UNIVERSITA' VITA-SALUTE SAN RAFFAELE

CORSO DI DOTTORATO DI RICERCA INTERNAZIONALE IN MEDICINA MOLECOLARE

CURRICULUM IN GENE AND CELL THERAPY

THE STUDY OF CELLULAR AGE ON iPSC-DERIVED β CELL FUNCTION

DoS: Prof. Lorenzo Piemonti

Second Supervisor: Prof. Francesco Dotta

Tesi di DOTTORATO di RICERCA di Laura Monaco

matr. 020256

Ciclo di dottorato XXXVII

SSD MED/13

Anno Accademico 2023/2024

CONSULTAZIONE TESI DI DOTTORATO DI RICERCA

I	Laura Monaco
Registration number	020256
Born at	Catania
On	23/06/1997

Author of the PhD Thesis title

The study of cellular age on iPSC-derived β cell function

☐ AUTHORIZES *the public release of the thesis*

☒ DOES NOT AUTHORIZE *the public release of the thesis for* 12 *months*

the PhD thesis date, specifically

From 01/04/2025 *To* 01/04/2026

Because:

☐ *The whole project or part of it might be subject to patentability;*

☒ *Parts of the thesis have been or are being submitted to a publisher or are in press;*

☐ *The thesis project is financed by external bodies that have rights over it and on its publication.*

Please Note: some parts of the thesis are not available in relation to the norm of the use of information protected by trade secret ***(To leave only if relevant)***

Copyright the contents of the thesis in whole or in part is forbidden

Data/ Date 10/03/2025 Signature Laura Monaco

DECLARATION

This thesis has been:

- composed by myself and has not been used in any previous application for a degree. Throughout the text I use both 'I' and 'We' interchangeably.
- has been written according to the editing guidelines approved by the University.

Permission to use images and other material covered by copyright has been sought and obtained. Figures 2,4,5,8,9,10,12,13,34 and 40 belong to an "open access" publication.

Part of the introduction paragraph "3.1.6. Innovative Cell Therapies for Diabetes Treatment" belongs to a review (Sordi et. al, 2023) where I contributed to the draft, and I am the second author.

All the results presented here were obtained by myself, except for:

1) Slices (Results, chapter 5.1, Figure 16) were processed by Dr. Amleto Fiocchi, Animal Histopathology Facility, San Raffaele Scientific Institute, Milan, Italy.
2) DNA sequencing (Results, chapter 5.5, Figure 24) was performed in collaboration with COSR-Centre for Omics Science, San Raffaele Scientific Institute, Milan, Italy.
3) Bioinformatic analysis on DNA sequencing (Results, chapter 5.5, Figure 24) was conducted in collaboration with Dr. Irene Franco and Dr. Jean Piero Margaria, Molecular Genetics of Renal Disorders, San Raffaele Scientific Institute, Milan, Italy.
4) The reprogramming of the iPMSC-iPSC line (Results, chapter 5.12, Figure 31) was performed in collaboration with Dr. Silvia Pellegrini, iPSC factory of CRB, San Raffaele Scientific Institute, Milan, Italy.
5) The results presented in chapters 5.7, 5.8, and 5.9 were obtained during my PhD period abroad at Beta Cell Aging Lab, in collaboration with Prof. Cristina-Aguayo Mazzucato, Dr. Kanako Iwasaki, Dr. Franscesko Hela and Cristopher Cahill, Joslin Diabetes Center, Boston, USA.
6) SOMAScan assay (Results, chapter 5.8, figure 27) was conducted in collaboration with BIDMC Genomics, Proteomics, Bioinformatics, and Systems Biology Center, Boston, USA.

Abstract

A reliable source of β cells is essential for advancing cell therapy in type 1 diabetes (T1D). Human induced pluripotent stem cells (iPSCs) can differentiate into insulin-producing β cells (iβ), effectively mimicking pancreatic development in vitro. While cellular senescence supports β cell formation during embryogenesis, aging-related β cell senescence impairs glucose sensing and insulin secretion. However, whether cellular senescence occurs during the transition from stem cells to mature endocrine cells and how it affects the final β cell phenotype remains unclear. This study investigates the role of aging in β cell differentiation and function.

Six clones of the iPSC cell line DRI2 were differentiated into β cells. Aging markers were assessed by measuring Senescence-associated β-Galactosidase activity (SA-β-Gal), histone H2AX phosphorylation (γH2AX), and superoxide production (mitoSOX) using flow cytometry. The expression of genes associated with the senescence-associated secretory phenotype (SASP) and cellular senescence was quantified via real-time qPCR. Somatic mutations were analyzed using TwinStrand Duplex sequencing. Proteomic analysis of iβ-conditioned media (CM) for specific β cell SASP factors was conducted with the SOMAScan assay. The effects of SASP factors in CM were evaluated on the human β cell line EndoC-βH5. The senescence state of the different clones at the iβ stage was correlated with their senescence profile and functional capacity. Finally, a senomorphic treatment was applied to iβ cells to determine the impact of senescence on β cell function.

Flow cytometry analysis revealed a significant increase in SA-β-Gal, γH2AX, and mitoSOX levels from iPSCs to iβ cells. Sequencing data indicated an increase in the Single Base Substitution 5 (SBS5) mutational signature during differentiation, a clock-like signature linked to aging. Transcriptomic analysis showed a significant upregulation of genes related to β cell SASP and cellular senescence, with a strong involvement of *p16* at the iβ stage. Proteomic analysis of iβ CM confirmed an enrichment of the $p16^{+}$ β cell SASP signature. When EndoC-βH5 cells were cultured with iβ CM, they exhibited increased SA-β-Gal activity, *p16* expression, and secretory function. Notably, the iPSC clone with higher *p16* expression at the iβ stage demonstrated superior function compared

to the clone with lower *p16* expression. Senomorphic treatment at the iβ stage reduced *p16* expression but also impaired iβ functionality in response to glucose.

These findings highlight a progressive increase in senescence during β cell differentiation, suggesting that $p16^{+}$ senescence may play a critical role in iβ maturation and function. Targeting senescence in iβ cells could provide a strategy to optimize cell therapy outcomes for T1D.

TABLE OF CONTENTS

1. **Acronyms and abbreviations**……..……....….4
2. **List of figures and tables**……..……..…7
3. **Introduction**……..…….…..10
   - **3.1. Type 1 Diabetes**……..……...10
     - ***3.1.1. Pathogenesis***……..12
     - ***3.1.2. Diagnosis***…… ….....13
     - **3.1.3. *Epidemiology***……..15
     - ***3.1.4. Therapy***……..15
     - ***3.1.5. Islet transplantation***……..18
     - ***3.1.6. Innovative Cell Therapies for Diabetes Treatment***……..20
   - **3.2. Pluripotent stem cells**…….……22
     - ***3.2.1. Generation of insulin-producing β cells from hPSCs***…..25
     - ***3.2.2. β cell replacement therapy***……..30
   - **3.3. Cellular aging and senescence**…… ..33
     - ***3.3.1. Senescence-associated secretory phenotype***……..37
     - ***3.3.2. Physiological and pathological role of senescence***……..39
     - **3.3.3. *β cell aging***……..44
     - ***3.3.4. Senotherapeutic approaches***……..50
   - **3.4. Cellular senescence of hPSCs from reprogramming to differentiation**……..…….55
4. **Aim of the work**……...60
5. **Results**…….……61
   - **5.1. iPSCs differentiate into β cells**……...…61
   - **5.2. Progressive increase in lysosomal activity highlights senescence dynamics during β cell differentiation**……..68
   - **5.3. DNA damage accumulates during the differentiation process**……...…….70

5.4. Elevated oxidative damage reflects senescence progression during β cell differentiation……..72
5.5. Single-base substitution analysis reveals an increase in signature aging mutation throughout the differentiation process…….……75
5.6. Transcriptomic data show an increase in senescence and SASP factors gene expression on EN and iβ stage……...76
5.7. Senescence in iβ differentiation is affected by *p16* and cells express specific β cell SASP factors……..77
5.8. Enrichment of SASP proteins in iβ secretome confirms the role of *p16* in iβ cell senescence……..79
5.9. iβ SASP factors induce secondary senescence and enhance insulin content in a human β cell line……81
5.10. iPSC clones exhibit different senescence profiles at the iβ stage…….……83
5.11. Senomorphic treatment on iβ decreases *p16* gene expression and insulin secretion……...85
5.12. iβ cells and human islets derived from the same donor present distinct senescence profiles……...88
6. Discussion……...95
7. Materials and methods……113
7.1. iPSC reprogramming……113
7.2. EndoC-βH5 culture (Joslin Diabetes Center)……..113
7.3. Human islets culture……..113
7.4. Pancreatic-mesenchymal stromal cells (pMSCs) culture……...…114
7.5. iPMSC-iPSCs reprogramming……...…114
7.6. iPSC differentiation into mature insulin-producing cells……...….114
7.7. iβ Senomorphic treatment……...119

7.8. Flow cytometry…….....119
7.9. Immunofluorescence staining…….....121
7.10. RNA extraction……...…124
7.11. RNA extraction (Joslin Diabetes Center)……..…125
7.12. Reverse transcription……125
7.13. Reverse transcription (Joslin Diabetes Center)……..126
7.14. TaqMan Gene Expression Assay……126
7.15. TaqMan Real-Time PCR ……130
7.16. Quantitative Real-Time PCR (Joslin Diabetes Center)……...130
7.17. SOMAScan Assay (Joslin Diabetes Center)……..……131
7.18. Static glucose-stimulated insulin secretion (Joslin Diabetes Center)…….……133
7.19. Collection of EndoC-βH5 cells for insulin and DNA content quantification (Joslin Diabetes Center)…….133
7.20. Dynamic glucose-stimulated insulin secretion……134
7.21. ELISA…….....…...134
7.22. DNA extraction……...135
7.23. DNA extraction (Joslin Diabetes Center)…….135
7.24. DNA sequencing……135
7.25. Statistical analysis……..136
8. References……138

1. Acronyms and abbreviations

AER	Apical Ectodermal Ridge
APCs	Antigen Presenting Cell
APD	Artificial Pancreas Device
AUC	Area Under the Curve
CA	Cardiac Tissue
cAMP	Cyclic AMP
CiPSC	Chemically Induced Pluripotent Stem-cell
CITR	Collaborative Islet Transplant Registry
CM	Conditioned Media
COPD	Chronic Obstructive Pulmonary disease
DDR	DNA Damage Response
DE	Definitive Endoderm
DM	Diabetes Mellitus
DNAm	DNA Methylation
DSBS	DNA Double-Strand Breaks
ECM	Extracellular Matrix
EN	Endocrine Cell
EP	Endocrine Progenitor
ESCs	Embryonic Stem Cell
EVS	Extracellular Vesicles
G6P	Glucose-6-Phosphate
GADA	Glutamic Acid Decarboxylase Autoantibody
GSIS	Glucose Stimulated Insulin Secretion
HbA1c	Glycated Hemoglobin
HF	Human Fibroblasts
HI	Human Islets
HIP	Hybrid Insulin Peptides
HLA	Human Leucocyte Antigen
HMGB1	High-Mobility Group Box 1

HPSCs	Human Pluripotent Stem Cell
HSCs	Hepatic Stellate Cell
IA-2A	Islet Antigen 2 Autoantibody
IAA	Insulin Autoantibody
iβ	iPSC-Derived β Cells
IBMX	3-Isobutyl-1-Methylxanthine
IEQ	Islet Equivalent
I-HF	Induced Human Fibroblast
iPSCS	Induced Pluripotent Stem Cell
MEF	Mouse Embryonic Fibroblasts
MitoSOX	Mitochondrial Superoxide Indicator
MMP	Matrix Metalloproteinases
MODY	Maturity-Onset Diabetes Of The Young
MSCs	Mesenchymal Stem Cell
NGS	Next-Generation Sequencing
NK	Natural Killer
NOD	Non-Obese Diabetic Mice
OGTT	Glucose Tolerance Test
OIS	Oncogene-Induced Senescence
PDE	Phosphodiesterase
PDL-1	Programmed Death-Ligand 1
PE	Pancreatic Endoderm
PECs	PEC-Direct Device
PERV	Porcine Endogenous Retroviruses
PF	Posterior Foregut
PGT	Primitive Gut Tube
PHPI	Purified Human Pancreatic Islets
pMSC	Pancreatic Mesenchymal Stromal Cell
ROS	Reactive Oxygen Species
RPE	Retinal Pigment Epithelium
SA-β-gal	Senescence-Associated β Galactosidase Activity

SAHF	Senescence-Associated Heterochromatin Foci
SASP	Senescence-Associated Secretory Phenotype
SBS	Single Base Substitution
SC-islet	Pancreatic Islet-Like Aggregate
SERPINs	Serine/Cysteine Proteinase Inhibitors
T1D	Type 1 Diabetes
T1DM	Type 1 Diabetes Mellitus
T2DM	Type 2 Diabetes Mellitus
TIMP	Tissue Inhibitors of Metalloproteinases
TIS	Therapy-Induced Senescence
TME	Tumor Microenvironment
UMIs	Unique Molecular Identifiers
uPAR	Urokinase Plasminogen Activator Receptor
UPR	Unfolded Protein Response
ZnT8A	Zinc Transported 8 Autoantibody
γH2AX	Phosphorylation of the histone H2AX

2. List of figures and tables

Figure 1. Simplified mechanism of T1D autoimmunity.

Figure 2. The stages of T1D.

Figure 3. Schematic illustration of the entire process from islet isolation to intraportal transplantation.

Figure 4. Innovative technologies and alternative sources of insulin-producing cells for β cell replacement.

Figure 5. The two faces of β cell development.

Figure 6. D'Amour et al. differentiation protocol.

Figure 7. Rezania et al. differentiation protocol.

Figure 8. Otonkoski et al. differentiation protocol.

Figure 9. Triggers and features of cellular senescence.

Figure 10. Physiological and pathological conditions of senescence.

Figure 11. Functional release of insulin.

Figure 12. Senotherapy in the context of senescent β cells.

Figure 13. Scheme of aging modifications during three main processes: reprogramming, iPSC culture, and differentiation.

Figure 14. Morphological changes on the differentiation process from iPSC into β cells.

Figure 15. Stage markers during the differentiation process from iPSC into β cells.

Figure 16. Representative immunofluorescence on iPSC and iβ clusters.

Figure 17. Gene expression assessment at Day 0 (iPSC), Day 21 (EN) and Day 30 (iβ) stages and GSIS.

Figure 18. SA-β-Gal activity during differentiation stages from iPSC into β cells.

Figure 19. Representative immunofluorescence of iβ cluster.

Figure 20. γH2AX during differentiation stages from iPSC into β cells.

Figure 21. Representative immunofluorescence of iβ cluster.

Figure 22. Superoxide production across the developmental stages from iPSC to β cells.

Figure 23. Representative immunofluorescence of iβ cluster.
Figure 24. Somatic mutation outcome during the differentiation process.
Figure 25. Heatmaps of differentially expressed genes at the stage of iPSC, EN, and iβ.
Figure 26. Specific senescence and SASP gene expression analysis during iβ differentiation.
Figure 27. Proteomic analysis on iβ CM.
Figure 28. Evaluation of iβ SASP factors effects on EndoC-βH5.
Figure 29. Evaluation of different senescence profiles between DRI2 clones.
Figure 30. Effects of Baricitinib on iβ.
Figure 31. Reprogramming of pMSCs and differentiation into iβ.
Figure 32. Senescence analysis of iβ in flow cytometry and transcriptomic analysis.
Figure 33. Senescence analysis in human islets and comparison with iβ derived from the same donor.
Figure 34. Otonkoski et al. differentiation protocol.
Figure 35. Cell morphology during the main stages of differentiation process.
Figure 36. RNA extraction process.
Figure 37. RNA extraction process.
Figure 38. RNA reverse transcription process.
Figure 39. RNA reverse transcription thermal profile.
Figure 40. TaqMan Array Card.
Figure 41. Duplex sequencing technology.
Table 1. SA-β-Gal positive cells during the differentiation stages for each clone.
Table 2. γH2AX positive cells during the differentiation stages for each clone.
Table 3. MitoSOX positive cells through the differentiation stages for each clone.
Table 4. Islets and iβ senescence and SASP gene expression from the same donor.
Table 5. List of the basal media used.
Table 6. List of the supplements used.
Table 7. Antibodies used in flow cytometry.

Table 8. CellEvent™ Senescence Green Flow Cytometry Assay Kit components.

Table 9. γH2AX Phosphorylation assay kit components.

Table 10. MitoSOX™ Red Mitochondrial Superoxide Indicator assay kit component.

Table 11. Primary antibodies used in immunofluorescence.

Table 12. Secondary antibodies used in immunofluorescence.

Table 13. Senescence marker's antibodies used in immunofluorescence staining.

Table 14. A list of specific differentiation marker genes analyzed using the Gene Card assay.

Table 15. List of the genes analyzed with the TaqMan Real-Time PCR.

Table 16. List of the genes analyzed with the Quantitative Real-Time PCR.

Table 17. List of specific β cell $p16^+$ SASP factors analyzed with SOMAScan.

Table 18. List of specific β cell $p21^+$ SASP factors analyzed with SOMAScan.

3. INTRODUCTION

3.1 Type 1 Diabetes

The pancreas, a complex organ, has both endocrine and exocrine functions. The exocrine pancreas consists of acinar cells, which secrete digestive enzymes, and ductal cells that transport pancreatic juices to the duodenum (Jennings *et al*, 2015). The endocrine part, composed of islets of Langerhans, includes insulin-secreting β cells, glucagon-secreting α cells, somatostatin-secreting δ cells, pancreatic polypeptide-secreting γ cells, and ghrelin-secreting ε cells. Focusing on β cells, they produce insulin, a peptide hormone crucial to carbohydrate, fat, and protein metabolism, facilitating glucose absorption from the bloodstream into cells. Thus, insulin is vital for regulating glucose levels (Vecchio et al, 2018).Diabetes mellitus (DM) is a metabolic disorder characterized by abnormally high blood sugar levels. DM encompasses several types, including Type 1, Type 2, maturity-onset diabetes of the young (MODY), gestational diabetes, neonatal diabetes, and secondary diabetes caused by endocrinopathies or steroid use. The two main types of DM are Type 1 diabetes mellitus (T1DM) and Type 2 diabetes mellitus (T2DM). T1DM typically results from insufficient insulin secretion, whereas T2DM arises from impaired insulin action. T1DM often appears in children or adolescents, whereas T2DM commonly affects middle-aged and older adults due to prolonged hyperglycemia linked to lifestyle and dietary factors. The underlying mechanisms of T1DM and T2DM differ significantly, leading to distinct causes, symptoms, and treatments for each type (Sapra & Bhandari, 2023). T1DM, called simply Type 1 Diabetes (T1D), also known as juvenile diabetes or insulin-dependent diabetes, is a chronic autoimmune disorder characterized by a lack of insulin and subsequent hyperglycemia, affecting millions globally (DiMeglio *et al*, 2018). The disease starts from the immune-mediated destruction of pancreatic β cells, which produce insulin (Gillespie, 2006). Patients diagnosed with T1D require lifelong insulin therapy and face numerous related complications. T1D often develops in children or young adults but can occur at any age. It is usually preceded by islet autoimmunity, indicated by specific autoantibodies: insulin (IAA), glutamic acid decarboxylase (GADA), islet antigen 2 (IA-2A), and zinc transported 8 (ZnT8A). Although asymptomatic initially, this phase can predict T1D development, with seroconversion

occurring early in genetically predisposed individuals (Frohnert *et al*, 2017). Moreover, the development of T1D can be related to multiple genetic and environmental factors. Key genetic risk factors are located in the class II Human Leucocyte Antigen (HLA) region, with around 600 additional non-HLA loci also contributing to disease susceptibility. Significant loci include HLA-DR and HLA-DQ, with certain haplotypes (DR4-DQ8, DR3-DQ2) common in 90% of children with T1DM, while DR15-DQ6 is rare (Ilonen *et al*, 2019).

Over the past century, lifestyle changes, including increased hygiene and environmental exposures, have significantly influenced T1D prevalence. Recent studies suggest that enteroviral infections, especially cosackie B viruses, may trigger autoimmune responses against β cells, leading to T1D. This hypothesis is backed by the observation that T1D incidence follows a seasonal pattern, with diagnosis peaks occurring from late autumn to early spring. During these colder months, viral infections are more common, and factors like reduced sunlight exposure, decreased outdoor activity, dietary shifts, and increased proinflammatory cytokines contribute to a shift towards proinflammatory gene networks. This increases β cells' vulnerability to enteroviral infections. Certain genetic mutations in the viral response pathway in T1D may amplify the immune response to the virus, leading to an increase of proinflammatory cytokines and chemokines. This results in the hyperexpression of HLA I molecules, attracting cytotoxic T cells and macrophages, ultimately causing the destruction of β cells and the onset of T1D (Onkamo *et al*, 1999; Geravandi *et al*, 2020). Additionally, nutrition also plays a crucial role. Diets rich in unsaturated fish oils, vitamin E, and vitamin D are associated with a protective effect, while heavy consumption of cow's milk, the introduction of gluten-containing foods after 9 months, and solid foods high in fiber before 4 months, have been linked to an increased risk of developing islet autoimmunity in the first three years of life (Niinistö *et al*, 2017; Uusitalo *et al*, 2008; Dong *et al*, 2013). Numerous studies have highlighted the complex interplay of these factors, emphasizing the importance of early nutritional interventions and lifestyle choices in modulating T1D risk (Beyerlein *et al*, 2014; Hakola *et al*, 2018).

3.1.1. Pathogenesis

Type 1 Diabetes (T1D) arises from interactions between pancreatic β cells and both the innate and adaptive immune system. In genetically predisposed individuals, an unidentified immune insult initiates a chronic, low-grade immunological process known as priming (Krogvold *et al*, 2015). The exact trigger for this immune response against β cells remains debated, with some suggesting specific stimuli while others consider it may be random. The initial immune response involves the infiltration of the innate immune cells like monocytes and natural killer (NK), along with autoreactive B cells, into the pancreatic islets. The primary site for antigen-presenting cells like B cells and dendritic cells, present islet antigens in the pancreatic lymph node to $CD4^+$ T lymphocytes. These T lymphocytes then activate auto-reactive $CD8^+$ T cells, specifically targeting insulin-producing β cells while leaving other endocrine cells in the islet unaffected. $CD4^+$ and $CD8^+$ T cells infiltrate the islets through vascularization leading to the islet basement membrane impairment, causing severe damage and the death of β cells. Immune cells release cytokines like tumor necrosis factor-alpha (TNF-α), interferon-gamma (IFN-γ), and interleukin 1 beta (IL-1β), which together drive β cell apoptosis. Moreover, T cells activated within the pancreatic lymph node also stimulate B lymphocytes to produce autoantibodies against β cell proteins. These autoantibodies can be detected in the bloodstream and are considered a definitive biomarker for T1D (**Figure 1**). On the other hand, regulatory T cells can potentially block this process in its early stages, but this cannot happen in the later stages of the disease (Hull *et al*, 2017; Padgett *et al*, 2013). During the early stages, immune therapies show the potential to regenerate partially destroyed β cells. Without intervention, the β cell population continues to decline (Bluestone *et al*, 2010).

Moreover, it has been demonstrated that hybrid insulin peptides (HIPs), which are novel antigens derived by the covalent fusion of proinsulin fragments and other β cell peptides, play a crucial role in the development of T1D. Researchers found that $CD4^+$ T cells from islets of individuals with T1D recognize HIPs, suggesting a central role for them in breaking immune tolerance and contributing to β cell destruction in both non-obese diabetic (NOD) mice and humans (Delong *et al*, 2016). In the context of immune activation, the expression of an alternatively spliced insulin gene (INS) product was investigated in human pancreatic islets. Specifically, δ cells could release INS products

derived from alternative splicing and activate preproinsulin-specific cytotoxic T lymphocytes *in vitro*, suggesting a potential role in islet autoimmunity (van Tienhoven *et al*, 2023). This concept is in line with a recent study where researchers measured preprandial and postprandial blood glucose concentrations in over 1,000 participants aged between 4 months and 3.6 years. They could observe that children who developed islet autoantibodies exhibited early elevations in blood glucose concentrations, suggesting that β cell dysfunction initiate several months before autoantibodies are seen (Warncke *et al*, 2022).

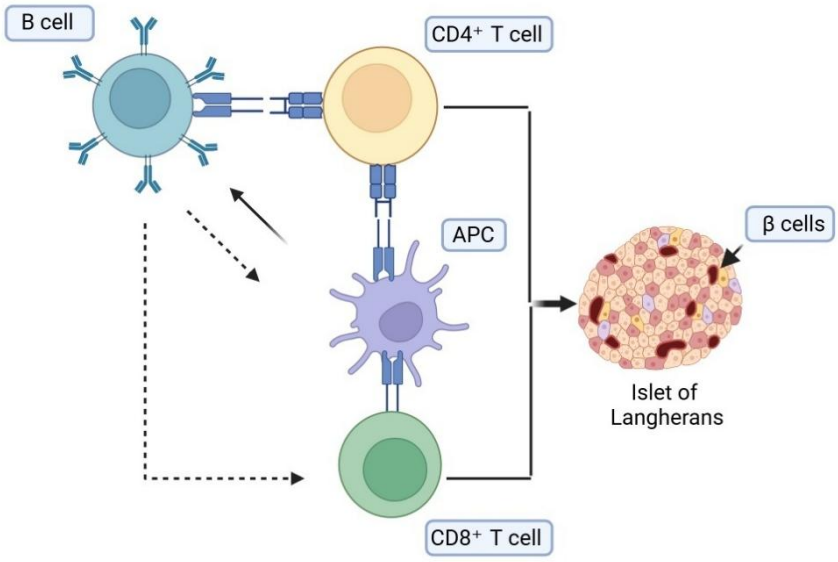


Figure 1. Simplified mechanism of T1D autoimmunity. *The immune response is initiated by β cell peptides presented by antigen-presenting cells (APCs). These APCs transport autoantigens to the pancreatic lymph nodes and engage with autoreactive CD4⁺ T lymphocytes, activating CD8⁺ T cells and B cells to produce autoantibodies. Once activated, the CD8⁺ T cells return to the islets and attack β cells displaying immunogenic self-antigens on major histocompatibility complex class I molecules (created with biorender.com).*

3.1.2 Diagnosis

Based on guidelines from the American Diabetes Association, diabetes is diagnosed with glucose criteria related to fasting blood glucose, postprandial glucose during a 75 g oral glucose tolerance test (OGTT), or glycated hemoglobin (HbA1c) levels. Going into details, fasting plasma glucose has to be ≥ 126 mg/dL on multiple occasions, random plasma glucose ≥ 200 mg/dL with typical hyperglycemia symptoms, plasma glucose ≥ 200 mg/dL two hours after a 75 g OGTT and HbA1C level ≥ 6.5% (Elsayed *et al*, 2022). Generally, T1D is considered primarily a childhood disease, even if it can occur also in

adults. For this reason, it can be confused with T2D. To exclude it, is fundamental to search for the pancreatic autoantibodies including ICA, IAA, GADA, IA2A, and ZnT8 because most T1D patients have one or more positive autoantibodies at diagnosis. The risk of progressing to T1D is relatively low with a single autoantibody, but children with two or more autoantibodies face a significantly higher risk, about 84%, of developing clinical T1D by age 18 (Ziegler *et al*, 2013). Based on this, T1D stages have been refined. Stage 1 and stage 2 are included in the presymptomatic phase. Stage 1 is related to children who present two or more autoantibodies and are still normoglycemic. For them, the chances to develop symptomatic type 1 diabetes are about 44% within five years, 70% within ten years, and nearly certain over their lifetime. Stage 2 is like stage 1, but in this case, the children having autoantibodies present dysglycemia due to the loss of β cell mass. Stage 3 is the symptomatic stage where the patients have typical symptoms that include frequent urination (polyuria), excessive thirst (polydipsia), and unintended weight loss (Insel *et al*, 2015) (**Figure 2**).

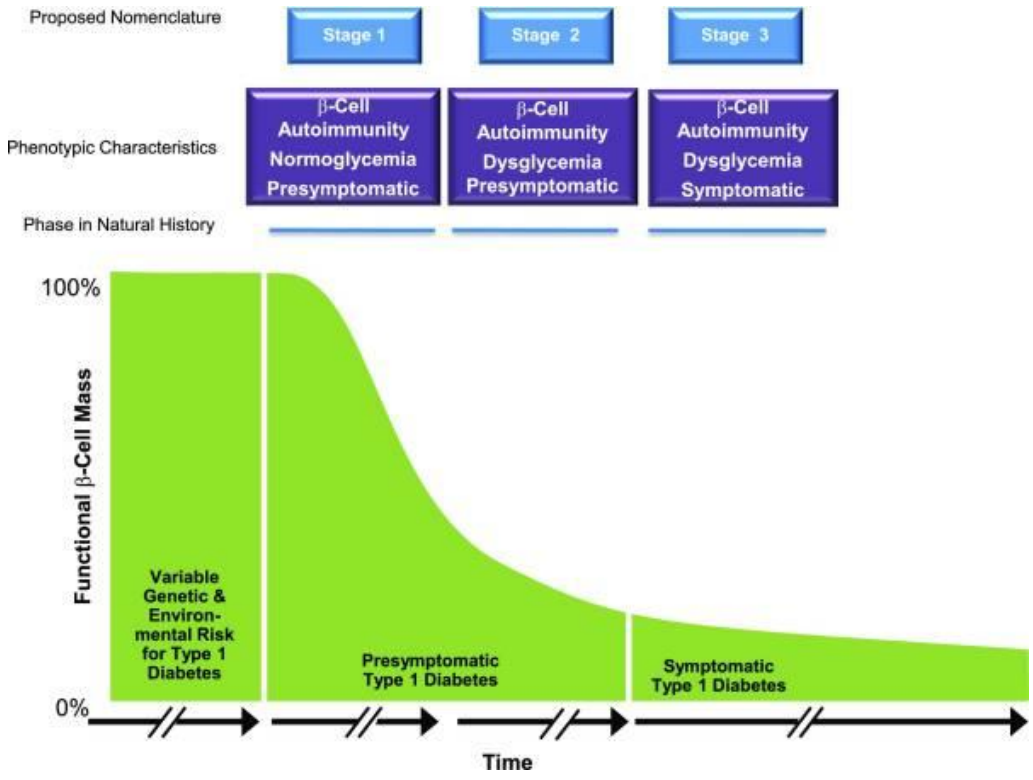


Figure 2. The stages of T1D. *The progression of T1D is linked to the progressive loss of functional β cell mass during time. The time is divided into two main phases. The first phase, the presymptomatic one, includes Stage 1 and Stage 2. The second phase, the symptomatic one, includes Stage 3* (Insel *et al*, 2015).

3.1.3 Epidemiology

The increase annually in the prevalence of T1D is 0.34% in adolescents and young adults being a big concern today for healthcare. In 2021, an estimated 8.4 million people worldwide were living with type 1 diabetes (T1DM), with 500.000 new cases recorded that year. Projections indicate that by 2040, the number of individuals with T1DM will rise between 13.5 and 17.4 million. The average life expectancy for a 10-year-old diagnosed with T1DM is only 13 years in low-income countries, compared to 65 years in high-income countries (Gregory *et al*, 2022). Extensive research has explored how environmental factors initiate the autoimmune process that destroys β-cells, suggesting that perinatal elements like delivery methods and maternal and childhood diets, ecological factors such as air pollution and climate, may be linked to the prevalence of T1D. Moreover, the rise in obesity can contribute to insulin resistance and lipid abnormalities speeding up the onset of T1D in those who are genetically predisposed (Buzzetti *et al*, 2020). In a recent study, data were analyzed from 193 articles spanning from 1990 to 2019, and it was found that the incidence of T1D was very different depending on the different continental regions. China and Venezuela report the lowest rates of type 1 diabetes at 0.1 per 100,000 people per year, whereas Finland and Sardinia have the highest rates at 37 per 100,000 per year. Regarding sex incidence, although many autoimmune diseases are more prevalent in females, T1D generally affects young boys and girls equally (Mobasseri *et al*, 2020).

3.1.4. Therapy

Currently, insulin replacement therapy remains the primary treatment for type 1 diabetes (T1D). The use of exogenous insulin was introduced by Banting and Best in 1921, who utilized crude animal pancreas extracts for their glucose-lowering effects. By 1922, commercial preparations of animal-derived insulin became available but with some issues related to the insulin's pharmacokinetics, particularly in its absorption causing extended periods of hypoglycemia. Since then, numerous humanized insulin analogs have been developed, mimicking endogenous insulin's biological actions and offering improved pharmacokinetic profiles: rapid-acting, short-acting, intermediate-acting, and long-acting insulin. Rapid-acting insulin starts working in 10-30 minutes, peaks in 30-90 minutes, and lasts 3-5 hours. Short-acting insulin begins in 30-60 minutes, peaks in 2-4 hours, and

lasts 5-8 hours. Intermediate-acting insulin starts in 1-2 hours, peaks in 4-12 hours, and lasts 12-18 hours. Long-acting insulin starts in a few hours, has a minimal peak, and lasts up to 24 hours. Insulin can be administered through injections, or, for many individuals, insulin pumps are preferred (Pathak *et al*, 2019). However, insulin pumps have very high costs, and inconsistent insurance coverage open new way to treat diabetes like smart insulin pens. "Smart insulin" is an innovative type of insulin designed to automatically adjust its activity based on blood glucose levels: they function similarly to traditional insulin pens but with added technology that helps track and optimize insulin delivery. This means it can turn on when blood sugar is high and turn off when it's low, helping to prevent dangerous hypoglycemic events and maintain better glucose control. One example of smart insulin is NNC2215, which has shown promise in early-stage research. It contains a glucose-responsive switch that activates the insulin when glucose levels rise and deactivates it when glucose levels fall simplifying diabetes management, even if patients still need to administer injections themselves, which can be inconvenient (Singh *et al*, 2023; Sacks, 2024). Indeed, T1D patients often use a continuous glucose monitor (CGM) to track blood glucose levels. These devices have some limitations, such as the need to replace the sensor every seven days and, in some cases, the requirement for calibration creating a significant workload for managing blood glucose levels. To address these challenges, closed-loop artificial pancreas devices (APD) are widely used. This device comprises three main components: a glucose sensor, insulin pump, and control algorithm that determines the amount of insulin to administer, mimicking the function of a healthy pancreas in response to real-time glucose levels. The ADP improvements, like the third generation one that comprises fully automated multi-hormones with insulin added with glucagon or amylin, are likely to maximize performance and user comfort (Dermawan & Kenichi Purbayanto, 2022; Nadia Ahmad *et al*, 2021).

Given that T1D is an autoimmune disease, attempts to reverse or prevent the autoimmune attack have focused on the immune system. While single-target immunotherapies have met specific objectives, they have not been effective in achieving long-term glycemic control or significantly preserving insulin secretion. Refining and combining these immunotherapies might improve glycemic control, but so far, combination therapies have not completely reversed T1D. Single-target immunotherapies like teplizumab serve T-cell modulation targeting the CD3 receptor on T-cells. In 2019 was conducted a randomized,

double-blind, placebo-controlled trial was conducted, enrolling 76 participants who were relatives of patients with T1D and had at least two diabetes-related autoantibodies along with dysglycemia. Participants received a single 14-day course of teplizumab or a placebo, and the results demonstrated that teplizumab significantly delayed the progression to clinical diabetes. Over a median follow-up period of 2 years, 19% of participants in the teplizumab group developed diabetes, compared to 62% in the placebo group (Herold *et al*, 2019). In 2022, the American Food and Drug Administration (FDA) approved teplizumab to delay the progression to stage 3 of T1D in high-risk children with stage 2 disease, characterized by the presence of autoantibodies.

Another approach is expanding a patient's own regulatory T cells in the laboratory and then infusing them back into the patient to help suppress the autoimmune response. Strategies to increase the number of Tregs are both safe and tolerable, and they hold promises for potentially controlling type 1 diabetes. In a study children recently diagnosed with T1D were included, and there was some improvement in β cell function following the infusion of expanded autologous Tregs (Marek-Trzonkowska *et al*, 2012). Furthermore, a phase 1/2 randomized, double blind, placebo-controlled trial including low-dose interleukin-2 (IL-2) therapy has demonstrated an ability to boost the number of Tregs (Hartemann *et al*, 2013).

One promising future treatment for T1D is the replacement of β cells from external sources. Pancreas transplants, performed for over 50 years, are a standard treatment for individuals with end-stage renal failure who also need a kidney transplant. In the 70% of the cases, a simultaneous pancreas-kidney transplant is done, that can lead to insulin independence in up to 80% of patients for over five years. In the 20% of the cases, T1D patients are subjected to a pancreas after kidney transplant that usually occurs after a living donor kidney transplant or a previous simultaneous pancreas-kidney transplant where the pancreas graft has failed. Rarely performed, in the 10% of T1D patients, is the pancreas transplant alone. This is done just for patients who have preserved renal function but poor glycemic control, leading to frequent hypoglycemia and hypoglycemic unawareness. However, whole pancreas transplants are common in adults but rare in children due to the low incidence of chronic complications, preference for intensive insulin therapy, and surgical challenges (Kochar & Jain, 2021). For this reason, islet cell transplants are a promising alternative.

Transplantation of donated pancreatic islets has long been a hopeful treatment for T1D patients, even if patients need to be under immunosuppressive treatment. These transplants can now offer significant glycemic control and the potential to eliminate the need for exogenous insulin (Christoffersson, 2022).

3.1.5. Islet transplantation

A groundbreaking advancement was the creation of the semiautomatic method for controlled pancreatic digestion using the Ricordi Chamber. This method enables the separation of islets from the exocrine tissue within a digestion chamber, where a mechanically enhanced, continuous enzymatic process takes place. As the pancreatic tissue is gradually digested, the released materials are constantly collected in a large volume of solutions to inhibit further enzyme activity (Agarwal & Brayman, 2012). The islet isolation process begins with the preparation of the pancreas where specific digestive enzymes break down the connective tissue preserving the islets of Langerhans. The pancreas is then placed inside the Ricordi Chamber where it undergoes a process of gentle mechanical agitation through glass beads. Concurrently, a continuous flow of enzymatic solutions is maintained within the chamber, enhancing the breakdown of the tissue. All the process is maintained at 37° to optimize enzyme activity and ensure effective digestion. While the pancreatic tissue is broken, the resulting mixture undergoes a filtration process where the islets are separated from the exocrine tissue. After this step, the islets are purified through a density gradient that creates distinct layers based on the weight particles, allowing the isolation of pure islets. Once purified, the islets are cultured for either transplantation or further research. Throughout the entire process, the integrity and functionality of the islets are carefully monitored to ensure they meet the required standards for clinical or research use **(Figure 3)** (Ricordi *et al*, 1989; Shapiro *et al*, 2016)**.** Data from the Collaborative Islet Transplant Registry (CITR) indicates that 1,086 patients underwent allogenic islet transplantation between 1999 and 2015. Over the years, specific conditions have been identified for achieving successful outcomes, such as the use of proper immunosuppressants, an islet equivalent (IEQ) count of ≥5000/Kg, a recipient age of ≥35, and a BETA-2 score of ≥15. The BETA-2 score is a composite metric to assess islet graft function following islet transplantation (>6 indicates a good graft function). It incorporates multiple clinical parameters to provide an evaluation of graft performance: HbA1c (5%), insulin dose (U/kg/day), fasting blood glucose (mg/dL), fasting C-peptide

(ng/mL) (Lam *et al*, 2022). Related to this, it is important to mention the use of C-peptide: is a small protein fragment that is released when proinsulin is cleaved to produce insulin in a ratio 1:1 and it serves as a marker of endogenous insulin production (from the patient's pancreas or β cell graft, and not by exogenous insulin administration). For this reason, C-peptide detectable levels post-transplant indicate successful engraftment and insulin production by the transplanted islets, assessing graft viability and guiding therapeutic decisions (Masset *et al*, 2021).

A multicenter, single-arm, phase 3 study of the investigational product purified human pancreatic islets (PHPI) was conducted at eight centers in North America. A significant number, specifically 48 patients with type 1 diabetes, were transplanted, and they achieved stable glycemic control with HbA1c <7% without severe hypoglycemia (85.5% at 1 year and 71% at 2 years). Similarly, sustained C-peptide stimulation was observed for over 5 years after islet transplantation in a Japanese group. However, long-term immunosuppression has been associated with a decrease in glomerular filtration rate, a higher risk of infections, and 73% of recipients needing islet re-infusion because of the survival of the transplanted islet graft. In a Canadian cohort, the average graft survival was approximately 5.9 years, and only 8% of patients remained insulin-independent 20 years post-transplantation (Lee & Yoon, 2022; Hering *et al*, 2016). A Lancet study just published this year, showed a retrospective cohort study with 79 individuals aged 18 to 67 years with type 1 diabetes who underwent intraportal or intrahepatic islet transplantation alone in Italy (Milan) between 2001 and 2023. A total of 159 islet infusions were performed, with a median total islet mass of 9637 islet equivalents IEQ/kg. Patients presented a notable reduction in HbA1c levels and daily insulin requirements, with 44% of patients achieving insulin independence for a median of 6 years. However, 35 of 79 patients experienced adverse events related to immunosuppressive therapy (Catarinella *et al*, 2025). Despite the progress, donor shortages and complications related to immunosuppression present significant challenges for the widespread adoption of islet transplantation.

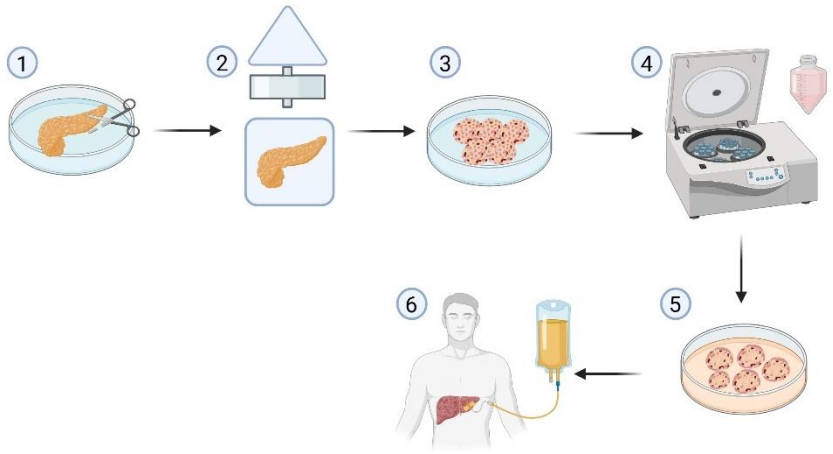


Figure 3. Schematic illustration of the entire process from islet isolation to intraportal transplantation. *The process can be divided into 7 main steps. The pancreas is extended and perfused with collagenase (1), then passed into the Ricordi chamber (2) and digested (3). The islet purification is done through continuous density centrifugation (4) and the highly purified human islets are maintained in culture (5) until the percutaneous transhepatic portal venous cannulation (6) (created with biorender.com).*

3.1.6. Innovative Cell Therapies for Diabetes Treatment

The field of cellular therapies for diabetes treatment is advancing rapidly, marking the dawn of an exciting new era (**Figure 4**). Significant efforts are underway to enhance islet transplantation in various ways, developing strategies for better engraftment and survival of transplanted islets. An example is to engineer ideal bio-artificial environments to support islet survival in culture and after transplantation with the addition of extracellular matrix (ECM) components that are lost during isolation or developing a novel approach to bio-fabricate functional, vascularized islet organs *ex vivo* (Tremmel & Odorico, 2018; Citro *et al*, 2019). Moreover, researchers are also working on hydrogel polymers to prevent direct contact between the transplanted cells and the host's immune system or on gene editing techniques to make the cells invisible to the immune system (Basta *et al*, 2020; Hu *et al*, 2024). Despite this, the challenges related to the procurement of human islets become more evident. Due to the limited number of pancreas donors and the challenges of safely managing rejection and recurrent autoimmunity, islet transaplantation cannot currently be extended to a large number of T1D patients. Moreover, achieving long-term normoglycemia in T1D patients often requires the contribution of two or more donors, as many islets are lost within the first 60 minutes of intraportal transplantation making widespread clinical implementation unfeasible

(Shapiro *et al*, 2000). For this reason, alternative sources of insulin-producing cells are studying. One of the possibilities is the xenotransplantation of pig islets. Pigs are considered a promising source for islet transplantation for several reasons: (i) pigs are genetically similar to human islets making them suitable for transplantation; (ii) pigs can be bred very easily and their pancreas contains a large number of isles that respond well to glucose stimulation; (iii) the use of CRISPR-Cas9 allow the modification of pigs that can be genetically modified to express human protective genes reducing the risk of immune rejection. There is already evidence of preclinical success, where in non-human primates researchers have shown that pig islets can maintain normoglycemia for extended periods, demonstrating their potential effectiveness (Shin *et al*, 2015). These factors and promising research make pig islets a viable and promising option for addressing the shortage of human islet donors and advancing diabetes treatment. However, the glucose-stimulated insulin secretion (GSIS) capacity of both adult and juvenile pig islets is lower than that of human islets: the insulin secretion capacity of adult pig islets is about one-third, and juvenile pig islets is about one-sixth, compared to human islets. This means that a significantly larger number of porcine islets are needed to achieve the same effect in reversing hyperglycemia as human islets (Cooper *et al*, 2024). Apart from this, the main limitations of pig islet xenotransplantation are immune rejection, which requires extensive and potentially risky gene editing to control, and the risk of transmitting porcine endogenous retroviruses (PERVs) (Citro *et al*, 2023). This is also accompanied by ethical concerns that need to be taken into consideration which, particularly pigs, raises ethical questions about animal welfare and the moral implications of using animals for medical purposes (Naqvi *et al*, 2023). Because of these limitations, human pluripotent stem cells, both embryonic stem and induced pluripotent stem cells, are considered as the best candidates for making β cells (Sordi *et al*, 2023).

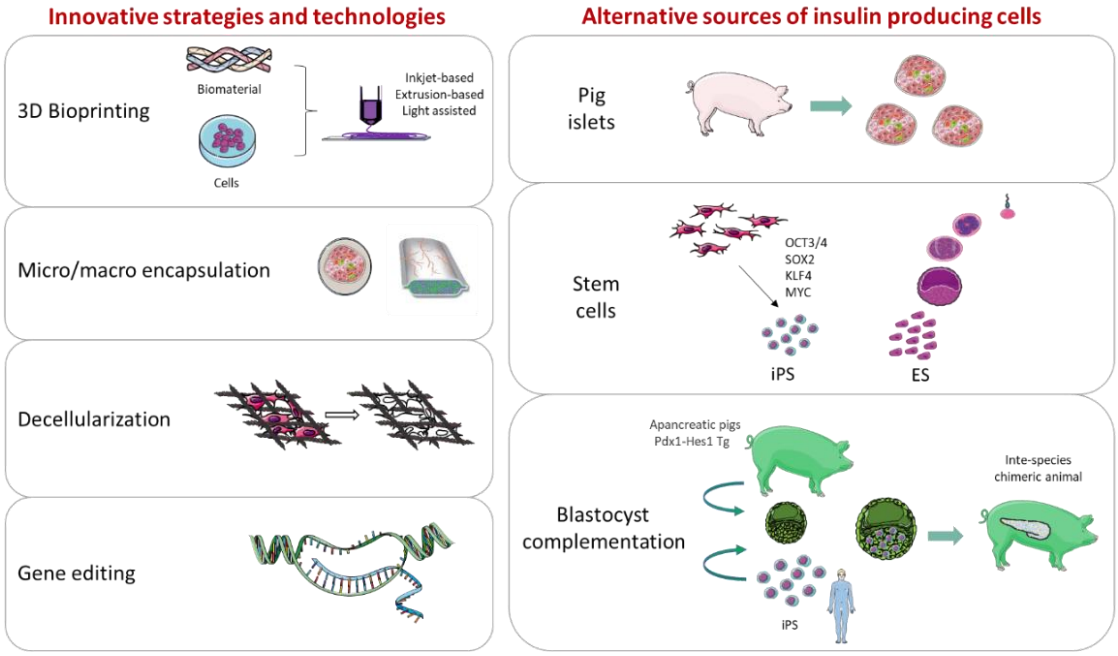


Figure 4. Innovative technologies and alternative sources of insulin-producing cells for β cell replacement. *On the left are described innovative strategies and technologies such as 3D bioprinting, micro/macro encapsulation, scaffold decellularization, and gene editing to enhance islet transplantation. On the right, are shown the alternative sources of insulin-producing cells: pig islets, stem cells (induced pluripotent stem cells and embryonic stem cells), and the blastocyst complementation mixing apancreatic pigs and stem cells to obtain an inter-species chimeric animal* (Sordi *et al*, 2023).

3.2 Pluripotent stem cells

Stem cells are unique, unspecialized cells in the human body with the remarkable ability to transform into any cell type and the capability to self-renew. These cells are found in both embryos and adults, progressing through various stages of specialization. The term "stem cell" was first coined by German biologist Ernst Haeckel in 1868 to describe the fertilized egg's potential to develop into all the cells of an organism. Stem cell therapy has evolved over the past 60 years into a promising treatment modality for numerous incurable diseases, including neurological disorders, pulmonary dysfunctions, metabolic and endocrine-related diseases, reproductive disorders, skin burns, and cardiovascular conditions. There are three main types of stem cells. Embryonic stem cells (ESCs) derived from early-stage embryos: these cells are pluripotent, meaning they can develop into any cell type in the body. ESCs have vast potential for regenerative medicine but also raise ethical concerns due to the destruction of embryos. On the other hand, adult stem cells are found in various tissues such as bone marrow, blood, and the brain, these cells are

multipotent. They have a more limited ability to differentiate compared to ESCs but play a crucial role in maintaining and repairing the tissue in which they are found. Hematopoietic stem cells (HSCs), which generate blood cells, and mesenchymal stem cells (MSCs), which can become bone, cartilage, and fat cells, are examples of adult stem cells (Hoang *et al*, 2022; Zakrzewski *et al*, 2019). In the early 2000s, researchers were searching for ways to harness the potential of stem cells without the ethical concerns associated with embryonic stem cells (ESCs). The Japanese stem cell biologist Shinya Yamanaka and the postdoctoral fellow Takahashi aimed to develop a method to reprogram adult cells back to a pluripotent state, making them functionally equivalent to ESCs. These efforts culminated in the creation of induced pluripotent stem cells (iPSCs) from mouse embryonic fibroblasts (MEFs) in 2006. They selected 24 potential reprogramming factors, including key transcription factors necessary for maintaining the ESC state. Through meticulous screening, Yamanaka and Takahashi identified four critical transcription factors: *OCT4*, *SOX2*, *KLF4*, and *MYC* (collectively known as Yamanaka factors). These transcription factors were cloned into retroviral vectors designed to carry and introduce these genes into the MEFs. These factors were sufficient to induce pluripotency in MEFs exhibiting properties similar to ESCs, including the ability to differentiate into various cell types (Takahashi & Yamanaka, 2006). One year later, Yamanaka and James Thomson independently showed that human fibroblasts could also be reprogrammed into iPSCs. Yamanaka used the same OSKM factors, while Thomson employed a different combination: *OCT4*, *SOX2*, *NANOG*, and *LIN28*. These breakthroughs demonstrated that it was possible to reprogram adult human cells to a pluripotent state, opening new avenues for regenerative medicine and research. In 2012 Yamanaka and John B. Gurdon were awarded the Nobel Prize in Physiology or Medicine for their contributions to the field of stem cell research. Since then, various modifications to the original cocktail of reprogramming factors have been developed to enhance the efficiency and safety of iPSC generation. The advent of iPSCs has revolutionized the field of regenerative medicine, providing a versatile tool for disease modeling, drug discovery, and potential cell-based therapies. By bypassing the ethical issues associated with ESCs, iPSCs have paved the way for new treatments and a deeper understanding of human biology (Cerneckis *et al*, 2024). Reprogramming somatic cells into iPSCs can be achieved through various viral and non-viral methods. Each approach has its advantages and

challenges. The viral methods include the use of retrovirus and lentivirus which insert reprogramming genes into the host genome, leading to stable expression of these genes. However, this integration poses a risk of insertional mutagenesis, where the insertion of viral DNA may disrupt important genes, potentially leading to cancer. Lentiviruses can infect non-dividing cells, broadening their applicability compared to retroviruses. For this reason, the use of Sendai virus method is the preferable one: it is an RNA virus that avoids genomic integration, reducing the risk of insertional mutagenesis and being diluted out of the cells after approximately 10 passages post-infection. It is highly efficient and transient, with demonstrated effectiveness in reprogramming neonatal and adult fibroblasts. This method is safer than retroviral and lentiviral methods, even if it is more challenging to handle compared to lentiviruses and residual virus can sometimes be difficult to eliminate completely with the need to culture the cells at high temperature (39°C) to ensure complete removal (Malik & Rao, 2013). Non-viral methods offer a safer, more flexible, and potentially more acceptable approach for reprogramming iPSCs, making them an attractive alternative to traditional viral methods. An exciting example is the method that involves introducing synthetic mRNA that encodes reprogramming factors directly into cells. It provides high reprogramming efficiency and avoids genomic integration requiring repeated transfection due to the transient nature of mRNA. Advancements in this reprogramming technique include the use of microRNAs (miRNA) to boost efficiency. It was shown that the combined effect of synthetically modified mRNAs encoding reprogramming factors and miRNA-367/302s, delivered as mature miRNA mimics, significantly enhance the efficiency of reprogramming human primary fibroblasts into iPSCs (Artero Castro *et al*, 2018; Kogut *et al*, 2018). Another exciting method is the use of chemical reprogramming, which includes the use of small molecules that can replace some or all reprogramming factors, facilitating the reprogramming process without altering the genome. It recreates a chemical-induced dedifferentiation, mimicking the dedifferentiation process that occurs in axolotl limb regeneration. This method is still under development with promising results (Guan *et al*, 2022). Indeed, this year an advancement in this technique was published, which provides a faster chemical reprogramming in less than 10 days, presenting a consistent 100% success rate of 15 different donors reprogramming (Wang *et al*, 2025). In general, each method offers unique benefits and limitations, and the choice often depends on the specific requirements

of the experiment or therapeutic application. Researchers continue to develop and refine these techniques to enhance the efficiency and safety of iPSC generation.

3.2.1. Generation of insulin-producing β cells from hPSC

Human pluripotent stem cells can proliferate indefinitely *in vitro* and maintain the ability to differentiate into all cell types from the three germ layers: ectoderm, mesoderm, and endoderm. Indeed, hPSCs can potentially produce unlimited human cells *in vitro* for transplantation therapies, including pancreatic β cells and other cells relevant to diabetes treatment. Moreover, in the context of cell therapy, iPSCs can be personalized for patients, potentially reducing immune rejection. Understanding the morphogenesis and expression profiles of key lineage-specific genes during pancreatic development *in vivo* is crucial for differentiating pancreatic β cells from stem cells *in vitro.* The development of β cells begins with the formation of the endoderm during the process of gastrulation in early embryonic development. Gastrulation results in the formation of three germ layers: ectoderm, mesoderm, and endoderm. The endoderm is the innermost layer and gives rise to the gastrointestinal tract, lungs, liver, and pancreas. The definitive endoderm arises from a particular anterior part of the primitive streak. This process is primarily governed by the transforming growth factor-β (*TGF-β*) superfamily, which includes Nodal/Activin A and bone morphogenetic protein (*BMP*) signaling, as well as the Wingless and Int-1 (*WNT*) signaling pathways (D'Amour *et al*, 2005). From the definitive endoderm, the cells undergo folding and closing to form the primitive gut tube. Within the posterior foregut, which is a region of the primitive gut tube, the activation of transcription factors like Forkhead box protein A2 *(FOXA2)* and hepatocyte nuclear factor 1 homeobox B *(HFN1B)* is essential (Wilson *et al*, 2003). The dorsal and ventral buds at the posterior foregut region grow and fuse to form the pancreatic endoderm after gut rotation. Key transcription factors, such as Pancreatic and Duodenal Homeobox 1 (*PDX1*), are crucial for the growth and differentiation of these buds. *PDX1* is expressed in both the dorsal and ventral buds and is necessary for their development. The pancreatic epithelium, consisting of multipotent progenitor cells, transforms morphologically to create both exocrine and endocrine components. *PDX1* promotes the expansion and differentiation of pancreatic progenitors in concomitance with NK6 Homeobox 1 *(NKX6.1)*, which is restricted to β cell formation later (Lyttle *et al*, 2008). As the pancreatic epithelium expands, endocrine progenitors begin to commit to specific lineages. A subset of progenitors will transition

to an endocrine fate. The expression of the transcription factor Neurogenin 3 *(NGN3)* and Neurogenic differentiation 1 (*NEUROD1*), key regulators of endocrine differentiation, marks this process (Gu *et al*, 2010; Schwitzgebel *et al*, 2000). The endocrine progenitors then aggregate to form clusters known as islets of Langerhans. Within these islets, different endocrine cell types differentiate, including insulin-producing β cells, glucagon-producing α cells, somatostatin-producing δ cells, pancreatic polypeptide-producing PP cells, and ghrelin-producing ε cells which produce, respectively, the hormones insulin, glucagon and somatostatin, and the pancreatic polypeptide. The β cells undergo further maturation, acquiring the ability to produce and secrete insulin in response to glucose levels. Critical transcription factors such as *PDX1*, MAF BZIP Transcription Factor A *(MAFA), NKX6.1* play significant roles in the maturation and function of β cells (Wang *et al*, 2006). Mature β cells are then functionally integrated into the pancreatic islets, working together with other endocrine cells to regulate blood glucose levels. Understanding these developmental processes is crucial for developing *in vitro* differentiation protocols to generate functional pancreatic β cells from pluripotent stem cells, providing a potential avenue for diabetes treatments, including cell replacement therapies. Mimicking *in vivo* pancreatic development with small molecules and growth factors, stepwise differentiation enables hPSCs to be first induced to definitive endoderm, then specialized into pancreatic progenitors, and finally directed through the pancreatic endocrine progenitor stage to become pancreatic β cells (Hebrok, 2012) (**Figure 5)**.

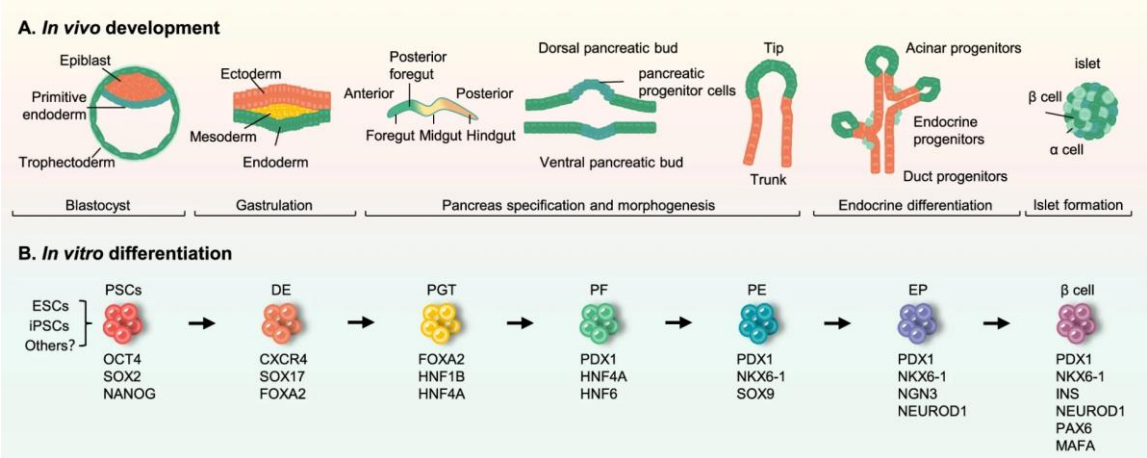


Figure 5. The two faces of β cells development. *The signaling pathways that govern embryonic pancreas development and the differentiation of human stem cells into β cells are intricate and multifaceted. In vivo development: pancreatic cells originate from the definitive endoderm, which forms during gastrulation and subsequently develops into the primitive gut tube. The development*

goes on from the primitive gut to the posterior foregut, by which, from the dorsal and ventral region, arises the pancreatic endoderm composed of pancreatic progenitors. The pancreatic epithelium then expands and differentiates into endocrine progenitor cells, which eventually develop into β cells. In vitro development: various signaling factors are employed to drive the differentiation process from hPSCs to pancreatic β cells. Mimicking the in vivo development, stem cells undergo a series of differentiation steps to form the pancreatic lineage and ultimately generate β cells: Definitive Endoderm (DE), Primitive Gut Tube (PGT), posterior foregut (PF), Pancreatic Endoderm (PE), and Endocrine Precursors (EP) (Jin & Jiang, 2022) .

In 2006, *D'amour et. al* published the first differentiation protocol from hPSC into β cells composed of 5 main stages (**Figure 6**). They established an efficient method with ESC using activin A, WNT3a, and low serum to direct up to 80% of ESCs toward the definitive endoderm lineage. The endodermal cells then differentiate into the primitive gut tube with the help of FGF10 and retinoic acid and are next directed to form the posterior foregut through BMP4 and inhibition of TGF-β signaling, leading to the development of pancreatic progenitors. These progenitors then were expanded and differentiated into pancreatic endoderm under the influence of factors like Noggin and cyclopamine and induced to form endocrine progenitors, marked by *NGN3* expression, and aggregated into islet-like clusters. One limitation was to achieve full maturation of the β cells, especially in the later stage of the protocol where the efficiency decreased. Many derived β cells did not display key markers such as *NKX6.1* and *PDX1*. They were still expressing markers of immaturity with a low ability to respond dynamically to glucose levels and secrete appropriate amounts of insulin (D'Amour *et al*, 2006).

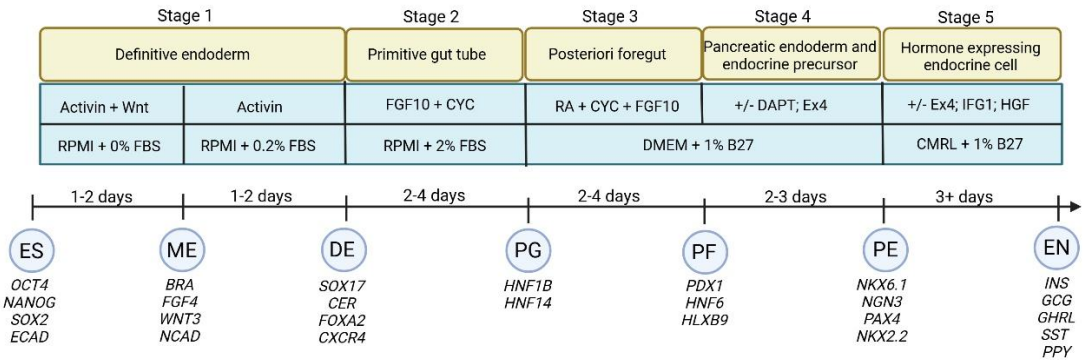


Figure 6. D'Amour et al. differentiation protocol. *The differentiation protocol is divided into five stages and the growth factors, medium, and range of duration for each stage are shown. Several markers characteristic of each cell population is listed. CYC, KAAD-cyclopamine; RA, all-trans retinoic acid; DAPT, γ-secretase inhibitor; Ex4, exendin-4; ES, hES cell; ME, mesendoderm; DE, definitive endoderm; PG, primitive gut tube; PF, posterior foregut endoderm; PE, pancreatic*

endoderm and endocrine precursor; EN, hormone-expressing endocrine cells (created with biorender.com).

In 2008, *Kroon et al.* showed that hESC-derived pancreatic endoderm cells efficiently reverse diabetes in mice after a couple of months. Indeed, the cells differentiate until the endocrine cells stage directly *in vivo* and protect mice against streptozotocin-induced hyperglicemia (Kroon *et al*, 2008). To obtain glucose responsiveness *in vitro*, subsequent protocol refined the differentiation process having differentiated hPSCs into PDX1 and NKX6.1 positive pancreatic progenitors, leading to the generation of β cells. Moreover, the 3D culture system was introduced, mimicking the in vivo environment and improving cell maturation. *Rezania et al.* and *Pagliuca et al.* managed to produce ESC-derived β cells with different levels of functionality: even if the produced cells had lower glucose-stimulated insulin secretion (GSIS) compared to human islets, they had the potential to reverse diabetes in diabetic mice following transplantation. In particular, *Rezania et. al* differentiation process included two more stages compared to the previous differentiation protocol: definitive endoderm (stage 1), primitive gut tube (stage 2), posterior foregut (stage 3), pancreatic endoderm (stage 4), pancreatic endocrine precursors (stage 5), immature β cells (stage 6), and maturing β cells (stage 7) resulting cells expressed key mature β cell markers like MAFA, PDX1/NKX6.1, and INS (**Figure 7**) (Pagliuca *et al*, 2014; Rezania *et al*, 2014).

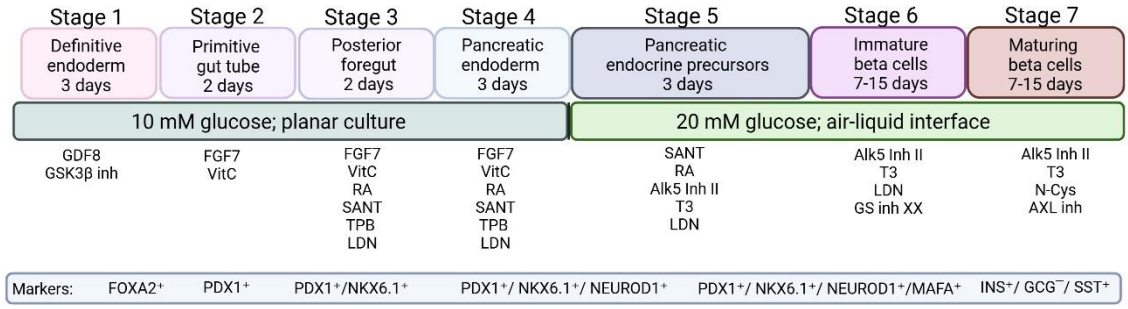


Figure 7. Rezania et al. differentiation protocol. *The differentiation protocol is divided into seven stages and the growth factors, way of culture, and range of duration for each stage are shown. In stage 1 hPSCs are induced into the definitive endoderm stage with Activin A that guides this step with FOXA2 as a marker of success. Stage 2, Stage 3, and Stage 4 involved the foregut endoderm and the pancreatic endoderm formations, achieved with factors like FGF7 and Retinoic acid with PDX1 and NKX6.1 as a marker of success. Stage 5 is the pancreatic endocrine precursors stage, where the cells express high levels of PDX1 and NKX6.1 and then they transition to Stage 6 as immature β cells until the final Stage 7 which focuses on the complete maturation of these cells into functional β-like cells positive for the Insulin marker (created with biorender.com).*

Recent progress has resulted in techniques that generate cells exhibiting more robust and dynamic GSIS. Indeed, *Nair et al*. discovered that isolating INS-positive cells at an early immature stage and then reaggregating them into clusters enhances beta cell maturation and *Velazco-Cruz et al.* found that by selectively modulating TGF-β signaling and resizing cell clusters could improve dynamic GSIS response (Nair *et al*, 2020; Velazco-Cruz *et al*, 2019). A significant advance was made with the optimized differentiation protocol introduced by Otonkoski and colleagues. In 2022, they published a refined method that successfully generated pancreatic islet-like aggregates (SC-islets) from iPSCs exhibiting dynamic glucose-responsive insulin secretion and an endocrine cell composition similar to primary human islets after 44 days of culture. By approximately day 44, the derived SC-islets display dynamic glucose-sensitive functionality. Using this protocol, the endocrine cell composition included around 30-50% β -like cells and 30-50% alpha-like cells, with a small proportion of δ-like cells (approximately 4%) and less than 5% of cells showing a polyhormonal (α/β) identity. This could be because the protocol emphasizes prolonged differentiation periods, allowing cells more time to mature and acquire functional characteristics. Moreover, the protocol includes a critical step where pancreatic progenitors are transferred from a planar culture into microwell plates, facilitating the formation of uniformly sized aggregates. This uniformity ensures consistent sizes and compositions of endocrine progenitor aggregates by excluding non-pancreatic lineages that typically do not re-aggregate after dissociation, promoting the homogeneity of the resulting SC-islets and improving the overall quality and functionality of the resulting beta cells (**Figure 8**) (Barsby *et al*, 2022). The advancements in deriving β cells from hPSCs enhance the potential to restore glucose-responsive insulin secretion in patients with T1D. However, clinical trial outcomes for stem cell therapy in T1DM remain unsatisfactory, with numerous questions and technical challenges still to be addressed: the improvement of β cell differentiation efficiency, the safeguard of the implanted β cells from autoimmune attacks, the generation of a sufficient number of islets for clinical transplantation and achievement of insulin independence. Despite these challenges, stem cell-based therapy for T1DM represents the most advanced approach to curing the disease (Krentz, 2021).

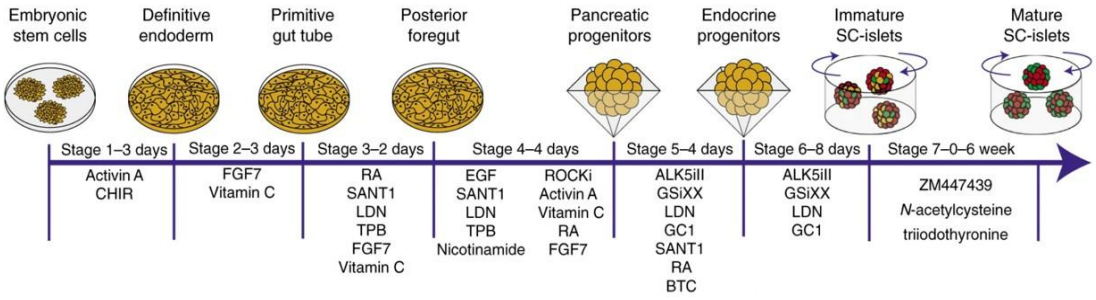


Figure 8. Otonkoski et al. differentiation protocol. *Stage 1 of the protocol is essential for generating a dense layer of definitive endoderm (DE), which will give rise to the posterior foregut and pancreatic lineage identities in subsequent steps. Stages 2 to 4 are also conducted within a planar cell culture environment, during which specific factors are introduced to trigger differentiation from primitive gut tube (Stage 2) to pancreatic progenitor stage (Stage 4). At stage 5, the pancreatic progenitors are transferred from the planar culture into microwell plates. This transition facilitates the formation of uniformly sized aggregates. At stage 6, the aggregates are transferred to a rotating suspension culture. Through further maturation steps, these aggregates gain downstream cellular identities and form SC-islets. The final two stages (Stage 6 and Stage 7) of the protocol maintain and further develop the endocrine progenitor aggregates into terminally differentiated endocrine lineages, stabilizing and functionally maturing the resultant SC-islets* (Barsby *et al*, 2022).

3.2.2. β cell replacement therapy

Transplanting human islets from deceased donors has shown that cell replacement therapy for diabetes is feasible. However, high numbers of islets are needed for successful grafts, often requiring multiple donor pancreases. The limited availability of donor pancreases and the use of cells from multiple donors can increase the risk of immune rejection and graft failure. Additionally, the purification process can damage islets before transplantation. These challenges can potentially be overcome by providing an unlimited supply of insulin-producing cells for transplantation. Stem cell-derived islets (SC-islets) can be generated from a single-cell source using a standardized process, resulting in a well-characterized cell product with predictable transplant outcomes (Hogrebe *et al*, 2023). Recent advancements in stem cell technologies have led to the first human clinical trials using SC-derived pancreatic products. Firstly, ViaCyte starting from hESC, developed an SC-derived pancreatic endoderm population called PEC-01, which matures into insulin-producing endocrine cells *in vivo* in rodent models. To use PEC-01 in human clinical trials, they created a macroencapsulated device to contain the transplanted cells.

These devices containing PEC-01 were called VC-01 and they were implanted subcutaneously without immunosuppressive treatment because of the cell-impermeable membrane of the device. The initial human trial in 2014, included 19 patients which received the implant and it was safe and well tolerated. The device shielded the cells from immune rejection, enabling survival for up to 24 months, though outcomes varied due to a foreign body response. A part from this, were detected islet cell markers, confirming β-cell presence. These findings highlight the device's immune protection, but the trial was blocked due to inconsistent cell survival because of the foreign body response to the encapsulation devices, leading to no insulin secretion in the transplanted patients (HENRY *et al*, 2018). To address this, the PEC-Direct device (PECs) was developed with membrane openings to allow vascularization, enhancing nutrient exchange and cell survival. However, because host cells could penetrate the device, immunosuppression was required post-transplantation. Using PECs, an open-label, first-in-human phase 1/2 study was started in 2017 and it was published a report that presents a one-year data analysis from the first cohort of 15 patients at a single trial site. These results showed that the implanted cells were well tolerated with no teratoma formation. Six months after the implantation, researchers could observe an increase in fasting and glucose-responsive C-peptide levels, along with mixed meal-stimulated C-peptide secretion, but no one reached insulin independence. Moreover, explanted grafts displayed cells with a mature β cell phenotype, immunoreactive for insulin, islet amyloid polypeptide, and MAFA (Ramzy *et al*, 2021). SC-islets have also been transplanted into human T1D patients in a clinical trial by Vertex Pharmaceuticals, starting in 2021. In this trial fully differentiated, allogeneic stem cell-derived pancreatic islets obtained from hESC were transplanted into the liver in 12 patients with T1D through the portal vein and treated with immunosuppression. Patients presented HbA1C ≤7% and >70% time-in-range (70-180 mg/dL), and 11 of 12 patients reduced or eliminated the use exogenous insulin. In particular, this clinical trial is now approved for Phase 3 and is called Zimislecel (VX-880). Are currently enrolled patients with type 1 diabetes (T1D) experiencing severe hypoglycemic events and impaired hypoglycemia awareness across the U.S., Canada, U.K., and EU. The company anticipates completing enrollment and dosing by 2025, with plans to seek approval following one year of insulin-free follow-up, assuming that the data will be positive. Recently, *Wang et. al* presented the results of a first-in-human phase

I clinical trial of autologous transplantation of chemically induced pluripotent stem-cell-derived (CiPSC) islets, transplanted in the abdominal anterior rectus. The patient maintained insulin independence from 75 days post-transplantation onwards without any transplant-related abnormalities after one year from the transplant, suggesting promising results for further clinical studies to evaluate autologous CiPSC islets and transplantation in diabetes (Wang *et al*, 2024b). SC-islets transplantation will also continue to require the use of chronic, systemic immunosuppression, due to the continued vulnerability of these islets to both direct and indirect allorecognition pathways.

In Type 1 Diabetes (T1D), β cell destruction is primarily driven by an autoimmune response mediated by T cells. Thus, the field of islet immunoengineering is focusing on developing strategies to increase the applicability of islet transplantation posing a significant challenge for stem cell-derived β cell therapies. Assessing the impact of diabetogenic T cells on human stem cell-derived β cells is difficult because animal models do not fully replicate human autoimmune conditions. While encapsulation techniques can reduce the risk of $CD8^+$ T cell-mediated cytotoxicity, unencapsulated β cells might achieve better vascularization, leading to higher graft survival rates. One approach to mitigate autoimmune attacks is modifying the transplanted cells to express immune-evasive features. For example, programmed death-ligand 1 (PD-L1) is naturally upregulated in islet transplants and can help suppress T cell activity. Another approach is to engineer β cells to lack HLA class I molecules and overexpress PD-L1 to be less vulnerable to diabetogenic T cells. This highlights the potential for developing stem cell-derived β cells with enhanced resistance to autoimmune responses (Karimova *et al*, 2022). Additionally, in January 2025, the company Sana Biotechnology announced the first-in human study where they provided evidence that their platform, based on hypoimmunogenic human islets, after transplant, evades immune rejection and produces insulin without immunosuppression. Advances in stem cell technology hold promise for diabetes cell therapy as a potential definitive cure. This therapy could benefit a broader patient population, including those with T1D and T2D who are insulin-dependent, as well as individuals undergoing pancreatectomy. However, the accelerated differentiation process in stem cell therapy involves rapidly converting stem cells into specific cell types, such as the β cells, in a shorter time frame than traditional methods. While this can speed up research and potential treatments, it may introduce stress to the cells. Stress can

accelerate cellular aging, reducing the cell's lifespan and functionality after transplantation. Therefore, just as we stand at a crucial moment for diabetes cell therapy marked by the first pioneering clinical experiences and advancements *in vitro* differentiation methods it is of fundamental importance to ensure that the cellular product for transplantation is of high quality, in terms of identity, function, and long-term survival.

3.3 Cellular aging and senescence

Aging can be defined as the gradual, time-dependent decline in the physiological functions and biological processes of an organism. This process leads to the progressive deterioration of the body's cells, tissues, and organs, ultimately impairing an individual's ability to maintain homeostasis, adapt to stress, and recover from injuries. Over time, there is an accumulation of damage in cellular components such as DNA, proteins, and lipids leading to decreased cellular efficiency and increased risk of disease. Living organisms are constantly exposed to external and internal agents that cause damage, but, when aging occurs, the repair mechanisms fail, leading to the accumulation of tissue damage and accelerated aging (Gorbunova *et al*, 2007). Since the repair mechanisms fail, somatic mutations can occur and persist over time, leading to cellular dysfunction, tissue degeneration, and an increased risk of diseases such as cancer. However, the underlying mechanisms of aging are complex and challenging to define. For this reason, researchers have identified cellular and molecular mechanisms linked to aging: cellular senescence is considered as a central hallmark in the aging process (Dodig *et al*, 2019; Ren *et al*, 2024). Cellular senescence is a state in which cells permanently lose their ability to divide and proliferate, while remaining metabolically active. The discovery of cellular senescence was first described in 1961 by Hayflick and Moorhead, who observed that primary human fibroblasts *in vitro* ceased to divide after approximately 50 cycles suggesting a link between senescence and aging. Subsequent findings, revealing that senescent cells accumulate in aged tissues, have reinforced the hypothesis that senescence itself can drive the aging process. Initially, the discovery that cells have a limited capacity to proliferate suggested that cellular senescence acts as a protective mechanism, preventing uncontrolled cell growth and serving as a barrier to cancer development. Now, senescence is recognized as a multifaceted phenomenon with various roles in tissue homeostasis,

regeneration, and pathology. Senescence also plays crucial physiological roles during normal development, working alongside apoptosis to facilitate embryonic morphogenesis. In adult tissues, senescence is primarily triggered in response to cellular damage, acting to suppress potentially dysfunctional, transformed, or aged cells. However, the accumulation of senescent cells with age can have detrimental effects (Mansfield *et al*, 2024; McHugh & Gil, 2018). The pathway of cellular senescence is a complex process involving multiple triggers and signaling cascades. Various stressors can lead to cellular senescence, with nuclear DNA damage being a common underlying cause. This typically involves DNA double-strand breaks (DSBs) that trigger the DNA damage response (DDR) pathway. When DSB occurs, the histone protein H2AX becomes phosphorylated at the serine 139 residue, resulting in a form known as γH2AX. This phosphorylation is a rapid and sensitive marker of DNA damage. Moreover, DNA damage leads to the activation of the kinases ATM and ATR. These sensors then activate the Tumor suppressor p53 (*TP53*) pathway, leading to the expression of *p21*, a cyclin-dependent kinase inhibitor (CDKI) that halts cell cycle progression and a crucial mediator of senescence-associated cell cycle arrest. Another key player for cell cycle arrest is *p16*, a CDK4 and CDK6 inhibitor, which becomes active later in senescence to help maintain the senescent state. In particular, *p16* leads to hyperphosphorylation of the retinoblastoma (Rb) protein which binds to E2F transcription factors, preventing the transcription of genes required for cell cycle progression. When DNA damage is not repaired, it results in prolonged DDR signaling and extended cell cycle arrest, leading to cellular senescence. Another form of DDR that can lead to cellular senescence is telomere shortening. The role of telomeres, the protective caps at the ends of chromosomes, is particularly significant. During DNA replication, each cell loses between 50 and 200 base pairs from the telomeres because DNA polymerase cannot replicate the very ends of chromosomes. As telomeres shorten over successive cell divisions, they eventually reach a critical length where they can no longer adequately protect chromosome ends. When this happens, the exposed chromosome ends resemble DNA DSBs. This triggers a DDR, which activates various cellular pathways that halt the cell cycle, preventing further division. Oncogene-induced senescence (OIS) is driven by the overexpression of oncogenes and the inactivation of tumor suppressor genes. Oncogenes are mutated versions of normal genes, known as proto-oncogenes, which regulate essential cellular functions under normal

conditions. However, when these genes are mutated or overexpressed, they initiate a period of rapid cell proliferation. Examples of oncogenes that can induce OIS include *RAS*, *BRAF*, and *MYC*. This rapid proliferation causes DNA replication stress, leading to errors and damage during DNA replication. Excessive proliferation stretches the cellular machinery, resulting in DSBs leading to DDR response and cell cycle arrest. In this context, reactive oxygen species (ROS), which accumulate in tumors, not only damage DNA but also function as signaling molecules that enhance the effects of oncogenes. Indeed, it was discovered that ROS generated by NADPH oxidases can induce cellular senescence by intensifying the initial hyperproliferative phase of OIS and associated DNA damage (Mylonas & O'Loghlen, 2022; Di Micco *et al*, 2020). All these triggers cause specific senescence features. As described before, the prolonged cell cycle arrest mediated by *p53/p21* and *p16/pRB* plays essential roles in maintaining the senescence phenotype. In particular, *p21* plays a crucial role in initiating cell cycle arrest and is one of the key targets of *p53* transcriptional activity in senescent cells. The *p21*-induced cell cycle arrest serves as a temporary safeguard for cells with low to moderate levels of damage, preventing their progression into the S-phase under conditions that are not conducive to DNA replication. If the damage is successfully repaired, cells can resume their cell cycle. However, if the arrest is prolonged, it leads to the upregulation of *p16*, which subsequently activates the transcriptional regulator Rb, ensuring a more permanent cell cycle arrest (Stein *et al*, 1999)(**Figure 9**).

Oxidative stress is a significant factor in inducing cellular senescence. ROS are natural by-products of normal oxygen metabolism and regulate several physiological functions such as signal transduction, gene expression, and cell proliferation. The major sources of ROS in cells include mitochondria, cell membranes, and the endoplasmic reticulum. Oxidative stress occurs when there is an imbalance between oxidants and antioxidants leading to structural damage to macromolecules like DNA, proteins, and lipids. An increase in lifespan is often associated with low ROS concentrations, whereas high ROS concentrations can promote the maintenance of the senescent phenotype. This involves responses to DNA damage, epigenetic regulation, and the activation of tumor suppression pathways (Dodig *et al*, 2019)(**Figure 9**).

Senescent cells often become larger and more flattened compared to their proliferating counterparts. This change in morphology is due to alterations in the cytoskeleton and cell

membrane dynamics, with a nucleus that may show structural abnormalities, such as an enlarged and irregular shape. Additionally, during senescence there is extensive chromatin reorganization. Senescence-associated heterochromatin foci (SAHF) are formed because of this reorganization, leading to the clustering of chromatin into dense foci. SAHF contributes to stable cell cycle arrest by silencing proliferation-promoting genes, maintaining the senescent phenotype by stabilizing the chromatin structure in the absence of DNA replication (Aird & Zhang, 2013).

Among the various biomarkers used to identify senescence, senescence-associated β-galactosidase staining (SA-β-Gal) is the most widely employed enzymatic method. This enzymatic assay leverages the increased lysosomal β-galactosidase activity observed in senescent cells. SA-β-Gal refers to the increased activity of the lysosomal enzyme β-galactosidase at a suboptimal pH (typically pH 6.0) in senescent cells. This contrasts with normal β-galactosidase activity, which is typically detected at a more acidic pH of around 4.0. This is due to the increased accumulation of damaged macromolecules that need to be degraded. Specifically, to detect it, lysosomal β-galactosidase catalyzes the hydrolysis of the soluble chromogenic substrate 5-bromo-4-chloro-3-indoyl β-D-galactopyranoside, producing an insoluble blue product. SA-β-Gal is a robust marker to detect the senescence phenotype, but it may not detect all types of senescent cells, as some cells may not exhibit increased β-galactosidase activity or sometimes accumulate in serum-starved or overconfluent cells, leading to potential false positives. For this reason, it is important to take in consideration a large number of senescence features (Muthamil *et al*, 2024) (**Figure 9**).

Another feature is the high resistance to apoptosis. Indeed, senescent cells often up-regulate anti-apoptotic members of the *BCL-2* family, such as *BCL-2* and *BCL-XL*. These proteins inhibit the pro-apoptotic factors *BAX* and *BAK*, preventing the release of cytochrome C from mitochondria, which is crucial for the initiation of the apoptotic cascade. Additionally, in the senescence phenotype, there is the activation of alarmins, which are proteins produced within cells released in response to tissue stress or damage. One of the most notable alarmins is the high-mobility group box 1 (HMGB1) protein, which functions as a structural chromatin-binding factor by interacting with histones and transcription factors. When cells are stressed, HMGB1 swiftly moves to the cytoplasm and is then secreted into the extracellular space, where it affects surrounding cells. The

release of HMGB1 from the nucleus to the cytoplasm is one of the early indicators of senescence and can be detected *in situ* (Ogrodnik *et al*, 2024).

3.3.1. Senescence-associated secretory phenotype

Senescent cells remain metabolically active and are commonly present in tissues undergoing chronic inflammation or frequent regeneration. They actively release a variety of signaling molecules to interact with and influence neighboring cells. The acquisition of the Senescence-Associated Secretory Phenotype (SASP) drives the secretory activity of senescence cells. The primary function of SASP is to induce the elimination of senescent cells. However, in the absence of efficient clearance, as seen in older individuals, senescent cells accumulate, leading to structural, degenerative, and irreversible tissue damage and fibrosis. Chronic senescence, driven by prolonged cellular stress or gradual macromolecular damage, involves complex effector pathways distinct from those in acute senescence, due to the heterogeneity of SASP factors and the high resistance of senescent cells to immune clearance. This chronic state has detrimental effects on cells and tissues. Essentially, SASP enables senescent cells to communicate with nearby cells by releasing inflammatory signals in a paracrine manner leading the cells around to enter senescence. The SASP consists of various factors: cytokines, chemokines, growth factors, metalloproteases, and extracellular vesicles (EVs). The primary cytokine in the SASP process is the pro-inflammatory IL-6, driven by sustained DNA damage in cells like keratinocytes, melanocytes, and epithelial cells. Another key interleukin upregulated in senescent cells is IL-1, with both IL-1α and IL-1β being overexpressed across different cell types. SASP profile includes soluble molecules such as growth factors (e.g., IGFBPs, VEGFs, PDGFs, HGFs) and interleukins. In addition to pro-inflammatory factors, senescent cells also secrete enzymes involved in ECM remodeling, such as matrix metalloproteinases (MMPs), particularly MMP1, MMP3, and MMP9, as well as serine/cysteine proteinase inhibitors (SERPINs) and tissue inhibitors of metalloproteinases (TIMPs). However, the specific composition of SASP widely varies depending on the cell type, tissue context, and the stimuli that triggered senescence. This variability is essential for the diverse roles that SASP plays in different physiological and

pathological processes (González-Gualda *et al*, 2021; Bulbiankova *et al*, 2023) (**Figure 9**).

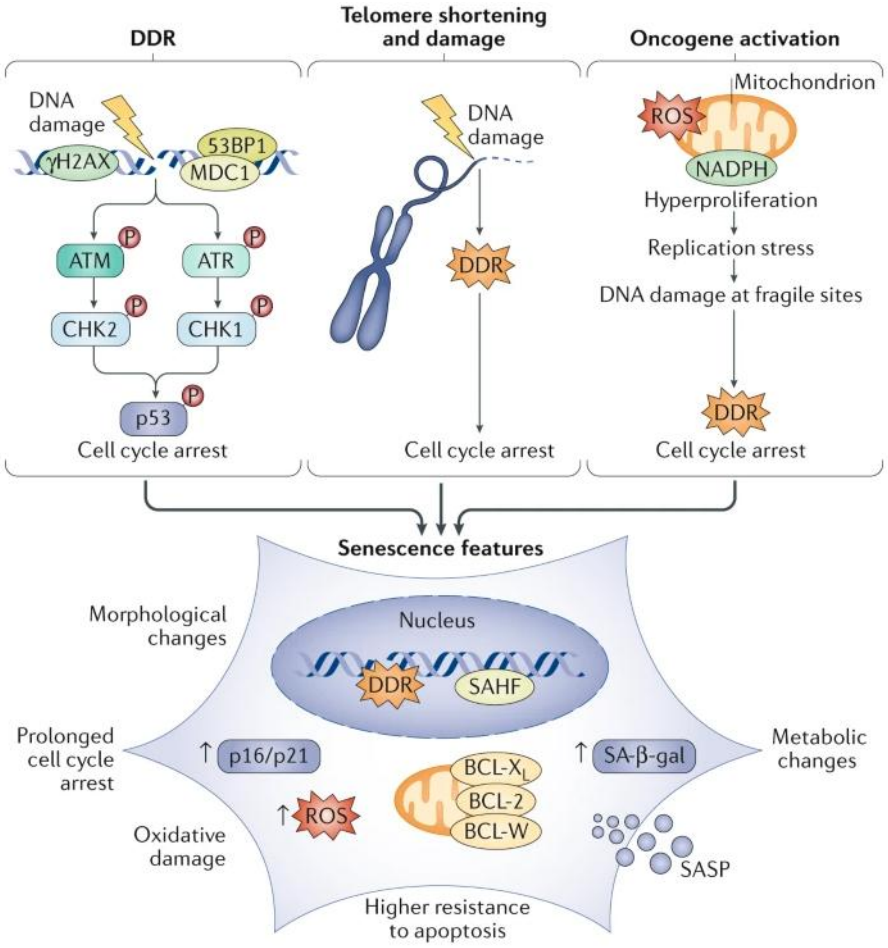


Figure 9. Triggers and features of cellular senescence. *When DNA damage occurs, it activates the DDR that involves proteins such as γH2AX, 53BP1, and MDC1. These signals lead to the activation of the kinases ATM, ATR, CHK2 and CHK3 that ultimate the activation of p53, initiating the cell cycle arrest. DDR could also be activated through telomere shortening and damage, and oncogene activation. Activated oncogenes, often through the production of reactive oxygen species (ROS), cause hyperproliferation and altered DNA replication, leading to replication stress and DNA damage at fragile sites, including telomeres. With prolonged DDR activation, there is the establishment of cellular senescence. Cellular senescence is characterized by several features: cell cycle arrest with the upregulation of p16 and p21, oxidative damage with the increase of ROS production, resistance to apoptosis and metabolic changes with higher β galactosidase activity and the secretion of SASP factors* (Di Micco *et al*, 2020).

3.3.2. Physiological and pathological role of senescence

Cellular senescence plays several important physiological roles in the body, contributing to various processes that are essential for maintaining health and preventing disease. Cellular senescence acts as a critical tumor suppression mechanism by preventing the proliferation of cells that could potentially become cancerous. The irreversible cell cycle arrest in cells undergoing OIS makes this mechanism particularly effective in preventing tumor formation following oncogene activation. It is a natural defense against tumor formation by causing a stable growth arrest in premalignant cells, reinforced by cyclin-dependent kinase inhibitors like p16 and p21. Moreover, senescent cells release SASP that could contribute to tumor suppression in an extrinsic manner enhancing immune surveillance, leading to the clearance of senescent cells (Burton & Krizhanovsky, 2014). SASP factors can also induce paracrine senescence or a stable growth arrest in nearby cancer cells. It was shown that OIS plays a crucial role in preventing the development of lymphoma and enhancing therapeutic responses: it is indicated as therapy-induced senescence (TIS) in tumors. In transgenic mice engineered to bypass the senescence response to oncogenic N-Ras, invasive T-cell lymphomas developed, whereas control mice only developed non-lymphoid neoplasms in a later stage. In another study, combining inhibitors of MEK and CDK4/6 has been shown to effectively induce cellular senescence and activate an NF-κB-driven SASP in a Kras-mutant mouse model of lung cancer: SASP components TNFα and ICAM1 triggered NK cell-mediated immunosurveillance, contributing to tumor regression. Therefore, targeting key factors that regulate innate or adaptive immune responses is a promising approach to enhance the clearance of premalignant OIS cells and prevent tumor progression (Schmitt *et al*, 2022).

In addition to their role in tumor suppression, senescent cells may also have beneficial effects in non-cancerous conditions by limiting tissue fibrosis and promoting tissue healing. When tissue damage occurs, certain cells in the affected area enter a state of senescence. These senescent cells, while no longer dividing, are metabolically active and secrete SASP factors: by balancing the inflammatory response and preventing excessive cell proliferation, senescence ensures that damaged tissues are effectively repaired and returned to a healthy state. It was shown that hepatic stellate cells (HSCs) can become senescent in the liver following activation and hyper-proliferation. Senescent HSCs reduce the secretion of ECM components and increase the secretion of ECM-degrading

enzymes, which helps to limit the formation of fibrotic scars (Sagiv *et al*, 2012). Moreover, *Demaria et al.* developed a BAC transgenic mouse model called p16-3MR to detect, isolate, and selectively eliminate senescent cells in living animals. They found that senescent fibroblasts and endothelial cells appeared at wound sites shortly after skin injury. Eliminating these senescent cells delayed wound closure, with the most significant delay occurring six days post-injury. The senescent fibroblasts at wound sites enhance healing by secreting platelet-derived growth factor (PDGF-A), a SASP factor that promotes myofibroblast differentiation and speeds up wound closure (Demaria *et al*, 2014). In cutaneous wound healing, *Jun et al.* revealed that during skin repair the communication network factor 1 (*CCN1*) is dynamically expressed at wound repair sites and can induce fibroblast senescence through an oxidative stress mechanism, associated with an increased DNA damage response and activation of the *p53* and RAC1–NOX1 complex. In particular, CCN1-induced senescent cells prevent excessive fibrosis, whereas mice expressing a senescence-defective *CCN1* mutant show elevated fibrosis. Additionally, they also demonstrated that topical application of another *Ccn* family member, *CCN2*, also induced senescence and reduced fibrosis in skin wounds in mice (Jun & Lau, 2010, 2017). Furthermore, highly concentrated trehalose induces SA-β-gal activity in fibroblasts via the *p21* pathway, upregulating various factors like dermapontin, fibroblast growth factor 2 (FGF2), epiregulin, vascular endothelial growth factor (VEGF), and angiopoietin-2. These factors lead to angiogenesis and keratinocyte proliferation, promoting repair in a living skin equivalent (Muto *et al*, 2023).

Cellular senescence has recently been recognized as playing a significant role in embryonic development. These studies were first done on mouse embryos, and then also observed in humans and chickens. Researchers explored the essential role of cellular senescence during mammalian embryogenesis. They found that senescence occurs in multiple embryonic structures, including the mesonephros, endolymphatic sac, and apical ectodermal ridge (AER). In these structures, they confirmed senescence not only by SA-β-Gal staining but also by markers such as Ki67 to confirm the absence of proliferation, increased heterochromatin markers, and elevated expression of cell cycle inhibitors such as *p15, p21*, and *p27* (Storer *et al*, 2013). Overall, researchers demonstrated that senescence in development is a process that is controlled by the cell cycle inhibitor p21, independent of DNA damage, but controlled by TGFβ–SMAD and PI3K–forkhead box

protein O (*FOXO*) pathways, leading to the secretion of growth factors and signaling molecules, such as FGF4 and FGF8, which contribute to tissue patterning and morphogenesis (Muñoz-Espín *et al*, 2013). Considering the physiological roles of senescence, the development in embryo is guided by reciprocal signaling between secreted factors, such as *TGF*β, and is mediated by *p21*. Once the cells enter in senescence, they start to secrete SASP factors, inducing functional changes in neighboring cells, affecting patterning, plasticity, proliferation, angiogenesis, and epithelial-mesenchymal transition. Moreover, SASP factors release a mixture of cytokines to recruit immune cells, like macrophages and NK cells. Indeed, once senescent cells have played their role during development, they are cleared from the developing embryo by immune cells. This removal eliminates the source of damage and SASP in stress or damage situations. In general, the physiological role of senescence seems to involve a temporary surge during the initial stages of development and regeneration, followed by prompt removal. In contrast, pathological senescence is marked by a long-lasting buildup after tissue damage. In chronic and disease conditions, the clearance of senescence is diminished, creating an amplifying loop of senescence and paracrine instruction. The increased number of senescent cells amplifies or alters the SASP with a prolonged secretion of ECM-modifying factors that can change tissue structure, contributing to age-related declines in tissue renewal and increased fibrosis. The role of SASP in inducing plasticity or dedifferentiation persists in aging, and this could lead to more tumor-initiating stem cells at risk of transformation. Aging tissues fail to clear senescent cells effectively due to increased production of SASP factors, immune system dysfunction and clearance, or altered recognition, leading to more senescent cells and elevated SASP (Rhinn *et al*, 2019) (**Figure 10**).

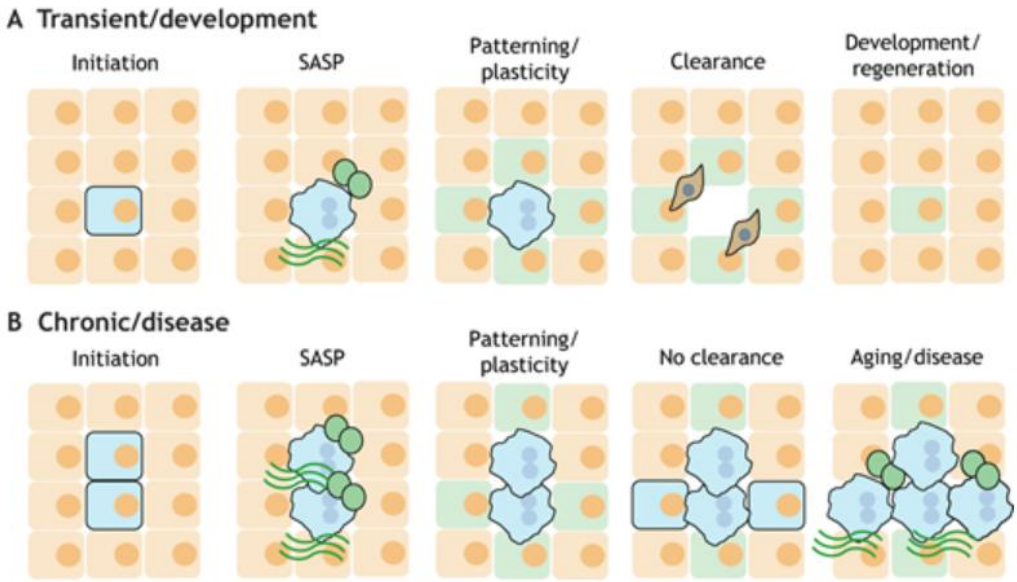


Figure 10. Physiological and pathological conditions of senescence. *In physiological conditions, senescence is transient because senescent cells are cleared, and it is a fundamental process for development and regeneration. Meanwhile, in pathological conditions senescence is not transient but persists with no clearance of senescent cells, leading to aging and senescence-related disease* (Rhinn *et al*, 2019).

For this reason, senescence is considered detrimental in different conditions. Cellular senescence can paradoxically contribute to tumor development through several mechanisms. One key factor is the release of SASP factors, which can initially help in recruiting immune cells to clear senescent cells but can also create a pro-tumorigenic environment. SASP in fact can alter the tumor microenvironment (TME), allowing senescent cells to alter the TME and encouraging more aggressive cancer traits. Persisting senescent cells in the TME can also foster tumor growth, drive metastasis, and lead to therapy resistance. Moreover, persistent senescent cells can evade immune surveillance, allowing tumor cells to escape detection and destruction (D'Ambrosio & Gil, 2023; Dong *et al*, 2024). It was shown from different studies that the accumulation of reactive oxygen species in senescent cells may promote stem cell aging and exhaustion. Aged human MSC present oxidative damage with high ROS levels, and increased *p21* and *p53*, suggesting a loss of MSC fitness with age. *Vilas et al.* utilized a mouse model with depletion of *SOX2*$^{+}$ stem cells, and, following a period of repetitive depletion of this stem cell population, they observed signs of premature aging in the mice with increased kyphosis, hair graying, and reduced fat mass. Another group presented a study where mice

hematopoietic stem cells (HSCs) with a high level of ROS were exhausted with bad self-renewal potential compared to the low level one, presenting elevated expression of activated *p38 MAPK* and *mTOR* (Oh *et al*, 2014; Vilas *et al*, 2018). In support of this, it is important to mention the chronic inflammation caused by the release of SASP factors by senescent cells. Indeed, in this condition immune cells are crucial for recognizing and eliminating senescent cells, but if this persists, they can also be affected by SASP, leading to a condition called "immunosenescence". This condition will diminish their function and ability to remove senescent cells and inflammatory substances, perpetuating a harmful cycle of inflammation and senescence. Continuous high levels of inflammation in organs like bone marrow, liver, and lungs lead to organ damage and diseases associated with aging. For example, it was shown that in mice, senescence can interfere with the normal migration of neutrophils across epithelial layers in injured tissues via a CXCL1-dependent mechanism, which leads to irregular neutrophil movement and causes damage to distant organs (Li *et al*, 2023). *Yousefzadeh et al.* worked with a mouse model with the ERCC1 gene deletion, which is crucial for DNA repair. In this model, senescent macrophages presented a significant rise in SASP factors release such as TNF-α, IL-6, and IL-1β and showed a marked increase in the expression of cell-cycle checkpoint inhibitors *p16* and *p21*, exhibiting reduced glycolysis and mitochondrial oxidative phosphorylation that reduced their functionality (Yousefzadeh *et al*, 2021).

All the diseases whose pathogenesis is related to cellular senescence are called "senopathies". Senopathies encompass a range of conditions, including cardiovascular, metabolic, musculoskeletal, liver, kidney, and lung diseases, as well as neurodegeneration. For example, in the context of osteoarthritis, senescent chondrocytes and adipocytes release inflammatory factors, contributing to cartilage degradation and inflammation (Surmachevska & Rubio, 2024). Extensive research indicates that cellular senescence contributes to the onset and progression of cardiovascular diseases, such as atherosclerosis. Atherosclerosis, characterized by the presence of plaques in larger arteries, accounts for nearly 30% of global deaths. Markers of cellular senescence have been found in both endothelial cells and vascular smooth muscle cells within atherosclerotic plaques in experimental mice, as well as in the vessel walls of patients with the disease (Grootaert, 2024). In a neurodegenerative context, there is increasing evidence that senescence could be linked to Alzheimer's disease and Parkinson's disease

(Wang *et al*, 2024c). Moreover, in lung tissues from patients with chronic obstructive pulmonary disease (COPD) and idiopatic pulmonary fibrosis were found biomarkers of senescence with the upregulation of *p53, p21* and *p16*. Additionally, in a mouse model of COPD, an elevated expression of pro-inflammatory cytokines such as MCP-1, KC, MIP-1α, IL-12 and G-CSF was found (Aghali *et al*, 2022). With aging, the accumulation of dysfunctional senescent β cells is likely to contribute to impaired glucose tolerance and the onset of diabetes. However, limited attention has been given to the specific role of β cell aging and senescence in diabetes, and the precise SASP profile of β cells remains to be elucidated.

3.3.3. β cell aging

Numerous human studies consistently report an age-dependent decline in β cell function in the context of type 2 diabetes (Basu *et al*, 2003). Indeed, different studies performed on islet cells revealed that islet from young donors exhibited significantly higher glucose-stimulated insulin secretion (GSIS), both static and dynamic, with an age-dependent loss of insulin secretion (Ihm *et al*, 2006). Moreover, in one study, islets from old and young donors were transplanted in diabetic mouse model, and 96% of recipients who received islets from younger donors reversed diabetes, compared to 68% of those who received islets from older donors (Gregg *et al*, 2016). Apart from *in vitro* measurement, this decline was also observed in a Chinese study, where an oral glucose tolerance test was performed in 32,245 subjects without diabetes, divided in three groups on age basis: 20-39 (young age), 40-59 (middle age), and more or equal to 60 years (old age). This study revealed variations in insulin insufficiency across different age groups, with poorer insulin secretion and better insulin sensitivity in the old group (Xiao *et al*, 2014).

In the past, β cells were considered as a single population, whereas recently it has been proposed that four distinct subtypes of human β cells exist, expressing varied profiles, as well as unique basal and GSIS patterns. *Dorrel et al.* showed that this heterogeneous distribution is significantly altered in type 2 diabetes with one subtype much more prevalent exhibiting higher basal insulin secretion and reduced response to glucose stimulation (Dorrell *et al*, 2016).

Following this study, *Aguayo-Mazzucato et al.* proposed that β cells exhibit different markers and functional properties at various stages of life, contributing to the development of T2D. They found typical aging markers in β cells such as *p16*, *p53*, and SA-β-Gal. In addition, they also discovered new aging markers including *IGF1R*, *CD99,* and *BAMBI*, which correlated with age and dysfunction. These new markers exhibited significant variability both within and between islets in the pancreas of mice and humans, confirming a heterogeneous distribution of β cell aging markers (Aguayo-Mazzucato *et al*, 2017). Regarding the *Igf1r* marker, this was also confirmed when two mouse models with diminished IGF1/IGF1R signaling presented suppressed cellular senescence and enhanced glucose tolerance. Moreover, to determine if metabolic stress could trigger cellular aging regardless of chronological age, they administered to 7-months-old C57BL/6J mice the insulin receptor antagonist S961. They discovered that this acute induction of insulin resistance led to increased expression of aging markers, shedding light on how metabolic stress might accelerate β cell dysfunction and decline (Iwasaki *et al*, 2023b).

Later on, *Aguayo-Mazzucato et al.* isolated senescent (β-Gal$^+$) β cells from 7-8-months-old mice and observed downregulation of critical β cell identity genes, including *INSULIN*, *MAFA*, *NKX6.*1, and *PDX1*, compared with non-senescent (β-Gal$^-$) β cells. Simultaneously, there was an upregulation of genes typically repressed in β cells, known as "disallowed genes", such as *LDHA* and *CATALASE*. This "fate drift" phenomenon reflects age-related transcriptional instability and endocrine cell reprogramming, potentially contributing to β cell dysfunction with aging (Aguayo-Mazzucato *et al*, 2019).

Besides, researchers have explored age-related changes in β cell proliferation capacity and components of stimulus-secretion coupling as potential factors contributing to senescent β cell dysfunction, finding a reduction in the expression of genes related to glycolysis, cellular depolarization (ATP-dependent K^+ channels, chloride channels, cation channels, voltage-gated calcium channels, and sodium channels), incretin pathway receptors, and the components of insulin granules (Westacott *et al*, 2017) (**Figure 11**).

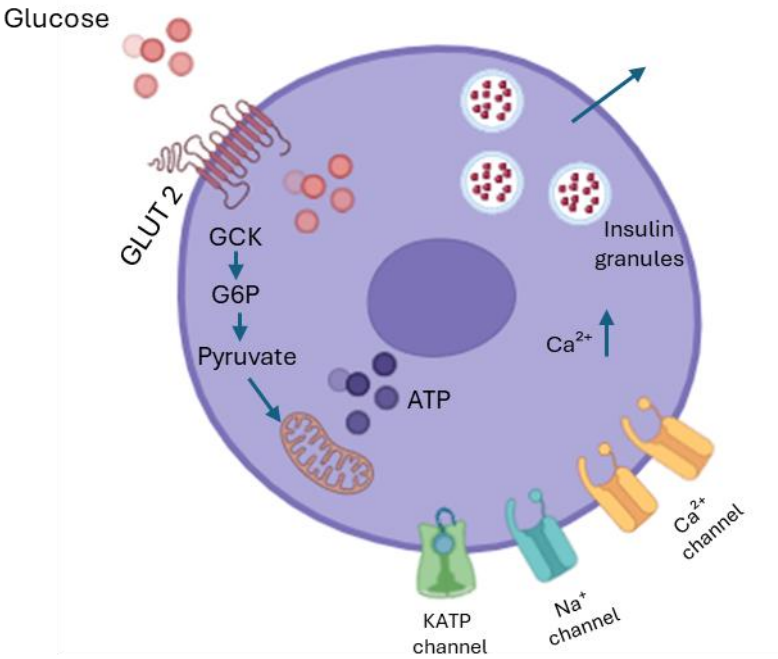


Figure 11. Functional release of insulin. *Glucose enters the pancreatic β cells through the glucose transporter GLUT2. Inside the cell, glucose is then metabolized through glycolysis: glucose is first phosphorylated to form glucose-6-phosphate (G6P) and then used to produce pyruvate, yielding on the production of ATP. The rise in ATP levels causes a higher ATP/ADP ratio in the cells, leading to the closure of ATP-sensitive potassium (KATP) channels. This closure results in membrane depolarization that opens the Na^+ and Ca^{2+} channels allowing calcium influx that triggers exocytosis of insulin-containing secretory granules (**created with biorender.com**).*

Another important feature of insulin secretion is mitochondrial activity. *Gregg et al.* explored this with a novel assay using NAD(P)H fluorescence lifetime imaging (FLIM) to directly visualize islet metabolism, finding that decreased mitochondrial activity is a key factor in the age-related reduction of insulin secretion in human and mouse islets. Additionally, using a novel bioenergetic workflow, it was found that T2D β cells present a shift in bioenergetic control because of responsiveness to elevated glucose levels due to diminished glucose metabolism rates before entering the TCA cycle and increased sensitivity to reduced ATP demand. Furthermore, the same study revealed higher mitochondrial oxidative stress in T2D β cells at both low and high glucose concentrations suggesting that the dysfunction is localized within the mitochondria, rather than resulting from upstream metabolic impairments (Gregg *et al*, 2016; Gerencser, 2015).

In 2021, a study was published where a SASP signature was identified in β cells, characterized by the secretion of factors linked to inflammation, cellular stress response, and ECM remodeling. They used both single-cell transcriptomic and proteomic analysis and defined the cell SASP using conditioned media from mouse, human senescent β cells, and a chemically induced-senescent mouse model of DNA damage. Their time-course experiments suggested that *p21* may act as an initial driver of β cell senescence and was linked to the transcription of β cell SASP factors *GSTP1*, *GDF15*, *DUSP3*, and *HSP90AA1*, while *p16* could help to maintain this state.

This study shed light on the fact that SASP in β cells is not just a mix of immune inflammatory molecules but is a much more complex secretome. In particular, β-cells from different individuals uniformly upregulate harmful SASP factors when aging and senescence occur. In T2D donors, similar changes in SASP secretion and transcriptome were observed, supporting the role of β cell senescence in the disease's pathology (Midha *et al*, 2021).

Another emerging novel mechanism of β cell failure is β cell dedifferentiation, a process in which β cells lose their differentiated state and revert to a progenitor-like stage or even reprogram into other endocrine cell types. It was initially observed in 1999, where *Jonas et al.* showed that chronic hyperglycemia leads to the loss of β cell identity and function in rats by decreased expression of key genes and transcription factors involved in insulin secretion and differentiation (Jonas *et al*, 1999). Lately, this was confirmed in β cell-specific Forkhead box O1 (*FoxO1*) deficient mice and has also been noted in mouse models of obesity and T2D (Talchai *et al*, 2012). Human studies have confirmed the existence of β cell dedifferentiation in T2D, marked by an increase in hormone-negative/chromogranin A-positive endocrine cells in islets. Interestingly, the gene profiles of senescent rodent β cells were found to resemble those of dedifferentiated β cells, suggesting a potential link between senescence and dedifferentiation. These findings suggest that accelerated β cell senescence, reflecting cellular aging, contributes to declining glucose metabolism (Cinti *et al*, 2016; Aguayo-Mazzucato, 2020).

Adipose tissue senescence plays a significant role in the development and progression of T2D. As we age, adipose tissue can become dysfunctional and accumulate senescent cells secreting SASP factors and leading to chronic inflammation and insulin resistance.

Studies have shown that senescent adipose cells exhibit increased markers of senescence, such as *p16* and *p21*, and reduced expression of genes involved in insulin signaling, like PPAR-γ and GLUT4 (Gustafson *et al*, 2022). This dysfunction in adipose tissue can exacerbate metabolic disturbances and promote the progression of T2D. To confirm this, several different models where senescence was cleared were studied, discovering that obesity-related metabolic dysfunctions like T2D were alleviated (Murakami *et al*, 2022). The hypothesis that cellular senescence could also be involved in the development of T1D is emerging. Indeed, during T1D development, some β cells respond to DNA damage by entering in a state of senescence. Senescence features, in particular the role of SASP factors on the islet microenvironment and the immune system, shed light on the role of senescent β cells in the pathogenesis of T1D. In 2019, *Thompson et al.* used both human T1D and non-obese diabetic (NOD) mice models to demonstrate, with transcriptomic and proteomic analysis, that β cells present hallmarks of DNA-damage-induced senescence and SASP in the prediabetic stage. This SASP could trigger an autoimmune response, drawing more self-reactive lymphocytes to invade the islets (insulitis) and destroying additional β cells, creating a cycle that leads to T1D onset. Moreover, the senescent β cells presented an upregulation of the anti-apoptotic gene *Bcl-2*, marking their entry in senescence. Treating preclinical mouse models with anti-apoptotic treatment showed the elimination of senescent β cells, halting the immune-mediated destruction and preventing the pathogenesis of T1D (Thompson *et al*, 2019).

In a recent review, the role of senescence in modifying extracellular vesicles (EVs) from β cells and its implication in T1D were also discussed. This review proposes that the SASP factors released by senescent β cell in T1D may alter the release of autoantigens and the miRNA profiles of β cells EVs, promoting inflammation and immune responses within the pancreatic islets (Motlagh *et al*, 2024). The observation that aged β cells exhibit elevated insulin secretion under baseline (low glucose) conditions, with little increase in response to high glucose, suggests that senescence may negatively impact glucose homeostasis, potentially contributing to chronic reductions in insulin sensitivity. In particular, patients with insulinomas display unregulated basal insulin secretion, leading to secondary insulin resistance (Helman *et al*, 2016a). However, these findings are in contrast with the beneficial effect of senescence in diabetes. Indeed, it was found that senescence could be activated when β cells encounter significant stress and help to switch

on mechanisms to survive. Disruption of the unfolded protein response (UPR) mediators in β cells of T1D mouse model before insulitis, induces the *p21* senescence phenotype and modifies the secretome, enhancing the recruitment of M2 macrophages to islets. The recruited M2 macrophages stimulate anti-inflammatory responses and immune surveillance, slowing the autoimmune β cell loss rate and preventing diabetes (Lee *et al*, 2023).

A lot of effort was given to study the expression of *p16* in β cells. *Helman et al.* showed that *p16* in β cells has significant importance in maturation and development rather than being a stress response. They observed that activating *p16* in transgenic mice models determined an increase in GSIS, and this was confirmed in diabetic mice where the induction of *p16* resulted in better glucose regulation. In particular, β cells expressing *p16* present typical signs of senescence, such as cell enlargement and increased glucose uptake and mitochondrial activity, which was related to the boost of insulin secretion. Additionally, they induced *p16*-driven senescence in a human β cell line (EndoC-βH2) and this process enhanced insulin secretion, showing that this process was partly dependent on the activity of the mechanistic target of rapamycin (mTOR) and peroxisome proliferator-activated receptor (PPAR)-γ proteins (Helman *et al*, 2016b). Later on, in another interesting work, single-cell transcriptomic data of 31 adult islet donors were analyzed: data showed that $p16^{+}$ cells present senescence signatures such as *p21* and *p53* upregulation and, at the same time, were enriched for genes of β cell maturation such as *MAFA*, *NKX6.1*, and *SIX3*. Interestingly, senescent human β cell like (EndoC-βH3) presented a downregulation of proliferation genes and, at the same time, an increase of β cell maturation genes such as *MAFA*. In this model and human islets, inflammatory SASP factors were almost absent but an upregulation on HLA-I levels in response to IFNα treatment was observed, suggesting that senescent β cells presents higher immunogenicity (Patra *et al*, 2024). These data raised the possibility of a novel functional role for senescence in β cells.

3.3.4. Senotherapeutic approaches

Senescent cells are often seen as key players in age-related dysfunctions, even if they can also contribute to tissue repair, regeneration, and development, suggesting that removing them could be detrimental. For this reason, it is crucial to understand the pathophysiological setting in which senescence is present and create targeted therapeutic strategies for specific senescent cell groups. These therapeutic approaches are called "senotherapeutic"(Quarta & Demaria, 2024). The first class of senotherapeutic is the "senolytic" drugs, which are pharmacological agents designed to remove senescent cells (**Figure 12**).

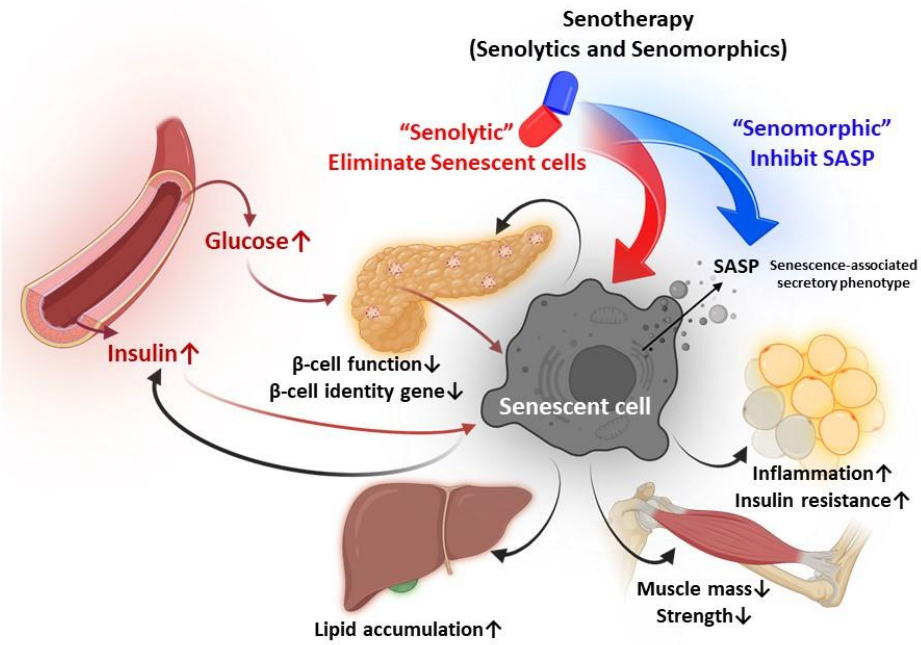


Figure 12. Senotherapy in the context of senescent β cells. *Senescent β cells in the pancreas are related to a decrease in β cell function and identity. This condition increases lipid accumulation in the liver, a reduction in muscle mass and strength, and an increase in inflammation and insulin resistance. Senescent β cells could be directly eliminated with the use of senolytic drugs or the spread of senescence could be blocked using senomorphic drugs, that inhibit SASP release* (Iwasaki *et al*, 2023a).

Senescent cells upregulate anti-apoptotic modulators, indeed one of the most used senolytic agents is the Navitoclax (also known as ABT-263 or ABT-737), which inhibits the activity of the *BCL-2* family of antiapoptotic proteins. This agent promotes cell death

in senescent cells, thereby clearing them from the body. Using p16-3MR transgenic mice, Navitoclax eradicated senescent hematopoietic stem cells, leading to the rejuvenation of the prematurely aged hematopoietic system. A study showed that Navitoclax effectively eliminated senescent endothelial cells in mice subjected to whole-brain irradiation, leading to decreased blood-brain barrier permeability and improved microvascular density (Gulej *et al*, 2023). Moreover, in the cancer context, research demonstrated that Navitoclax targets senescent tumor cells induced by chemotherapy (vinblastine) and MAPK inhibitors (dabrafenib or trametinib) in pediatric low-grade gliomas (Guiho *et al*, 2021). Indeed, Navitoclax has entered phase I and phase II clinical trials for treating various cancers, including small-cell lung cancer and acute lymphocytic leukemia (Skwarska & Konopleva, 2023). In the context of T2D, it was shown that the use of ABT-263 in different models such as transgenic INK-ATTAC, aged and insulin resistance mice models decreased the senescence markers, the SASP profile while improving glucose metabolism and β cell function (Aguayo-Mazzucato *et al*, 2019).

Venetoclax (also called ABT-199) is already approved for the treatment of chronic lymphocytic leukemia and acute myeloid leukemia. *Thompson et al.* showed that treating the normoglycemic non-obese diabetic mice model with ABT-199 prevented the development of diabetes compared to control groups (Thompson *et al*, 2019). Dasatinib and quercetin (D&Q) have been extensively studied for their anti-apoptotic activity, to eliminate senescence cells selectively. In particular, dasatinib is an FDA-approved tyrosine kinase inhibitor for treating myeloid leukemia, and Quercetin is a naturally occurring flavonoid promoting apoptosis. A study demonstrated that D&Q treatment selectively eradicated senescent human skin fibroblasts *in vitro* and *in vivo*, leading to increased collagen density and suppression of the SASP (Takaya & Kishi, 2024). Another study conducted on middle-aged non-human primates showed that D&Q reduced senescence marker gene expression in adipose tissue and improved immune cell profiles, with significant improvements in metabolic health and reduced glycosylated hemoglobin A1c levels when combined with caloric restriction (Ruggiero *et al*, 2023). In the context of metabolic disorders, in 2020 it was shown that the combination of D&Q in obese mice led to the reduction of senescence markers in the white adipose tissue. Moreover, the mix of D&Q and navitoclax treatment in mice increased insulin sensitivity and glucose tolerance (Islam *et al*, 2023; Sierra-Ramirez *et al*, 2020).

Senolytic CAR-T cells are an innovative therapeutic approach that exploits the precision of chimeric antigen receptor therapy to eliminate senescent cells. Senescent cells have a distinctive antigen protein on the surface which is the urokinase plasminogen activator receptor (uPAR). By targeting these antigens, senolytic CAR-T cells can selectively eliminate senescent cells without harming healthy cells. Recent studies have demonstrated the effectiveness of senolytic CAR-T cells in aged mice, showing promising results in mitigating age-related declines and metabolic dysfunction. *Amor et al.* treated a high-fat diet mouse model with anti-uPAR CAR-T cells, and this treatment showed lower basal insulin levels after fasting, followed by a significant rise in insulin levels 15 minutes post-glucose load, indicating enhanced pancreatic β cell function. Moreover, these treated mice showed improved peripheral insulin sensitivity and exercise capacity 2.5 months after treatment (Amor *et al*, 2024).

The second group of senotherapeutics are called “senomorphic” drugs, they don't eliminate senescent cells but instead modulate their harmful secretions of SASP factors, mitigating inflammation and other detrimental effects associated with cellular senescence. Different molecular mechanisms mostly regulate inflammatory SASP factors: the activation of *p16* and *p21* pathways, DDR, the nuclear-factor (NF-Kb), p38/mitogen-activated protein kinase (MAPK) pathway, cyclic GMP-AMP synthase (cGAS)-stimulator of interferon gene (STING) pathways, transcription factor GATA-binding protein 4 (GATA4) and the JAK/STAT pathway. Rapamycin, resveratrol, and metformin are well-known examples of senomorphics. Additionally, promising senomorphics include aspirin, NF-κB inhibitors, p38MAPK inhibitors, janus kinase/signal transducer (JAK/STAT) inhibitors, ATM inhibitors, and statins. Metformin is one of the most used senomorphic drugs, which has direct impacts on mTORC1, PGC1-α, Insulin-IGF1 signaling, SIRT1, NF-κB signaling, and pro-inflammatory cytokines. Moreover, metformin has long been employed to treat T2D by lowering blood glucose levels through the inhibition of hepatic gluconeogenesis (Palmer *et al*, 2015) . Indeed, the use of metformin improves insulin secretion and overall β cell function in a context of exposure to free fatty acids or high glucose (Patanè *et al*, 2000). It has been shown that it reduces senescence in pancreatic β cells, decreasing the release of SASP factors through the inhibition of the transcription factors NF-κB (Moiseeva *et al*, 2013).

Moreover, in diabetic kidney complications, metformin alleviates high glucose-induced senescence and fibrosis of renal tubular epithelial cells, by downregulating the expression of *E2F1* (Liang *et al*, 2022). A study on the effect on T cells found that metformin decreased the number of senescent $CD8^+$ T cells and inhibited the secretion of pro-inflammatory cytokines like IL-6, while promoting telomerase activity and genes related to stemness. In Parkinson's disease, the use of metformin on mouse model of the disease normalized mitochondrial function and reduced mitochondrial DNA release, leading to delayed astrocyte senescence and improved dopamine neuron survival (Yang *et al*, 2023; Wang *et al*, 2024a).

Another interesting compound with senomorphic activity is curcumin. Indeed, the use of curcumin has been shown to ameliorate cellular senescence in D-galactose-induced senescent neurons in rats, by reducing β-gal positive cells, *p16*, and *p21* levels and to mitigate D-galactose-induced cellular senescence in cardiomyocytes by promoting autophagy through the SIRT1/AMPK/mTOR pathway (Lee *et al*, 2020; Yang *et al*, 2022). In diabetes context, curcumin was used to assess the delay of T2D in prediabetic population. In this study, they evaluated β cell function, insulin resistance (HOMA-IR) and anti-inflammatory cytokine levels. After 9 months of treatment, the patients treated with curcumin presented better β cell function with reduced number of individuals that developed T2D compared to the placebo group, suggesting the beneficial effects of curcumin (Chuengsamarn *et al*, 2012).

Curcumin has been suggested to inhibit the JAK/STAT pathway for SASP secretion, showing its therapeutical potential (Iwasaki *et al*, 2023a). In particular, the JAK/STAT pathway plays a crucial role in the production of SASP factors including growth factors, hormones, colony-stimulating factors, interferons and interleukins. The JAK family is composed of four members: JAK1, JAK2, JAK3 and tyrosine kinase 2 (TYK2). JAKs are activated when the receptors bind specific cytokine, which facilitates the phosphorylation of signal transducers and activators of transcription (STAT) protein. These tyrosine-phosphorylated STATs then dimerize and are transported into the nucleus, where they regulate specific genes. JAK1 and JAK2 are crucial for inflammatory signaling and the regulation of growth hormone and other endocrine signals, whereas JAK3 is predominantly involved in erythropoietin signaling and immune functions. Senescent human primary preadipocytes and human umbilical vein endothelial cells released SASP

and were treated with JAK inhibitors. Using the conditioned medium (CM) from the non-treated senescent preadipocytes induced macrophage migration *in vitro* causing inflammation in healthy adipose tissue and preadipocytes. In contrast, using the CM from the senescent cells treated with JAK inhibitors such as momelotinib (JAK1/2 inhibitor), has resulted in reduced inflammation (Xu *et al*, 2015). The use of JAK2 inhibitor has been shown to enhance antitumor response and to improve muscle stem cell function and regeneration. Ruxolitinib is a senomorphic treatment that inhibits JAK2/STAT3 signaling both *in vivo* and *in vitro*: it was shown that in mice model of senescence in septic cardiomyopathy it alleviated mitochondrial-mediated apoptosis and restored antioxidant system balance. Furthermore, it led to a significant reduction in cardiac senescence markers, such as *p21* and *p53*, and SASP-associated genes such as CXCL1, CXCL5, MMP3, IL-1α, IL-6, CXCL10, and IL-1β . Additionally, the use of the senomorphics ruxolitinib and tofacitinib (JAK1/3 inhibitors) have effectively promoted hair growth (Yang *et al*, 2024; Hu *et al*, 2021; Xu *et al*, 2016).

In the context of diabetic kidney disease, ruxolitinib treatment in diabetic mice showed a reduction in proteinuria and improved renal inflammation (El-Kady *et al*, 2021). Baricitinib, a JAK inhibitor selective to JAK1 and JAK2, was used in a clinical trial for patients with T2D and it was observed to reduce albuminuria compared to placebo control (Tuttle *et al*, 2018). Moreover, in 2023 a study with baricitinib was published in the context of T1D. In particular, 91 patients with T1D were treated with baricitinib daily and the data published are up to 48 weeks of treatment. The treated patients, compared to the placebo ones, presented an increase in the mean C-peptide levels after a mixed-meal test, suggesting a better β cell function (Waibel *et al*, 2023). In general, in the last decades both synthetic and natural senolytics and senomorphic treatments as anti-aging have been proposed and early results showed that they may be administered to humans with safety (Boccardi & Mecocci, 2021). Considering the use of senomorphic agents during the differentiation of iPSCs into β cells in the vision of T1D cell therapy involves examining both beneficial and detrimental effects. Senomorphic compounds target senescent cells and their secretory phenotype SASP, potentially improving the efficiency and quality of β cell differentiation by reducing cellular senescence and promoting a healthier cellular environment. However, it's crucial to consider potential drawbacks and the beneficial

effect of senescence during the differentiation process, such as unintended impacts on cell viability or differentiation efficiency.

3.4 Cellular senescence of hPSCs from reprogramming to differentiation

Aging in hPSCs is a topic of significant interest in stem cell research. Both iPSCs and ESCs are pluripotent stem cells with the ability to differentiate into various cell types, making them valuable tools for regenerative medicine and disease modeling. Considering iPSCs, it is important to take in consideration what happens in terms of aging through the reprogramming, maintenance, and differentiation processes (**Figure 13**).

The process of reprogramming somatic cells into iPSCs has been shown to reset many aging-related characteristics. Studies have demonstrated that iPSCs derived from aged donors, including centenarians, exhibit a rejuvenated transcriptomic profile upon reprogramming (Zhang *et al*, 2020). In a study, fibroblasts from centenarians and individuals with disease-related mutations were reprogrammed into iPSCs. It was observed that the reprogramming efficiency was higher using the younger fibroblasts. However, once they differentiated them into fibroblasts, these presented the same transcriptomic profiles, suggesting a rejuvenation of their transcriptome. Moreover, the same was observed using the iPSC obtained from individuals with disease-related mutations, which could differentiate without a decrease in the differentiation efficiency, suggesting that the epigenome can be reset during the reprogramming, like a form of senescence reversal (Strässler *et al*, 2018). In general, even with the decreased efficiency in aged cells, somatic cell reprogramming can reset the molecular and cellular characteristics of the somatic cell of origin cellular features of aging cells. Different studies confirmed that the donor's age does not influence reprogramming (Soria-Valles & López-Otín, 2016). In another interesting study, vaginal fibroblasts from young and old women were used. In both groups, they could observe the same expression of genes like *NANOG*, *SOX-1*, *TRA-1-60* and *OCT-4* which indicate the same pluripotency level, and similar expression of the anti-apoptotic gene *BCL-2* and the senescence genes *p53* and *p21*. Age did not impact aging markers, the cells presented longer telomeres, lower oxidative stress, and gene expression patterns reverting aging cells to an embryonic-like condition (Wen *et al*, 2013).

In one study, iPSCs from 18-months and 2-months mice were obtained and differentiated into cardiac tissue (CA). The obtained 18-month-old CA presented no upregulation of *p16* and *p53*, no telomere shortening, and just a slight alteration in mitochondrial ultrastructure with reactive oxygen species. In general, they found no significant differences between the 2-month-old CA and 18-month-old CA, suggesting that the reprogramming can lead to partial rejuvenation (Cheng *et al*, 2017). Additionally, in another study, *Suzuki et. al* showed that iPSCs derived from young mouse embryonic fibroblasts and 21-months-old mouse bone marrow mice were both capable of regulating angiogenic vascular response in the same way (Suzuki *et al*, 2012). Another aspect to take into consideration is that, with aging, there is also an increase in senescence. Indeed, replicative senescence represents a challenge for iPSCs reprogramming: several studies have suggested that the increased expression of *p53*, *p16*, and *p21* may be a barrier to the decline in reprogramming efficiency. In a study, using a six-factor gene cocktail, it was observed that the presence of senescent cells did not affect the reprogramming. The authors reprogrammed fibroblasts derived from 74-year-old-donor fibroblasts (not senescent and replicative senescence-induced) and centenarian fibroblasts from a 96-year donor. Surprisingly, all the resulting iPSCs are indistinguishable from hESCs, indicating that senescence and aging from the fibroblasts did not affect efficiency reprogramming (Lapasset *et al*, 2011). These results strongly support the idea that these cells maintain a youthful state. Additionally, both *in vivo* and *in vitro* studies have shown that reprogramming factors completely remodel the chromatin structure, recovering the levels of H3K9me3 and H4K20me3 (Koche *et al*, 2011)**.** However, the complete reprogramming *in vivo* using the Yamanaka factors lead to teratoma formation. *Ocampo et al.* used aged mice model to demonstrate that partial reprogramming through the short-term induction of Yamanaka factors improved the lifespan of the mice, with higher regenerative capacity of the pancreas and faster recovery from muscle injury(Ocampo *et al*, 2016).

A predictive model was developed by Horvath to estimate DNA methylation (DNAm) age across various tissues and cell types, utilizing a dataset of 8,000 samples from 82 Illumina DNA methylation arrays, including 51 healthy tissues and cell types. This research conducted by *S. Horvath* has shown that human ESCs and iPSCs exhibit an epigenetic age (eAge) (Horvath, 2015). It was consistently observed that ESCs displayed an eAge close to zero across five different datasets. Furthermore, due to the similarities

between iPSCs, which are artificially generated pluripotent stem cells, and ESCs, *Horvath* confirmed that iPSCs have a significantly younger DNAm age compared to their corresponding primary cells. The significant discovery made by *Horvath* was also corroborated by the work of *Kerepesi* and colleagues. They analyzed iPSCs and ESCs using multiple available datasets to further investigate the aging process in these cells. Their findings revealed that the epigenetic age of these cells remained very low, even after more than 100 passages. They exposed the cells to artificial culture conditions, such as high oxygen levels and could not see any changes in the epigenetic age. This was also confirmed in cell culture with a high number of passages, which can potentially lead to the accumulation of mutations (Kerepesi *et al*, 2021).

It's worth noting that hPSCs cells tend to experience a decline in proliferation and differentiation potential after a limited number of cell divisions, and cell passaging, commonly referred to as splitting cells, can lead to an increase in DNAm age (Horvath, 2015). Moreover, some studies suggest that, while iPSCs differentiate into mature cells, the cellular aging process restarts, resulting in shorter telomeres, epigenetic modifications, increased senescence markers, and mitochondrial dysfunction (Strässler *et al*, 2018).

Unlike primary cells, such as MSC, the reprogrammed iPSCs avoid replicative senescence. In particular, replicative senescence is present after a limited number of cell divisions and is related to the loss of proliferation and differentiation potential. This condition can be associated with specific senescence-associated DNA methylation (SA-DNAm) changes. In a study, researchers showed that iPSCs do not present SA-DNAm alterations, and this is probably related to their ability to evade cellular senescence. However, when iPSCs are differentiated into MSCs and are maintained in culture, they re-enter in replicative senescence with DNAm changes similar to the primary MSCs, with similar morphology and immunophenotype. This process seemingly begins with the loss of the pluripotent state, once iPSCs enter the differentiation process, becoming the final product of the differentiation. This iPSC-derived MSCs do not display only modifications on DNAm, but also an increase in SA-β-Gal and share the same gene expression with primary MSC, particularly in metabolic processes. Going deep into it, iPSC-derived and primary MSC shared the same metabolome with features of senescence-associated alterations such as decreased nicotinamide ribonucleotide and increased orotic acid

levels. This change is probably due to the excessive release of ROS during the entry in senescence, in concomitance with the observation of mitochondrial dysfunction (Fernandez-Rebollo *et al*, 2020)**.** In support of this, in a study iPSCs were differentiated into fibroblasts to check their re-enter in replicative senescence after prolonged culture. The differentiated fibroblasts displayed increased SA-β-Gal activity, shortened telomeres, and elevated expression of *p16* and *p21* (Koch *et al*, 2013).

In 2010, it was demonstrated that cells derived from iPSC lines exhibit early senescence compared to those obtained from ESCs. Specifically, iPSC-derived endothelial cells displayed slow growth, with a majority showing a senescent-like phenotype, and 50% of the cells expressing SA-β-Gal. Conversely, ESC-derived endothelial cells maintained normal morphology and robust growth, with fewer than 5% staining positive for SA-β-Gal. To investigate whether this phenomenon was limited to hemangioblastic lineages, researchers generated retinal pigment epithelium (RPE) from both ESCs and iPSCs. Notably, iPSC-derived RPEs exhibited abnormal senescent-like characteristics, such as large vacuolated cells with irregular morphology already at the first passage with positive cells for SA-β-Gal (Feng *et al*, 2010). *Goyer et. al* examined and compared the cellular senescence pathways in iPSC-derived human fibroblasts (i-HF) to the primary skin fibroblasts (HF). The researchers found that i-HFs presented higher sensitivity to various stressors, with pronounced activation of senescence pathways, and elevated SASP release compared to the primary one. Moreover, they underlined the fact that it is crucial to consider that the functionality of iPSC-derived cells is influenced by the differentiation protocol used (Goyer *et al*, 2024).

In the context of iPSC-derived β cells, it is important to take into consideration the longtime of culture to complete the differentiation process. It has been shown in cardiomyocytes, neurons, and MSCs that extended culture periods of iPSC-derived cells induce an aging phenotype, including changes in DNAm, elevated ROS, and an increase in *p21* and SA-β-Gal activity (Pitrez *et al*, 2024). Cellular senescence during iPSC differentiation into β cells is a significant concern as it can impact the efficiency and functionality of the resulting cells, considering the stress induced by the differentiation process per se. However, it is important to consider that in the context of differentiation, senescence could have a positive role. During development, senescence acts as a barrier to prevent cells from reverting to a less differentiated state, ensuring they maintain their

specialized functions. Moreover, it can promote local proliferation, cell plasticity, and tissue patterning, creating a supportive environment for stem cells and balancing cell growth and differentiation, ensuring proper development (Ring *et al*, 2022; Saito *et al*, 2024). However, due to controversial results regarding the senescence state of iPSC, further investigation into the cellular age of these cells is necessary. Especially, further investigation is essential to explore the impact of senescence in the context of the differentiation process from iPSC into β cells, where a lot of aspects remain largely unexplored.

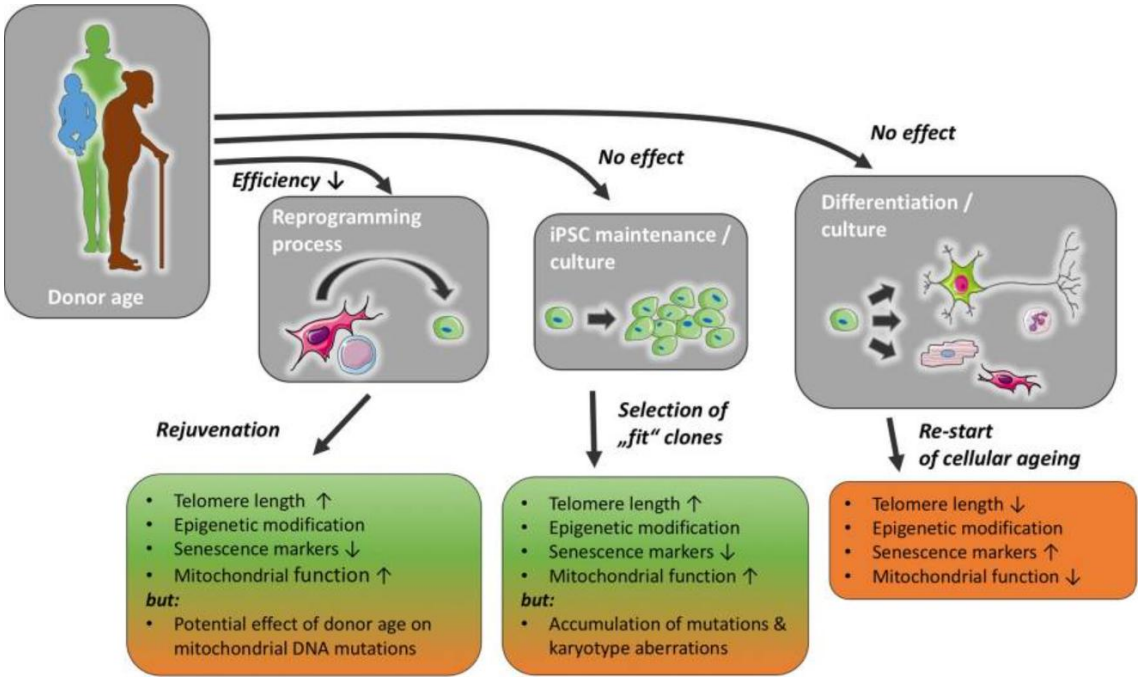


Figure 13. Scheme of aging modifications during three main processes: reprogramming, iPSC culture, and differentiation. *The reprogramming process from somatic cells has lower efficiency with old donors. However, after the reprogramming, the cells are rejuvenated with longer telomeres, mitochondrial function, and lower expression of senescence markers. While iPSCs are maintained in culture, they can accumulate mutation and karyotype aberrations. The differentiation process is where cellular aging and senescence restart: cells present shorter telomeres, decreased mitochondrial function, and an increase in senescence markers* (Strässler *et al*, 2018).

4. Aim of the work

Type 1 diabetes (T1D) is a chronic autoimmune disease characterized by the destruction of insulin-producing β cells in the pancreas. While pancreatic islet transplantation from cadaveric donors offers a potential cure, its clinical application is severely limited by donor scarcity and the requirement for lifelong immunosuppression. Human induced pluripotent stem cells (iPSCs) provide an alternative source, as they can differentiate into insulin-producing β cells (iβ), effectively recapitulating pancreatic development in vitro.

Cellular senescence plays a dual role in biology: while it can support tissue development during early life, it may later impair cellular function and contribute to the development of diseases. However, whether senescence occurs during the differentiation of iPSCs into mature endocrine cells and how it affects the final β cell phenotype remains unclear. Reprogramming somatic cells into iPSCs resets many aging markers, such as senescence-associated gene expression, telomere length, and mitochondrial activity, effectively rejuvenating the cells. However, during differentiation, aging-related processes re-emerge, leading to telomere shortening, epigenetic modifications, increased senescence markers, and mitochondrial dysfunction. Some studies suggest that aging-associated β cell senescence negatively affects glucose sensing and insulin secretion, while others propose that senescence, particularly linked to *p16* expression, enhances β cell function and maturation. Understanding how senescence influences β cell differentiation is crucial for optimizing iPSC-derived β cell therapies for T1D.

This study aims to determine whether cells undergo senescence during differentiation by analyzing iPSC clones from the same donor at key differentiation stages. The investigation focuses on transcriptomic data, including senescence and β cell SASP gene expression, as well as proteomic data, with a particular emphasis on the β cell SASP signature and its effects on the microenvironment. Additionally, the study examines the correlation between iPSC clone senescence and differentiation efficiency and evaluates the impact of senescence on iβ function using senomorphic treatment.

5. Results

5.1 iPSCs differentiate into mature β cells

An iPSC line (DRI2) from a healthy donor was differentiated *in vitro* into mature β cells. The differentiations were conducted using six different clones from the same line (DRI2#3, DRI2#4, DRI2#9, DRI2#13, DRI2#14, DRI2#15), each differentiated three times. To evaluate the progress of the differentiation from iPSC into β cells, the morphology of the cells was monitored at the main stages of the differentiation process: Day0 (iPSC), Day 4 (DE), Day 11 (PE), Day 21 (EN) and Day 30 (iβ) (**Figure 14**). Additionally, flow cytometry staining was conducted at the five main stages (**Figure 15A**). On Day 0 and Day 4 we assessed the positivity of the cells for OCT4 and the chemokine receptor CXCR4, respectively known as key markers related to pluripotency and definitive endoderm (Jin & Jiang, 2022). At the stage of iPSC, clones presented a high percentage of cells expressing OCT4 (99.6%±0.5%), while this percentage was strongly reduced at the stage of DE (1.7%±1.9%). Conversely, at the stage of iPSC, the cells were CXCR4 negative (2.5%±1.6%) and became CXCR4 positive at the stage of DE (97.8%±2.2%), marking the complete transition into definitive endoderm (**Figure 15B**). Once it was assessed, an additional measure of quality control of the differentiation was evaluated from the stage of PE to iβ by examining important markers associated with pancreatic progenitor and mature β cells: NKX6.1, PDX1 and INSULIN (Jin & Jiang, 2022) . Moreover, to ensure the purity of the differentiation, the presence of GLUCAGON positive cells was evaluated. To check the pancreatic progenitor formation we analyzed the presence of NKX6.1 positive cells, which increased from PE to EN stage (PE: 41.4% ±4%: EN: 53.1%±6.1%), whereas declined at the stage of iβ (39.8%± 3.8%). Additionally, the percentage of PDX1 positive cells was high at the stage of PE (59.6%±7%) and slightly declined over time reaching lower levels at EN and iβ stage (EN:44.1%±5%; iβ: 18.8%±2.9%). As expected, at the iβ stage the percentage of cells positive for INSULIN was high (45.5%± 2%) while the percentage of cells expressing GLUCAGON remained lower (11.1%± 1.5%), confirming the quality and efficiency of the differentiation process (**Figure 15C**). Additionally, the evolution of iPSC into iβ was analyzed with staining of key markers by immunofluorescence. At the stage of iPSC, their pluripotency was confirmed with OCT4 and SSEA4 (**Figure 16A**). At the last stage of iβ,

clusters presented both GLUCAGON and CHROMOGRANIN positive cells, and NKX6.1 and INSULIN positive cells (**Figure 16B**). By exploiting TaqMan array card technology, the expression of 47 genes related to the differentiation process and insulin machinery was measured. In particular, the gene expression was assessed at three stages: iPSC (Day0), endocrine progenitors (Day21), and mature β cells (Day30). Specifically, it was observed a high expression of pluripotency genes (*SOX2, NANOG, POUF51*) at the stage of iPSC, whereas the genes associated with endocrine progenitors and β cell development (such as *PDX1, NKX2.2, NKX6.1, INSULIN, MAFA*) demonstrated a high expression at the stage of EN and iβ (**Figure 17A**). Moreover, the genes related to glucose sensing and insulin secretion were not expressed at the stage of iPSC, then went up from EN to iβ stage, marking the full maturation of β cells at the end of the differentiation process (**Figure 17B**). Finally, the effective maturation and capacity to respond to glucose of the obtained iβ was evaluated with dynamic glucose-stimulated insulin secretion (GSIS). In this test, iβ cells were exposed to varying glucose concentrations, both low and high, in the presence or absence of IBMX as a secretagogue. This was followed by a forced insulin release using KCl as a depolarizing stimulus. Insulin secretion in response to these stimuli was measured in the collected medium at closely timed intervals. iBeta cells exhibited a fold increase in insulin secretion in response to high glucose stimulation, which was significantly enhanced by IBMX compared to glucose alone. Upon the removal of IBMX and glucose, insulin secretion declined during the recovery phase. Subsequent depolarization with KCl induced another insulin release peak, confirming the cells' responsiveness to membrane depolarization, a hallmark of functional β cells. (**Figure 17C, Figure 17D**).

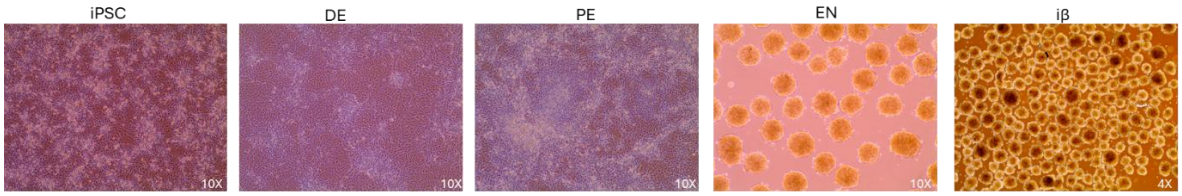
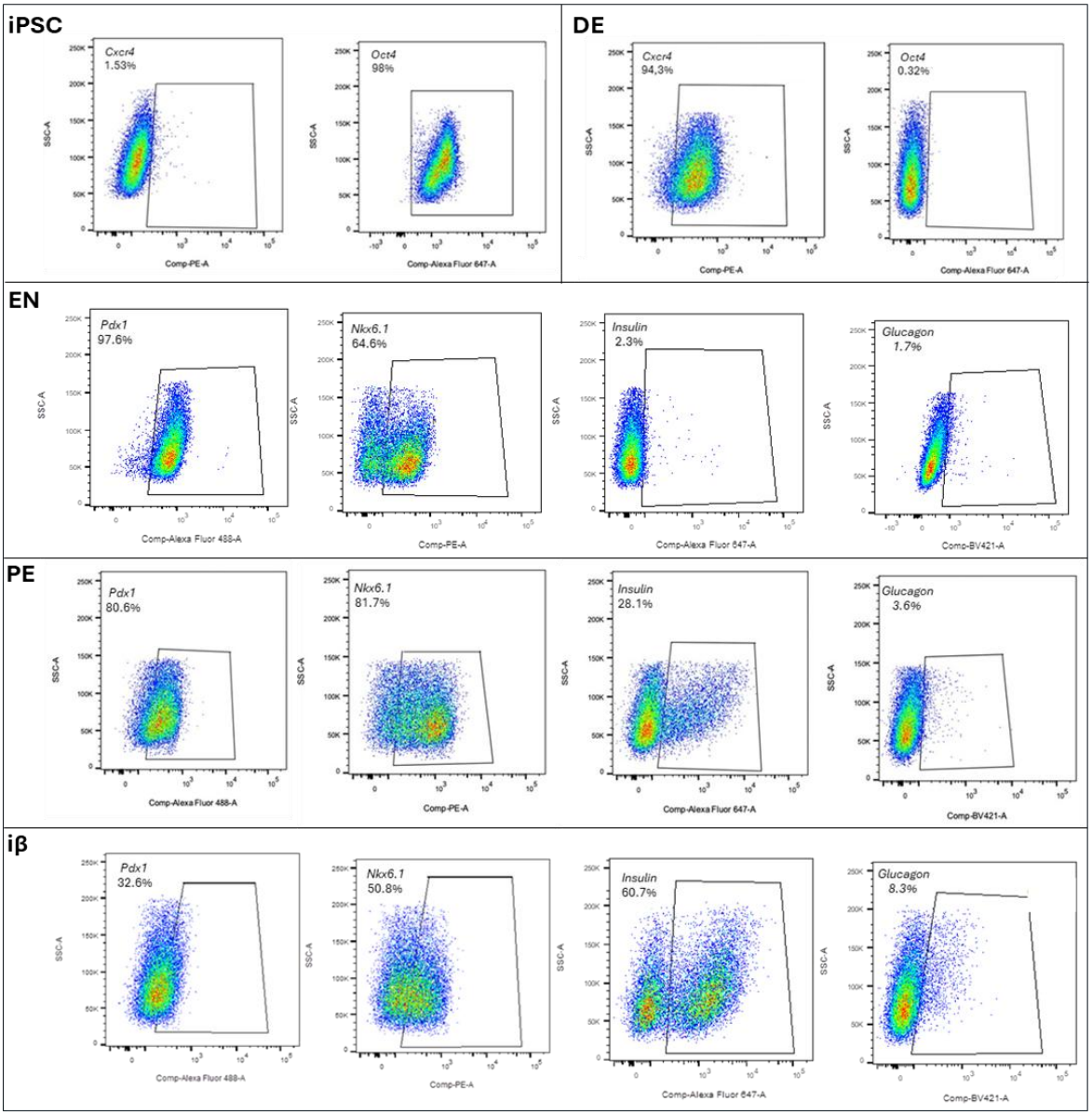


Figure 14. Morphological changes on the differentiation process from iPSC into β cells. *Representative pictures of a DRI2 clone through the main stages of the differentiation process: iPSC, DE, PE, EN, and iβ. At the stage of iPSC, DE, and PE the cells are attached to the plate. From iPSC stage to PE stage, there is a high confluence of the cells until they form 3D layers. From stage EN, the cells are passed in suspension and maintained in agitation until they reach a clear and defined form of cluster. Magnification 4X and 10X.*


A
Singlets
53,4%
Cells
71%
Live cells
88.2%
FSC-H
FSC-A
SSC-A
Comp-APC-Cy7-A
iPSC
Cxcr4
1.53%
Oct4
98%
DE
Cxcr4
94,3%
Oct4
0.32%
EN
Pdx1
97.6%
Nkx6.1
64.6%
Insulin
2.3%
Glucagon
1.7%
PE
Pdx1
80.6%
Nkx6.1
81.7%
Insulin
28.1%
Glucagon
3.6%
iβ
Pdx1
32.6%
Nkx6.1
50.8%
Insulin
60.7%
Glucagon
8.3%
Comp-PE-A
Comp-Alexa Fluor 647-A
Comp-Alexa Fluor 488-A
Comp-BV421-A

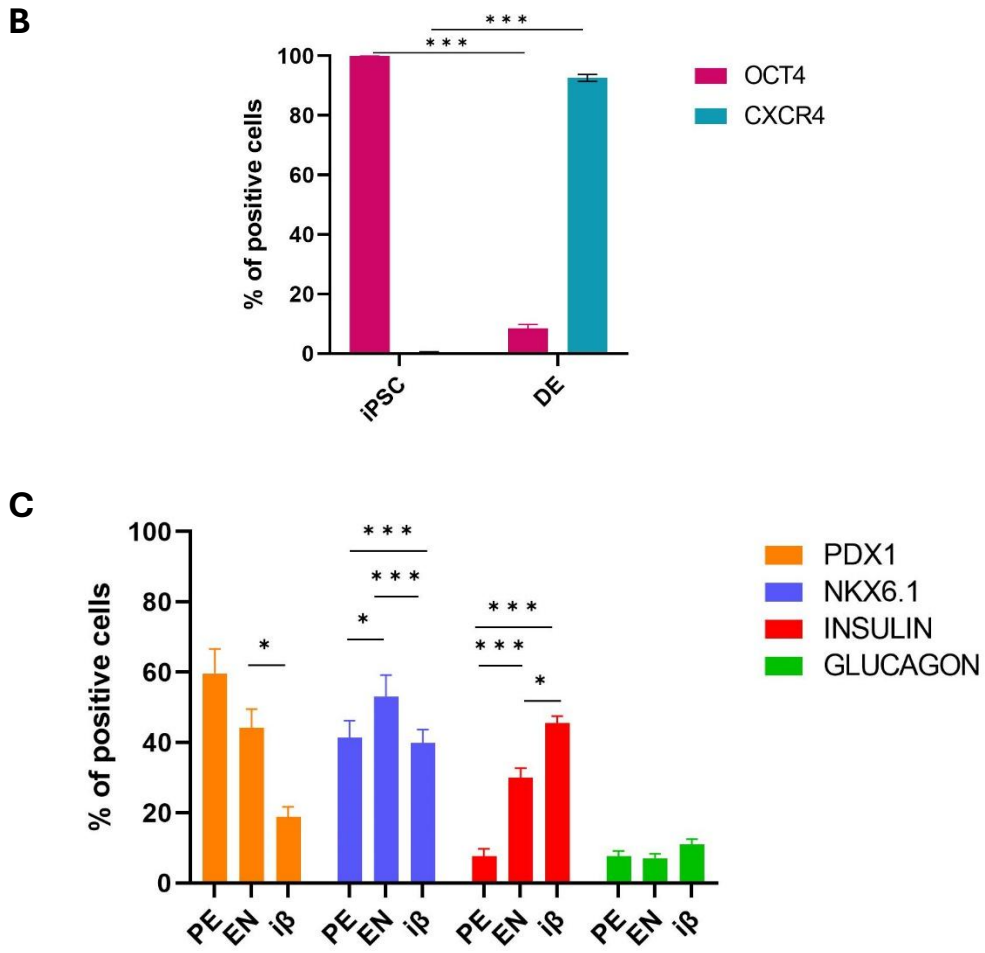


Figure 15. Stage markers during the differentiation process from iPSC into β cells. *Representative example of a gating strategy starting from FSC-H/FSC-A profile, then selected for SSC-A/FSC-A and subgated for live cells. Based on gated live cells, specific markers are gated through the main stages of the differentiation process of a representative DRI2 clone (A). Bar plots show the percentage of positive cells for OCT4 and CXCR4 at the stage of iPSC compared to DE (B) and the evolution of the key differentiation markers NKX6.1, PDX1, INSULIN and GLUCAGON comparing DE, EN, and iβ stages (C). The analysis considers the mean percentage of all clones during the differentiation process (Two-way ANOVA, n=18). Results are expressed as mean ± SEM. *p<0.05; ** p<0.01; ***p<0.001. iPSC: induced pluripotent stem cells; DE: definitive endoderm; PE: pancreatic endoderm; EN: endocrine cells; iβ: iPSC-derived β cells.*

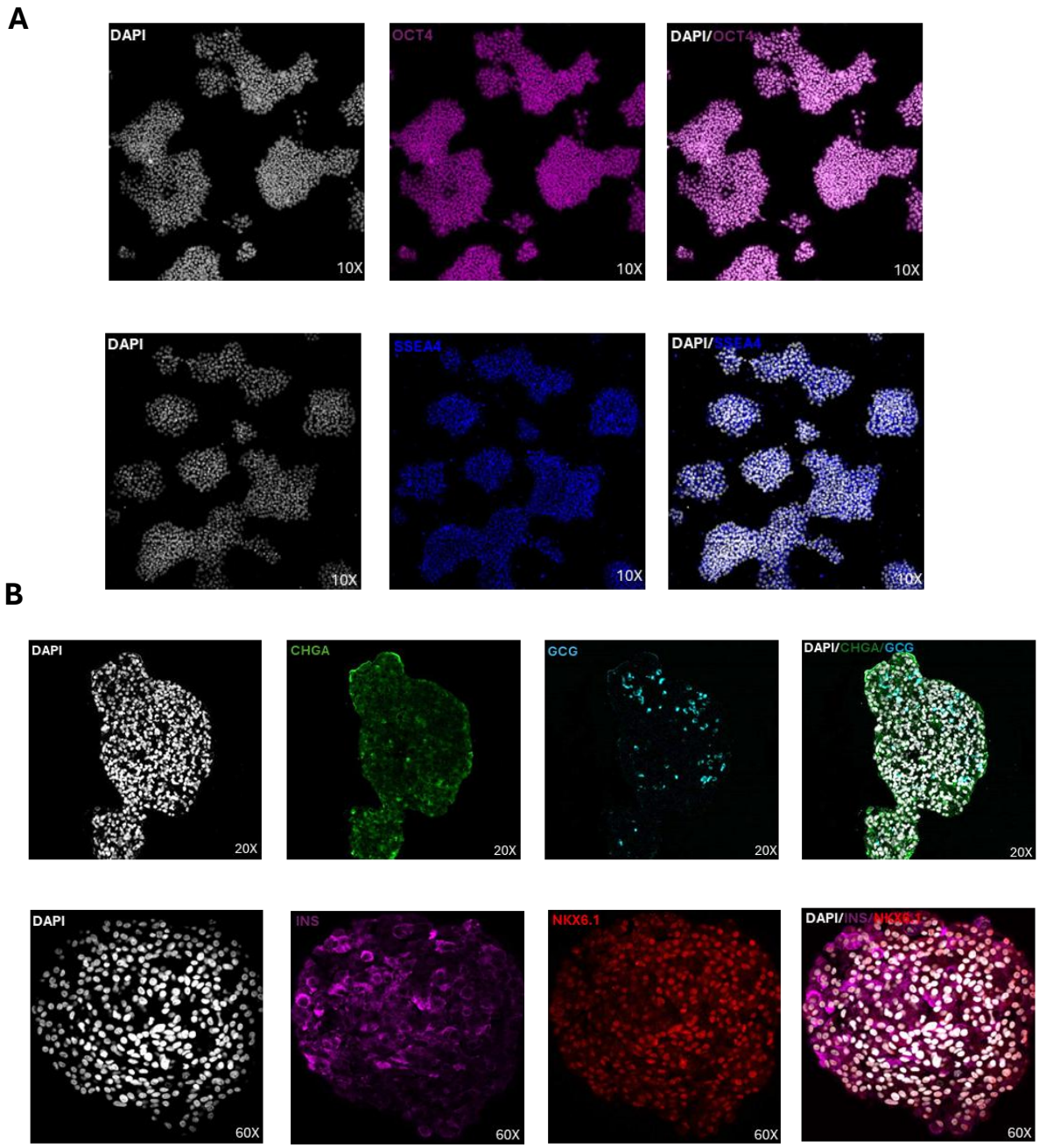
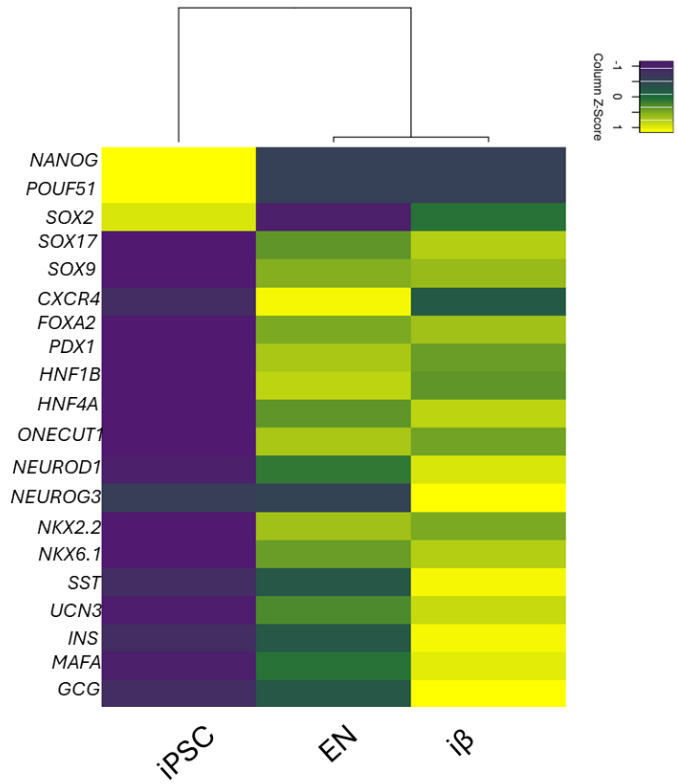
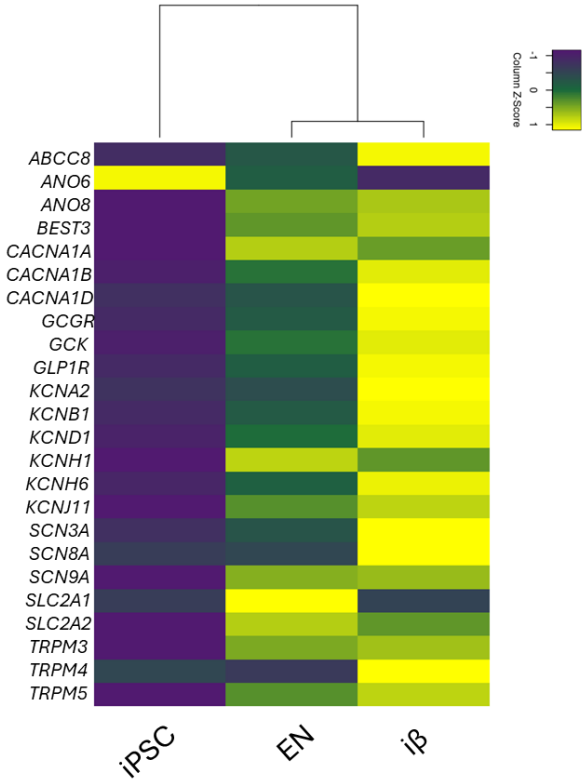


Figure 16. Representative immunofluorescence on iPSC and iβ clusters. *Single staining on iPSC for OCT4 (violet) and SSEA4 (blue) (A). Double staining of iβ clusters: CHGA (green) and GLUCAGON (light blue), and INSULIN (violet) and NKX6.1 (red) (B). For all the images, nuclei are stained in white (Hoechst). Single channels and merged images are shown. Magnification 10X, 20X and 60X.*

A


Column Z-Score
-1
0
1
NANOG
POUF51
SOX2
SOX17
SOX9
CXCR4
FOXA2
PDX1
HNF1B
HNF4A
ONECUT1
NEUROD1
NEUROG3
NKX2.2
NKX6.1
SST
UCN3
INS
MAFA
GCG
iPSC
EN
iβ

B


Column Z-Score
-1
0
1
ABCC8
ANO6
ANO8
BEST3
CACNA1A
CACNA1B
CACNA1D
GCGR
GCK
GLP1R
KCNA2
KCNB1
KCND1
KCNH1
KCNH6
KCNJ11
SCN3A
SCN8A
SCN9A
SLC2A1
SLC2A2
TRPM3
TRPM4
TRPM5
iPSC
EN
iβ

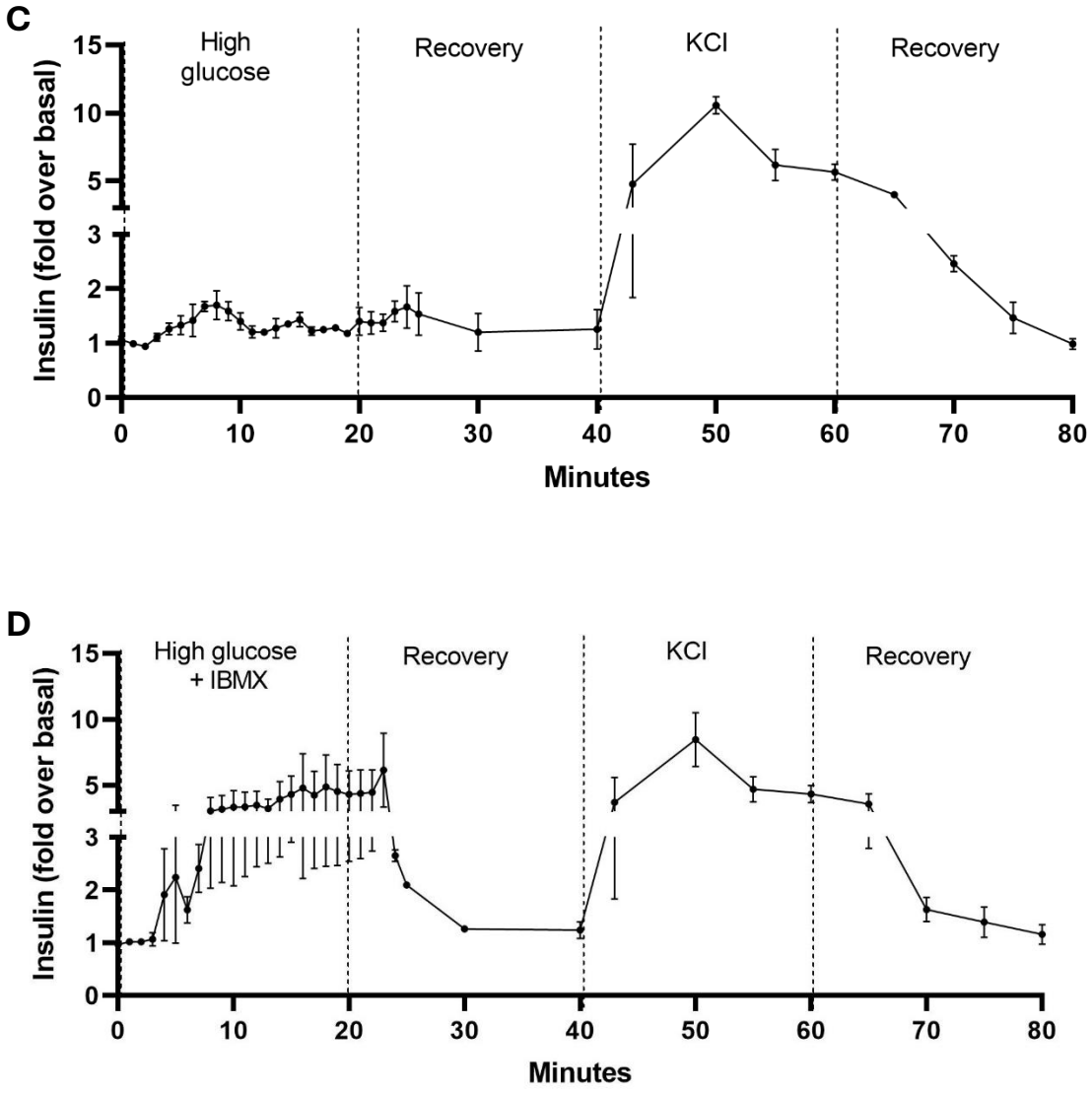


Figure 17. Gene expression assessment at Day 0 (iPSC), Day 21 (EN) and Day 30 (iβ) stages and GSIS. *Heatmaps show the expression of gene markers involved in β cell development (A) and in glucose sensing and insulin secretion Heatmaps are produced by considering the mean gene expression of all clones during the differentiation process (Spearman's ranking, n = 12). iPSC: induced pluripotent stem cells; EN: endocrine cells; iβ: iPSC-derived β cells. (B). Dynamic GSIS of a representative DRI2 clone at the iβ stage. Insulin is expressed as fold over basal in response to high glucose (11mM), Recovery (low glucose 0.5mM), and depolarizing KCl (C). Dynamic GSIS of a representative DRI2 clone at the iβ stage. Insulin is expressed as fold over basal in response to high glucose (11mM) + IBMX, recovery (low glucose 0.5mM), and depolarizing KCl (D) (n=2).*

5.2. Progressive increase in lysosomal activity highlights senescence dynamics during β cell differentiation

To assess the senescence state of cells during differentiation, lysosomal activity was evaluated using senescence-associated β-galactosidase (SA-β-gal) enzyme activity. Flow cytometry was used to determine the percentage of SA-β-Gal-positive cells at five key time points throughout the developmental stages of differentiation: Day0 (iPSC), Day4 (EN), Day11 (PE), Day21 (EN) and Day30 (iβ) (**Figure 18A**). For all differentiated clones, the increase in the percentage of positive cells was evaluated from the iPSC stage to the final stage of mature β cells. (**Table 1**). Based on this analysis of all the clones, the results were treated as a single differentiation process, showing a general increase in SA-β-Gal activity from iPSC to iβ cells. (iPSC: 9.6% ± 0.4%; iβ: 42.1% ± 1.4%). In particular, the increase in this marker became significantly relevant starting at the stage of endocrine cells (EN:35.3% ± 5.7%). Furthermore, this trend was validated by the fold change in SA-β-Gal expression relative to iPSCs, showing a significant increase at each stage. There was a gradual rise from definitive endoderm (DE) to pancreatic endoderm (PE) and endocrine progenitors (EN), peaking at the iβ stage. (DE:1.3±0.13; PE:1.7±0.2; EN: 3.8±0.2; iβ: 4.9± 0.3) (**Figure 18B, Figure 18C**). A qualitative analysis using the immunofluorescence procedure was performed to confirm the SA-β-Gal activity at the mature β cell stage. The immunofluorescence staining at the iβ stage showed positive results for the SA-β-Gal senescence marker (**Figure 19**).

iPSC clone (n=3)	iPSC	DE	PE	EN	iβ
DRI2#3	9.6%±3.7	19.6%±9.1	17.7%±12.8	35.6%±2.54	39.53%±6.02
DRI2#4	8.2%±2.9	10.8%±5.3	15.4%±4	32.1%4.7	46.6%±6.2
DRI2#9	10.8%±2.9	20.2%±13.4	18.3%±7.2	37.1%±9.8	39.9%±5.9
DRI2#13	9.7%±1.1	8.8%±1.9	10.2%±2.2	40.2%±6.8	44.7%±1.7
DRI2#14	10.7%±4.9	11.7%±3.3	13.6%±1.3	32.6%±2.5	44.1%±7.9
DRI2#15	10.2%±0.6	11.1%±2.4	12.6%±2.6	34.6%±6	43.6%±8.2

Table 1. SA-β-Gal positive cells during the differentiation stages for each clone. *All results are expressed as means ± SD. iPSC: induced pluripotent stem cells; DE: definitive endoderm; PE: pancreatic endoderm; EN: endocrine cells; iβ: iPSC-derived β cells.*

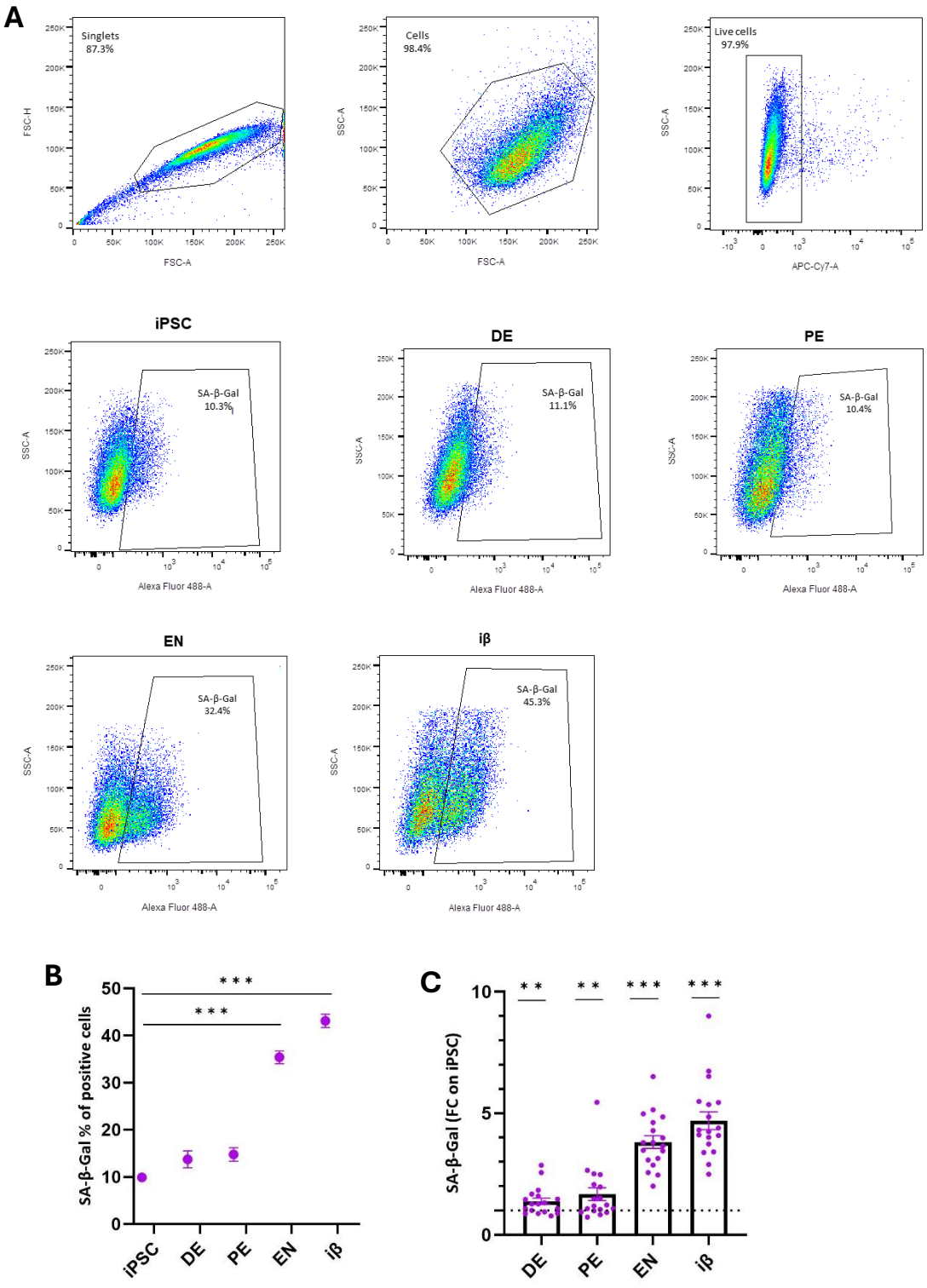


Figure 18. SA-β-Gal activity during differentiation stages from iPSC into β cells. *An illustrative example of a gating strategy starting from FSC-H/FSC-A profile, then selected for SSC-A/FSC-A and subgated for live cells. Based on gated live cells, the percentage of SA-β-Gal positive cells of a representative experiment is reported during the steps of the differentiation (iPSC, DE, PE, EN, iβ) (A). Dot plot of the percentages of SA-β-Gal positive cells during the stages of the differentiation process, combining the differentiation data from each clone. (B). SA-β-Gal activity expressed as fold change relative to iPSC (C). (Two-way ANOVA, One-sample t-test, n=18).*

*Results are expressed as mean ± SEM. *p<0.05; ** p<0.01; ***p<0.001. iPSC: induced pluripotent stem cells; DE: definitive endoderm; PE: pancreatic endoderm; EN: endocrine cells; iβ: iPSC-derived β cells.*

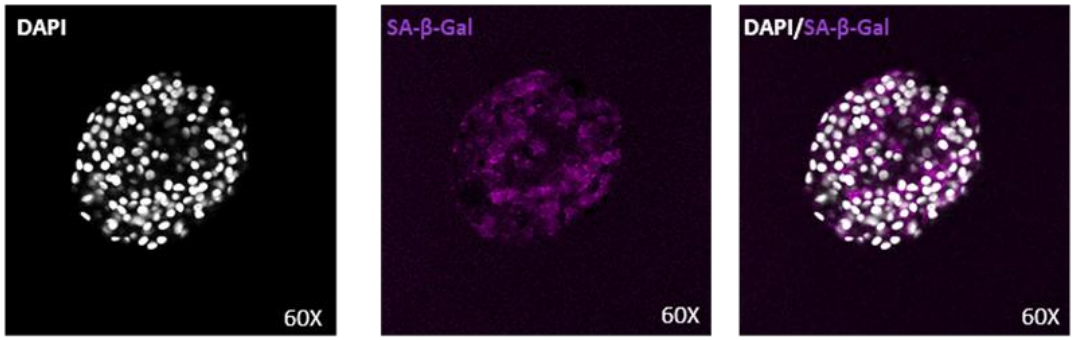


Figure 19. Representative immunofluorescence of iβ cluster. *Single staining of iβ for SA-β-Gal activity (purple). Nuclei are stained in white (Hoechst). Single channels and merged images are shown. Magnification 60X.*

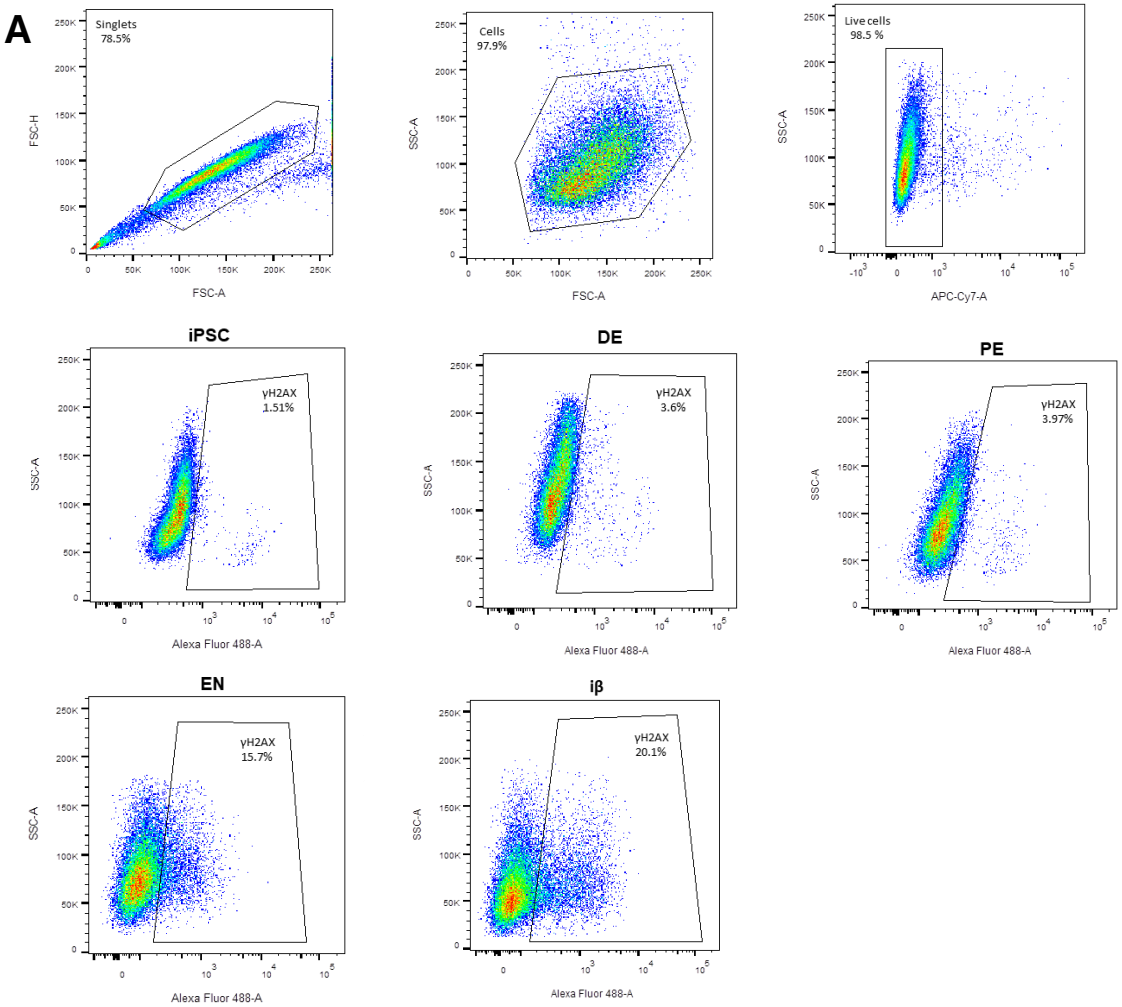
5.3 DNA damage accumulates during the differentiation process

The accumulation of DNA damage leads to detectable nuclear foci of extended chromatin modification like the phosphorylation of histone H2AX (γH2AX), which contributes to cell cycle arrest. To evaluate the DNA damage accumulation during the differentiation process, the percentage of positive cells for γH2AX was evaluated. Flow cytometry staining was performed during the differentiation time points described for SA-β-Gal (**Figure 20A**). For each clone, the rise in the percentage of positive cells across the differentiation process was evaluated (**Table 2**). When analyzing all the clones together, the results were considered as a unified differentiation process, showing an increase in DNA damage during the transition from iPSC to mature β cells. (iPSC: 3.5% ± 0.5%, iβ: 18% ± 0.9%). Similar to the trend observed in SA-β-Gal activity, this increase was particularly prominent starting at the endocrine cell stage of differentiation (EN: 17.2% ± 3.6%). This pattern was confirmed by the fold change in γH2AX expression relative to iPSCs, which showed a significant rise at each stage of differentiation. The levels gradually increased from the definitive endoderm (DE), peaking at the EN stage. (DE: 2± 0.2; PE: 3± 0.5; EN: 7.3 ±1.5; iβ: 6.5± 1.1) **(Figure 20B, Figure 20C**). Moreover, a qualitative assessment of DNA damage was conducted using immunofluorescence staining. Mature iβ were stained for γH2AX, showing positive results for γH2AX in the

nuclei. These results reinforced the presence of senescence-associated characteristics at this developmental stage (**Figure 21**).

iPSC clone (n=3)	iPSC	DE	PE	EN	iβ
DRI2#3	4.8%±1.2	4.7%±1.1	8.7%±0.3	13.4%±3.2	17.7%±2.6
DRI2#4	4.2%±1.8	6%±2.8	11.5%±6.4	17.3%±2.2	14.4%±1.4
DRI2#9	3.8%±3.2	5.9%±2.5	8%±1.1	16.9%±2.8	15.5%±2.4
DRI2#13	2%±1.2	4.7%±1	5.9%±1.7	20.3%±2.3	16.5%±3.3
DRI2#14	3.2%±1.5	5.1%±2	7%±2.3	17.6%±6.6	15.6%±1.3
DRI2#15	3.2%±1.4	6.7%±2.7	6.8%±2.6	17.6%±2.5	20.7%±2.5

Table 2. γH2AX positive cells during the differentiation stages for each clone. *All results are reported as means ± SD. iPSC: induced pluripotent stem cells; DE: definitive endoderm; PE: pancreatic endoderm; EN: endocrine cells; iβ: iPSC-derived β cells.*



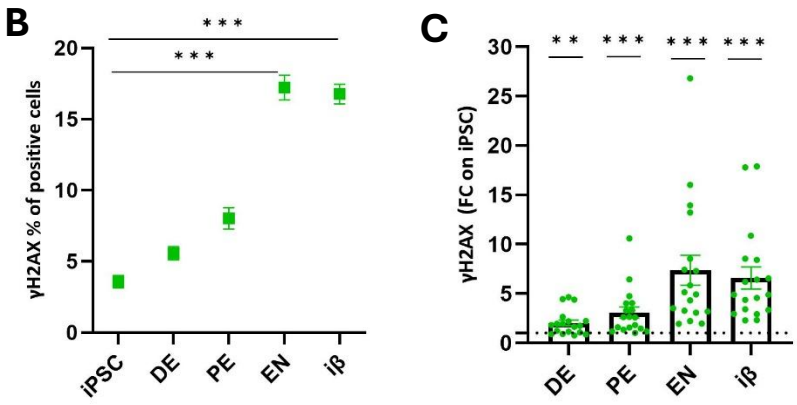


Figure 20. γH2AX during differentiation stages from iPSC into β cells. *The analysis begins with a gating strategy starting with the FSC-H/FSC-A profile, followed by selection based on SSC-A/FSC-A, and subgating for live cells. The percentage of γH2AX-positive cells is shown in a representative experiment across the differentiation stages (iPSC, DE, PE, EN, and iβ) (A). The dot plot illustrates the percentage of γH2AX-positive cells across differentiation stages, combining data from the differentiation experiments for each clone (B). γH2AX is expressed as fold change relative to iPSCs. (C) (Two-way ANOVA, One-sample t-test n=18). Results are expressed as mean ± SEM. *p<0.05; ** p<0.01; ***p<0.001. iPSC: induced pluripotent stem cells; DE: definitive endoderm; PE: pancreatic endoderm; EN: endocrine cells; iβ: iPSC-derived β cells.*

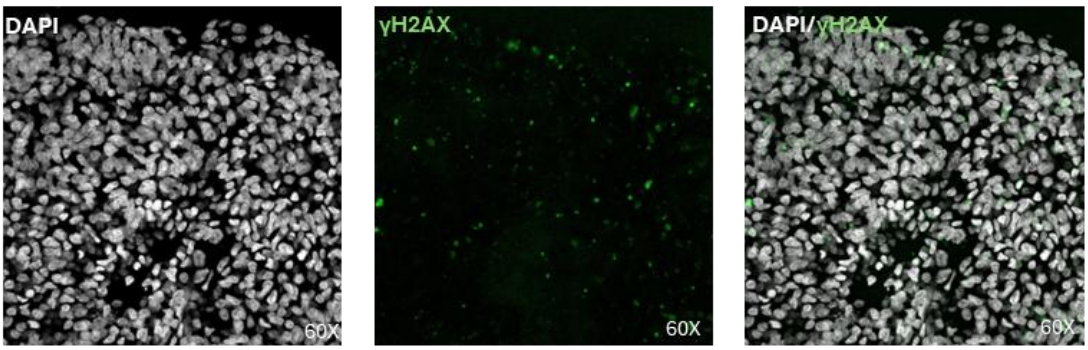


Figure 21. Representative immunofluorescence of iβ cluster. *Staining of iβ for γH2AX (green). Nuclei are stained in white (Hoechst). Single channels and merged images are shown. Magnification 60X (C).*

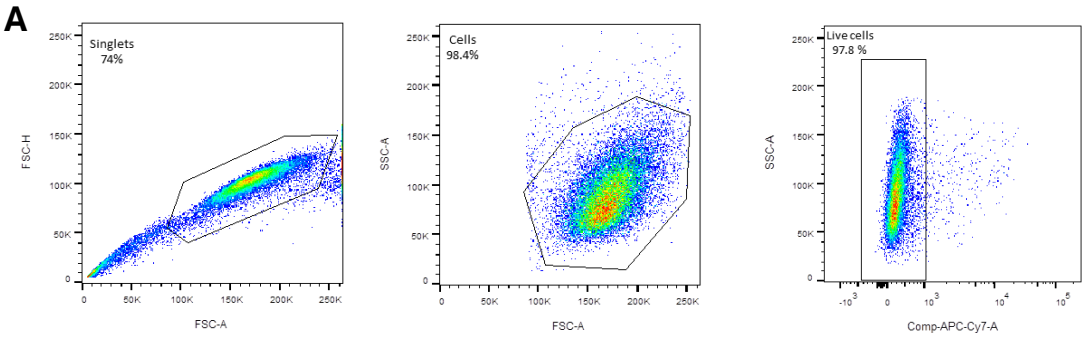
5.4. Elevated oxidative damage reflects senescence progression during β cell differentiation

To assess the senescence state of the cells, oxidative stress and superoxide production in the mitochondria were evaluated using flow cytometry analysis. The cells were stained during the differentiation time points described for SA-β-Gal and γH2AX (**Figure 22A)**. The percentage of positive cells was analyzed for each individual clone throughout the differentiation process **(Table 3).** As with the other senescence markers, the results were

treated as a unified differentiation process, revealing an increase in superoxide production from iPSC to mature β cells (iPSC: 5.6% ± 0.6%; iβ: 25.4% ± 4%). Similar to the patterns observed in lysosomal activity and DNA damage, this increase was particularly noticeable, especially beginning at the endocrine cell stage of the differentiation process (EN: 18.3%± 4.8%). This trend was validated by the fold change in MitoSOX relative to iPSCs, which showed a progressive increase from the PE stage, reaching its peak at the iβ stage. (DE: 1.2± 0.1; PE: 1.7± 0.1; EN: 3.5 ±0.3; iβ: 5± 0.6) (**Figure 22B, Figure 22C**). Finally, a qualitative evaluation of superoxide production was done with immunofluorescence staining in iβ live cells, showing positive results for superoxide within mitochondria. This underscores the existence of traits linked to senescence at this specific stage of development (**Figure 23**).

iPSC clone (n=3)	iPSC	DE	PE	EN	iβ
DRI2#3	4.2%±0.9	6.9%±2.6	4.1%±2	11.8%±2.2	14.4%±0.9
DRI2#4	5.9%±0.5	6.7%±1.1	11.8%±5.3	22.3%±6.7	20%±5
DRI2#9	3.6%±0.7	6.6%±2.5	7.6%±1.8	17.7%±5.9	32.2%±8.5
DRI2#13	7.7%±1.3	5.1%±1.1	10.4%±4.8	19.4%±4.4	27.4%±7.6
DRI2#14	6.9%±2.2	7.4%±3	9.4%±2.3	19.9%±2.2	33.5%±3.4
DRI2#15	5.9%±0.3	7.7%±3.6	11.5%±5.3	18.8%±1.1	32.1%±5.2

Table 3. MitoSOX positive cells through the differentiation stages for each clone. *All data are expressed as means ± SD. iPSC: induced pluripotent stem cells; DE: definitive endoderm; PE: pancreatic endoderm; EN: endocrine cells; iβ: iPSC-derived β cells.*



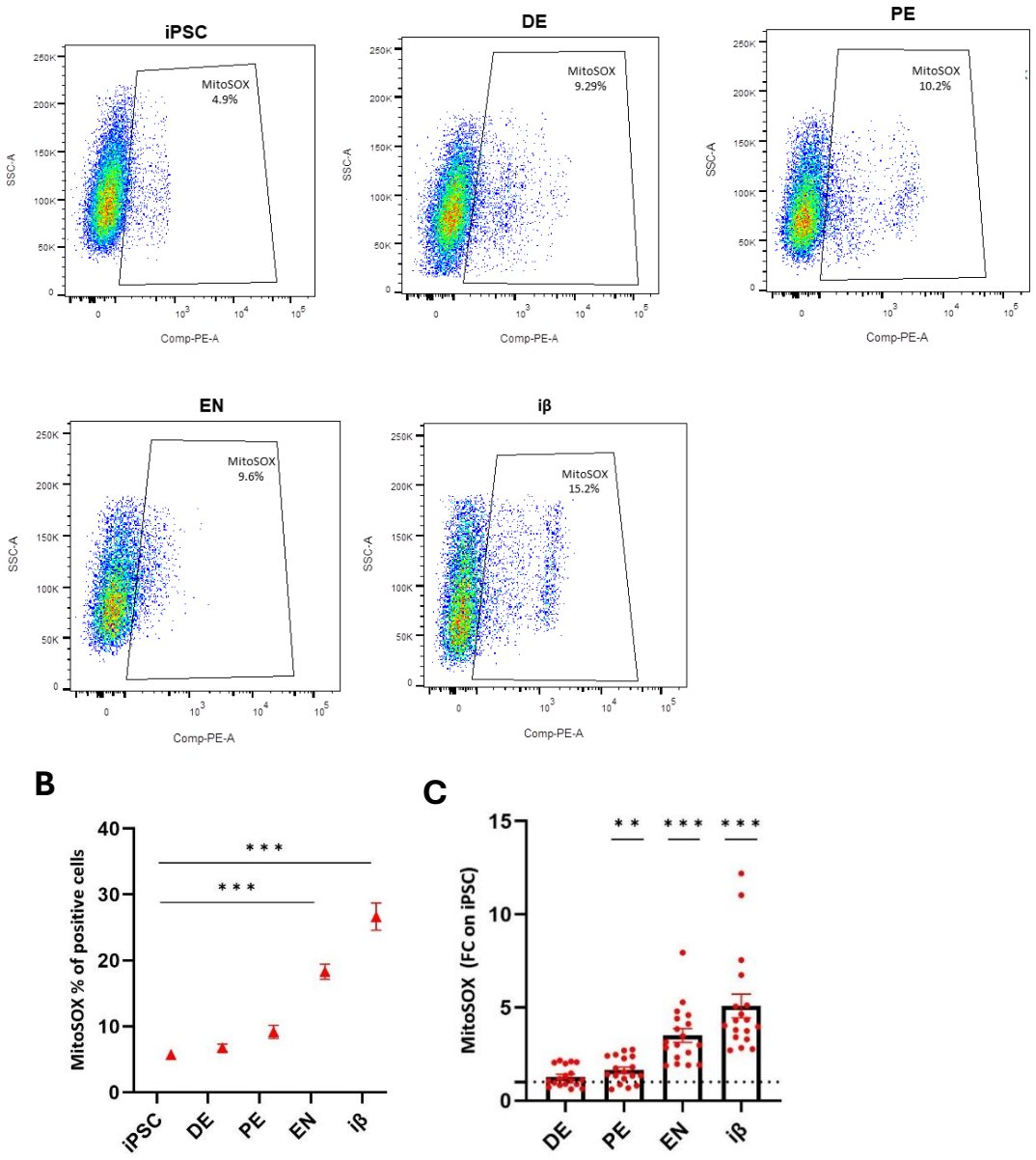


Figure 22. Superoxide production across the developmental stages from iPSC to β cells. *Gating strategy starting with the FSC-H/FSC-A profile, followed by selection based on SSC-A/FSC-A, and subgated for live cells. The percentage of MitoSOX positive cells is illustrated across the differentiation steps (iPSC, DE, PE, EN and iβ) in a representative experiment (A). Dot plot displays the percentage of MitoSOX-positive cells across the differentiation phases, combining data from the differentiation experiments for each clone. (B). MitoSOX expressed as fold change relative to iPSC (C) (Two-way ANOVA, One-sample t-test n=18). Results are expressed as mean ± SEM. *p<0.05; ** p<0.01; ***p<0.001. iPSC: induced pluripotent stem cells; DE: definitive endoderm; PE: pancreatic endoderm; EN: endocrine cells; iβ: iPSC-derived β cells.*

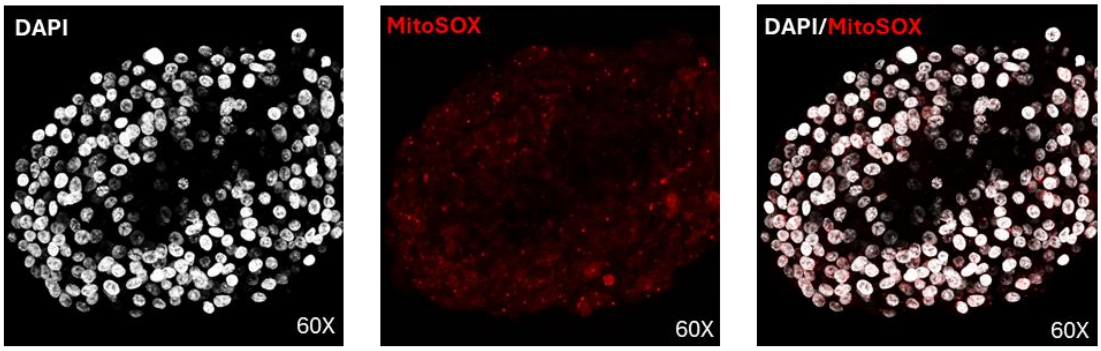


Figure 23. Representative immunofluorescence of iß cluster*. Single staining of live iß for MitoSOX (red). Nuclei are stained in white (Hoechst). Single channels and merged images are shown. Magnification 60X.*

5.5. Single-base substitution analysis reveals an increase in signature aging mutation throughout the differentiation process

Somatic mutations accumulate over time and are thought to contribute to the aging process by causing cellular dysfunction. To assess somatic mutation burden during differentiation, mutation frequency was quantified at the iPSC, PE, EN, and iβ stages. The results indicate a decrease in mutation frequency from iPSC to the EN stage, followed by a sharp increase in iβ cells (**Figure 24A**). Next, the distribution of SBS signatures across differentiation stages was analyzed to identify the predominant mutational processes. The main signatures identified were SBS5 (associated with aging), SBS40 (of unknown origin but frequently observed in various tissues), and SBS1 (a clock-like process linked to the deamination of methylated cytosines). Notably, the proportion of SBS5 increased progressively from the iPSC to iβ stage (iPSC: 14.25%; iβ: 68.06%), suggesting a cumulative effect of aging-related mutational processes during differentiation (**Figure 24B**).

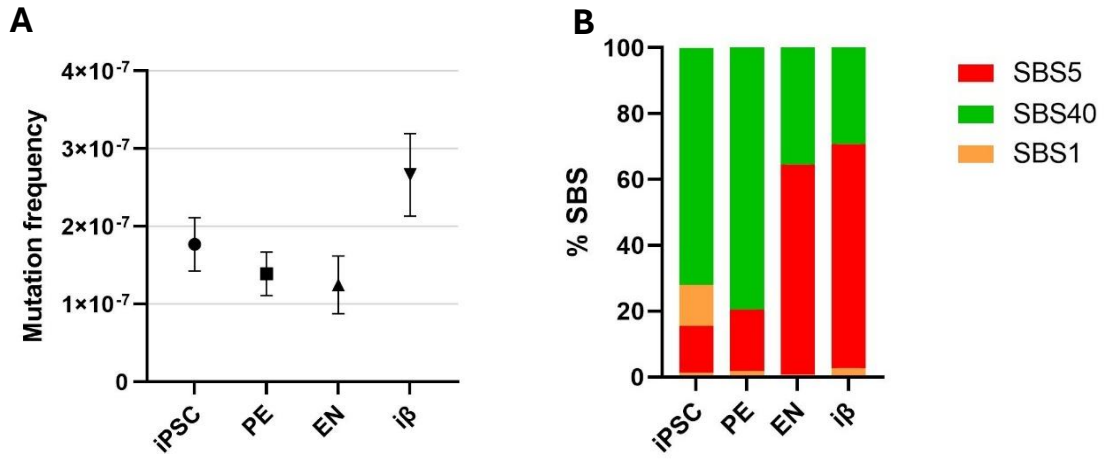


Figure 24. Somatic mutation outcome during the differentiation process. *Somatic mutations are quantified at four main stages of the differentiation process: iPSC, PE, EN, and iβ. The mutation frequency is determined by dividing the mutation count (total number of mutations observed) by the total duplex bases (the total number of base pairs successfully sequenced) (A). Bar graph of the percentage of the contribution of SBS signatures (SBS5, SBS40, and SBS1) at different stages (B). (n=2). Results are expressed as mean ± SEM.*

5.6 Transcriptomic data show an increase in senescence and SASP factors gene expression on EN and iβ stages

Since there are no universal markers to evaluate the senescence state of the cells, transcriptomic analysis was conducted to evaluate better this condition during iβ differentiation process. General senescence and SASP factors genes were analyzed at three main stages of the differentiation process: Day 0 (iPSC), Day 21 (EN), and Day 30 (iβ) (**Table 14**). The heatmap displayed an increase in general senescence genes at the EN and iβ stages, including genes associated with DNA damage such as *ATM*, cell cycle arrest markers like *p21, p16, CDKN1B*, and inflammation-related genes like *STAT3* and *GATA4* (**Figure 25A**). Moreover, most of the genes related to SASP factors were upregulated at the iβ stage such *as CXCL10*, *IGFBP3,* and *SERPINE1*, whereas others at the iPSC stage, such as *IGFBP4* and *IL6* (**Figure 25B**).

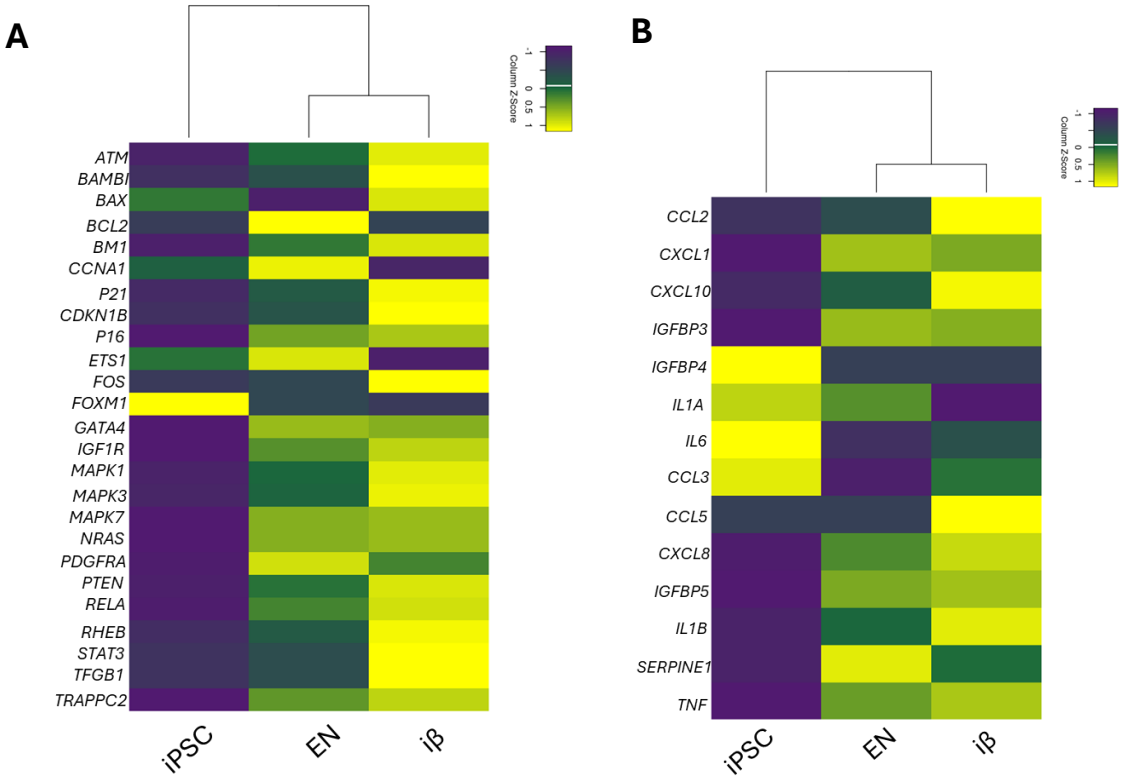


Figure 25. Heatmaps of differentially expressed genes at the stage of iPSC, EN, and iβ. *Differential expression of senescence-associated genes (A). Differential expression of general SASP genes (B). Heatmaps were created by combining the average gene expression data from all clones. (Spearman's ranking, n =12). iPSC: induced pluripotent stem cells; EN: endocrine cells; iβ: iPSC-derived β cells.*

5.7 Senescence in iβ differentiation is affected by *p16* and cells express specific β cell SASP factors

TP53 gene expression is known to be upregulated in response to stress, which could lead to both apoptosis and senescence (Mijit *et al*, 2020). At the PE stage, cells undergo strong mechanical stress to detach from the planar culture, leading to a significant increase in DNA damage, as indicated by the elevated expression of *ATM* and *ATR* genes. The expression level of the *TP53* at the stage of EN was significantly increased compared to the iPSC stage and this was accompanied by both an upregulation of apoptosis-like genes, as *CAS8* and *CYCS*, and one of the main senescence effectors, *p16.* On the contrary, the absence of a significant increase in *p21* gene expression, suggests that senescence is influenced by *p16* (**Figure 26A**). Additionally, specific transcriptomic analysis was

performed to check for the presence of known specific β cells SASP factors released by senescent islets, already published in other works by *Aguayo Mazzucato et al.* (Midha *et al*, 2021) (**Table 16**). Throughout the iβ differentiation process, these specific SASP factors were found significantly increased at the EN and iβ stages, marking the senescent state of the cells (**Figure 26B**).

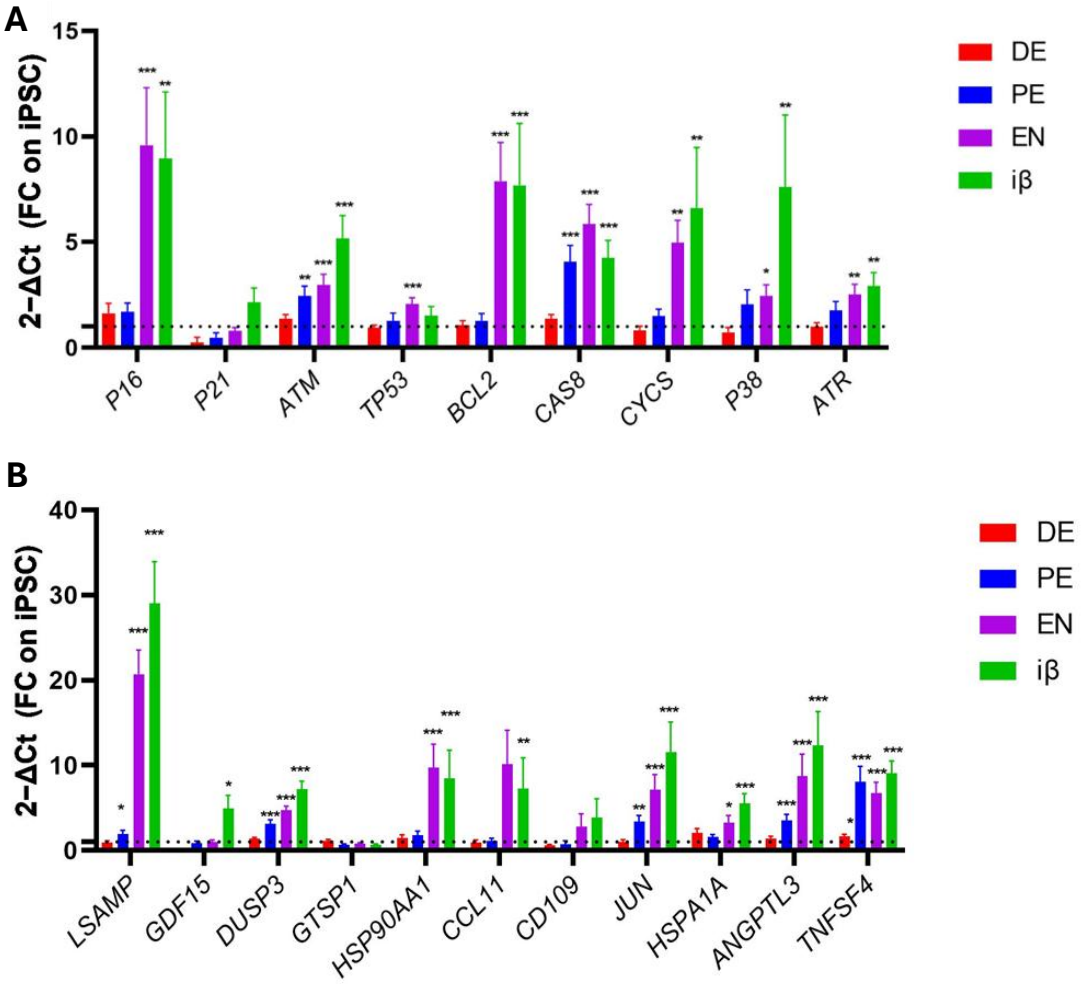
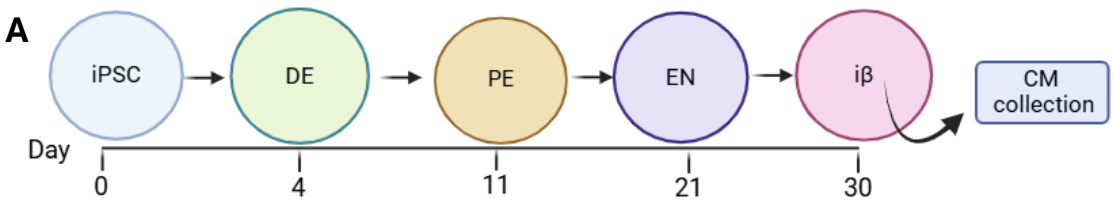


Figure 26. Specific senescence and SASP gene expression analysis during iβ differentiation. *The bar graph represents the fold change in gene expression levels at different differentiation stages (DE, PE, EN, iβ) relative to the iPSC stage. Expression of senescence and stress genes (A). Expression of specific iβ SASP genes (B). The analysis was performed based on the average expression of all clones throughout the differentiation process (One-sample t-test, n=18). Results are expressed as mean ± SEM. *p<0.05; ** p<0.01; ***p<0.001. iPSC: induced pluripotent stem cells; DE: definitive endoderm; PE: pancreatic endoderm; EN: endocrine cells; iβ: iPSC-derived β cells.*

5.8. Enrichment of SASP proteins in iβ secretome confirms the role of *p16* in iβ cell senescence

The iβ cells were cultured in serum-free media for 24 hours to generate the conditioned media (CM) which was then collected (**Figure 27A**). The iβ CM was used to analyze the SASP proteome and was compared to the negative control. The CM sample analysis was performed using the aptamer-based SOMAscan proteomics platform, which quantified the concentrations of 7000 different proteins. Based on these results, the analysis first focused on the secretion of SASP proteins known to be released from senescent islets (Midha *et al*, 2021). Additionally, the SASP factors known to be released from the unique secretory profile of senescent $p16^{+}$ (**Figure 27B**) and $p21^{+}$ (**Figure 27C**) β cells were analyzed (**Table 17, Table 18)**. When compared to the negative control, the iβ secretome exhibited the presence of SASP proteins. The analysis of *p16* and *p21* SASP factors revealed that the CM was enriched with these proteins with the *p16* group showing a significantly higher concentration compared to the *p21* SASP group. These findings align with the transcriptomic data, where the iβ population demonstrated a significant increase in *p16* expression (**Figure 27D)**. This confirms that the rise of senescence during the differentiation is reflected in the secretome of the later stage of the differentiation process.



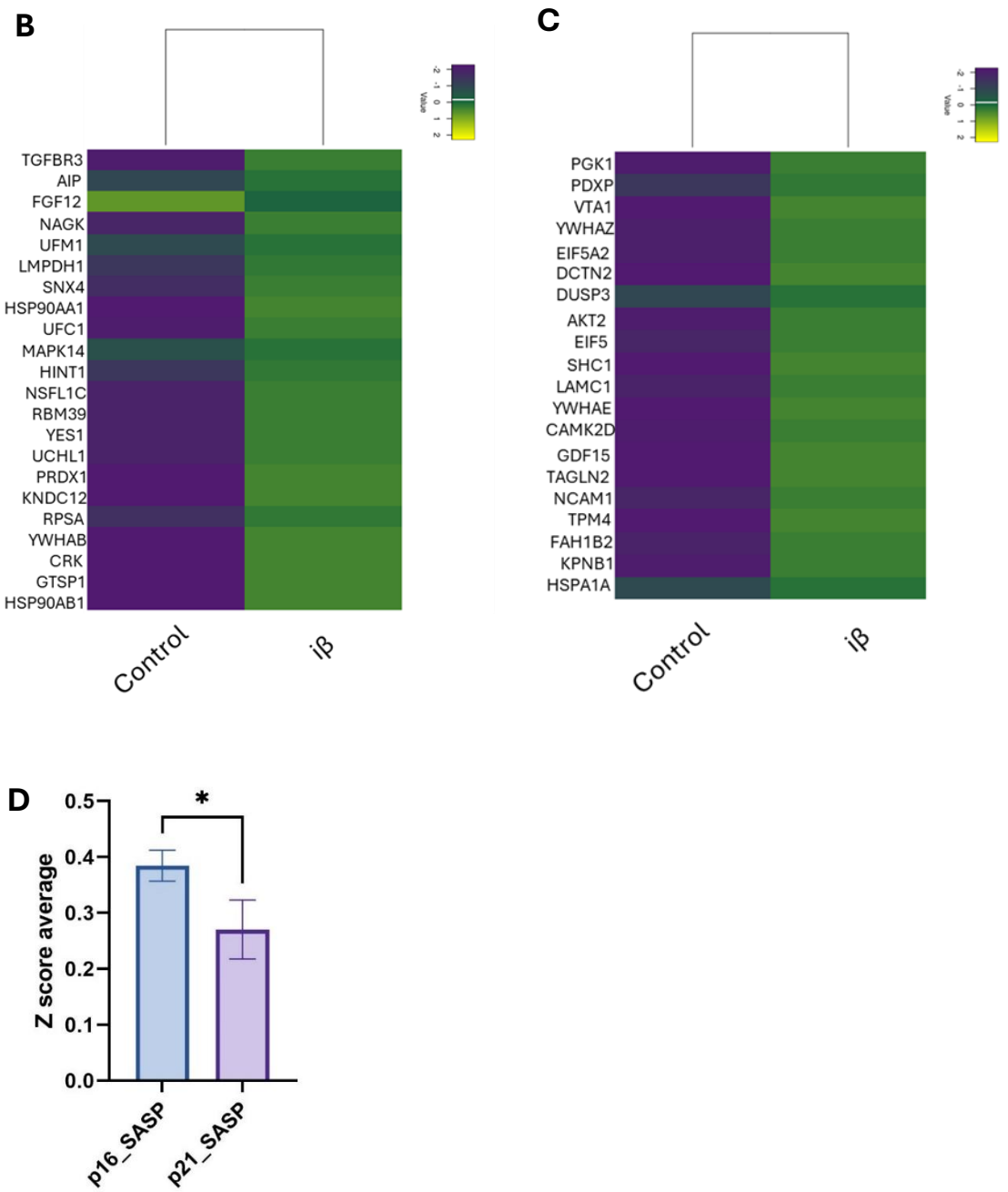


Figure 27. Proteomic analysis on iβ CM. *Representative scheme of the sample collection (A). The heatmap shows the release of p16 SASP factors (B) and p21 SASP factors (C) by iβ, compared to negative control. Z-score average distribution of released SASP factors from all the DRI2 clones at the iβ stage. The Z-score indicates the deviation of protein release levels from the mean across all samples, standardized to unit variance. Z score is used to compare the two SASP factors populations (D). The analysis was performed based on the average release of all clones at the iβ stage. (Mann Whitney t-test, n=6). Results are expressed as mean ± SEM. *p<0.05; ** p<0.01; ***p<0.001. iβ: iPSC-derived β cells; CM: conditioned media.*

5.9. iβ SASP factors induce secondary senescence and enhance insulin content in a human β cell line

To investigate the effects of the SASP factors released from iβ on the microenvironment as secondary senescence, the iβ CM was used to culture the human islet model EndoC-βH5 To ensure that the observed effects were not due to the basal medium, the EndoC-βH5were also cultured in parallel with iβ medium lacking SASP factors as a negative control. EndoC-βH5 cells were treated with iβ CM for 6 hours, followed by 2 days of recovery to appreciate the effects of the secondary senescence induced by the SASP factors (**Figure 28A**). The SA-β-Gal activity was evaluated, and showed a significant increase in cells cultured with iβ CM compared to the control (Control: 20.1%±0.1; iβ: 51%±6.8) (**Figure 28B**). Additionally, transcriptomic analysis revealed a significant increase in *p16* gene expression, while *p21* remained unaffected compared to the control without SASP, indicating that senescence was driven by *p16*. At the same time, iβ CM led to a significant increase in *NKX6.1* expression and a slight increase in *INSULIN* expression (**Figure 28C**). Quantification of insulin content, normalized to DNA concentration, revealed a significant increase in EndoC-βH5 treated with iβ CM (**Figure 28D**). These results were further supported by static GSIS data, which showed an increased secretion index in EndoC-βH5 cells treated with iβ CM (Control: 0.8±0.1; iβ CM: 1.2± 0.08) (**Figure 28E**).

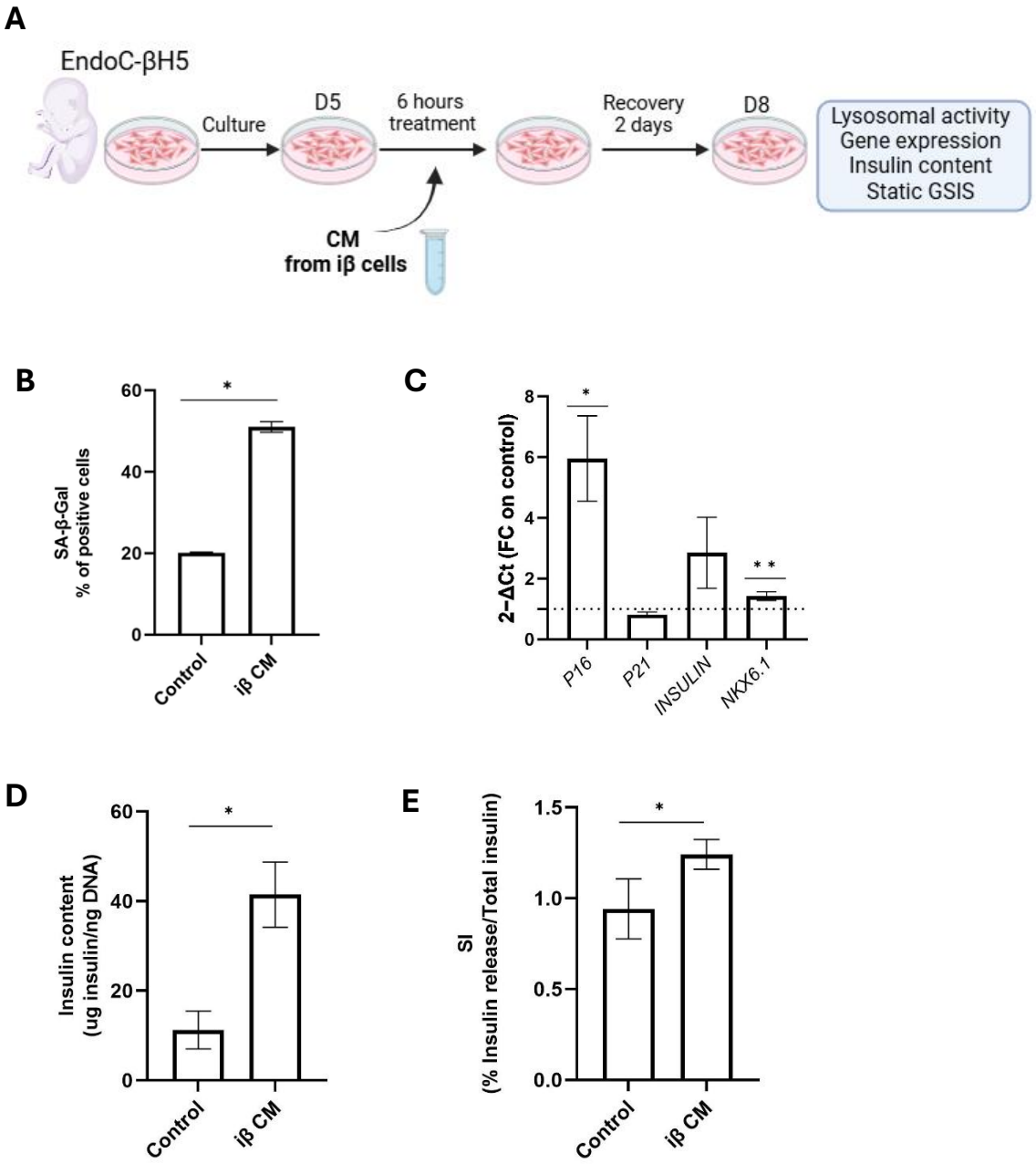
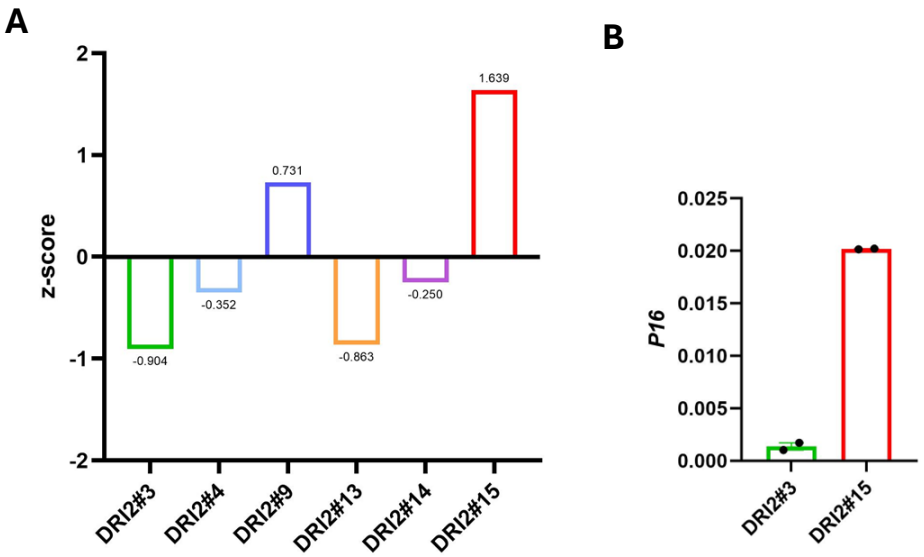


Figure 28. Evaluation of iβ SASP factors effects on EndoC-βH5. *Representative scheme of the workflow experiment (A). Percentage of SA-β-Gal activity of EndoC-βH5 compared to control (B). Columns represent the fold change in gene expression levels of EndoCβ-H5 (iβ CM treated) relative to control (C). Comparison of insulin content normalized to DNA concentration (D). The secretion index (SI) is calculated as the ratio of the percentage of insulin release (normalized to the total insulin) at high glucose (11 mM) to the percentage of insulin release (normalized to the total insulin) at low glucose (0.5 mM). (E). (One sample t-test, Unpaired t-test, n=4). Results are expressed as mean ± SEM. *p<0.05; ** p<0.01; ***p<0.001. iβ: iPSC-derived β cells; CM: conditioned media; SI: secretion index.*

5.10 iPSC clones exhibit different senescence profiles at the iβ stage

To explore the differences in terms of senescence between DRI2 clones (DRI2#3, 2#4, 2#9, 2#13, 2#14, 2#15) at the iβ stage, transcriptomic data based on *p16* gene expression were used to calculate the z-score. This analysis revealed that the clones exhibited different senescence profiles, as indicated by different senescence z-scores. Notably, DRI2#3 and DRI2#15 showed opposite profiles, suggesting divergent senescence-associated signatures (DRI2#3: -0.904; DRI2#15: 1.693) (**Figure 29A, Figure 29B**). These differing senescence profiles of 2#3 and 2#15 clones were also linked to their functional performance in dynamic GSIS (**Figure 29C, Figure 29D**). The area under the curve (AUC), calculated from the total area of insulin secretion, showed a trend toward a better response in the 2#15 clone compared to 2#3 (DRI2#3: 147±4.9; DRI2#15: 218.9±10.1) (**Figure 29E**). To confirm this data, the average z-score was calculated based on the expression of insulin machinery genes (**Table 14**). The z-score confirmed the same trends and profiles observed in dynamic GSIS, showing a similar division of DRI2#3 and DRI2#15 based on their senescence profiles. This suggests a parallel relationship between increased *p16*-related senescence and functionality (**Figure 29F**).



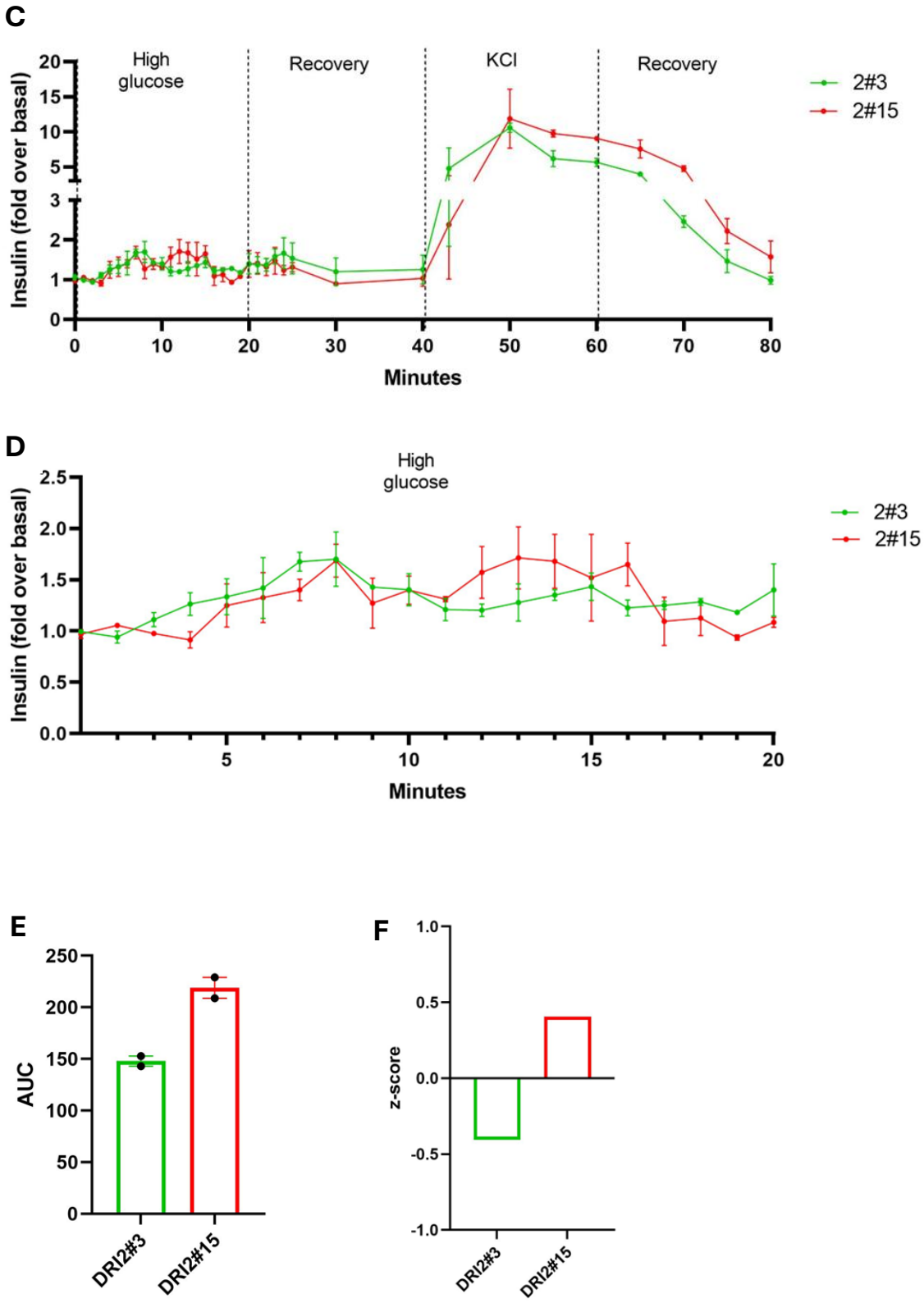
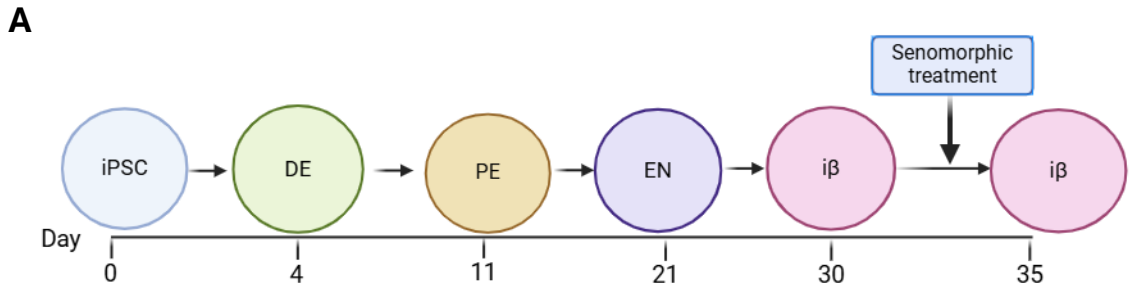


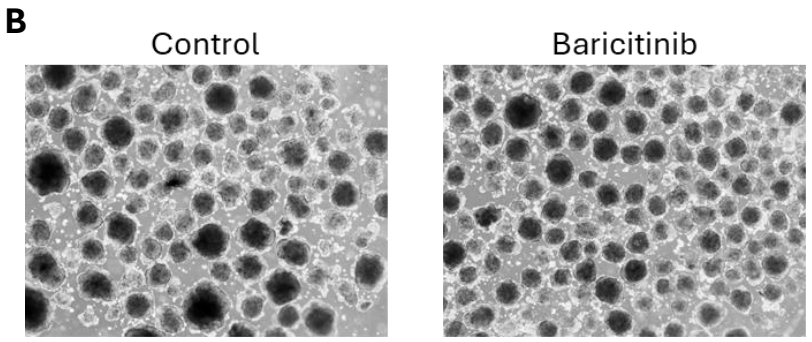
Figure 29. Evaluation of different senescence profiles between DRI2 clones. *Z-score overall distribution of senescence gene expression in DRI2 clones (2#3, 2#9, 2#13, 2#14, 2#15) at the iβ stage. The Z-score indicates the deviation of expression levels from the mean across all samples,*

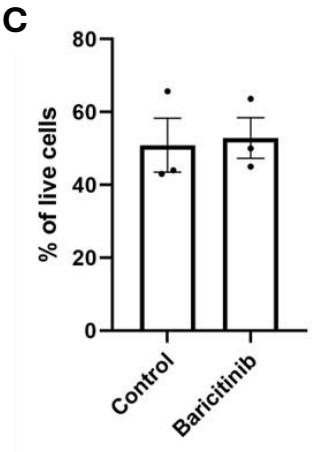
*standardized to unit variance. The division of DRI2 clones is based on their upregulation and downregulation of gene expression relative to the mean. (A). Differential expression of p16 comparing 2#3 and 2#15 clone (B). Insulin expressed as fold over basal of glucose-stimulated insulin secretion (GSIS) profiles of 2#3 and 2#15 clones (C). The profile of insulin release focuses on the high glucose step, highlighting the insulin secretion response at 11 mM glucose. (D). Area under the curve (AUC) calculated on insulin secretion profile of GSIS of 2#3 and 2#15 clones (E). Z-score overall distribution of insulin machinery gene expression in DRI2 clones (2#3 and 2#15) at the iβ stage. The Z-score indicates the deviation of expression levels from the mean across all samples, standardized to unit variance (E) (n=2 technical replicates for each clone). Results are expressed as mean ± SEM. *p<0.05; ** p<0.01; ***p<0.001.*

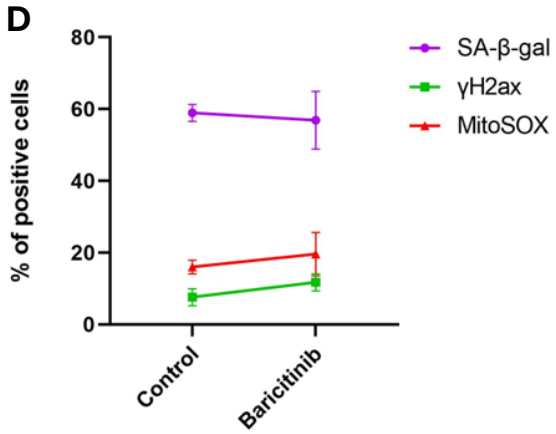
5.11. Senomorphic treatment on iβ decreases *p16* gene expression and insulin secretion

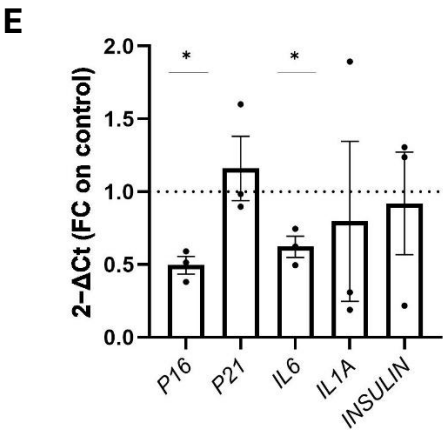
Senomorphic treatment was employed to assess the effects of senescence on β cell differentiation, using Baricitinib, a senomorphic drug that inhibits the JAK/STAT pathway. Baricitinib was used in the late stage of iβ differentiation process, from Day 30 to Day 35 (**Figure 30A**). After the treatment, the Baricitinib-treated group did not present any changes compared to the control, exhibiting well-defined, homogeneous clusters and no differences in the percentage of live cells, suggesting that Baricitinib as not toxic to the cells (Control: 50.9%±7.4; Baricitinib: 52.8%±5) (**Figure 30B, 30C**). Furthermore, flow cytometry analysis of senescence markers (SA-β-Gal, γH2AX, and MitoSOX) showed no detectable differences between the Baricitinib and control groups: SA-β-Gal (Control: 58.9± 4.1; Baricitinib: 56.9%±13.9 %); γH2AX (Control: 7.6%±4; Baricitinib: 11.7%±4.1%); and MitoSOX (Control: 16%± 3.2%; Baricitinib: 19.6%± 10.3%) (**Figure 30D**). However, transcriptomic analysis revealed the effects of Baricitinib at the mRNA level, showing a significant reduction in *p16* and *IL6* gene expression compared to untreated iβ, indicating an impact on the iβ senescence state (**Figure 30E**). These results were complemented by functional analysis of iβ after treatment. Dynamic GSIS revealed two different secretion profiles between the control and Baricitinib-treated group (**Figure 30F, 30G**). Indeed, when the area under the curve of the entire insulin secretion profile of both groups was calculated, the Baricitinib-treated group exhibited a significant functional decrease compared to the control, suggesting that senescence plays an important role in iβ function and maturation (Control: 339.2±93.1; Baricitinib: 124.1±25) (**Figure 30H**).


A
Senomorphic treatment
iPSC
DE
PE
EN
iβ
iβ
Day
0
4
11
21
30
35


B
Control
Baricitinib


C
% of live cells
80
60
40
20
0
Control
Baricitinib


D
% of positive cells
80
60
40
20
0
SA-β-gal
γH2ax
MitoSOX
Control
Baricitinib


E
2−ΔCt (FC on control)
2.0
1.5
1.0
0.5
0.0
*
*
P16
P21
IL6
IL1A
INSULIN

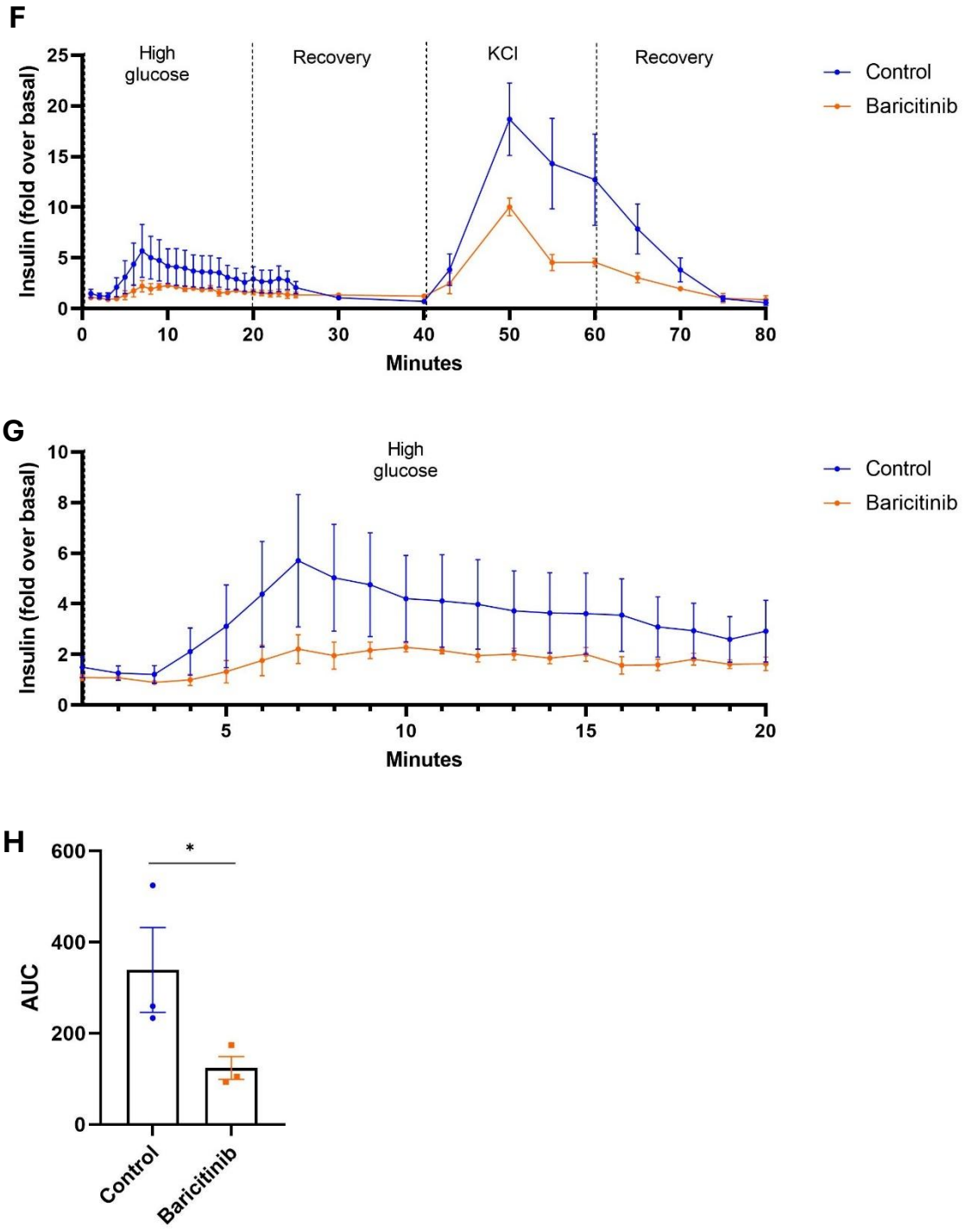


Figure 30. Effects of Baricitinib on iβ. *Representative scheme of the workflow experiment (A). Cell morphology of control and Baricitinib-treated groups. Magnification 4X (B). Flow cytometry analysis of the percentage of live cells and markers (SA-β-Gal, γH2AX and MitoSOX) in the control and Baricitinib-treated group (C, D). Columns represent the fold change in gene expression levels of Baricitinib-treated iβ relative to the control (E). Insulin expressed as fold over basal of glucose-stimulated insulin secretion (GSIS) profiles of control and Baricitinib-treated groups (F). The profile of insulin release focuses on the high glucose step, highlighting the insulin secretion response at 11 mM glucose. (G). Area under the curve (AUC) calculated on insulin secretion profile of GSIS of control and Baricitinib-treated groups (H). (One-sample t-test, Unpaired t-test, n=3). Results are expressed as mean ± SEM. *p<0.05; ** p<0.01; ***p<0.001.*

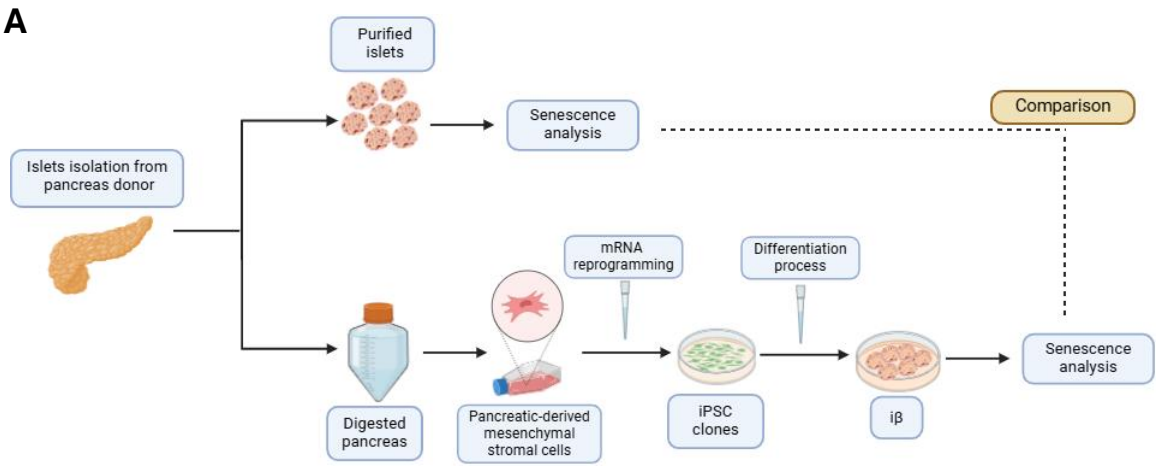
5.12. iβ cells and human islets derived from the same donor present distinct senescence profiles

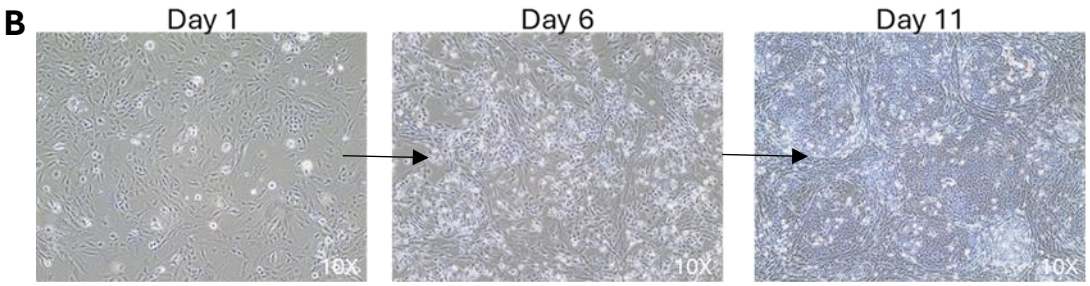
Purified islets were received and cultured after islets isolation from a donor to evaluate their senescence profile. At the same time, the digested pancreas material derived from the same donor, was cultured to obtain pancreatic-derived mesenchymal stromal cells (pMSCs) (Khiatah *et al*, 2019) (**Figure 31A**). These pMSCs were then used to generate iPSC clones through mRNA reprogramming: on Day 1 they still displayed fibroblasts-like morphology, which began to change by Day 6, and by Day 11 distinct iPSC colonies were fully formed (**Figure 31B**). The iPSCs colonies were manually picked and cleaned to establish two stabilized iPSCs clones (iPMSC#3, #56), which were subsequently differentiated into mature β cells (**Figure 31C**).

Since this is the first study to use a reprogramming protocol starting from pMSCs, the quality of the iPSC clones was evaluated based on their capacity to differentiate into β cells using key β cell identity markers such as PDX1, NKX6.1, INSULIN and GLUCAGON. The differentiated iβ cells exhibited a high percentage of these markers (PDX1: 37.2% ± 20%; NKX6.1: 71.9% ± 3.4%; INSULIN: 68% ± 7%; GLUCAGON: 5.6% ± 4.6%) (**Figure 31D**). Moreover, the function of the differentiated iβ was tested with dynamic GSIS, where the cells slightly responded to high glucose stimulation, whereas they responded at the KCl stage (**Figure 31E**).

During these differentiation processes, their senescence profile of the obtained iPSC clones from iPSC to β cell stage was also studied. Senescence markers and gene expression profiles were analyzed at two stages of the differentiation process: iPSC (Day 0) and iβ (Day 30). Flow cytometry data revealed a significant increase in SA-β-Gal (iPSC: 14.2%±9.9; iβ: 39.2%± 15.4) and MitoSOX (iPSC: 12.2%± 16.1; iβ: 18.4%± 5.7) from iPSC into β cells, with a slight decrease in γH2AX (iPSC: 4.2%±2.7; iβ: 3.5%±2.6) (**Figure 32A**). Moreover, at the stage of iβ, there was a significant increase in *ATM, JUN, INSULIN,* and *NKX6.1* expression, with a trend in *p16* increase, and no significant changes observed in other senescence and SASP-related genes (**Figure 32B**). Human islets were cultured overnight and their morphology was checked, showing a well-defined islets (**Figure 33A**). Flow cytometry analysis of human islets revealed that 56.6% of cells were alive and a percentage of 22.5% of cells presented oxidative damage, as indicated by MitoSOX staining for senescence markers (**Figure 33B, 33C**). To evaluate the

differences in the senescence profile of islets and iβ derived from the same donor, the percentage of cells positive for SA-β-Gal, γH2AX, and MitoSOX was compared, showing no significant difference between the two groups. Notably, SA-β-Gal positive cells were more in iβ than in islets (iβ: 39.2%± 15.4; Islets: 9.1%), while γH2AX (iβ: 3.5%±2.6; Islets: 10.5%) and MitoSOX (iβ: 18.4%± 5.7; Islets: 22.5%) levels appeared to be higher in the islets (**Figure 33D**). Transcriptomic analysis, which is more sensitive, revealed two distinct senescence profiles on iβ and islets based on the z-score of senescence and SASP gene expression (**Table 4**). Specifically, the islets presented a higher Z-score, indicating an increased expression of senescence and SASP-related genes (**Figure 33E**).





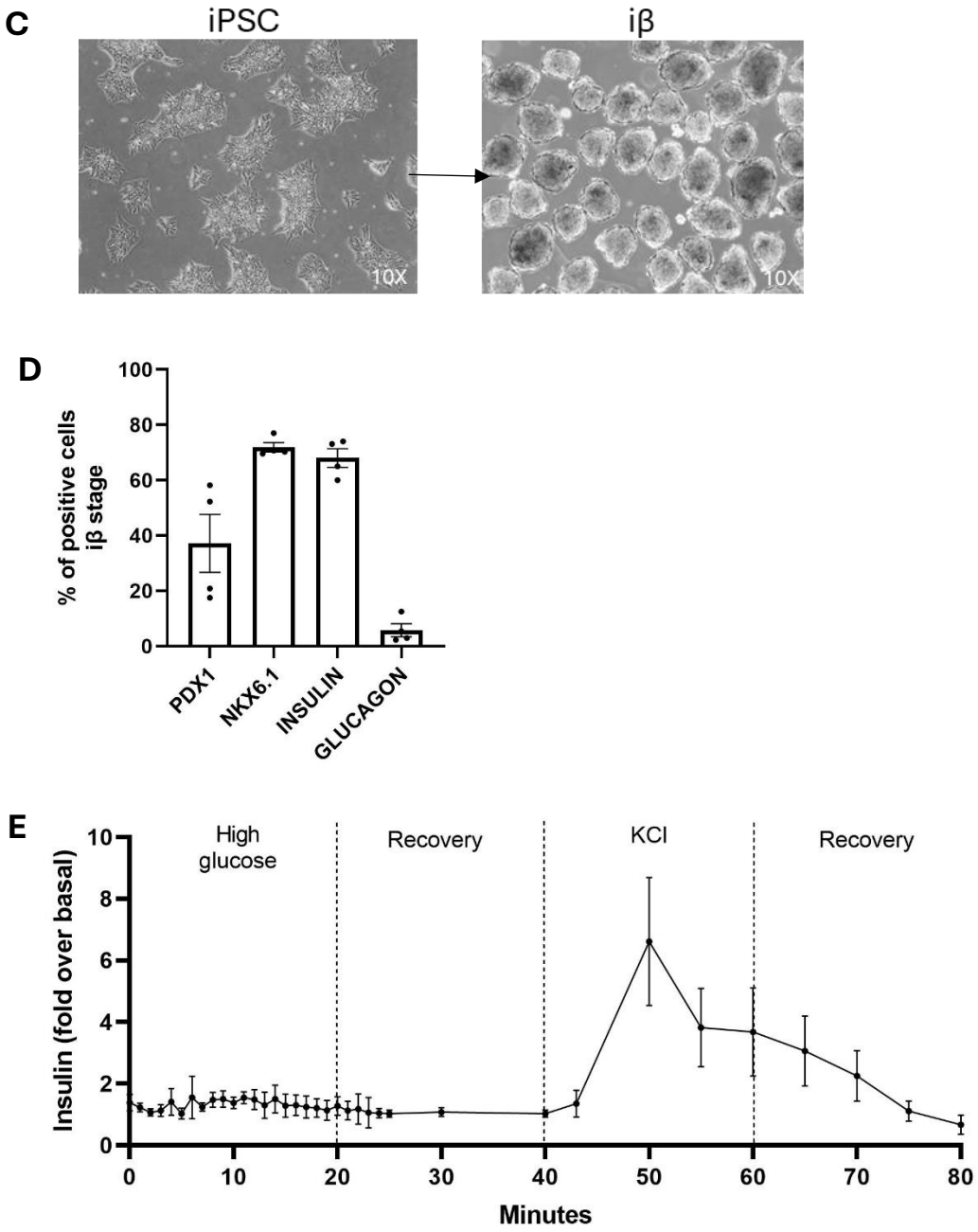
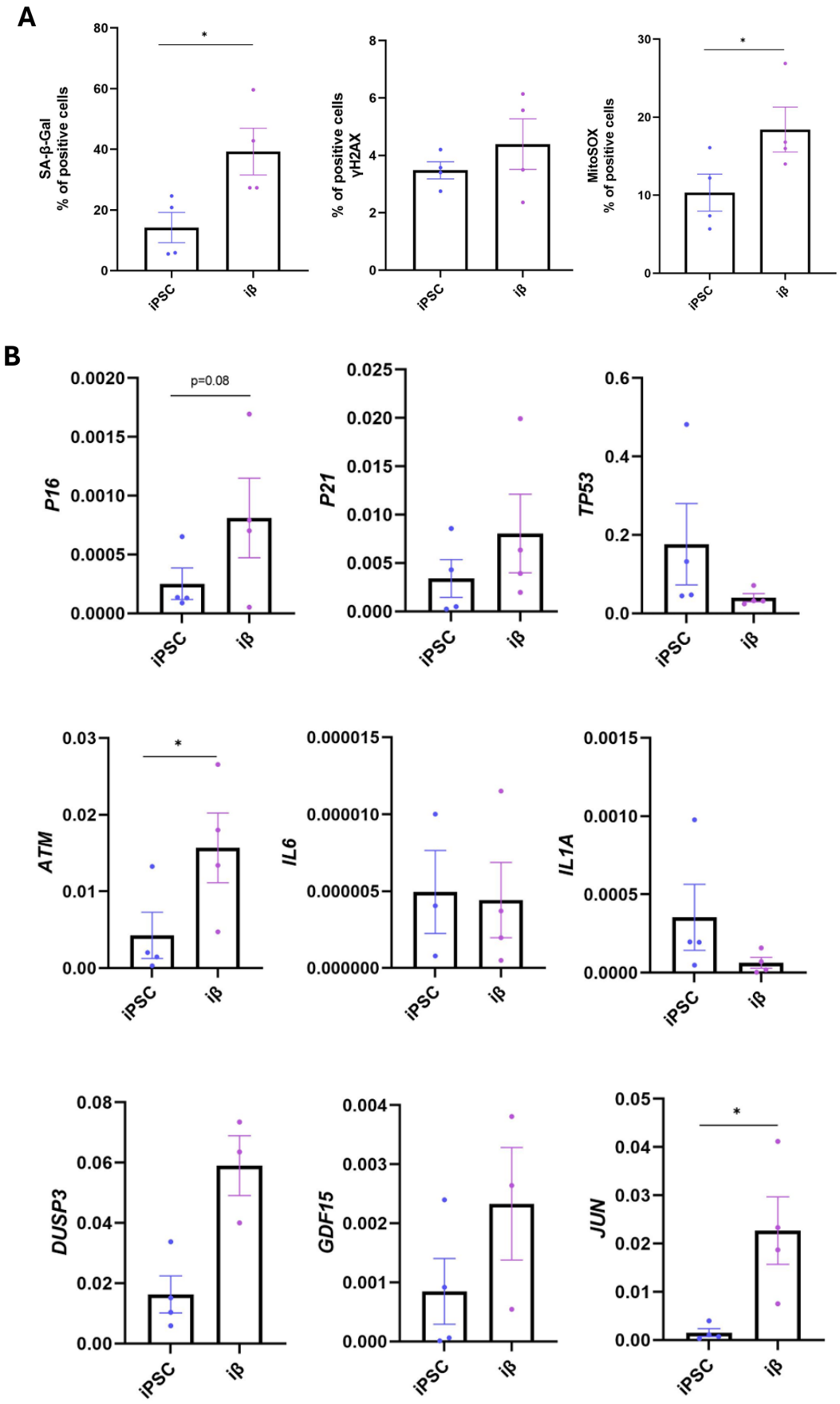


Figure 31. Reprogramming of pMSCs and differentiation into iβ. *Representative scheme of the workflow experiment (A). Morphological changes through the mRNA reprogramming, starting from Day 1 with pMSC culture until the formation of iPSC colonies at Day 6 and defined iPSC colonies at Day 11(B). Morphological changes from the obtained iPSC into β cells. Magnification 10X (C). Flow cytometry analysis showing the percentage of positive cells for PDX1, NKX6.1, INSULIN and GLUCAGON at the iβ stage (D). Insulin expressed as fold over basal of glucose-stimulated insulin secretion (GSIS) profiles (E) (n=2 technical replicates for each clone). Results are expressed as mean ± SEM. *p<0.05; **p<0.01; ***p<0.001. iPSC: induced pluripotent stem cells; iβ: iPSC-derived β cells.*


A
SA-β-Gal
% of positive cells
% of positive cells
γH2AX
MitoSOX
% of positive cells
iPSC
iβ
B
P16
P21
TP53
ATM
IL6
IL1A
DUSP3
GDF15
JUN
p=0.08
*

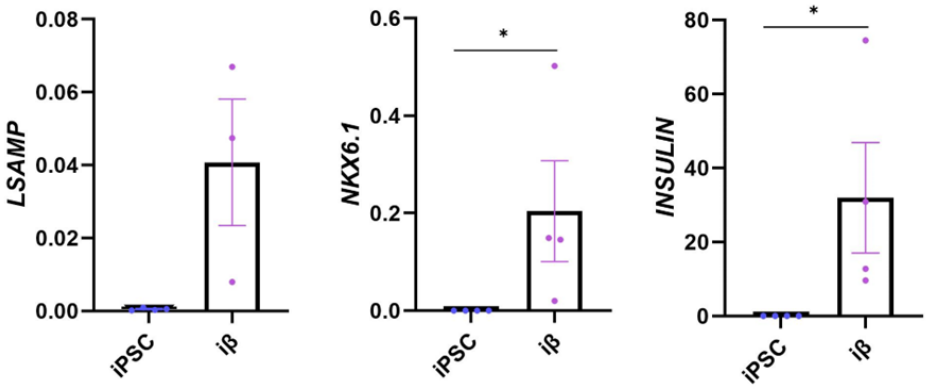
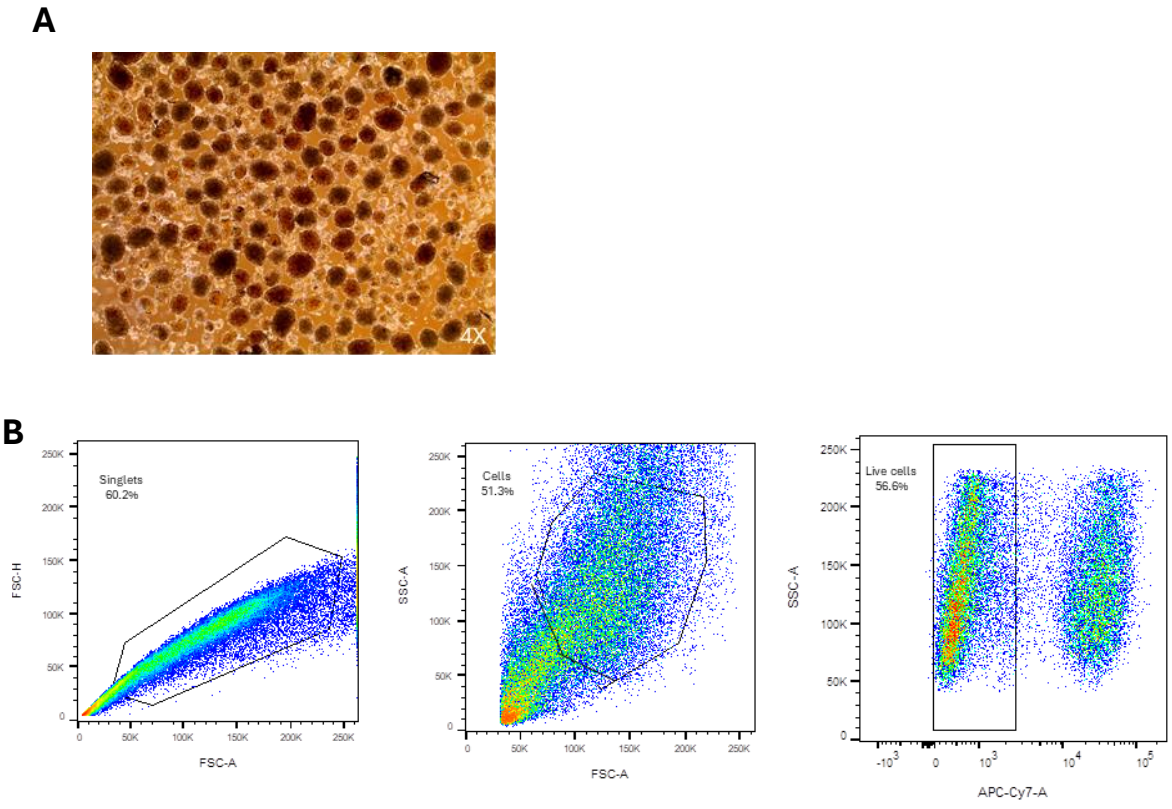


Figure 32. Senescence analysis of iβ in flow cytometry and transcriptomic analysis. *Percentage of positive cells for senescence markers (SA-β-Gal, γH2AX, and MitoSOX) comparing iPSC and iβ stages (A). Bar graphs show gene expression ($2^{-\Delta Ct}$) of senescence, SASP factors, and β cell identity genes comparing iPSC and iβ stage (B). (Unpaired t-test, Mann-Whitney t-test, n=2 technical replicate for each clone). Results are expressed as mean ± SEM. *p<0.05; ** p<0.01; ***p<0.001. iPSC: induced pluripotent stem cells; iβ: iPSC-derived β cells.*



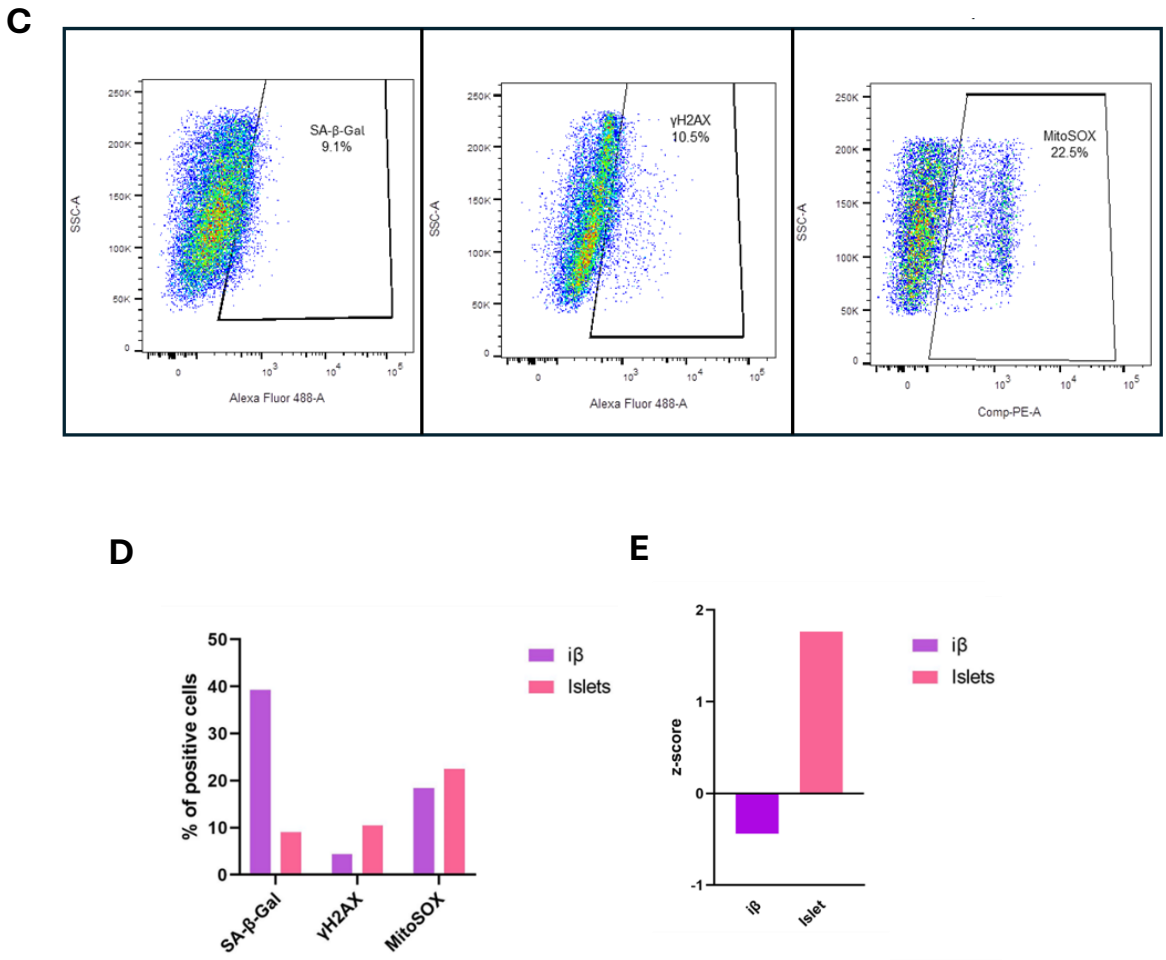


Figure 33. Senescence analysis in human islets and comparison with iβ derived from the same donor. *Representative picture of human islets received from the donor. Magnification 4X. (A). The analysis of human islets begins with a gating strategy on FSC-H/FSC-A profile, followed by selection based on SSC-A/FSC-A, and subgating for live cells (B). Percentage of positive cells for senescence markers (SA-β-Gal, γH2AX, and MitoSOX) of human islets (C). Bar graphs show flow cytometry data based on the percentage of positive cells senescence markers (SA-β-Gal, γH2AX, and MitoSOX) comparing iβ and human islets from the same donor (D). Z-score overall distribution of senescence and SASP gene expression in iβ and islets from the same donor. The Z-score indicates the deviation of expression levels from the mean across all samples, standardized to unit variance. Islets and iβ classification based on Z-score. (E). (n=1 for islets and n=2 technical replicates for each clone). iβ: iPSC-derived β cells.*

Gene	iβ (2^-ΔCt)	Islets (2^-ΔCt)
p21	0.008043438	0.504519347
p16	0.00081032	0.08349045
TP53	0.039906673	0.060980192
ATM	0.015686278	0.04001222
IL6	4.42264E-06	0.005193396
IL1A	6.28572E-05	0.001702328
JUN	0.022670393	0.065160049
DUSP3	0.180774306	0.285695259
GDF15	0.013555273	0.309638335
LSAMP	0.146923548	0.013159254

Table 4. Islets and iβ senescence and SASP gene expression from the same donor*. iβ gene expression is presented as the mean expression of two differentiations for each clone (n=2 technical replicates for each clone). Islets gene expression is one sample. Data are expressed as 2^-ΔCt. iβ: iPSC-derived β cells.*

6. Discussion

Type 1 Diabetes (T1D) is a worldwide chronic, immune-mediated disease characterized by the destruction of insulin-producing β cells in the pancreas (DiMeglio *et al*, 2018). This condition leads to a decrease in insulin secretion, development of hyperglycemia, and ultimately the onset of clinical T1D, which is correlated to secondary complications, like renal failure, cardiovascular disease, retinopathy, and neuropathy (Nathan, 2014). Although the use of exogenous insulin administration can ameliorate hyperglycemia, it cannot provide physiological regulation of blood glucose. Therefore, the ideal treatment for diabetes should restore both insulin production and insulin secretion regulation by glucose in patients. Clinical pancreas or islet transplantation has been considered a feasible treatment option for T1D patients with poor glycemic control, especially in adults, but is rare in children due to the low incidence of chronic complications, preference for intensive insulin therapy, and surgical challenges (Kochar & Jain, 2021). For this reason, islet cell transplants are a promising alternative. Despite the progress, donor shortages and complications related to immunosuppression present significant challenges for the widespread adoption of islet transplantation. For this reason, intensive studies have been conducted for the generation of insulin-producing cells *in vitro* since pluripotent stem cells have been proposed for application in regenerative medicine (Chen *et al*, 2020). Indeed, hPSCs (both ESC and iPSCs) hold great promise for the manufacturing of an unlimited number of specific human cell types *in vitro*, making them a valuable resource for transplantation therapies, including pancreatic β cells (Kim *et al*, 2020). In our work, we used two lines of iPSCs. The first one, called DRI2, was obtained from $CD34^+$ enriched blood cells from a 25-year-old healthy donor using Sendai virus reprogramming, and we differentiated six different clones (DRI2#3, 2#4, 2#9, 2#13, 2#14, 2#15) from this line into β cells. The second one, called iPMSC, was obtained from pancreatic mesenchymal stromal cells (pMSCs) from a 51-year-old healthy donor using mRNA reprogramming, and we differentiated two clones (iPMSC#6, #53) from this line into β cells.

Thanks to significant advancements over the past two decades, SC-β cells can now be generated through *in vitro* differentiation, and they are already being transplanted in clinical trials. Extensive experience in islet transplantation has refined our understanding

of optimal purity, dosage, and infusion protocols, as well as the selection of suitable transplantation sites. In recent years, various strategies have been developed to protect transplanted islets from immune rejection, including immunosuppressive drugs and encapsulation technologies.

However, a key challenge remains: the long-term survival and functional persistence of these SC-islets in recipients is still not fully understood (Gamble *et al*, 2018). Indeed, in our study, we focused on understanding the mechanisms behind the aging of β cells from iPSCs, exploring a potential connection between aging and long-term functionality. In the context of islet transplantation, several studies have evaluated the longevity of transplanted islets and the necessity for re-infusion procedures. A specific ten-year outcome study of islet transplantation alone or after kidney transplantation in T1D patients was conducted to evaluate the long-term results. Graft survivals were 82% and 78% after 5 and 10 years, respectively, in the entire study group (Vantyghem *et al*, 2019). A comprehensive study in Canada involving 255 T1D patients who underwent islet transplantation reported a median graft survival of approximately 5.9 years. Notably, 70% of the grafts remained functional during the follow-up period, with insulin independence achieved in 32% of patients at the five-year mark, decreasing over time (Marfil-Garza *et al*, 2022). A ten-year follow-up study within the Swiss-French network, indicated that islet graft survival was 95.55%, 79.9%, and 51.9% respectively at 1, 5 and 10 years (Lablanche *et al*, 2021). In summary, while islet transplantation offers significant benefits in managing T1D, with many patients experiencing improved glycemic control and reduced insulin requirements, the longevity of graft function varies, and insulin independence may not be sustained long term. This is related to a combination of immune rejection, islet loss post-transplant, decline in β-cell function, and inadequate engraftment, requiring up to three sequential islet infusions, aiming to achieve adequate metabolic control. In the context of the SC-islets transplantation, pre-clinical studies showed that SC-islets demonstrated better vascular and neural engraftment than human islets after 3 months from the transplant, indicating positive long-term implications (Thorngren *et al*, 2024). The data from the SC-islets human clinical trial from ViaCyte with PEC-01 showed an initial survival, then compromised due to immune response and fibrosis. With the use of the open-device PECs, six out of 17 patients produced glucose-reactive C-peptide six months after transplantation, indicating that the SC-islets not only survived

but also functioned to some extent, though C-peptide levels were still low, which could point to some limitations in the long-term survival and function of the SC-islets (Ramzy *et al*, 2021). With Vertex clinical trials, VX-880 demonstrated islet cell engraftment and glucose-responsive insulin production by Day 90 (REICHMAN *et al*, 2023). The Chinese clinical trial demonstrated that the recipient's insulin requirements began to decline within two weeks post-engraftment, achieving complete insulin independence by day 75, and it was sustained for at least 12 months, highlighting the potential for durable graft function (Wang *et al*, 2024b). Human β cells are remarkably long-lived, with evidence suggesting minimal turnover in adulthood. Studies indicate that human β cells primarily form during the first 30 years of life and persist for decades, with limited proliferation in later years. Markers of cellular aging, such as lipofuscin accumulation, further support the notion that β cells in adults are largely postmitotic and may endure for the organism's lifetime (Kushner, 2013). However, the duration and persistence of SC-islets in recipients still need further research to be fully established. Given the chronic nature of T1D, it becomes imperative to transplant cells with a lasting lifespan, preferably spanning decades or even a lifetime. Since SC-β cells undergo a non-physiological *in vitro* transformation with an artificial and accelerated process, this raises critical questions about their cellular age.

To study the cellular age from iPSC into β cells, we used six clones from an iPSC line, and we specifically evaluated the senescence state of the cells at particular time points of differentiation. Cellular senescence is characterized by a permanent arrest in cell division while maintaining metabolic activity, triggered by DNA damage, telomere shortening, or oncogene-induced stress (OIS). This process is mainly controlled by the *P53/p21* and *p16/Rb* pathways, where *p21* initiates the arrest and *p16* sustains it in a stable, irreversible state (Stein *et al*, 1999). Since no single marker can define senescence, a combination of features, like SA-β-Gal activity, γH2AX expression, and increased mitochondrial ROS, are required for accurate detection. Senescent cells also release a mix of SASP factors, such as cytokines, chemokines, and growth factors, which influence surrounding cells and tissue environments (Suryadevara *et al*, 2024). Although senescence supports development and tissue repair, the accumulation of senescent cells can promote inflammation and age-related dysfunction (Hernandez-Segura *et al*, 2018).

During the differentiation process from iPSCs to β cells, our cells may undergo senescence. The role of β cell senescence is still debated, with different hypotheses proposed. One widely accepted theory suggests that aging leads to an accumulation of senescent β cells, which contribute to impaired glucose sensing and insulin secretion, playing a role in the development of T2D. Key hallmarks of β cell senescence include the upregulation of DNA damage markers (γH2AX) alongside increased expression of *p16* and *p21*, elevated SA-β-Gal activity, activation of anti-apoptotic pathways, and the establishment of a functional SASP (Cha *et al*, 2023). However, some studies propose an alternative perspective, suggesting that β cell senescence, particularly the increase in *p16* expression, supports better maturation and enhanced functionality of β cells (Helman *et al*, 2016b; Patra *et al*, 2024) .

In this study, we investigated senescence during the differentiation process into β cells in six iPSC DRI2 clones derived from the same donor. The protocol of differentiation of human iPSC into β cells is well established in our lab and is based on Otonkoski's lab protocol, with a 7-stage protocol that follows pancreatic developmental stages, exploiting 2D and 3D cultures. The Otonkoski protocol at Stage7 (Day 30), typically presents 40% $INSULIN^+$ cells, 15–20% $INSULIN^+GLUCAGON^+$, 5% $GLUCAGON^+$ cells, 4% $SOMATOSTATIN^+$, and 13% serotonin-producing enterochromaffin-like cells (ECs), with the remaining 20–25% consisting of endocrine progenitors and undefined cells (Balboa *et al*, 2022). Our cultures displayed a similar complexity, with 19% $PDX1^+$ cells, 40% $NKX6.1^+$ cells, 45.5% $INSULIN^+$ cells, and 11% $GLUCAGON^+$ cells. Specifically, immunofluorescence at iβ stage revealed many $NKX6.1^+INSULIN^-$ cells, which may represent endocrine progenitor cells or ECs. Furthermore, employing TaqMan array card technology to measure the expression of 43 genes associated with β cell development and function, we found that terminally differentiated cells expressed genes related to glucose-stimulated response and insulin secretion, demonstrating their effective differentiation. We observed an increased expression of genes related to insulin secretion (*ABCC8*), exocytosis-related genes (*KCNJ11*), the glucose transporter *SLC2A2*, and receptors associated with β cell function (*GCGR*), providing support for the reaching of mature β cells. Moreover, the resultant population exhibited specific biological markers of primary β cells such as *NEUROD1*, *PDX1*, *NKX6.1*, and mature β cell indicators such as *INSULIN* and *UCN3*. However, at the iβ stage, the expression of *NEUROG3* and *GLUCAGON* was

highly represented, marking that our samples presented a mixed composition of cells from different developmental stages. Moreover, iβ responded to the exposure of different glucose stimuli (Low glucose 0.5 mM and High glucose 11mM) and depolarizing KCl. The iβ we obtained did not present a strong insulin release in the presence of glucose alone. Indeed, to achieve a robust response to glucose stimulation, they required IBMX (3-isobutyl-1-methylxanthine), which is a non-specific phosphodiesterase (PDE) inhibitor that increases intracellular cyclic AMP (cAMP) and enhances calcium-mediated exocytosis of insulin granules (Siegel *et al*, 1980). *Pratt et. al* found that inhibiting PDE with IBMX potentiated GSIS in INS-1 cells. Specifically, PDE inhibition increased cAMP levels, and improved insulin secretion under high glucose conditions. Furthermore, PDE inhibition in human β cells enhanced insulin secretion, indicating its potential as a strategy to boost GSIS in pancreatic β cells (Pratt *et al*, 2019). In a previous study conducted in our lab by Pellegrini *et al*., insulin secretion from iβ cells was assessed in response to glucose and KCl. The iβ cells showed a weak response compared to human islets (HI) and EndoC-βH1 cells. However, the addition of IBMX enhanced insulin secretion in all three cell types. These findings suggest that iβ cells have the potential to secrete insulin, but their response is still immature, with lower basal secretion levels than HI cells, indicating an underdeveloped functionality similar to EndoC-βH1 cells (Pellegrini et al, 2018). This data suggested that the dependency on IBMX indicates an immature (still at the endocrine progenitor stage) or dysfunctional β cell phenotype of our iβ, as mature β cells should be able to mount a strong insulin secretion response to glucose alone.

We examined the cellular age across five distinct time points: iPSC, DE, PE, EN, and iβ, evaluating the presence of three markers associated with senescence. Specifically, we employed SA-β-Gal to evaluate lysosomal activity, γH2AX to evaluate DNA damage, and MitoSOX to assess mitochondrial dysfunction and oxidative damage. Our analysis aligns with the notion that senescence occurs during differentiation. Indeed, some studies suggest that the aging process can be reactivated during iPSC differentiation into mature cells. For example, iPSC-derived retinal pigment epithelial (RPE) cells and fibroblasts show early signs of senescence, such as abnormal morphology, increased SA-β-Gal, and stress sensitivity. iPSC-derived fibroblasts also secrete more SASP factors than primary fibroblasts, highlighting the influence of the differentiation protocol on cell function

(Feng *et al*, 2010; Goyer *et al*, 2024). Additionally, our differentiation process from iPSC into β cells requires at least 30 days to end, and some studies presented that prolonged culture times for differentiating iPSC-derived cells into cardiomyocytes, neurons, and MSCs, can trigger aging features, including increased ROS, altered DNA methylation, and elevated expression of senescence markers like *p21* and SA-β-Gal activity (Pitrez *et al*, 2024). The three markers under consideration (SA-β-Gal, γH2AX and MitoSOX) exhibited a significant increase from iPSC stage to the EN and iβ stage. However, it is important to mention that our senescence analysis was conducted on the entire population at the late stage of differentiation, rather than specifically on the β cell population. This represents a key limitation of the study, as our differentiated cultures are a heterogeneous mixture of cell populations, including 45.5% $INSULIN^+$ cells, 11% $GLUCAGON^+$ cells, and other non β endocrine populations. For instance, we do not know whether the senescence markers we detected are primarily derived from the β cells, or whether other endocrine cell types, such as α cells, also play a significant role. To resolve this limitation in future studies, specific strategies could be employed to assess senescence in defined cell populations. For example, immunofluorescence staining with multiple markers could allow the co-localization of senescence features with β cell identity markers. Additionally, sorting cells based on SA-β-Gal activity and analyzing the expression of β cell markers in each subpopulation could help to clarify the contribution of senescent β cells versus non β cells. Alternatively, single-cell RNA seq could be used to deconvolute the transcriptional profiles of individual cell types within the culture, directly identifying senescence-associated gene expression patterns in β cells compared to other populations.

Numerous studies have demonstrated that cellular aging in long-lived organisms is a complex and stochastic process characterized by the gradual accumulation of molecular damage and genomic alterations over time (López-Otín *et al*, 2013; Enge *et al*, 2017). While both aging and senescence are interconnected biological processes, it is important to distinguish between them: aging refers to the progressive decline in function and integrity over time, whereas senescence is a stress-induced, often acute, cellular program leading to a stable cell cycle arrest and a distinct secretory phenotype (de Magalhães & Passos, 2018). In particular, when studying mutational signatures, the observed patterns reflect processes associated with chronological aging rather than senescence per se. Senescent cells can emerge rapidly in response to acute damage and do not necessarily

accumulate mutations in the same way aging cells do. To explore the emergence of somatic mutations during differentiation, we performed TwinStrand Duplex Sequencing on DNA samples collected at multiple stages of the differentiation process (iPSC, PE, EN, and iβ). The core principle of Duplex Sequencing involves sequencing both strands of a DNA molecule and comparing the results to eliminate errors that affect only one strand, eliminating sequencing errors, and enabling the detection of ultra-low frequency variants that are often undetectable by conventional NGS methods. Duplex Sequencing technology has been utilized to study somatic mutations associated with aging. One study, for instance, applied Duplex Sequencing to profile mitochondrial genomes, identifying mutational hotspots and providing insights into mitochondrial DNA mutations throughout aging (Serrano *et al*, 2024). Our sequencing results revealed a noticeable pattern of increasing base alterations from iPSC to iβ, indicating the occurrence of an aging process that induces the accumulation of somatic mutations during differentiation. Using COSMIC mutational signature database, three main Single-Base substitutions (SBS) were found: SBS1, SBS40, and SBS5. SBS signatures are patterns of somatic mutations found in cancer and normal tissues, reflecting different mutational processes. Unlike SBS1 and SBS5, which are well-characterized aging-related signatures, SBS40 remains poorly understood, with an unknown underlying mechanism. SBS1 and SBS5 are commonly associated with "clock-like" mutations in normal aging and endogenous mutation. In particular, SBS1 is primarily driven by DNA replication at a consistent rate, whereas SBS5 accumulates with time in all cell types implying a replication-independent mechanism linked to DNA repair errors (Sondka *et al*, 2024; Spisak *et al*, 2024). Our data showed that SBS1 was mostly present at the iPSC stage, suggesting that the reprogramming and the rapid proliferation with extensive cell divisions led to the increase of SBS1, acting as a replication-driven "clock-like" signature. On the contrary, the enrichment of SBS5 at the iβ stage suggested that this mutational accumulation at this stage is not dependent on replication but influenced by endogenous stress and DNA repair processes. It is possible that, since iβ cells are differentiated and postmitotic, their exposure to oxidative stress and imperfect DNA repair mechanisms could drive to slow accumulation of SBS5. Importantly, it must be noted that these findings remain preliminary. Our analysis was conducted on two differentiation replicates from a single representative clone, and the sequencing covered both coding and non-coding regions of

the genome without the resolution to map mutations to specific genes or functional outcomes. Therefore, while we can detect specific patterns of somatic mutations with aging-related signatures, we cannot directly attribute these mutations to precise phenotypes.

In summary, our study reveals that the differentiation of iPSCs into β cells undergoes an aging process. To better understand the molecular mechanisms underlying the observed senescence with flow cytometry, we examined the expression levels of 39 genes associated with the senescence process. We conducted RNA expression analysis on six distinct clones of iPSCs that were differentiated into β cells. In the first part of the work, gene expression was performed at three key time points: during the iPSC stage, EN stage, and in the mature β cells. The gene panel analyzed encompassed genes related to the general SASP and markers associated with senescence. Most of the genes related to general senescence were increased at the iβ stage, with the cell cycle inhibitors such as *p16*, *p21,* and *CDKN1B* and genes involved in OIS and stress response as *MAPK1, MAPK3*, and *MAPK7* (Bloom & Cross, 2007; Anerillas *et al*, 2020). Moreover, the iβ stage presented an increase in *NRAS, ETS1,* and *FOS*, which are involved in regulating senescence by promoting the upregulation of *p16* and *p21*, as well as modulating inflammatory and stress responses. At the iPSC stage, there was the upregulation of *FOXM1*, which normally promotes cell cycle progression but is downregulated in senescent cells (Wierstra, 2013). At the iβ stage, certain genes known to modulate senescence by regulating pro-inflammatory and growth factor signaling, such as *TGFB1, STAT3*, *RELA*, and *PDGFRA*, were upregulated (Ueda *et al*, 2021; Pang *et al*, 2024; Ijima *et al*, 2023). Noteworthy, findings included an increased expression of *CCL2*, known to induce death in mice with accelerated aging, suggesting its potential as a biomarker for a higher senescent cell burden (Luciano-Mateo *et al*, 2020). *CXCL10*, known to be elevated in older adults compared to the young, was also identified (Bradburn *et al*, 2018). Moreover, *TNF*, a crucial pro-inflammatory cytokine secreted by senescent cells that can trigger senescence in both mouse and human cells, showed increased expression (Kandhaya-Pillai *et al*, 2017). Finally, *IGFBP5*, a key factor regulating cell senescence and proliferation, showed elevated expression levels at iβ stage (Sanada *et al*, 2018). On the other hand, some genes associated with senescence displayed unexpected patterns during the differentiation process. *SERPINE1*, a well-known promoter of senescence, and

IL-6, important for its role in inducing and maintaining senescence, decreased their expression levels throughout the differentiation stages, suggesting their transient activation in the early stage of reprogramming, reflecting a combination of reprogramming stress, epigenetic memory, and dynamic regulation of pluripotency with differentiation-related pathways (Wang *et al*, 2023; Ortiz-Montero *et al*, 2017).

In the experimental work I conducted at the Beta Cell Aging Lab at the Joslin Diabetes Center in Boston, I performed further analyses on senescence gene expression using RNA samples from the five main stages of the differentiation process: iPSC, DE, PE, EN and iβ. In particular, to better understand the data obtained from flow cytometry, where a significant increase of senescence markers (SA-β-Gal, γH2AX and MitoSOX) was observed starting at the EN stage, *TP53* gene expression was evaluated. *TP53* is known to be upregulated to trigger both apoptosis and senescence (Zuckerman *et al*, 2009). In the passage from PE to EN stage, the cells are subjected to strong mechanical stress to be detached from the planar culture and passed into the suspension culture. This is reflected in the marked increase in DNA damage, as evidenced by the elevated expression of *ATM* and *ATR* genes at the EN stage. This is linked to a significant increase in the expression level of *TP53* gene, which is accompanied by both upregulation of apoptosis-like genes, such as *CAS8* and *CYCS*, and senescence effectors as *p16* and *BCL-2.* At the iβ stage, *TP53* decreased, whereas *p16* levels were significantly maintained, suggesting that the mechanical stress induced apoptosis in part of the cell population, while others entered a senescent state. It is critical to note that our samples were collected at specific timepoints, and the transition from PE to EN spans approximately 10 days, which is a considerable window where dynamic molecular changes could occur. It could be possible that *TP53* appears between PE and EN stages to play a role in the early and potentially reversible stages of senescence, maintaining a high expression at EN stage and diminishing its activity over time. *TP53* is fundamental to activate early senescence with *p21* (Mijit *et al*, 2020). Although we did not detect a significant *p21* expression in our samples, it is plausible that *p21* levels transiently increased within this 10-day window, initiating early senescence, and subsequently declined as *p16* expression increased and stabilized. In all the differentiation timepoints, *p21* expression remained low overall, even if there was a slight increase at the iβ stage, although not statistically significant, suggesting that a subset of cells may still reside in an early senescent state. The significant increase of *p16*

activity at the iβ stage, as suggested by *Beausejour et al.,* may contribute to a senescent state with a distinct and long-lasting senescence phenotype (Beauséjour *et al*, 2003). Our gene expression data aligns with this idea, as we observed an increase in *p16* levels during the differentiation process, suggesting that senescence in this context is affected and maintained by *p16.*

Previous research has shown that each type of senescence leads to a distinct SASP profile, with only a limited number of factors overlapping between different conditions. This complexity makes it challenging to establish a universal SASP signature. Therefore, the varied expressions of senescence-associated genes in our study could reflect the unique senescence profile specific to β cell aging. During my period in Boston at the Beta Cell Aging Lab, led by Professor Aguayo Mazzucato, my colleagues identified a distinct β SASP signature by cross-referencing the single-cell RNASeq data and the proteomic data already published of mouse and human islets (Midha *et al*, 2021). This "signature" provides a molecular profile of senescent β cells, revealing key factors involved in their secretory phenotype. Although these findings are not published yet, they served as preliminary data for my transcriptomic and proteomic analysis of SASP factors where I used this gene list to further investigate the secreted factors and validate the functional impact on iβ senescence. Transcriptomic data revealed a significant increase in β cell SASP signature such as *LSAMP, DUSP3, JUN,* and *ANGPTL3*. Specifically, the β cell SASP signature was deeply investigated by distinguishing the $p16^{+}$ and $p21^{+}$ SASP β cell signatures. The collected iβ conditioned media (CM) presented both $p16^{+}$ and $p21^{+}$ proteomic SASP signatures. This could be related to the fact that, in our analysis of senescence gene expression at iβ stage, we found that senescence appears to be primarily affected by *p16*, even if a small part of the cells still express, not significantly, *p21*. To further validate this, we compared the proteomic data of $p16^{+}$ and $p21^{+}$ SASP groups, and we found enrichment on $p16^{+}$ SASP, while SASP typically linked to $p21^{+}$ were less represented, confirming that *p16* plays a dominant role in affecting senescence during iβ differentiation, shaping also the secretory profile of these cells.

After confirming the presence of SASP factors in iβ CM, we investigated their effects on a human β cell line. Specifically, we wanted to understand if the released SASP factors could influence "secondary senescence" through paracrine signaling in neighboring non-senescent cells, resulting in a spread of the senescent phenotype within the

microenvironment (Admasu *et al*, 2021). In the context of T2D, senescence in adipose tissue has emerged as a critical factor in the development of the disease. With aging and obesity, adipose tissue undergoes dysfunction and accumulates senescent cells that secrete a range of SASP, playing a key role in the disruption of insulin signaling pathways, thus exacerbating metabolic disturbances associated with T2D (Gustafson *et al*, 2022). Studies have demonstrated that senescent adipocytes exhibit elevated levels of senescence markers such as *p16* and *p21*, alongside a reduction in the expression of critical genes for insulin sensitivity, including PPAR-γ and GLUT4 (Murakami *et al*, 2022). Moreover, in T1D context, Thompson *et al.* demonstrated that using both human T1D samples and non-obese diabetic (NOD) mouse models, β cells exhibit hallmarks of DNA-damage-induced senescence and SASP during the prediabetic stage. The SASP not only recruits self-reactive lymphocytes, exacerbating insulitis, but also induces "paracrine senescence" in nearby β cells, creating a feedforward loop that accelerates β cell loss and disease progression (Thompson *et al*, 2019).

We used the human cell line EndoCβ-H5, which is a widely used human pancreatic β cell model. They are a commercial human β cell line, obtained through the insertion of immortalizing genes (hTERT and SV40 large T) into human fetal pancreatic tissue using integrative gene transfer. They have a ready-to-use nature, coupled with physiological insulin secretion and responsiveness to metabolic and inflammatory stimuli, which makes them a valuable tool for studying β cell function (Blanchi *et al*, 2023). Additionally, they have already been used in previous studies on β cell senescence. *Brawerman et al.* treated EndoC-βH5 cells with bleomycin to investigate how DNA damage influences β-cell senescence. Post-treatment, EndoC-βH5 presented increased expression of DDR markers, such as γH2AX, and early senescence markers, including *p21*, *p16*, and elevated expression levels of *CXCL8*, indicating the initiation of the senescence program in response to DNA damage (Brawerman *et al*, 2022). In our experiments, the EndoCβ-H5 were treated with iβ CM and, as a negative control, we treated them with Basal Stage 7 media of the differentiation process. Specifically, we decided to use EndoC-βH5 because they are a pure β cell line, allowing us the direct assessment of SASP effects on β cell senescence and function without interference from other cell types. EndoCβ-H5 treated with iβ CM presented an increase in SA-β-Gal activity and in *p16* gene expression, indicating their transition into senescence. Interestingly, we also found a significant

increase in insulin content and glucose response compared to the non-treated EndoCβ-H5. These data suggest that the increase in senescence, influenced by *p16*, correlates with β cell function, additionally supported by a significant increase in *NKX6.1* gene expression. In our experiment, the secretion index, defined as the ratio of the percentage of insulin release (normalized to total insulin content) at high glucose (11 mM) to that at low glucose (0.5 mM), was 1.2 in iβ CM compared to 0.9 in controls. While this indicates a modest increase in glucose response, both values are lower than what would be expected from well-functioning EndoC-βH5 cells (Blanchi *et al*, 2023). To this, there is a key factor that may explain this: the CM used in our study was derived from iβ culture conditions, which differ from the optimized media typically used for EndoC-βH5 cells, and its composition could affect insulin secretion dynamics, limiting the responsiveness of the cells.

After analyzing the senescence profile and its link to secondary senescence, we wondered whether there was a difference in senescence profile, and consequently in function, among the DRI2 clones that we differentiated (DRI2#3, 2#4, 2#9, 2#13, 2#14, 2#15). A study conducted alongside my thesis project, to which I contributed in part, analyzed the differences between clones and identified an early-stage gene signature for selecting the best β cell differentiation-prone iPSC clone from a patient (Zamarian, Monaco, et al, manuscript in preparation). In this study we observed high heterogeneity among DRI2 clones in terms of differentiation potential into β cells and their functionality. Here, I explored the possibility that part of this variability could be due to the senescence state of iPSC clones. To assess it, we performed transcriptomic analysis of the cells at the iβ stage obtained from the different clones, focusing on *p16* gene expression. We calculated the average Z-score based on the expression levels of *p16* and subsequently classified the clones on the basis of their senescence profile: DRI2#3 presented the lowest expression of *p16*, whereas DRI2#15 had the highest expression of *p16*. To assess whether the senescent state observed in iβ cells influenced their function, we analyzed dynamic GSIS in *p16* high and *p16* low clones and found distinct secretion patterns. To quantitatively assess insulin secretion dynamics, we calculated the area under the curve (AUC), a key metric representing total insulin secretion over time in response to high glucose stimulation and KCl. A higher AUC indicates better overall insulin secretion, while a lower AUC points to impaired function. Notably, the DRI2#3 clone, which had reduced

p16 expression, showed a low AUC, whereas the DRI2#15 clone, with higher *p16* expression, tended to have a higher AUC. These findings suggest that senescence during differentiation affects positively β cell function. On this line, in 2016, *Helman et al.* demonstrated that the parallel activation of *p16* in transgenic mouse models and diabetic mice, enhanced GSIS, playing a crucial role in β-cell maturation and development rather than serving just as a stress response marker. Notably, β cells expressing *p16* exhibited classical senescence traits, including cellular enlargement, increased glucose uptake, and heightened mitochondrial activity, which correlated with enhanced insulin secretion (Helman *et al*, 2016b). Expanding on these findings, in 2024, *Patra et al.* analyzed single-cell transcriptomic data from 31 adult islet donors, revealing that $p16^{+}$ β cells exhibited senescence-associated signatures, including upregulation of *p21* and *TP53*, alongside enrichment of key β-cell maturation genes such as *MAFA, NKX6.1,* and *SIX3*. Similarly, senescent β-cell-like EndoC-βH3 cells displayed downregulation of proliferation-associated genes while showing increased expression of β cell maturation markers, such as *MAFA* (Patra *et al*, 2024). Our studies, in particular the experiments with the EndoCβH-5 experiments and the analysis on the clones, align with previous literature highlighting the role of cellular senescence, particularly *p16* expression, as a key driver of improved β cell function. However, despite these promising findings, our study has the limitation that the number of iPSC clones analyzed was small, requiring a higher number of differentiations to validate the observed relationship between *p16* expression and iβ function.

The next phase of our research shifted toward a senotherapeutic approach in the last stage of iβ differentiation process, evaluating its effect on iβ function and maturation. The senotherapeutic approach could involve the use of senolytics and senomorphics drugs. Senolytic drugs, specifically targeting anti-apoptotic pathways to selectively eliminate senescent cells, have shown promising results and have been employed in the context of both T1D and T2D. In T2D context, *Aguayo-Mazzucato et al.* used as a mice model treated with S961, an insulin receptor antagonist, which developed insulin resistance. They treated the mice with two types of senolytics: dasatinib and quercetin (D+Q) and ABT26, which respectively target the HIF1α and Bcl-2 pathways. Both treatments resulted in enhanced glucose metabolism and β cell identity gene expression (Aguayo-Mazzucato *et al*, 2019). In T1D context, *Thompson et al.* showed that treating the

normoglycemic non-obese diabetic mice model with ABT-199, which specifically targets Bcl-2, prevented the development of diabetes compared to control groups (Thompson *et al*, 2019). However, a potential drawback is the reduction in β cell mass, which is undesirable for maintaining transplanted cells in the recipient. In this regard, senomorphics drugs emerge as a viable option. They target SASP-related pathways, and block SASP secretion, without inducing cell death, offering a balance between addressing senescence and preserving β cell mass in transplantation scenarios (Rubin de Celis & Bonner-Weir, 2023). We investigated the effects of Baricitinib, a JAK/STAT inhibitor with senomorphic properties, on iβ cells. Baricitinib is a selective inhibitor of Janus kinases 1 and 2 (JAK1/JAK2), which are key signaling molecules in the JAK/STAT pathway (Tuttle *et al*, 2018). By inhibiting JAK1 and JAK2, Baricitinib blocks this signaling cascade, preventing the downstream activation of STAT proteins. This leads to a reduction in inflammatory and senescence-associated gene expression, particularly affecting IL6-related pro-inflammatory signaling (Choi *et al*, 2018). In order to clearly see the effects of senomorphic treatment on iβ function using dynamic GSIS, we decided to conduct this experiment on a different clone compared to the others presented above, which had a particularly robust secretion. The treatment was applied during the iβ stage of differentiation (From Day 30 to Day 35) to assess its impact on senescence markers, transcriptomic profiles, and functional insulin secretion. Our findings indicate that Baricitinib treatment did not alter the morphological integrity or viability of iβ cells, confirming that the drug was not cytotoxic under the tested conditions. Furthermore, flow cytometry analysis revealed no significant changes in classical senescence markers, including SA-β-Gal, γH2AX, and MitoSOX, suggesting that senomorphic effects of Baricitinib were not readily detectable using these assays. However, transcriptomic analysis provided more sensitive insights, showing a significant downregulation of *p16* and *IL6* gene expression in Baricitinib-treated cells, indicating a blockage of paracrine senescence spread within the microenvironment. These findings indicate that, although phenotypic markers of senescence remain unchanged, Baricitinib effectively modulated the transcriptional profile of senescence-associated pathways, particularly those related to inflammation and cell cycle arrest. The reduction in *IL6,* a key component of the SASP, suggests that Baricitinib could mitigate inflammatory signaling within the iβ population. Interestingly, functional GSIS analysis demonstrated that Baricitinib treatment led to a

significant reduction in insulin secretion, as evidenced by a lower insulin AUC, compared to untreated iβ cells. This decline in function suggests that the senescence process, despite often being associated with cellular aging, may play a beneficial role in iβ maturation and insulin secretion. These findings align with our previous observations that more senescent iβ cells exhibited enhanced insulin secretion, reinforcing the concept that senescence, particularly mediated by *p16*, could contribute positively to β cell functional competency (Helman *et al*, 2016b; Patra *et al*, 2024).

In the last part of the project, our research aimed to compare iβ and human islets obtained from the same cadaveric donor in terms of their senescence profile. At San Raffaele Hospital, we have access to human islets for research purposes, allowing us to receive both freshly isolated islets and the discarded digested pancreatic tissue from the same donor. In our lab, it has been previously demonstrated that it is possible to isolate a population of mesenchymal stromal cells from this post-digestion pancreatic tissue (Sordi *et al*, 2010). This unique opportunity enabled us to simultaneously study native β cells and generate iPSCs from pancreatic mesenchymal stromal cells (pMSCs) obtained from the digested pancreas (Khiatah *et al*, 2019). To my knowledge, this is the first time that pMSCs are reprogrammed into iPSCs, which are then efficiently differentiated into iβ cells. However, our findings suggest that comparing the senescence profiles of iβ cells and donor islets presents significant challenges, due to the fundamentally different origins and conditions of these cells. Flow cytometry data on senescence markers revealed that iβ cells exhibit a higher percentage of SA-β-Gal positive cells compared to donor islets, suggesting a form of senescence that is likely associated with cellular maturation rather than stress. On contrary, islets tend to have elevated γH2AX and MitoSOX, indicative of DNA damage response and mitochondrial oxidative stress. These signs of senescence could be a consequence of a stress response derived from pancreas digestion during the islet isolation process. Moreover, this difference in the senescence profile is further supported by the Z-score analysis, based on senescence and SASP gene expression, which highlights a markedly lower senescence score in iβ compared to native islets. In general, we encountered significant difficulties in analyzing the native islets, as they were highly stressed due to the isolation process. This stress likely affected their functionality, and as a result, we were unable to perform GSIS analysis to assess their insulin secretion capacity. These issues highlight the challenges of comparing two models with such

distinct backgrounds, where the conditions of one model (the native islets) are heavily influenced by the isolation process and the subsequent stress that occurs during digestion. Moreover, the low sample size limits the power of our analysis. Probably a direct comparison of pre-digestion pancreatic tissue would provide a more relevant baseline for evaluating senescence profiles. For future studies, a potentially useful modification could involve fixing a portion of the pancreas before digestion and performing immunostaining to directly compare pre- and post-digestion senescence markers, minimizing the confounding effects introduced by the isolation process and offering a clearer comparison of senescence between native and differentiated β cells.

In conclusion, our study focused on understanding the mechanisms of senescence and aging during the differentiation of iPSCs into iβ. One of the main strengths of our study lies in the use of the iPSC-derived β cell model, which represents a powerful and reproducible system for studying human β cell biology and the effects of senescence in a controlled context. We adopted a multifaceted approach to analyze senescence in β cells, combining phenotypic analysis (SA-β-Gal, γH2AX, MitoSOX), transcriptomic, and proteomic profiling. Furthermore, collaboration with the Beta Cell Aging Lab at the Joslin Diabetes Center significantly enriched our analysis, allowing us to characterize specific SASP factors in β cells and their paracrine effects. This cross-fertilization allowed us to identify a correlation between *p16*-driven senescence with iβ function and maturation. Our work suggests that senescence may have a positive role in β cell maturation and function, challenging the traditional view of senescence as purely detrimental, and opening new questions about the role of senescence in other cell types and differentiation processes, such as neuronal or muscle differentiation. However, this aspect requires further investigation by increasing the number of experiments and testing our approach on another iPSC line to determine whether differences in senescence levels and functionality are reproducible across different clones. Moreover, to further explore the role of senescence in iβ, a potential future approach could be the use of targeted gene silencing techniques. One option would be to employ CRISPR-Cas9 to delete the *p16* gene at the iPSC stage, followed by differentiation into iβ, to assess the impact of *p16* absence on β cell maturation and insulin secretion. Alternatively, transient silencing of *p16* using siRNA at the iβ stage could provide insights into the immediate effects of reduced *p16* expression on iβ function and maturation.

From a translational perspective, particularly in the context of T1D cell therapy, our findings present both opportunities and challenges. The observation that senescent β cells may contribute to enhanced maturation and function raises the possibility of intentionally promoting senescence in iβ cells to improve their therapeutic potential. One possible strategy to increase the proportion of senescent β cells could be to extend the culture period in the last stage of the differentiation process, allowing more time for senescence programs to become fully established. Another approach might involve the use of CDK4/6 inhibitor drugs, such as Palbociclib, which can induce *p16*-driven senescence without causing DNA damage. These compounds are extensively studied in oncology, particularly in breast cancer, where they have shown not only anti-proliferative effects but also good immunomodulatory properties (Lee *et al*, 2024) . Given the important role we observed for *p16*-mediated senescence in our model, applying CDK4/6 inhibitors during iβ differentiation may represent an interesting strategy to selectively enhance beneficial senescence programs.

While β cell senescence may enhance their maturation and function, it also raises concerns about increased immunogenicity. This is supported by recent evidence showing that senescent β cells exhibit elevated HLA-I levels in response to IFNα treatment, indicating enhanced visibility to the immune system (Patra et al., 2024). Moreover, in the context of iPSC-derived β cells, in a previous study conducted in our lab by *Chimienti et al.,* presented that undifferentiated iPSCs exhibited low levels of HLA class I molecules, whereas, when differentiation progressed towards the iβ stage, there was an upregulation of classical HLA class I molecules, including HLA-A, HLA-B, and HLA-C (Chimienti *et al*, 2022). Moreover, in iβ stage we found a higher expression of genes known to modulate senescence by regulating pro-inflammatory and growth factor signaling, such as *TGFB1, STAT3*, *RELA*, and *PDGFRA*, which may further exacerbate immune recognition and rejection post-transplantation. To address these limitations, future therapeutic strategies may need to incorporate protective measures to mitigate the heightened immunogenicity of senescent β cells. One of the most actively investigated approaches is the use of advanced encapsulation devices. However, developing an ideal encapsulation system remains a major challenge, particularly for ensuring long-term viability and function of iβ cells *in vivo*. For instance, Vertex Pharmaceuticals clinical trial VX-264, which involves implanting encapsulated SC-islets without

immunosuppression, was recently suspended due to a lack of therapeutic efficacy, highlighting the technical difficulties in translating this approach. On the other hand, targeting immunogenicity at the cellular level through immune engineering represents a promising strategy. In NOD mouse model, *Gerace et al.* has demonstrated that genetically modifying SC-islets to both evade immune detection and promote localized immune tolerance can support long-term graft function in autoimmune settings (Gerace *et al*, 2023). In immunocompetent allogeneic rhesus macaques, researchers transplanted hypoimmune SC-islets by deleting genes responsible for HLA class I and II expression and overexpressing CD47, and they survived for at least 16 weeks without the need for immunosuppressive therapy, whereas wild-type cells were rejected (Hu *et al*, 2023). Clinically, in January 20205, Sana Biotechnology reported promising early outcomes from the first patient treated with hypoimmunogenic-engineered islets, which survived without any immunosuppressive therapy. Despite their higher immunogenicity, combining encapsulation technologies with immune engineering could offer a powerful way to protect senescent iβ cells.

In summary, our study provides new perspectives on the role of senescence in β cell differentiation and maturation, opening new research directions to modulate senescence on iβ, potentially enhancing the efficacy of cell therapy for patients with T1D.

7. Materials and methods

7.1 iPSC reprogramming

The human iPSC clones DRI2 (DRI2#3, 2#4, 2#9, 2#13, 2#14, 2#15), were generated at Diabetes Research Institute in December 2019, from $CD34^+$ enriched blood cells of a healthy donor, through episomal expression of *OCT4, MYC, SOX2, KLF4,* and *LIN28* genes with CytoTuneTM-iPS 2.0 Sendai Reprogramming Kit following manufacturer's instructions. After reprogramming, DRI2 clones were selected based on their star-shaped morphology, and when dedifferentiated cells appeared, they were manually removed by scraping and aspirating under the microscope in sterile conditions. Clone stabilizations were done by manually picking the iPSC colonies and culturing them in the presence of CloneR (*StemCell Technologies*) in 24-well plates (*Corning Incorporated, Costar*) monitoring its growth and the presence of dedifferentiated cells.
Stabilized clones were cultured in six-well plates (*Corning Incorporated, Costar*) with 0.5 μg/cm² Vitronectin Recombinant human protein (*ThermoScientific*) in Essential 8 Basal Medium (*Gibco*) supplemented with 1% Pen/Strep (*Lonza*) and cultured at 37°C and 5% CO_2. Cells were passed every 3–4 days using 0.5 mM EDTA (*ThermoScientific*). Cells were imaged using an EVOS microscope (*ThermoScientific*).

7.2 EndoC-βH5 culture (Joslin Diabetes Center)

EndoC-βH5 cells (*Human Cell Design)* were seeded in a 96-well plate (*Corning*) with a concentration of $1x10^5$ cells/well. Cells were cultured at 37°C and 5% CO_2 with complete EndoC-βH5 medium Ultiβ1 (*Human Cell Design*). After 4 days, cells were cultured with iβ conditioned media (CM) for 6 hours, followed by a recovery of 2 days. On Day 7 cells were detached with Trypsin/EDTA (*Merck*), and collected for FACS, RNA and DNA analysis. Moreover, cells were used for static GSIS to assess the insulin content.

7.3 Human islets

Human islets were isolated from a cadaveric organ donor in the Pancreatic Islet Processing Unit of the Diabetes Research Institute at IRCCS San Raffaele Hospital in Milan, Italy. Islets presented a purity of 70% and were cultured for 24 hours with CMRL 1066 (*Corning*), 10% FBS (*Lonza*), 1% P/S (*Lonza*), 1% L-glutamine (*Lonza*)

supplemented with Nicotinamide (1:200, *Sigma-Aldrich*), Y-27632 (1:1000, *Selleckchem*) and DNase 100U (1:200, *Merck*) at 37°C and 5% CO_2 on an orbital shaker (60 rpm).

7.4 Pancreatic-mesenchymal stromal cells (pMSCs)

Pancreatic-mesenchymal stromal cells (pMSCs) were obtained from the discarded fractions of pancreatic tissue after islets isolation in the Pancreatic Islet Processing Unit of the Diabetes Research Institute at IRCCS San Raffaele Hospital in Milan, Italy. The digested pancreas was maintained on ice and 500 µL were transferred into a 50mL Falcon tube (*Corning*) and washed three times at 300g for 8 minutes with cold PBS (*Lonza*). After washing steps, the cells were cultured in T75 Flasks (*Corning*) in AlphaMEM (*Euroclone*), 10% FBS (*Lonza*), 1% P/S (*Lonza*), 1% L-glutamine (*Lonza*). Cells were maintained at 37°C and 5% CO_2 and passed every 5–6 days using Tryple (*ThermoScientific*). Cells were imaged using an EVOS microscope (*ThermoScientific*).

7.5 iPMSC-iPSCs reprogramming

The human iPMSC-iPSC line, was reprogrammed at Diabetes Research Institute in April 2023, from pancreatic-derived mesenchymal stromal cells (pMSCs) with StemRNA 3rd Gen Reprogramming Kit (*Reprocell*) following manufacturer's instructions. After reprogramming, two clones (iPMSC#6, #53) were selected based on their star-shaped morphology, and when dedifferentiated cells appeared, they were manually removed by scraping and aspiring under the microscope in sterile conditions. Clone stabilizations were done by manually picking the iPSC colonies and culturing them in the presence of CloneR (*StemCell Technologies*) in 24-well plates (*Corning Incorporated, Costar*) monitoring its growth and the presence of dedifferentiated cells. Stabilized iPMSC clones were cultured in six-well plates coated with 0.5 µg/cm² Vitronectin Recombinant human protein in Essential 8 Basal Medium supplemented with 1% Pen/Strep and cultured at 37°C and 5% CO_2. Cells were passed every 3–4 days using 0.5 mM EDTA. Cells were imaged using an EVOS microscope (*ThermoScientific*).

7.6 iPSC differentiation into mature insulin producing cells

Human iPSCs were differentiated into insulin-producing cells following a seven-stage protocol established for PSCs (Barsby *et al*, 2022). The protocol lasts 30 days, including

planar culture for the initial stages and transition to suspension culture for the final maturation steps (**Figure 34**).

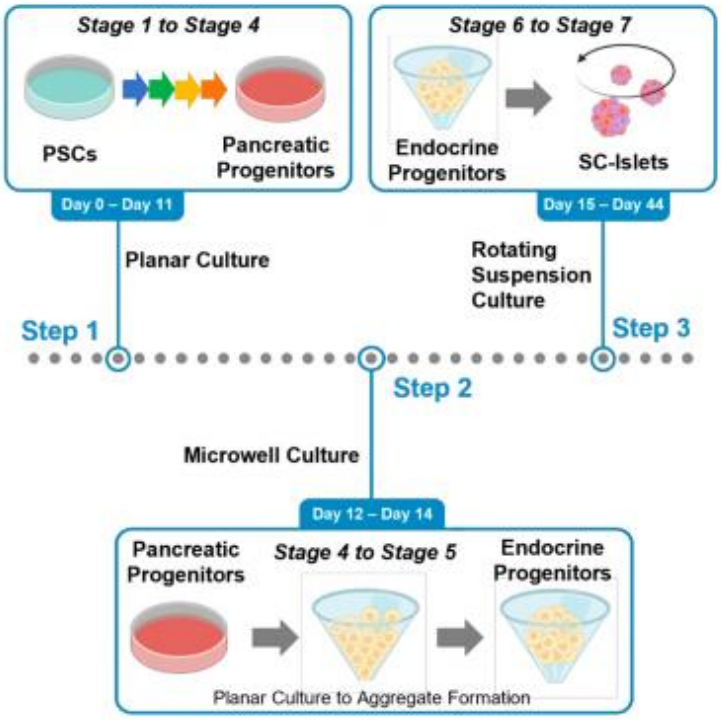


Figure 34. Otonkoski et al. differentiation protocol. *Graphical abstract of the seven-stage differentiation protocol.*

At day 0 of the differentiation process, iPSCs were cultured on VTN-coated 6-well with a concentration of $1.6x10^6$ cells/well in Essential 8 Basal medium (*Gibco*) with Y-27632 (*Selleckchem*, 1:1000) to allow a fully confluent seeding that enables the efficient induction of definitive endoderm.

From this point, the differentiation protocol is divided into 7 stages as follows:

- Stage 1 (Day 1-3): Basal 1 medium is used to culture cells, supplemented with Activin A 1 mg/ml (*QKine*) and CHIR-99021 10 mM (*Tocris*) for the first 2 days and only Activin A for the third one.
- Stage 2 (Day 4-6): Basal 1 medium is supplemented with Vitamin C 250 Mm (*Sigma-Aldrich*) and FGF-7 100 ng/µl (*Genscript*).
- Stage 3 (Day 7-8): Basal 2 Medium supplemented with Vitamin C 250 mM, FGF-7 100 ng/µl and Supplement 3.

- Stage 4 (Day 9-12): Basal 2 medium supplemented with Vitamin C 250 mM, FGF-7 100 ng/µl, hEGF 100 ng/µl (*Peprotech*), Activin A 1 mg/ml, Y-27632 10 mM, Nicotinamide 1 M (*Sigma-Aldrich*) and Supplement 4.

On day 11, pancreatic progenitors were transferred from planar culture into microwell plates (AggreWell 400, 6-well microwell plates; *Stemcell Technologies*) to promote the formation of uniformly sized aggregates.

- Stage 5 (Day 15-16): Basal 3 medium supplemented with Betacellulin 100 ng/µl (*Peprotech*), Y-27632 10 mM and Supplement 5.

During days 12 to 14, cells start to aggregate and assume a spherical morphology. On day 15, endocrine progenitor (EP) aggregates, from the AggreWell microwell plates, were transferred to a suspension culture on an ultra-low attachment (ULA, *Corning*) 6-well plate on an orbital shaker (95 rpm). These aggregates differentiated into pancreatic islet-like aggregates (SC-islets).

- Stage 6 (Day 17-23): Basal 3 medium and Supplement 6.

- Stage 7 (Day 23-30): Basal 4 medium supplemented with N-acetylcysteine 100 mM (*Sigma-Aldrich*), T3 10 mM (*Sigma-Aldrich*) and ZM-447439 5 mM (*Selleckchem*) (**Table 5**, **Table 6**).

All supplemented media were filtered with 0.22 *µm* filter units (Stericup Quick Release, *Corning*) before being added to the cells. The medium was freshly prepared every day and changed every 24 hours for the first 17 days, while from day 17 to 30, it was changed every 3 days. Cells were maintained at 37°C with 5% CO2. Cell morphology was observed during differentiation with the EVOS XL Core microscope (*ThermoScientific*) (**Figure 35**).

BASAL 1 MEDIUM (STAGE 1-2)		
Reagent	**Final concentration**	**Amount**
MCDB131	n/a	500 mL
GlutaMAX (100X)	1X	5 mL
Glucose (2.5 M)	10 mM	1 mL
$NaHCO_3$	1.5 g/L	750 mg
BSA	0.5%	2.5 g
Total	**n/a**	**506 mL**
BASAL 2 MEDIUM (STAGE 3-4)		
Reagent	**Final concentration**	**Amount**
MCDB131	n/a	500 mL
GlutaMAX (100X)	1X	5 mL
Glucose (2.5 M)	10 mM	1 mL
$NaHCO_3$	2.5 g/L	1250 mg
BSA	2%	10 g
ITS-X	0.5X	2.5 mL
Total	**n/a**	**508.5 mL**
BASAL 3 MEDIUM (STAGE 5-6)		
Reagent	**Final concentration**	**Amount**
MCDB131	n/a	500 mL
GlutaMAX (100X)	1X	5 mL
Glucose (2.5 M)	20 Mm	3 mL
$NaHCO_3$	1.5 g/L	750 mg
BSA	2%	10 g
ITS-X	0.5X	2.5 mL
$ZnSO_4$ (10 mM)	10 µM	0.5 mL
Heparin (10 mg/mL)	10 µg/mL	0.5 mL
Pen/Step (100X)	1X	5 mL
Total	**n/a**	**516.5 mL**
BASAL 4 MEDIUM (STAGE 7)		
Reagent	**Final concentration**	**Amount**
CMRL	n/a	500 mL
GlutaMAX (100X)	1X	5 mL
Pen/Step (100X)	1X	5 mL
ITS-X	0.5X	2.5 mL
Sodium Pyruvate (100 mM)	0.5 mM	2.5 mL
$ZnSO_4$ (10 mM)	10 µM	0.5 mL
Heparin (10 mg/mL)	10 µg/mL	0.5 mL
Lipid concentrate (2000X)	1X	0.25 mL
Trace Element A (2000X)	1X	0.25 mL
Trace Element B (2000X)	1X	0.25 mL
BSA	2%	10 g
Total	**n/a**	**516.75 mL**

Table 5. List of the basal media used. *The table lists reagents, final concentrations and amounts of factors that compose the media.*

STAGE 3 SUPPLEMENT (2500X)		
Reagent	**Final concentration**	**Amount**
SANT1 (2.5 mM)	0.625 mM	100 µL
Retinoic Acid (10 mM)	2.5 mM	100 µL
LDN-193189 (1 mM)	0.25 mM	100 µL
TPB (2.5 mM)	0.5 mM	80 µL
DMSO	n/a	40 µL
Total	**n/a**	**400 µL**
STAGE 4 SUPPLMENT (2500X)		
Reagent	**Final concentration**	**Amount**
SANT1 (2.5 mM)	0.625 mM	100 µL
Retinoic Acid (10 mM)	0.25 mM	10 µL
LDN-193189 (1 mM)	0.5 mM	200 µL
TPB (2.5 mM)	0.25 mM	40 µl
DMSO	n/a	50 µL
Total	**n/a**	**400 µL**
STAGE 5 SUPPLMENT (1500X)		
Reagent	**Final concentration**	**Amount**
SANT1 (2.5 mM)	0.375 mM	100 µL
Retinoic Acid (10 mM)	75 µM	5 µL
LDN-193189 (1 mM)	0.15 mM	100 µL
GC1 (10 mM)	1.5 mM	100 µL
GSiXX (1 mM)	0.15 mM	100 µL
Alk5inhII (50 mM)	15 mM	200 µL
DMSO	n/a	62 µL
Total	**n/a**	**667 µL**
STAGE 6 SUPPLEMENT (2000X)		
Reagent	**Final concentration**	**Amount**
LDN-193189 (1 mM)	0.2 mM	100 µL
GC1 (10 mM)	2 mM	100 µL
GSiXX (1 mM)	0.2 mM	100 µL
Alk5inhII (50 mM)	20 mM	200 µL
Total	**n/a**	**500 µL**

Table 6. List of the supplements used*. The table lists reagents, final concentrations and amounts of each factor that compose the supplements.*

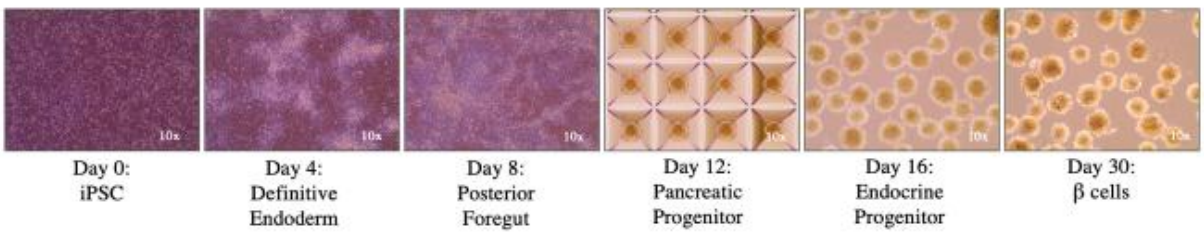


Figure 35. Cell morphology during the main stages of differentiation process. *At Day 0 (iPSC), a fully confluent seeding of cultured iPSCs facilitates the efficient induction of definitive endoderm at Day 4. The cell-layer then assumes a thicker morphology until the formation of Posterior foregut at Day 8. Between days 12 and 15, the pancreatic progenitors begin to aggregate and assume a spherical morphology. In the final stages, from Day 16 until Day 30, endocrine progenitors mature into iPSC-derived β cells (iβ cells) with the size remaining stable and the rounded morphology retained.*

7.7 iβ Senomorphic treatment

The senomorphic treatment with Baricitinib was performed at the iβ stage to evaluate its effects on iβ maturation and function. At day 30, iβ were treated with Baricitinib 100 nM (S2851, *Selleckchem*) until day 35. Untreated iβ were used as negative control. On Day 35, iβ cells were collected for a dynamic glucose-stimulated insulin secretion test, FACS analysis and RNA extraction.

7.8 Flow cytometry

Flow cytometry analysis was performed at day 0, 4, 11, 21 and 30 of the differentiation protocol to evaluate the expression levels of intracellular and extracellular stage-specific markers (**Table 7**). At day 0 the pluripotency marker OCT4 was evaluated and the CXCR4 definitive endoderm marker was quantified at day 4; from day 11 to 30 Insulin, Glucagon, PDX1, NKX6.1 were assessed.

Cells were counted and processed as follows: the cells were detached with Accutase (Merck) for 5 min at 37 °C, resuspended in 1 mL of PBS and stained with 1 µL of LIVE/DEAD Fixable Violet Stain Kit (*Invitrogen, APC-Cy7*) for 30 minutes at room temperature (RT) to assess cell viability. After that, cells were washed with FACS buffer (PBS + 0.2% BSA). Extracellular staining (CXCR4): the cells were marked with the Ab at room temperature for 15 minutes and fixed with Cytofix (*BD Cytofix/Cytoperm*, *BD Biosciences*) for 20 minutes at 4°C. Intracellular staining (OCT4, Insulin, Glucagon, PDX1, NKX6.1): after the fixation step, the cells were permeabilized with Perm Buffer Phosflow III (*BD Biosciences*) for 30 minutes at 4° C in the dark. After the permeabilization step, cells were marked with intracellular Ab for 30 minutes at 4°C in the dark. After each step cells were washed with FACS buffer and centrifuged at 1200 rpm for 5 minutes.

Antibody	Catalog#	Manufactures	Fluorophore
OCT4 (4µl x 10^6 cells)	16-202 (1 x 50 µg)	BD Biosciences	AlexaFluor 647
CXCR4 (6µl x 10^6 cells)	557145 (1 x 500 µL)	BD Biosciences	PE
PDX1 (5µl x 10^6 cells)	562274 (1 x 250 µL)	BD Biosciences	AlexaFluor 488
NKX6.1 (5µl x 10^6 cells)	563023 (1 x 250 µL)	BD Biosciences	PE
INSULIN (2µl x 10^6 cells)	565689 (1 x 25 µg)	BD Biosciences	AlexaFluor 647
GLUCAGON (2µl x 10^6 cells)	565891 (1 x 50 µg)	BD Biosciences	BV421-A

Table 7. Antibodies used in flow cytometry*. The table lists antibodies, catalog numbers, manufactures and fluorophores.*

During the differentiation protocol the cellular senescence was investigated through the evaluation of lysosomal activity (SA-β-Gal), DNA damage (γH2AX), and oxidative damage (MitoSOX). The senescence level of EndoCβ-H5 and human islets was also investigated.

Following the LIVE/DEAD staining procedure, as previously described, the staining for senescence markers is described below.

- SA-β-Gal staining: $3x10^5$ cells were fixed with PFA 4% for 10 minutes at RT. Then, the cells were washed in FACS buffer (PBS + 1% BSA) and resuspended in 100 µL of Working Solution, composed of the senescent green probe diluted in the senescent buffer. The unstained control cells were resuspended only in the senescent buffer. After that, cells were incubated for 1 hour and 30 minutes at 37°C in the dark. Then, the Working Solution was removed, and cells were washed with FACS buffer (PBS + 1% BSA) and resuspended with 100 µL of FACS buffer (PBS + 0.2% BSA). All wash steps were performed at 1200 rpm for 5 minutes (**Table 8**).

Component	Catalog #	Manufactures	Fluorophore
CellEvent™ Senescence green Probe (1000x)	C10851 (1 x 50 µL in DMSO)	Invitrogen	AlexaFluor 488
CellEvent™ Senescence Buffer	C10851 (1 x 50 mL)	Invitrogen	//

Table 8. CellEvent™ Senescence Green Flow Cytometry Assay Kit components*. The table lists components, catalog numbers, manufactures and fluorophores.*

- γH2AX staining: $1x10^5$ cells were fixed with Fixation solution for 20 minutes on ice. After washing step, cells were resuspended in the Permeabilization solution with an anti-phospho-Histone H2A.X (ser139) FITC conjugate antibody. As negative control a mouse IgG-FITC conjugate antibody was used. After 20 minutes of incubation on ice, cells were washed with the Wash solution and finally resuspended in FACS buffer (PBS + 0.2% BSA). All washing steps were performed at 1200 rpm for 5 minutes with PBS (**Table 9**).

Component	Catalog#	Manufactures	Fluorophore
Anti-phospho-H2A.X(ser139)	16-202 (1 x 370 µL)	Merck	AlexaFluor 488
Normal Mouse IgG	12-487 (1 x 350 µL)	Merck	AlexaFluor 488
Fixation Solution (16x)	20-257 (1 x 5 mL)	Merck	//
Wash Solution (10x)	20-258 (1 x 2 mL)	Merck	//
Permeabilization solution (10x)	20-259 (1 x 1 mL)	Merck	//

Table 9. γH2AX Phosphorylation assay kit components. *The table lists the component, catalog number, manufactures and fluorophore.*

- MitoSOX staining: $1x10^5$ cells were resuspended in HBSS/Ca/Mg (24020117, *GibcoTM*) and stained with mitoSOX Red Mitochondrial Superoxide indicator (1:1000) at 37 °C for 10 minutes. Finally, the cells were washed with HBSS/Ca/Mg and then analyzed. All washing steps were performed at 1200 rpm for 5 minutes (**Table 10**).

Component	Catalog #	Manufactures	Fluorophore
MitoSOX™ Red Mitochondrial Superoxide Indicator	M36008 (10 x 50 µg)	Invitrogen	PE

Table 10. MitoSOX™ Red Mitochondrial Superoxide Indicator assay kit component*. The table lists the component, catalog number, manufactures and fluorophore.*

All data were acquired with FACS Canto II HTS and analyzed using FlowJo 10.9.0 software.

7.9 Immunofluorescence staining

For immunofluorescence analysis, iPSCs were cultured on a chamber slide (*Corning*) and then fixed with PFA 4% for 10 minutes. After that, cells were washed with 1ml of PBS and incubated for 30 minutes at room temperature with blocking solution (2% BSA, 5% FBS, 0.2-0.4% Tryton, 0.05% NaN3 in PBS) to permeabilize the cells and block any non-specific binding. Cells were incubated at room temperature for 1 hour in the dark with the primary antibody diluted in Blocking solution. After 1 hour, chamber slides were washed 3 times with PBS for 2 minutes. Then, the secondary antibody and the nuclear staining Hoechst 33342 (*Invitrogen*, 1:1000) were added and incubated for 1 hour in the dark at RT. After 1 hour, slides were washed three times with PBS for 2 minutes. One drop of anti-fade mounting medium (05-1740, bio-optica) and a coverslip was placed on the slide. At iβ stage, cell aggregates were co-stained for Glucagon/Chromogranin and Insulin/NKX6.1. For Glucagon/Chromogranin staining, clusters were fixed in PFA 4% overnight, included in 1% Agarose (*Sigma*) and paraffin-embedded. Sections were incubated with pH 6 Citrate Buffer (10 mM citric acid anhydrous, 0.05% Tween 20 in

H_2O) for antigen retrieval, followed by Blocking solution to permeabilize the cells and block any non- specific binding. Slides were incubated at RT for 1 hour with primary antibodies diluted in Blocking solution. Then, the secondary antibody and the nuclear staining Hoechst 33342 (*Invitrogen*, 1:1000) were added and incubated for 1 hour in the dark at room temperature. After 1 hour, sections were washed three times with PBS for 2 minutes. One drop of anti-fade mounting medium (05-1740, bio-optica) and a coverslip were placed on the slide.

For Insulin/NKX6.1 co-staining, cell clusters were fixed in 4% PFA for 10 minutes and then incubated at 95°C for 20 minutes in pH 6 Citrate Buffer, followed by permeabilization with Perm Buffer (0.05% Tween 20, 0.2% Triton X-100 in PBS) for 10 minutes at RT. Next, clusters were blocked for 1 hour at RT using Blocking ASE Buffer (5% goat serum, 2% BSA, 0.1% H_2O_2, 10 mM glycine in PBS). After blocking, they were incubated overnight at 4°C with primary antibody diluted in Blocking ASE Buffer. The next day, clusters were washed twice with PBS for 5 minutes, followed by a 1-hour incubation at RT with the secondary antibody. After two additional PBS washes (5 minutes each), clusters were stained with Hoechst 33342 (*Invitrogen*, 1:1000) for 10 minutes at RT (**Table 11, Table 12**). Finally, the clusters were mounted with one drop of anti-fade mounting medium (05-1740, bio-Optica) on a glass slide, covered with a coverslip. Slides were examined at the Olympus FluoVIEW FV3000RS Confocal microscope. Slides were stored between 4°C in the dark.

Antibody	Catalog#	Species	Manufactures
OCT4 (1:500)	NBP2-15052	Mouse	Novos Biologicals
SSEA-4 (1:100)	AB16287	Mouse	Abcam
NKX6.1 (1:100)	MAB5857	Mouse	R&D
INSULIN (Ready to use)	IR002	Guinea pig	Dako
CHGA (1:20)	AB85554	Rabbit	Abcam
GLUCAGON (1:500)	G2654	Mouse	Merck

Table 11. Primary antibodies used in immunofluorescence. *The table lists beta cell marker's antibodies names, concentrations, catalog numbers, species and manufactures.*

Species	Catalog#	Derivation	Manufactures	Fluorophore
Mouse (1:500)	A11001	Goat	Thermo Fisher	Alexa Fluor 488
Mouse (1:500)	A11003	Goat	Thermo Fisher	Alexa Fluor 546
Guinea pig (1:500)	A21450	Goat	Thermo Fisher	Alexa Fluor 647
Rabbit (1:500)	A11008	Gaot	Thermo Fisher	Alexa Fluor 488

Table 12. Secondary antibodies used in immunofluorescence. *The table lists antibody species with concentrations, catalog numbers, derivation, manufactures and fluorophores.*

The senescence markers (**Table 13**) were subsequently evaluated by immunofluorescence staining via confocal microscopy at the stage of β cells:

- SA-β-Gal staining has been performed using the CellEvent™ Senescence Green Flow Cytometry Assay Kit. β cells were fixed in 4% PFA solution for 10 minutes, protected from light. Cells were washed with FACS buffer (1% BSA in PBS) and stained by adding the Working solution for 2 hours at 37°C. Afterward, cells were washed 3 times with PBS and stained with Hoechst 33342 (1:1000) for 10 minutes at RT. Finally, clusters were mounted on a glass slide with one drop of ant-fade mounting medium (05-1740, bio-optica) and a coverslip was placed on the slide.

- MitoSOX staining has been performed using the MitoSOX™ Red Mitochondrial Superoxide Indicator, for live-cell imaging. Clusters were put in a ULA (*Corning*) 24-well plate with HBSS/Ca/Mg and stained with mitoSOX Red Mitochondrial Superoxide Indicator (1:1000) and Hoechst 33342 (*Invitrogen*, 1:1000) at 37° for 10 minutes. After that, cells were washed with HBSS/Ca/Mg, transferred to Optical bottom plates 96-well (*Greiner*), and analyzed.

- γH2AX staining has been performed using the Gamma H2A.X Staining Kit. The positive senescence control was obtained by treating β cells with the DNA DSB Inducer (1:200) for 1 hour at 37°C with 5% CO_2. Cells were fixed with 4% PFA solution for 10 minutes, protected from light. Subsequently, the cells were permeabilized with 90% methanol at 4°C for 10 minutes. To prevent non-specific binding, PBS containing 1% BSA was added, and the cells were incubated for 30 minutes at RT on an orbital shaker. Then, the cells were stained with 1x Anti-Phospho-Histone H2A.X (Ser139) primary antibody, for 1 hour on an orbital shaker. Then, three washes were performed with Wash Buffer (PBST). After that, cells were stained with secondary antibody, FITC-Conjugate and Hoechst 33342 (*Invitrogen*, 1:1000) for 1 hour, on an orbital shaker. Finally, after 3

washes with Wash Buffer (PBST), cells were mounted with one drop of ant-fade mounting medium (05-1740, bio-optica) and a coverslip was placed on the slide.

Fluorescent dyes/Reagents	Catalog #	Manufactures	Fluorophore
CellEvent™ Senescence green Probe (1:1000)	C10851 (1 x 50 µL in DMSO)	Invitrogen	Alexa Fluor 488
MitoSOX™ Red Mitochondrial Superoxide Indicator (1:1000)	M36008 (10 x 50 µg)	Invitrogen	PE
Anti-phospho-H2A.X (ser139) (1:100)	16-202 (1 x 370 µL)	Abcam	//
Secondary Antibody (1:100)	16-202 (1 x 370 µL)	Abcam	Alexa Fluor 488

Table 13. Senescence marker's antibodies used in immunofluorescence staining*. The table lists antibodies and concentrations, catalog numbers, manufactures and fluorophores.*

The senescence markers images were acquired using the Olympus FluoView 3000 RS, using a silicone immersion 60X objective. The images were analyzed using ImageJ software.

7.10 RNA extraction

To evaluate the gene expression, the cells at different stages of differentiation (day 0, day 4, day 11, day 21, day 30) and human islets were lysate in 500 µL of Lysis solution (*Ambion*) and stored at -80 °C until RNA extraction. RNA extraction was performed using the mirVanaTM miRNA Isolation Kit (*Invitrogen*, AM1561). This Kit uses a rapid procedure to isolate RNA from tissues and cells by a glass fiber filter (GFF)-based method. The method isolates total RNA ranging in size from kilobases down to 10-mers. RNA extraction procedure was performed in accordance with the manufacturer's guidelines (**Figure 36**). Extracted RNA was quantified at Nanodrop and the RNA quality and purity was evaluated using the absorbance ratio A260/280 and 260/230, respectively.

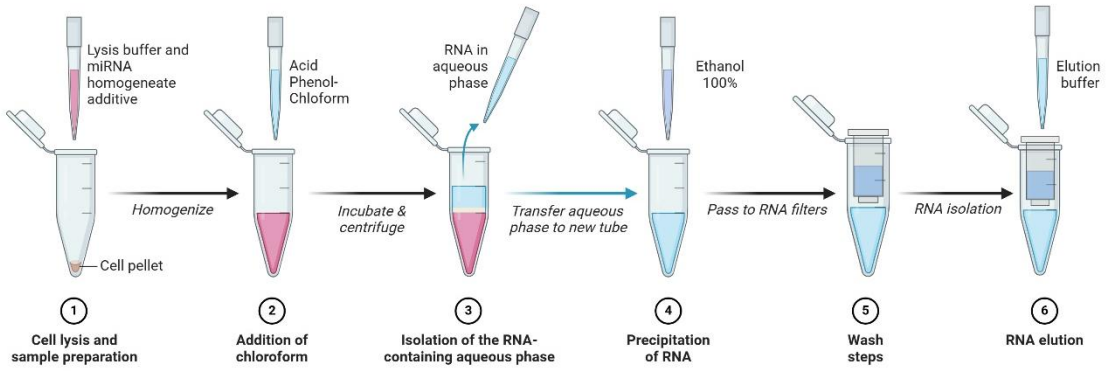


Figure 36. RNA extraction process. *Created with BioRender (created with biorendor.com).*

7.11 RNA extraction (Joslin Diabetes Center)

EndoCβ-H5 cells were harvested (1x10^5 cells), lysed with Buffer RLT, and stored at -80°. RNA was then extracted using RNeasy Micro Kit (74004, *Qiagen*) following the manufacturer's guidelines (**Figure 16**). Extracted RNA was quantified at Nanodrop the RNA quality and purity was evaluated by absorbance ratio A260/280 and 260/230, respectively.

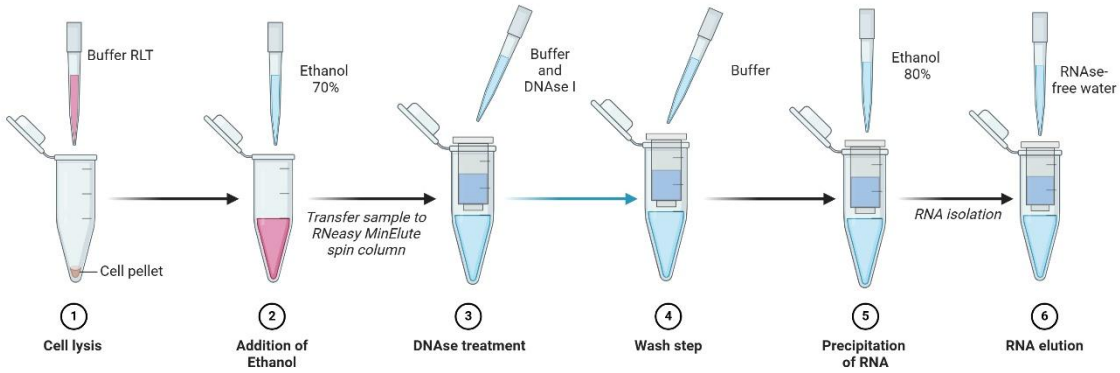


Figure 37. RNA extraction process. *Created with BioRender (created with biorendor.com).*

7.12 Reverse transcription

RNA from each sample was reverse transcribed using the SUPERSCRIPT III/IV kit (*Invitrogen*). Samples were thawed on ice and spin down. Residual genomic DNA was removed with DNAse treatment: the reaction includes 2 ug of total RNA, 1 µL of TURBO DNase buffer 10x, 1 µL of TURBO DNase, and Nuclease-free H_2O to reach a final volume of 8 µL. Samples were loaded into the thermal cycler (*BioRad*) using the following thermal profile: 30 minutes at 37°C, then 1.4 µl of EDTA was added and then 10 minutes at 75°C for DNase inhibition. After DNase treatment, the reverse transcription was performed as described below:

Two µL of MIX 1 (1 µL of RANDOM EXAMERS and 1 µL of DNTPs mix) was added to each tube of DNAse treated sample and after 5 minutes at 65°C, 7 µL of MIX 2 (5X SSIV FIRST STRAND BUFFER, 1 µL of DTT, 1 µL of RNASE OUT, 1 µL of SS IV RT) were added. The reverse transcription reaction took place using the following thermal profile: 10 minutes at 23°C, 10 minutes at 50°C and 10 minutes at 80°C. As final step, 1 µL of RNASE H was added and the reaction continued for 20 minutes at 37°C (**Figure 38**). The cDNA obtained was stored at -20°C until use.

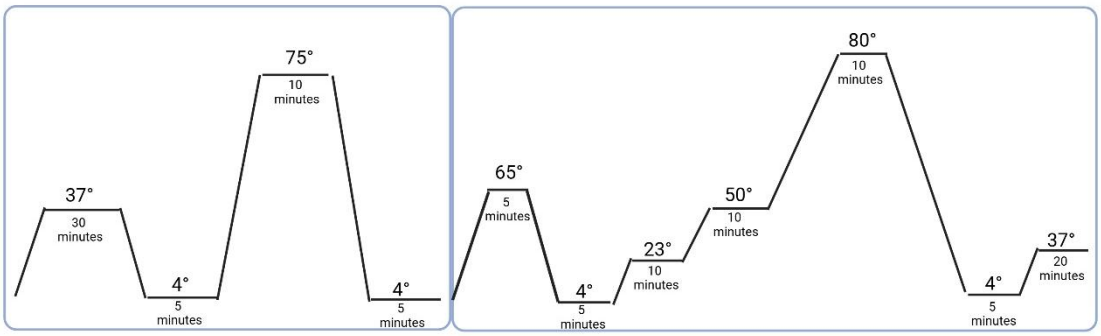


Figure 38. RNA reverse transcription process. *Therma profile of DNase treatment and reverse transcription process. Created with BioRender (created with biorendor.com).*

7.13 Reverse transcription (Joslin Diabetes Center)

The reaction included 100 ng of total RNA from each EndoC-Bh5 sample. It was reverse transcribed using the High-Capacity cDNA Reverse Transcription kit (*Thermofisher*). The 2X RT master mix (final volume 20 µL) was prepared with 10X RT Buffer, 25X dNTP Mix, 10X RT RANDOM PRIMERS, MultiSCRIBE Reverse Transcriptase, RNase Inhibitor and Nuclease-free H_2O. The reaction was performed under the following thermal profile: 10 minutes at 25°, 120 minutes at 37° and 5 minutes at 85° (**Figure 39**). The cDNA obtained was stored at -20°C until use.

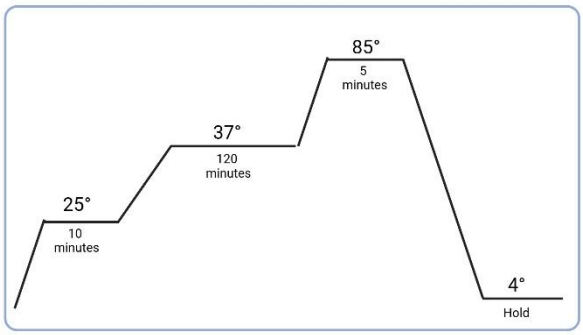


Figure 39. RNA reverse transcription thermal profile. *Created with BioRender (created with biorendor.com).*

7.14 TaqMan Gene Expression Assay

Gene expression was investigated at three main stages of the differentiation process (iPSC, EN, iβ) by real-time PCR using the Applied Biosystems TaqMan Arrays (4342259, *Applied Biosystems*) containing TaqMan Gene Expression Assays dried down in 96-well TaqMan Array plates. These qPCR arrays are ideal for gene expression profiling that

require the analysis of tens to thousands of targets (**Figure 40**). Customized TaqMan Array Card were used to analyze a panel of 96 genes. Each sample was analyzed with predesigned gene-specific primer and probe sets from TaqMan Gene Expression Assays (*Applied Biosystems*) related to specific genes for iβ differentiation, insulin machinery, cellular senescence and SASP factors (**Table 14).** The TaqMan Array Card is designed to perform 96 simultaneous Real-Time PCR (qPCR) reactions and support 4 samples. These cards provide highly reproducible and sensitive results with higher throughput. The following thermal profile was used: 50°C for 2 minutes, 92°C for 10 minutes and 40 cycles of 95°C for 1 second and 60°C for 20 seconds. In each lane of the Gene Card, it has been loaded a mix solution composed of 55 µL of TaqMan Fast Advanced Master Mix, 750 ng of cDNA and nuclease free H2O to reach a total volume of 100 µL for each lane. Afterward, the card was sealed, centrifuged at 331 xg for 1 minute twice, and PCR was performed using the QuantStudio 12K Flex instrument (Applied Biosystems). The geometric mean of the housekeeping genes, glyceraldehyde-3-phosphate dehydrogenase (*GAPDH*), β-actin (*ACTB*), Peptidylprolyl Isomerase A (*PPIA*) and Tata Binding Protein (*TBP*), was used for data normalization. Relative quantification of target genes was carried out after sample normalization using the $2^{-\Delta Ct}$ method.

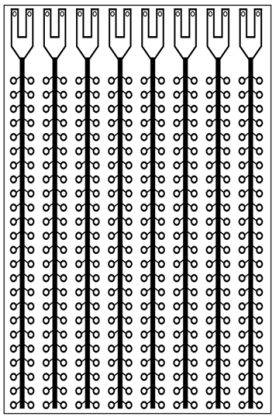


Figure 40. TaqMan Array Card. *Schematic representation of the Gene Card. In each reaction well is loaded 750 ng of sample* (Lappan *et al*, 2022).

Gene symbol	Gene name	Function
ATM	ATM serine/threonine kinase	Cellular senescence
BAMBI	BMP and activin membrane bound inhibitor	Cellular senescence
BAX	BCL2 associated X, apoptosis regulator	Cellular senescence
BCL2	BCL2, apoptosis regulator	Cellular senescence
BMI1	BMI1 proto-oncogene, polycomb ring finger	Cellular senescence
CCNA1	cyclin A1	Cellular senescence
CDKN1A (P21)	cyclin dependent kinase inhibitor 1A	Cellular senescence
CDKN1B	cyclin dependent kinase inhibitor 1B	Cellular senescence
CDKN2A (P16)	cyclin dependent kinase inhibitor 2A	Cellular senescence
ETS1	ETS proto-oncogene 1, transcription factor	Cellular senescence
FOS	Fos proto-oncogene, AP-1 transcription factor subunit	Cellular senescence
FOXM1	forkhead box M1	Cellular senescence
GATA4	GATA binding protein 4	Cellular senescence
IGF1R	insulin like growth factor 1 receptor	Cellular senescence
MAPK1	mitogen-activated protein kinase 1	Cellular senescence
MAPK3	mitogen-activated protein kinase 3	Cellular senescence
MAPK7	mitogen-activated protein kinase 7	Cellular senescence
NRAS	neuroblastoma RAS viral oncogene homolog	Cellular senescence
PDGFRA	platelet derived growth factor receptor alpha	Cellular senescence
PTEN	phosphatase and tensin homolog	Cellular senescence
RELA	RELA proto-oncogene, NF-kB subunit	Cellular senescence
RHEB	Ras homolog enriched in brain	Cellular senescence
STAT3	signal transducer and activator of transcription 3	Cellular senescence
TGFB1	transforming growth factor beta 1	Cellular senescence
TRAPCC2	trafficking protein particle complex subunit 2	Cellular senescence
CCL2	c-c motif chemokine ligand 2	SASP factors
CXCL1	c-x-c motif chemokine ligand 1	SASP factors
CXCL10	c-x-c motif chemokine ligand 10	SASP factors
IGFBP3	insulin like growth factor binding protein 3	SASP factors
IGFBP4	insulin like growth factor binding protein 4	SASP factors
IL1A	interleukin 1 alpha	SASP factors
IL6	interleukin 6	SASP factors
CCL3	c-c motif chemokine ligand 3	SASP factors
CCL5	c-c motif chemokine ligand 5	SASP factors
CXCL8	c-x-c motif chemokine ligand 8	SASP factors
IGFBP5	insulin like growth factor binding protein 5	SASP factors
IL1B	interleukin 1 beta	SASP factors
SERPINE1	serpin family e member 1	SASP factors
TNF	tumor necrosis factor	SASP factors

NANOG	Nanog homeobox	Marker of iβ differentiation
POU5F1	POU class 5 homeobox 1	Marker of iβ differentiation
SOX2	SRY-box 2	Marker of iβ differentiation
SOX17	SRY-box 17	Marker of iβ differentiation
SOX9	SRY-box 9	Marker of iβ differentiation
CXCR4	C-X-C motif chemokine receptor 4	Marker of iβ differentiation
FOXA2	forkhead box A2	Marker of iβ differentiation
PDX1	pancreatic and duodenal homeobox 1	Marker of iβ differentiation
HNF1B	HNF1 homeobox B	Marker of iβ differentiation
HNF4A	hepatocyte nuclear factor 4 alpha	Marker of iβ differentiation
ONECUT1	one cut homeobox 1	Marker of iβ differentiation
NEUROD1	neuronal differentiation 1	Marker of iβ differentiation
NEUROG3	neurogenin 3	Marker of iβ differentiation
NKX2-2	NK2 homeobox 2	Marker of iβ differentiation
NKX6-1	NK6 homeobox 1	Marker of iβ differentiation
SST	Somatostatin	Marker of iβ differentiation
UCN3	urocortin 3	Marker of iβ differentiation
INS	Insulin	Marker of iβ differentiation
MAFA	MAF bZIP transcription factor A	Marker of iβ differentiation
GCG	Glucagon	Marker of iβ differentiation
ABCC8	ATP binding cassette subfamily C member 8	Glucose sensing/Insulin secretion
ANO6	anoctamin 6	Glucose sensing/Insulin secretion
ANO8	anoctamin 8	Glucose sensing/Insulin secretion
BEST3	bestrophin 3	Glucose sensing/Insulin secretion
CACNA1B	calcium voltage-gated channel subunit alpha1 B	Glucose sensing/Insulin secretion
CACNA1A	calcium voltage-gated channel subunit alpha1 A	Glucose sensing/Insulin secretion
GCGR	glucagon receptor	Glucose sensing/Insulin secretion
GCK	Glucokinase	Glucose sensing/Insulin secretion
KCNA2	potassium voltage-gated channel subfamily A member 2	Glucose sensing/Insulin secretion
KCNB1	potassium voltage-gated channel subfamily B member 1	Glucose sensing/Insulin secretion
KCND1	potassium voltage-gated channel subfamily D member 1	Glucose sensing/Insulin secretion
KCNH1	potassium voltage-gated channel subfamily H member 1	Glucose sensing/Insulin secretion
KCNH6	potassium voltage-gated channel subfamily H member 6	Glucose sensing/Insulin secretion
KCNJ11	potassium voltage-gated channel subfamily J member 11	Glucose sensing/Insulin secretion
SCN3A	sodium voltage-gated channel alpha subunit 3	Glucose sensing/Insulin secretion
SCN8A	sodium-voltage gated channel alpha subunit 8	Glucose sensing/Insulin secretion
SCN9A	sodium-voltage gated channel alpha subunit 9	Glucose sensing/Insulin secretion
SLC2A1	solute carrier family 2 member 1	Glucose sensing/Insulin secretion
SLC2A2	solute carrier family 2 member 2	Glucose sensing/Insulin secretion
TRPM3	transient receptor potential cation channel subfamily M member 3	Glucose sensing/Insulin secretion
TRPM4	transient receptor potential cation channel subfamily M member 4	Glucose sensing/Insulin secretion
TRPM5	transient receptor potential cation channel subfamily M member 5	Glucose sensing/Insulin secretion

Table 14. A list of specific differentiation marker genes analyzed using the Gene Card assay. *The table lists gene symbols, names and functions quantified at iPSC, EN and iβ stages of the differentiation protocol.*

7.15 Taqman Real-Time PCR

Real time PCR was performed in a 7900 Real-Time PCR System (*Applied Biosystems*) using TaqMan Fast Advanced Master Mix (*Applied Biosystem*). Each sample was analyzed in duplicate with predesigned gene-specific TaqMan Gene Expression Assays (*Applied Biosystems*) (**Table 15**). The following thermal profile was used: 95°C for 20 seconds, and 40 cycles of 95°C for 1 second and 60°C for 20 seconds. Gene expression levels are normalized to *GAPDH* and reported as $2^{-\Delta Ct}$ or as a fold change relative to the control ($2^{-\Delta\Delta Ct}$).

Gene symbol	Gene name	TaqMan probe
CDKN2A (P16)	cyclin-dependent kinase inhibitor 2A	Hs00923894_m1
CDKN1A (P21)	cyclin dependent kinase inhibitor 1°	Hs00355782_m1
ATM	ATM serine/threonine kinase	Hs00175892_m1
TP53	tumor protein P53	Hs01034249_m1
JUN	jun proto-oncogene	Hs01103582_s1
IL1A	interleukin 1 alpha	Hs00174092_m1
IL6	interleukin 6	Hs00174131_m1
LSAMP	limbic system associated membrane protein	Hs01082652_m1
DUSP3	dual specificity phosphatase 3	Hs01115776_m1
GDF15	growth differentiation factor 15	Hs00171132_m1
NKX6.1	NK6 homeobox 1	Hs00232355_m1
INS	insulin	Hs00356618_m1
GAPDH	glyceraldehyde-3-phosphate dehydrogenase	Hs99999905_m1

Table 15. List of the genes analyzed with the TaqMan Real-Time PCR. In the table are reported gene symbols, gene names and TaqMan probe number.

7.16 Quantitative Real-Time PCR (Joslin Diabetes Center)

Real time PCR was performed in a QuantStudio 6 Pro System (*Applied Biosystems*). Fast Syber Green (*Applied Biosystems*) and custom designed primers were used to quantify the levels of target genes (*Eurofins*) (**Table 16**). The following thermal profile was used: 95°C for 30 seconds, and 40 cycles of 95°C for 3 seconds and 60°C for 30 seconds. Gene expression levels are normalized to *GAPDH* and reported as $2^{-\Delta Ct}$ or as a fold change relative to the control ($2^{-\Delta\Delta Ct}$).

Gene symbol	Gene name	Forward	Reverse
CDKN2A (P16)	cyclin-dependent kinase inhibitor 2a	CTTCGGCTGACTGGCTG	GCCTCCGACCGTAACTATTC
CDKN1A (P21)	cyclin dependent kinase inhibitor 1°	TGTCACTGTCTTGTACCCTTG	GCGTTTGGAGTGGTAGAAATC
ATM	atm serine/threonine kinase	CCGTGATGACCTGAGACAAGATG	CAAGAACACCACTTCGCTGAGAG
TP53	tumor protein p53	CCATCCTCACCATCATCACACTG	CACAAACACGCACCTCAAAGC
BCL2	jun proto-oncogene	AACGTGCCTCATGAAATAAAG	TTATTGGATGTGCTTTGCATTC
CAS8	caspase 8	CAGGCAGGGCTCAAATTTCT	TCTGCTCACTTCTTCTGAAATCTGA
CYCS	cytochrome c	GGCTGCAGTGTAGCTGTGAT	GATGGAGTTTCCTTTATCTGTTGC
MAPK14 (P38)	mitogen-activated protein kinase 14	CAGCAGCTGGAACGGGAGTA	GGTAGAACGTGGGCCTCTCC
ATR	serine/threonine kinase	TGCAGTAATGTCAATGGTTGG	CTGGAACTTCAAAGGTTTCTCC
LSAMP	limbic system associated membrane protein	CACTGGCAGAGGAGCATCCA	GGCTTTCATCCACAGCGAGC
DUSP3	dual specificity phosphatase 3	CTGTGGCTCAGGACATCCCC	TGGCATTGGTGTTGACGTGC
GDF15	growth differentiation factor 15	CCGAAGACTCCAGATTCCGA	CCCGAGAGATACGCAGGTG
HSP90AA1	heat shock protein 90 alpha family class a member 1)	ATGGCTGCTTCCCAGGTGAT	CTTCCTCCGCTCTTTGGGGT
CCL11	c-c motif chemokine ligand 11	CCCCTTCAGCGACTAGAGAG	TCTTGGGGTCGGCACAGAT
CD109	cd109 molecule	TTGAATTCCCAATCCTGGAG	TTGTTGCCACTAACCACCAA
JUN	jun proto-oncogene	CCGGCTGGAGGAAAAAGT	CCGACGGTCTCTCTTCAA
HSPA1A	heat shock protein family a member 1a	ACTCCCGTTGTCCCAAGGCTTC	TCTGTCGGCTCCGCTCTGAGAT
ANGPTL3	angiopoietin like 3	ACCATTTATAACAGAGGTGAACATACAAG	CCTGATATAACATCACAGTAGACATGAAAA
TNFSF4	tnf superfamily member 4	TGCTCTTCAGGTATCACATCGG	ATGACTGAGTTGTTCTGCACC
NKX6.1	nk6 homeobox 1	CTGGCCTGTACCCCTCATCA	CTTCCCGTCTTTGTCCAACAA
INS	insulin	GCAGCCTTTGTGAACCAACA	TTCCCCGCACACTAGGTAGAGA
GAPDH	glyceraldehyde-3-phosphate dehydrogenase	TTGAGGTCAATGAAGGGGTC	GAAGGTGAAGGTCGGAGTCA

Table 16. List of the genes analyzed with the Quantitative Real-Time PCR. *The table lists the gene symbols, gene names and primer sequences.*

7.17 SOMAScan assay (Joslin Diabetes Center)

At the iβ stage (DRI2#3, #4, #9, #13, #14, #15), cells were cultured for 24 hours in Stage 7 medium without BSA, generating iβ Conditioned media (CM). The iβ CM was then collected to perform proteomic analysis with SOMAScan assay v4.1 (*SomaLogic*) for the detection of specific released β cell *p16*$^{+}$ SASP factors (**Table 17**) and *p21*$^{+}$ SASP factors (**Table 18**). As negative control the basal Stage 7 media without BSA was analyzed. The experimental workflow consists of the following steps:
-Preparation of SOMAmer reagents: synthetic SOMAmer reagents (single-stranded DNA molecules modified for high-affinity protein binding) are prepared, and labeled with a fluorophore, a photocleavable linker and a biotin molecule.
-Protein capture: diluted samples are incubated with dilution-specific SOMAmers immobilized on streptavidin-coated beads via their biotin tags.
-Removal of unbound proteins: three washing steps are performed to remove non-specific and unbound proteins, ensuring that only specific protein-SOMAmer complexes remain.
-Protein labeling: the captured proteins are labeled with biotin to facilitate their identification.

- Release of Protein-SOMAmer Complexes: the photocleavable linker is broken using UV light, releasing the protein-SOMAmer complexes from the beads into the solution.
-Second capture on new beads: the released complexes are introduced into a new set of streptavidin beads, where the biotinylated proteins bind again, leaving free SOMAmer reagents in solution.
-Quantification of SOMAmer Reagents: the free SOMAmer molecules, which reflect the original protein abundance, are quantified using microarray hybridization techniques, where the fluorescence signal intensity correlates with protein concentration in the samples.

This assay was conducted at BIDMC Genomics, Proteomics, Bioinformatics, and Systems Biology Center (Boston), enabling the measurement of up to 7000 human proteins, using only 50 µL of sample.

Protein symbol	Protein name
TGFBR3	transforming growth factor beta receptor 3
AIP	aryl hydrocarbon receptor interacting protein
FGF12	fibroblast growth factor 12
NAGK	n-acetylglucosamine kinase
UFM1	ubiquitin fold modifier 1
IMPDH1	inosine monophosphate dehydrogenase 1
SNX4	sorting nexin 4
HSP90AA1	heat shock protein 90 alpha family class a member 1
UFC1	ubiquitin-fold modifier conjugating enzyme 1
MAPK14	mitogen-activated protein kinase 14
HINT1	histidine triad nucleotide binding protein 1
NSFL1C	nsfl1 cofactor
RBM39	rna binding motif protein 39
YES1	yes proto-oncogene 1
UCHL1	ubiquitin c-terminal hydrolase l1
PRDX1	peroxiredoxin 1
KNDC12	potassium two pore domain channel subfamily k member 12
RPSA	ribosomal protein sa
YWHAB	tyrosine 3-monooxygenase/tryptophan 5-monooxygenase activation protein beta
CRK	crk proto-oncogene
GTSP1	glutathione s-transferase pi 1
HSP90AB1	heat shock protein 90 alpha family class b member 1

Table 17. List of specific β cell p16⁺ SASP factors analyzed with SOMAScan. *The table lists the protein symbols and protein names.*

Protein symbol	Protein name
PGK1	phosphoglycerate kinase 1
PDXP	pyridoxal phosphatase
VTA1	vesicle trafficking 1
YWHAZ	tyrosine 3-monooxygenase/tryptophan 5-monooxygenase activation protein zeta
EIF5A2	eukaryotic translation initiation factor 5a2
DCTN2	dynactin subunit 2
DUSP3	dual specificity phosphatase 3
AKT2	akt serine/threonine kinase 2
EIF5	eukaryotic translation initiation factor 5
SHC1	shc adaptor protein 1
LAMC1	laminin subunit gamma 1
YWHAE	tyrosine 3-monooxygenase/tryptophan 5-monooxygenase activation protein epsilon
CAMK2D	calcium/calmodulin dependent protein kinase ii delta
GDF15	growth differentiation factor 15
TAGLN2	transgelin 2
NCAM1	neural cell adhesion molecule 1
TPM4	tropomyosin 4
FAH1B2	platelet activating factor acetylhydrolase 1b catalytic subunit 2
KPNB1	karyopherin subunit beta 1
HSPA1A	heat shock protein family a (hsp70) member 1a

Table 18. List of specific β cell p21⁺ SASP factors analyzed with SOMAScan. *The table lists the protein symbols and protein names.*

7.18 Static glucose-stimulated insulin secretion (Joslin Diabetes Center)

Static glucose-stimulated insulin secretion (GSIS) was performed on EndoC-βh5 cells. On Day 6 of culture, the cells were starved with UltiST medium (*Human Cell Design*) for 24 hours. On Day 7, cells were incubated with βKrebs (*Human Cell Design*) supplemented with 0.1% BSA (*Merck*) following these steps:

-Acclimatization step: pre-incubation of 60 minutes with βKrebs without glucose.

-Pre-stimulus step: incubation of 40 minutes with βKrebs supplemented without glucose.

-High glucose step: incubation of 40 minutes with βKrebs supplemented with 20mM of glucose.

After the low and high glucose steps, the supernatant from each well was carefully collected and stored at -80°. Once GSIS finished, the cells were collected from each well to analyze DNA concentration and the total insulin content.

7.19 Collection of EndoC-βH5 cells for insulin and DNA content quantification (Joslin Diabetes Center)

After static GSIS, $1x10^5$ EndoC-βH5 cells were detached with Trypsin/EDTA (*Merck*) and resuspended in 400 uL of PBS. The aliquot was frozen at -20° or sonicated immediately. Cells were sonicated following these steps: 10 seconds of sonication,

followed by 15 seconds on ice, repeated three times. Once the cells were sonicated, the total volume was divided into two equal aliquots of 200 µL to determine total insulin content and DNA quantity.

7.20 Dynamic glucose-stimulated insulin secretion

β cells were collected at the end of the differentiation protocol and tested to assess their ability to respond to a glucose stimulus by a dynamic perifusion analysis. In this process, terminally differentiated cells (Day 30) undergo exposure to various stimuli, including low glucose, high glucose, and depolarizing KCl using the perifusion machine (BioRep Perifusion V2.0.0). Cells were maintained into a chamber at 37°C and perfused with different concentrations of glucose with a speed flow of 30 µL/min in the first step and with a speed flow of 100 µL/min in the other steps with a pulsatile peristaltic pump. The eluate was collected in 96 well plates. The following protocol was used:
- Step 1 (Low glucose): cells were maintained in low glucose condition (0.5 mM) in a KREBS solution composed by NaCl 125 mM, KCl 5.9 mM, CaCl2 2.56 mM, MgCl2 1mM, HEPES 25mM, 0.1% BSA, pH 7.4 for 1 hour, this is the period of acclimatization.
- Step 2 (Low glucose): cells were maintained in a solution of glucose 0.5 mM for 20 minutes.
- Step 3 (High glucose or High glucose + IBMX): cells are stimulated with a solution of 11mM glucose for 20 minutes. For IBMX condition, cells are stimulated with a solution of 11mM glucose supplemented with IBMX 50 µM (*Gibco*).
- Step 4 (Low glucose): glucose concentration decreased to 0.5 mM for 20 minutes.
- Step 5 (KCl): a solution of KCl 30 mM for 20 minutes was used to depolarize the cells and allow insulin secretion in the intracellular deposits. -
- Step 6 (Low glucose): cells were maintained for 20 minutes with a 0.5 mM glucose concentration.
The eluate was collected and frozen at -80 °C until use.

7.21 ELISA

Insulin ELISA KIT (*Mercodia*) was used to quantify insulin content in the eluate collected from EndoC-βH5 static GSIS and from specific perifusion steps of iβ dynamic GSIS (minute 60 of step 1; minutes 15 and 20 of step 2; minutes 1 to 20 of step 3; minutes 1 to 5 and 10, 20 of step 4; minutes 3, 5, 10, 15, 20 of step 5; minutes 5, 10, 20 of step 6) using

the following protocol: standard calibrators and samples were loaded into the plate (25 µL per well), already coated with insulin antibody. Then, 100 µL of 1X Conjugated Enzyme mix was added to each well, including the standards. The plate was incubated with an orbital shaker for 1 hour at room temperature with a speed of 300 rpm. After one hour, the plate was washed six times with 1X Wash Buffer Solution using an automatic washer. After washes, 200 µL of TMB Substrate was added and the plate was incubated at room temperature for 15 minutes. After that, 50 µL of Stop Solution was added and the ELISA was read using the Bio-Rad spectrophotometer reader (Milan), or GloMax Promega reader (Joslin Diabetes Center).

7.22 DNA extraction

Cells at Day 0 (iPSCs), Day 11 (PE), Day 21 (EN), and Day 30 (iβ) were detached with Accutase (*Merck*) for 5 min at 37 °C, washed with PBS and the dry pellet was frozen at -80°C until DNA extraction. The MaxwellR RSC Instrument (*Promega*) was used to automatically extract the DNA with the MaxwellR RSC Blood DNA Kit (*Promega*) following the manufacturing procedure. The DNA was quantified by the Quantus Fluorometer (*Promega*), using the QuantiFluorR ONE dsDNA System. As a final step, the obtained extracted DNA was stored at -80°C until use.

7.23 DNA extraction (Joslin Diabetes Center)

EndoC-βH5 ($5x10^4$ cells) were sonicated, as previously described, resuspended in 200µL of PBS and stored at -20C° until DNA extraction. DNA was extracted using DNeasy Blood & Tissue Kit (69506, *Qiagen*) following the manufacturer guidelines and quantified with Nanodrop.

7.24 DNA sequencing

DNA at Day 0 (iPSCs), Day 11 (PE), Day 21 (EN), and Day 30 (iβ) were sequenced through Duplex Sequencing Technology, using the TwinStrand DuplexSeq Kit (*TwinStrand Biosciences*). TwinStrand Duplex Sequencing technology is a biochemical and informatics-based error correction approach that provides unprecedented sequencing accuracy and enables highly sensitive detection of ultra-low frequency genetic variants (**Figure 41**). The sequencing has been performed, according to the manufacture

instructions at the Center for Omics Sciences (COS) at IRCCS San Raffaele Hospital, in Milan.

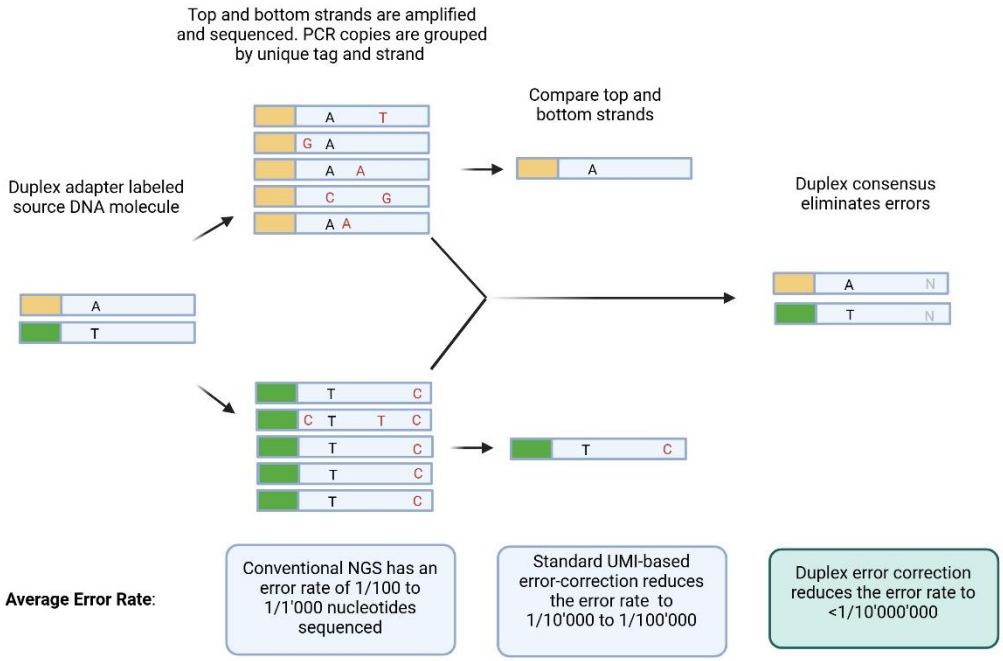


Figure 41. Duplex sequencing technology. *DNA molecules were first labeled with duplex adapters, containing unique molecular identifiers (UMIs) for both top and bottom strands. After PCR amplification, sequencing reads were grouped based on their unique tags and strand information. Conventional next-generation sequencing (NGS) produces errors at a rate of 1 in 100 to 1 in 1,000 nucleotides. To mitigate these errors, UMI-based error correction was applied, reducing the error rate to 1 in 10,000 to 1 in 100,000. Finally, a Duplex Consensus Sequence (DCS) was generated by comparing the complementary strands, eliminating PCR and sequencing artifacts. This duplex error correction resulted in an exceptionally low error rate of <1 in 10 million nucleotides, ensuring high-confidence variant detection. Created with BioRender (www.biorender.com).*

7.25 Statistical analysis

Statistical analysis was performed using GraphPad Prism software version 9. Data distribution was evaluated by applying a normality test (Shapiro-Wilk test).

FACS data comparisons among groups were performed using the ANOVA and One-Sample t-test, as data were normally distributed.

Quantification of gene expression data was carried out after sample normalization using the geometric mean of the housekeeping mRNA abundance using the $2^{-\Delta Ct}$ method or as a fold change relative to the control ($2^{-\Delta\Delta Ct}$). A Wilcoxon-Mann-Whitney or a t-test were applied for data normally or not normally distributed, respectively.

SOMAscan data were transformed into log2 and presented as their corresponding z-score. Wilcoxon-Mann-Whitney or t-test were applied for the statistical analysis.

The heatmap analysis was done using the Heatmapper online tool (http://www.heatmapper.ca/) using the mean values of gene expression for each time point of differentiation (Day 0, Day 21, Day 30) and of proteomic data applying the Spearman Rank method for not normally distributed data.

Statistical significance was accepted at p-value ≤ 0.05.

8. References

Admasu TD, Rae M & Stolzing A (2021) Dissecting primary and secondary senescence to enable new senotherapeutic strategies. *Ageing Res Rev* 70: 101412

Agarwal A & Brayman KL (2012) Update on islet cell transplantation for type 1 diabetes. *Semin Intervent Radiol* 29: 90–98

Aghali A, Ngassie MLK, Pabelick CM & Prakash YS (2022) Cellular Senescence in Aging Lungs and Diseases. *Cells* 11: 1781

Aguayo-Mazzucato C (2020) Functional changes in beta cells during ageing and senescence. *Diabetologia* 63: 2022–2029

Aguayo-Mazzucato C, Andle J, Lee TB, Midha A, Talemal L, Chipashvili V, Hollister-Lock J, van Deursen J, Weir G & Bonner-Weir S (2019) Acceleration of β Cell Aging Determines Diabetes and Senolysis Improves Disease Outcomes. *Cell Metab* 30: 129-142.e4

Aguayo-Mazzucato C, van Haaren M, Mruk M, Lee TB, Crawford C, Hollister-Lock J, Sullivan BA, Johnson JW, Ebrahimi A, Dreyfuss JM, *et al* (2017) β Cell Aging Markers Have Heterogeneous Distribution and Are Induced by Insulin Resistance. *Cell Metab* 25: 898-910.e5

Aird KM & Zhang R (2013) Detection of senescence-associated heterochromatin foci (SAHF). *Methods in Molecular Biology* 965: 185–196

Amor C, Fernández-Maestre I, Chowdhury S, Ho YJ, Nadella S, Graham C, Carrasco SE, Nnuji-John E, Feucht J, Hinterleitner C, *et al* (2024) Prophylactic and long-lasting efficacy of senolytic CAR T cells against age-related metabolic dysfunction. *Nature Aging 2024 4:3* 4: 336–349

Anerillas C, Abdelmohsen K & Gorospe M (2020) Regulation of senescence traits by MAPKs. *Geroscience* 42: 397

Artero Castro A, León M, Luna-Peláez N, Bernal AM, del Buey Furió V, Erceg S & Lukovic D (2018) Generation of a human iPSC line by mRNA reprogramming. *Stem Cell Res* 28: 157–160

Balboa D, Barsby T, Lithovius V, Saarimäki-Vire J, Omar-Hmeadi M, Dyachok O, Montaser H, Lund PE, Yang M, Ibrahim H, *et al* (2022) Functional, metabolic and transcriptional maturation of human pancreatic islets derived from stem cells. *Nature Biotechnology 2022 40:7* 40: 1042–1055

Barsby T, Ibrahim H, Lithovius V, Montaser H, Balboa D, Vähäkangas E, Chandra V, Saarimäki-Vire J & Otonkoski T (2022) Differentiating functional human islet-like aggregates from pluripotent stem cells. *STAR Protoc* 3: 101711

Basta G, Montanucci P & Calafiore R (2020) Microencapsulation of cells and molecular therapy of type 1 diabetes mellitus: The actual state and future perspectives between promise and progress. *J Diabetes Investig* 12: 301

Basu R, Breda E, Oberg AL, Powell CC, Man CD, Basu A, Vittone JL, Klee GG, Arora P, Jensen MD, *et al* (2003) Mechanisms of the Age-Associated Deterioration in Glucose ToleranceContribution of Alterations in Insulin Secretion, Action, and Clearance. *Diabetes* 52: 1738–1748

Beauséjour CM, Krtolica A, Galimi F, Narita M, Lowe SW, Yaswen P & Campisi J (2003) Reversal of human cellular senescence: roles of the p53 and p16 pathways. *EMBO J* 22: 4212–4222

Beyerlein A, Chmiel R, Hummel S, Winkler C, Bonifacio E & Ziegler AG (2014) Timing of gluten introduction and islet autoimmunity in young children: updated results from the BABYDIET study. *Diabetes Care* 37

Blanchi B, Taurand M, Colace C, Thomaidou S, Audeoud C, Fantuzzi F, Sawatani T, Gheibi S, Sabadell-Basallote J, Boot FWJ, *et al* (2023) EndoC-βH5 cells are storable and ready-to-use human pancreatic beta cells with physiological insulin secretion. *Mol Metab* 76: 101772

Bloom J & Cross FR (2007) Multiple levels of cyclin specificity in cell-cycle control. *Nat Rev Mol Cell Biol* 8: 149–160

Bluestone JA, Herold K & Eisenbarth G (2010) Genetics, pathogenesis and clinical interventions in type 1 diabetes. *Nature* 464: 1293–1300

Boccardi V & Mecocci P (2021) Senotherapeutics: Targeting senescent cells for the main age-related diseases. *Mech Ageing Dev* 197: 111526

Bradburn S, McPhee J, Bagley L, Carroll M, Slevin M, Al-Shanti N, Barnouin Y, Hogrel JY, Pääsuke M, Gapeyeva H, *et al* (2018) Dysregulation of C-X-C motif ligand 10 during aging and association with cognitive performance. *Neurobiol Aging* 63: 54–64

Brawerman G, Pipella J & Thompson PJ (2022) DNA damage to β cells in culture recapitulates features of senescent β cells that accumulate in type 1 diabetes. *Mol Metab* 62: 101524

Bulbiankova D, Díaz-Puertas R, Álvarez-Martínez FJ, Herranz-López M, Barrajón-Catalán E & Micol V (2023) Hallmarks and Biomarkers of Skin Senescence: An Updated Review of Skin Senotherapeutics. *Antioxidants 2023, Vol 12, Page 444* 12: 444

Burton DGA & Krizhanovsky V (2014) Physiological and pathological consequences of cellular senescence. *Cellular and Molecular Life Sciences* 71: 4373–4386

Buzzetti R, Zampetti S & Pozzilli P (2020) Impact of obesity on the increasing incidence of type 1 diabetes. *Diabetes Obes Metab* 22: 1009–1013

Catarinella D, Melzi R, Mercalli A, Magistretti P, Tentori S, Gremizzi C, Paloschi V, Cobelli F De, Esposto G, Costa S, *et al* (2025) Long-term outcomes of pancreatic islet transplantation alone in type 1 diabetes: a 20-year single-centre study in Italy. *Lancet Diabetes Endocrinol* 0

Cerneckis J, Cai H & Shi Y (2024) Induced pluripotent stem cells (iPSCs): molecular mechanisms of induction and applications. *Signal Transduction and Targeted Therapy 2024 9:1* 9: 1–26

Cha J, Aguayo-Mazzucato C & Thompson PJ (2023) Pancreatic β-cell senescence in diabetes: mechanisms, markers and therapies. *Front Endocrinol (Lausanne)* 14: 1212716

Chen S, Du K & Zou C (2020) Current progress in stem cell therapy for type 1 diabetes mellitus. *Stem Cell Res Ther* 11

Cheng Z, Peng HL, Zhang R, Fu XM & Zhang G Sen (2017) Rejuvenation of Cardiac Tissue Developed from Reprogrammed Aged Somatic Cells. *Rejuvenation Res* 20: 389–400

Chimienti R, Baccega T, Torchio S, Manenti F, Pellegrini S, Cospito A, Amabile A, Lombardo MT, Monti P, Sordi V, *et al* (2022) Engineering of immune checkpoints B7-H3 and CD155 enhances immune compatibility of MHC-I−/− iPSCs for β cell replacement. *Cell Rep* 40: 111423

Choi J, Cooper ML, Staser K, Ashami K, Vij KR, Wang B, Marsala L, Niswonger J, Ritchey J, Alahmari B, *et al* (2018) Baricitinib-induced blockade of interferon gamma receptor and interleukin-6 receptor for the prevention and treatment of graft-versus-host disease. *Leukemia* 32: 2483

Christoffersson G (2022) Towards effective beta-cell replacement through understanding and targeting of the autoreactive immune response during onset of type 1 diabetes. *J Immunol Regen Med* 15: 100057

Chuengsamarn S, Rattanamongkolgul S, Luechapudiporn R, Phisalaphong C & Jirawatnotai S (2012) Curcumin extract for prevention of type 2 diabetes. *Diabetes Care* 35: 2121–2127

Cinti F, Bouchi R, Kim-Muller JY, Ohmura Y, Sandoval PR, Masini M, Marselli L, Suleiman M, Ratner LE, Marchetti P, *et al* (2016) Evidence of β-Cell Dedifferentiation in Human Type 2 Diabetes. *J Clin Endocrinol Metab* 101: 1044–1054

Citro A, Moser PT, Dugnani E, Rajab KT, Ren X, Evangelista-Leite D, Charest JM, Peloso A, Podesser BK, Manenti F, *et al* (2019) Biofabrication of a vascularized islet organ for type 1 diabetes. *Biomaterials* 199: 40–51

Citro A, Neroni A, Pignatelli C, Campo F, Policardi M, Monieri M, Pellegrini S, Dugnani E, Manenti F, Maffia MC, *et al* (2023) Directed self-assembly of a xenogeneic vascularized endocrine pancreas for type 1 diabetes. *Nature Communications 2023 14:1* 14: 1–15

Cooper DKC, Mou L & Bottino R (2024) A brief review of the current status of pig islet xenotransplantation. *Front Immunol* 15: 1366530

D'Ambrosio M & Gil J (2023) Reshaping of the tumor microenvironment by cellular senescence: An opportunity for senotherapies. *Dev Cell* 58: 1007–1021

D'Amour KA, Agulnick AD, Eliazer S, Kelly OG, Kroon E & Baetge EE (2005) Efficient differentiation of human embryonic stem cells to definitive endoderm. *Nat Biotechnol* 23: 1534–1541

D'Amour KA, Bang AG, Eliazer S, Kelly OG, Agulnick AD, Smart NG, Moorman MA, Kroon E, Carpenter MK & Baetge EE (2006) Production of pancreatic hormone–expressing endocrine cells from human embryonic stem cells. *Nature Biotechnology 2006 24:11* 24: 1392–1401

Delong T, Wiles TA, Baker RL, Bradley B, Barbour G, Reisdorph R, Armstrong M, Powell RL, Reisdorph N, Kumar N, *et al* (2016) Pathogenic CD4 T cells in type 1 diabetes recognize epitopes formed by peptide fusion. *Science* 351: 711

Demaria M, Ohtani N, Youssef SA, Rodier F, Toussaint W, Mitchell JR, Laberge RM, Vijg J, VanSteeg H, Dollé MET, *et al* (2014) An essential role for senescent cells in optimal wound healing through secretion of PDGF-AA. *Dev Cell* 31: 722–733

Dermawan D & Kenichi Purbayanto MA (2022) An overview of advancements in closed-loop artificial pancreas system. *Heliyon* 8: e11648

DiMeglio LA, Evans-Molina C & Oram RA (2018) Type 1 diabetes. *Lancet* 391: 2449

Dodig S, Čepelak I & Pavić I (2019) Hallmarks of senescence and aging. *Biochem Med (Zagreb)* 29: 0–0

Dong JY, Zhang WG, Chen JJ, Zhang ZL, Han SF & Qin LQ (2013) Vitamin D Intake and Risk of Type 1 Diabetes: A Meta-Analysis of Observational Studies. *Nutrients 2013, Vol 5, Pages 3551-3562* 5: 3551–3562

Dong Z, Luo Y, Yuan Z, Tian Y, Jin T & Xu F (2024) Cellular senescence and SASP in tumor progression and therapeutic opportunities. *Molecular Cancer 2024 23:1* 23: 1–19

Dorrell C, Schug J, Canaday PS, Russ HA, Tarlow BD, Grompe MT, Horton T, Hebrok M, Streeter PR, Kaestner KH, *et al* (2016) Human islets contain four distinct subtypes of β cells. *Nat Commun* 7

El-Kady MM, Naggar RA, Guimei M, Talaat IM, Shaker OG & Saber-Ayad M (2021) Early renoprotective effect of ruxolitinib in a rat model of diabetic nephropathy. *Pharmaceuticals* 14: 608

Elsayed NA, Aleppo G, Aroda VR, Bannuru RR, Brown FM, Bruemmer D, Collins BS, Hilliard ME, Isaacs D, Johnson EL, *et al* (2022) 2. Classification and Diagnosis of Diabetes: Standards of Care in Diabetes—2023. *Diabetes Care* 46: S19

Enge M, Arda HE, Mignardi M, Beausang J, Bottino R, Kim SK & Quake SR (2017) Single-Cell Analysis of Human Pancreas Reveals Transcriptional Signatures of Aging and Somatic Mutation Patterns. *Cell* 171: 321-330.e14

Feng Q, Lu SJ, Klimanskaya I, Gomes I, Kim D, Chung Y, Honig GR, Kim KS & Lanza R (2010) Hemangioblastic Derivatives from Human Induced Pluripotent Stem Cells Exhibit Limited Expansion and Early Senescence. *Stem Cells* 28: 704–712

Fernandez-Rebollo E, Franzen J, Goetzke R, Hollmann J, Ostrowska A, Oliverio M, Sieben T, Rath B, Kornfeld JW & Wagner W (2020) Senescence-Associated Metabolomic Phenotype in Primary and iPSC-Derived Mesenchymal Stromal Cells. *Stem Cell Reports* 14: 201

Frohnert BI, Ide L, Dong F, Barón AE, Steck AK, Norris JM & Rewers MJ (2017) Late-onset islet autoimmunity in childhood: the Diabetes Autoimmunity Study in the Young (DAISY). *Diabetologia* 60: 998–1006

Gamble A, Pepper AR, Bruni A & Shapiro AMJ (2018) The journey of islet cell transplantation and future development. *Islets* 10: 80–94

Gerace D, Zhou Q, Kenty JHR, Veres A, Sintov E, Wang X, Boulanger KR, Li H & Melton DA (2023) Engineering human stem cell-derived islets to evade immune rejection and promote localized immune tolerance. *Cell Rep Med* 4: 100879

Geravandi S, Liu H & Maedler K (2020) Enteroviruses and T1D: Is It the Virus, the Genes or Both which Cause T1D. *Microorganisms* 8: 1017

Gerencser AA (2015) Bioenergetic Analysis of Single Pancreatic β-Cells Indicates an Impaired Metabolic Signature in Type 2 Diabetic Subjects. *Endocrinology* 156: 3496–3503

Gillespie KM (2006) Type 1 diabetes: pathogenesis and prevention. *CMAJ* 175: 165–170

González-Gualda E, Baker AG, Fruk L & Muñoz-Espín D (2021) A guide to assessing cellular senescence in vitro and in vivo. *FEBS J* 288: 56–80

Gorbunova V, Seluanov A, Mao Z & Hine C (2007) Changes in DNA repair during aging. *Nucleic Acids Res* 35: 7466

Goyer ML, Desaulniers-Langevin C, Sonn A, Mansour Nehmo G, Lisi V, Benabdallah B, Raynal NJM & Beauséjour C (2024) Induced Pluripotent Stem Cell-Derived Fibroblasts Efficiently Engage Senescence Pathways but Show Increased Sensitivity to Stress Inducers. *Cells* 13: 849

Gregg T, Poudel C, Schmidt BA, Dhillon RS, Sdao SM, Truchan NA, Baar EL, Fernandez LA, Denu JM, Eliceiri KW, *et al* (2016) Pancreatic β-cells from mice offset age-associated mitochondrial deficiency with reduced KATP channel activity. *Diabetes* 65: 2700–2710

Gregory GA, Robinson TIG, Linklater SE, Wang F, Colagiuri S, de Beaufort C, Donaghue KC, Magliano DJ, Maniam J, Orchard TJ, *et al* (2022) Global incidence, prevalence, and mortality of type 1 diabetes in 2021 with projection to 2040: a modelling study. *Lancet Diabetes Endocrinol* 10: 741–760

Grootaert MOJ (2024) Cell senescence in cardiometabolic diseases. *npj Aging 2024 10:1* 10: 1–14

Gu C, Stein GH, Pan N, Goebbels S, Hörnberg H, Nave KA, Herrera P, White P, Kaestner KH, Sussel L, *et al* (2010) Pancreatic β cells require NeuroD to achieve and maintain functional maturity. *Cell Metab* 11: 298

Guan J, Wang G, Wang J, Zhang Z, Fu Y, Cheng L, Meng G, Lyu Y, Zhu J, Li Y, *et al* (2022) Chemical reprogramming of human somatic cells to pluripotent stem cells. *Nature 2022 605:7909* 605: 325–331

Guiho R, Selt F, Stone T, Jacques T, Hargrave D, Gil J, Witt O, Milde T & Barbera JPM (2021) LGG-09. SENOLYTIC AGENT NAVITOCLAX TARGETS VINBLASTINE- AND MAPK INHIBITORS-INDUCED SENESCENT TUMOUR CELLS IN PAEDIATRIC LOW GRADE GLIOMAS. *Neuro Oncol* 23: i33–i33

Gulej R, Nyúl-Tóth Á, Ahire C, DelFavero J, Balasubramanian P, Kiss T, Tarantini S, Benyo Z, Pacher P, Csik B, *et al* (2023) Elimination of senescent cells by treatment with Navitoclax/ABT263 reverses whole brain irradiation-induced blood-brain barrier disruption in the mouse brain. *Geroscience* 45: 2983–3002

Gustafson B, Nerstedt A, Spinelli R, Beguinot F & Smith U (2022) Type 2 Diabetes, Independent of Obesity and Age, Is Characterized by Senescent and Dysfunctional Mature Human Adipose Cells. *Diabetes* 71: 2372–2383

Hakola L, Takkinen HM, Niinistö S, Ahonen S, Nevalainen J, Veijola R, Ilonen J, Toppari J, Knip M & Virtanen SM (2018) Infant Feeding in Relation to the Risk of Advanced Islet Autoimmunity and Type 1 Diabetes in Children With Increased Genetic Susceptibility: A Cohort Study. *Am J Epidemiol* 187: 34–44

Hartemann A, Bensimon G, Payan CA, Jacqueminet S, Bourron O, Nicolas N, Fonfrede M, Rosenzwajg M, Bernard C & Klatzmann D (2013) Low-dose interleukin 2 in patients with type 1 diabetes: a phase 1/2 randomised, double-blind, placebo-controlled trial. *Lancet Diabetes Endocrinol* 1: 295–305

Hebrok M (2012) Generating β Cells from Stem Cells—The Story So Far. *Cold Spring Harb Perspect Med* 2: a007674

Helman A, Avrahami D, Klochendler A, Glaser B, Kaestner KH, Ben-Porath I & Dor Y (2016a) Effects of ageing and senescence on pancreatic β-cell function. *Diabetes Obes Metab* 18 Suppl 1: 58–62

Helman A, Klochendler A, Azazmeh N, Gabai Y, Horwitz E, Anzi S, Swisa A, Condiotti R, Granit RZ, Nevo Y, *et al* (2016b) p16Ink4a-induced senescence of pancreatic beta cells enhances insulin secretion. *Nature Medicine 2016 22:4* 22: 412–420

HENRY RR, PETTUS J, WILENSKY J, SHAPIRO AMJ, SENIOR PA, ROEP B, WANG R, KROON EJ, SCOTT M, D'AMOUR K, *et al* (2018) Initial Clinical Evaluation of VC-01TM Combination Product—A Stem Cell–Derived Islet Replacement for Type 1 Diabetes (T1D). *Diabetes* 67

Hering BJ, Clarke WR, Bridges ND, Eggerman TL, Alejandro R, Bellin MD, Chaloner K, Czarniecki CW, Goldstein JS, Hunsicker LG, *et al* (2016) Phase 3 Trial of Transplantation of Human Islets in Type 1 Diabetes Complicated by Severe Hypoglycemia. *Diabetes Care* 39: 1230–1240

Hernandez-Segura A, Nehme J & Demaria M (2018) Hallmarks of Cellular Senescence. *Trends Cell Biol* 28: 436–453

Herold KC, Bundy BN, Long SA, Bluestone JA, DiMeglio LA, Dufort MJ, Gitelman SE, Gottlieb PA, Krischer JP, Linsley PS, *et al* (2019) An Anti-CD3 Antibody, Teplizumab, in Relatives at Risk for Type 1 Diabetes. *N Engl J Med* 381: 603

Hoang DM, Pham PT, Bach TQ, Ngo ATL, Nguyen QT, Phan TTK, Nguyen GH, Le PTT, Hoang VT, Forsyth NR, *et al* (2022) Stem cell-based therapy for human diseases. *Signal Transduction and Targeted Therapy 2022 7:1* 7: 1–41

Hogrebe NJ, Ishahak M & Millman JR (2023) Developments in stem cell-derived islet replacement therapy for treating type 1 diabetes. *Cell Stem Cell* 30: 530–548

Horvath S (2015) Erratum to DNA methylation age of human tissues and cell types [Genome Biology, 14, R115, (2013)]. *Genome Biol* 16: 1–5

Hu X, li J, Fu M, Zhao X & Wang W (2021) The JAK/STAT signaling pathway: from bench to clinic. *Signal Transduction and Targeted Therapy 2021 6:1* 6: 1–33

Hu X, White K, Olroyd AG, DeJesus R, Dominguez AA, Dowdle WE, Friera AM, Young C, Wells F, Chu EY, *et al* (2023) Hypoimmune induced pluripotent stem cells survive long term in fully immunocompetent, allogeneic rhesus macaques. *Nature Biotechnology 2023 42:3* 42: 413–423

Hu X, White K, Young C, Olroyd AG, Kievit P, Connolly AJ, Deuse T & Schrepfer S (2024) Hypoimmune islets achieve insulin independence after allogeneic transplantation in a fully immunocompetent non-human primate. *Cell Stem Cell* 31: 334-340.e5

Hull CM, Peakman M & Tree TIM (2017) Regulatory T cell dysfunction in type 1 diabetes: what's broken and how can we fix it? *Diabetologia* 60: 1839

Ihm SH, Matsumoto I, Sawada T, Nakano M, Zhang HJ, Ansite JD, Sutherland DER & Hering BJ (2006) Effect of Donor Age on Function of Isolated Human Islets. *Diabetes* 55: 1361–1368

Ijima S, Saito Y, Yamamoto S, Nagaoka K, Iwamoto T, Kita A, Miyajima M, Sato T, Miyazaki A & Chikenji TS (2023) Senescence-associated secretory phenotypes in mesenchymal cells contribute to cytotoxic immune response in oral lichen planus. *Immunity and Ageing* 20: 1–15

Ilonen J, Lempainen J & Veijola R (2019) The heterogeneous pathogenesis of type 1 diabetes mellitus. *Nature Reviews Endocrinology 2019 15:11* 15: 635–650

Insel RA, Dunne JL, Atkinson MA, Chiang JL, Dabelea D, Gottlieb PA, Greenbaum CJ, Herold KC, Krischer JP, Lernmark A, *et al* (2015) Staging Presymptomatic Type 1 Diabetes: A Scientific Statement of JDRF, the Endocrine Society, and the American Diabetes Association. *Diabetes Care* 38: 1964–1974

Islam MT, Tuday E, Allen S, Kim J, Trott DW, Holland WL, Donato AJ & Lesniewski LA (2023) Senolytic drugs, dasatinib and quercetin, attenuate adipose tissue inflammation, and ameliorate metabolic function in old age. *Aging Cell* 22: e13767

Iwasaki K, Abarca C & Aguayo-Mazzucato C (2023a) Regulation of Cellular Senescence in Type 2 Diabetes Mellitus: From Mechanisms to Clinical Applications. *Diabetes Metab J* 47: 441–453

Iwasaki K, Lalani B, Kahng J, Carapeto P, Sanjines S, Hela F, Abarca C, Tsuji T, Darcy J, Bartke A, *et al* (2023b) Decreased IGF1R attenuates senescence and improves function in pancreatic β-cells. *Front Endocrinol (Lausanne)* 14: 1203534

Jennings RE, Berry AA, Strutt JP, Gerrard DT & Hanley NA (2015) Human pancreas development. *Development* 142: 3126–3137

Jin W & Jiang W (2022) Stepwise differentiation of functional pancreatic β cells from human pluripotent stem cells. *Cell Regeneration 2022 11:1* 11: 1–19

Jonas JC, Sharma A, Hasenkamp W, Ilkova H, Patanè G, Laybutt R, Bonner-Weir S & Weir GC (1999) Chronic hyperglycemia triggers loss of pancreatic β cell differentiation in an animal model of diabetes. *Journal of Biological Chemistry* 274: 14112–14121

Jun J Il & Lau LF (2010) The matricellular protein CCN1 induces fibroblast senescence and restricts fibrosis in cutaneous wound healing. *Nat Cell Biol* 12: 676–685

Jun JII & Lau LF (2017) CCN2 induces cellular senescence in fibroblasts. *J Cell Commun Signal* 11: 15–23

Kandhaya-Pillai R, Miro-Mur F, Alijotas-Reig J, Tchkonia T, Kirkland JL & Schwartz S (2017) TNFα-senescence initiates a STAT-dependent positive feedback loop, leading to a sustained interferon signature, DNA damage, and cytokine secretion. *Aging* 9: 2411–2435

Karimova M V., Gvazava IG & Vorotelyak EA (2022) Overcoming the Limitations of Stem Cell-Derived Beta Cells. *Biomolecules* 12: 810

Kerepesi C, Zhang B, Lee SG, Trapp A & Gladyshev VN (2021) Epigenetic clocks reveal a rejuvenation event during embryogenesis followed by aging. *Sci Adv* 7: eabg6082

Khiatah B, Qi M, Du W, T-Chen K, Van Megen KM, Perez RG, Isenberg JS, Kandeel F, Roep BO, Ku HT, *et al* (2019) Intra-pancreatic tissue-derived mesenchymal stromal cells: A promising therapeutic potential with anti-inflammatory and pro-angiogenic profiles. *Stem Cell Res Ther* 10: 1–14

Kim MJ, Lee EY, You YH, Yang HK, Yoon KH & Kim JW (2020) Generation of iPSC-derived insulin-producing cells from patients with type 1 and type 2 diabetes compared with healthy control. *Stem Cell Res* 48

Koch CM, Reck K, Shao K, Lin Q, Joussen S, Ziegler P, Walenda G, Drescher W, Opalka B, May T, *et al* (2013) Pluripotent stem cells escape from senescence-associated DNA methylation changes. *Genome Res* 23: 248

Kochar IS & Jain R (2021) Pancreas transplant in type 1 diabetes mellitus: the emerging role of islet cell transplant. *Ann Pediatr Endocrinol Metab* 26: 86–91

Koche RP, Smith ZD, Adli M, Gu H, Ku M, Gnirke A, Bernstein BE & Meissner A (2011) Reprogramming factor expression induces rapid and widespread targeted chromatin remodeling. *Cell Stem Cell* 8: 96

Kogut I, McCarthy SM, Pavlova M, Astling DP, Chen X, Jakimenko A, Jones KL, Getahun A, Cambier JC, Pasmooij AMG, *et al* (2018) High-efficiency RNA-based

reprogramming of human primary fibroblasts. *Nature Communications 2018 9:1* 9: 1–15

Krentz NAJ (2021) Improvements in stem cell to beta-cell differentiation for the treatment of diabetes. *J Immunol Regen Med* 12: 100043

Krogvold L, Edwin B, Buanes T, Frisk G, Skog O, Anagandula M, Korsgren O, Undlien D, Eike MC, Richardson SJ, *et al* (2015) Detection of a low-grade enteroviral infection in the islets of langerhans of living patients newly diagnosed with type 1 diabetes. *Diabetes* 64: 1682–1687

Kroon E, Martinson LA, Kadoya K, Bang AG, Kelly OG, Eliazer S, Young H, Richardson M, Smart NG, Cunningham J, *et al* (2008) Pancreatic endoderm derived from human embryonic stem cells generates glucose-responsive insulin-secreting cells in vivo. *Nature Biotechnology 2008 26:4* 26: 443–452

Kushner JA (2013) The role of aging upon β cell turnover. *J Clin Invest* 123: 990–995

Lablanche S, Borot S, Wojtusciszyn A, Skaare K, Penfornis A, Malvezzi P, Badet L, Thivolet C, Morelon E, Buron F, *et al* (2021) Ten-year outcomes of islet transplantation in patients with type 1 diabetes: Data from the Swiss-French GRAGIL network. *American Journal of Transplantation* 21: 3725–3733

Lam A, Oram RA, Forbes S, Olateju T, Malcolm AJ, Imes S, Shapiro AMJ & Senior PA (2022) Estimation of Early Graft Function Using the BETA-2 Score Following Clinical Islet Transplantation. *Transplant International* 35: 10335

Lapasset L, Milhavet O, Prieur A, Besnard E, Babled A, Ät-Hamou N, Leschik J, Pellestor F, Ramirez JM, De Vos J, *et al* (2011) Rejuvenating senescent and centenarian human cells by reprogramming through the pluripotent state. *Genes Dev* 25: 2248

Lappan R, Jirapanjawat T, Williamson DA, Lange S, Chown SL & Greening C (2022) Simultaneous detection of multiple pathogens with the TaqMan Array Card. *MethodsX* 9

Lee DH, Imran M, Choi JH, Park YJ, Kim YH, Min S, Park TJ & Choi YW (2024) CDK4/6 inhibitors induce breast cancer senescence with enhanced anti-tumor immunogenic properties compared with DNA-damaging agents. *Mol Oncol* 18: 216–232

Lee H, Sahin GS, Chen CW, Sonthalia S, Cañas SM, Oktay HZ, Duckworth AT, Brawerman G, Thompson PJ, Hatzoglou M, *et al* (2023) Stress-induced β-cell early senescence confers protection against type 1 diabetes. *Cell Metab* 35: 2200

Lee J, Kim YS, Kim E, Kim Y & Kim Y (2020) Curcumin and hesperetin attenuate D-galactose-induced brain senescence in vitro and in vivo. *Nutr Res Pract* 14: 438–452

Lee J & Yoon KH (2022) β cell replacement therapy for the cure of diabetes. *J Diabetes Investig* 13: 1798–1802

Li X, Li C, Zhang W, Wang Y, Qian P & Huang H (2023) Inflammation and aging: signaling pathways and intervention therapies. *Signal Transduction and Targeted Therapy 2023 8:1* 8: 1–29

Liang D, Li Z, Feng Z, Yuan Z, Dai Y, Wu X, Zhang F, Wang Y, Zhou Y, Liu L, *et al* (2022) Metformin Improves the Senescence of Renal Tubular Epithelial Cells in a High-Glucose State Through E2F1. *Front Pharmacol* 13: 926211

López-Otín C, Blasco MA, Partridge L, Serrano M & Kroemer G (2013) The hallmarks of aging. *Cell* 153: 1194

Luciano-Mateo F, Cabré N, Baiges-Gaya G, Fernandez-Arroyo S, Hernandez-Aguilera A, Rodriguez-Tomas E, Arenas M, Camps J, Menendez JA & Joven J (2020) Systemic overexpression of C-C motif chemokine ligand 2 promotes metabolic dysregulation and premature death in mice with accelerated aging. *Aging (Albany NY)* 12: 20001

Lyttle BM, Li J, Krishnamurthy M, Fellows F, Wheeler MB, Goodyer CG & Wang R (2008) Transcription factor expression in the developing human fetal endocrine pancreas. *Diabetologia* 51: 1169–1180

de Magalhães JP & Passos JF (2018) Stress, cell senescence and organismal ageing. *Mech Ageing Dev* 170: 2–9

Malik N & Rao MS (2013) A Review of the Methods for Human iPSC Derivation. *Methods Mol Biol* 997: 23

Mansfield L, Ramponi V, Gupta K, Stevenson T, Mathew AB, Barinda AJ, Herbstein F & Morsli S (2024) Emerging insights in senescence: pathways from preclinical models to therapeutic innovations. *npj Aging 2024 10:1* 10: 1–33

Marek-Trzonkowska N, Wujtewicz MA, Myśliwiec M, Witkowski P, Dobyszuk A, Møynarski W, Grabowska M, Balcerska A, Techmańska I, Myśliwska J, *et al* (2012) Administration of CD4+CD25highCD127− Regulatory T Cells Preserves β-Cell Function in Type 1 Diabetes in Children. *Diabetes Care* 35: 1817–1820

Marfil-Garza BA, Imes S, Verhoeff K, Hefler J, Lam A, Dajani K, Anderson B, O'Gorman D, Kin T, Bigam D, *et al* (2022) Pancreatic islet transplantation in type 1 diabetes: 20-year experience from a single-centre cohort in Canada. *Lancet Diabetes Endocrinol* 10: 519–532

Masset C, Branchereau J, Karam G, Hourmant M, Dantal J, Giral M, Garandeau C, Meurette A, Kerleau C, Kervella D, *et al* (2021) Clinical utility of C-peptide measurement after pancreas transplantation with especial focus on early graft thrombosis. *Transplant International* 34: 942–953

McHugh D & Gil J (2018) Senescence and aging: Causes, consequences, and therapeutic avenues. *J Cell Biol* 217: 65

Di Micco R, Krizhanovsky V, Baker D & d'Adda di Fagagna F (2020) Cellular senescence in ageing: from mechanisms to therapeutic opportunities. *Nature Reviews Molecular Cell Biology 2020 22:2* 22: 75–95

Midha A, Pan H, Abarca C, Andle J, Carapeto P, Bonner-Weir S & Aguayo-Mazzucato C (2021) Unique Human and Mouse β-Cell Senescence-Associated Secretory Phenotype (SASP) Reveal Conserved Signaling Pathways and Heterogeneous Factors. *Diabetes* 70: 1098–1116

Mijit M, Caracciolo V, Melillo A, Amicarelli F & Giordano A (2020) Role of p53 in the Regulation of Cellular Senescence. *Biomolecules* 10: 420

Mobasseri M, Shirmohammadi M, Amiri T, Vahed N, Fard HH & Ghojazadeh M (2020) Prevalence and incidence of type 1 diabetes in the world: a systematic review and meta-analysis. *Health Promot Perspect* 10: 98

Moiseeva O, Deschênes-Simard X, St-Germain E, Igelmann S, Huot G, Cadar AE, Bourdeau V, Pollak MN & Ferbeyre G (2013) Metformin inhibits the senescence-associated secretory phenotype by interfering with IKK/NF-κB activation. *Aging Cell* 12: 489–498

Motlagh RA, Pipella J & Thompson PJ (2024) Exploring senescence as a modifier of β cell extracellular vesicles in type 1 diabetes. *Front Endocrinol (Lausanne)* 15: 1422279

Muñoz-Espín D, Cañamero M, Maraver A, Gómez-López G, Contreras J, Murillo-Cuesta S, Rodríguez-Baeza A, Varela-Nieto I, Ruberte J, Collado M, *et al* (2013) XProgrammed cell senescence during mammalian embryonic development. *Cell* 155: 1104

Murakami T, Inagaki N & Kondoh H (2022) Cellular Senescence in Diabetes Mellitus: Distinct Senotherapeutic Strategies for Adipose Tissue and Pancreatic β Cells. *Front Endocrinol (Lausanne)* 13: 869414

Muthamil S, Kim HY, Jang HJ, Lyu JH, Shin UC, Go Y, Park SH, Lee HG & Park JH (2024) Biomarkers of Cellular Senescence and Aging: Current State-of-the-Art, Challenges and Future Perspectives. *Adv Biol* 8: 2400079

Muto J, Fukuda S, Watanabe K, Dai X, Tsuda T, Kiyoi T, Kameda K, Kawakami R, Mori H, Shiraishi K, *et al* (2023) Highly concentrated trehalose induces prohealing senescence-like state in fibroblasts via CDKN1A/p21. *Commun Biol* 6

Mylonas A & O'Loghlen A (2022) Cellular Senescence and Ageing: Mechanisms and Interventions. *Frontiers in Aging* 3: 866718

Nadia Ahmad NF, Nik Ghazali NN & Wong YH (2021) Wearable patch delivery system for artificial pancreas health diagnostic-therapeutic application: A review. *Biosens Bioelectron* 189: 113384

Nair GG, Tzanakakis ES & Hebrok M (2020) Emerging routes to the generation of functional β-cells for diabetes mellitus cell therapy. *Nat Rev Endocrinol* 16: 506

Naqvi RA, Naqvi AR, Singh A, Priyadarshini M, Balamurugan AN & Layden BT (2023) The future treatment for type 1 diabetes: Pig islet- or stem cell-derived β cells? *Front Endocrinol (Lausanne)* 13: 1001041

Nathan DM (2014) The diabetes control and complications trial/epidemiology of diabetes interventions and complications study at 30 years: overview. *Diabetes Care* 37: 9–16

Niinistö S, Takkinen HM, Erlund I, Ahonen S, Toppari J, Ilonen J, Veijola R, Knip M, Vaarala O & Virtanen SM (2017) Fatty acid status in infancy is associated with the risk of type 1 diabetes-associated autoimmunity. *Diabetologia* 60: 1223–1233

Ocampo A, Reddy P, Martinez-Redondo P, Platero-Luengo A, Hatanaka F, Hishida T, Li M, Lam D, Kurita M, Beyret E, *et al* (2016) In Vivo Amelioration of Age-Associated Hallmarks by Partial Reprogramming. *Cell* 167: 1719

Ogrodnik M, Carlos Acosta J, Adams PD, d'Adda di Fagagna F, Baker DJ, Bishop CL, Chandra T, Collado M, Gil J, Gorgoulis V, *et al* (2024) Guidelines for minimal information on cellular senescence experimentation in vivo. *Cell* 187: 4150–4175

Oh J, Lee YD & Wagers AJ (2014) Stem cell aging: mechanisms, regulators and therapeutic opportunities. *Nat Med* 20: 870

Onkamo P, Väänänen S, Karvonen M & Tuomilehto J (1999) Worldwide increase in incidence of Type I diabetes - The analysis of the data on published incidence trends. *Diabetologia* 42: 1395–1403

Ortiz-Montero P, Londoño-Vallejo A & Vernot JP (2017) Senescence-associated IL-6 and IL-8 cytokines induce a self- and cross-reinforced senescence/inflammatory milieu strengthening tumorigenic capabilities in the MCF-7 breast cancer cell line. *Cell Commun Signal* 15

Padgett LE, Broniowska KA, Hansen PA, Corbett JA & Tse HM (2013) The role of reactive oxygen species and proinflammatory cytokines in type 1 diabetes pathogenesis. *Ann N Y Acad Sci* 1281: 16

Pagliuca FW, Millman JR, Gürtler M, Segel M, Van Dervort A, Ryu JH, Peterson QP, Greiner D & Melton DA (2014) Generation of functional human pancreatic β cells in vitro. *Cell* 159: 428–439

Palmer AK, Tchkonia T, LeBrasseur NK, Chini EN, Xu M & Kirkland JL (2015) Cellular Senescence in Type 2 Diabetes: A Therapeutic Opportunity. *Diabetes* 64: 2289–2298

Pang X, Gao S, Liu T, Xu FX, Fan C, Zhang JF & Jiang H (2024) Identification of STAT3 as a biomarker for cellular senescence in liver fibrosis: A bioinformatics and experimental validation study. *Genomics* 116: 110800

Patanè G, Piro S, Rabuazzo AM, Anello M, Vigneri R & Purrello F (2000) Metformin restores insulin secretion altered by chronic exposure to free fatty acids or high glucose: a direct metformin effect on pancreatic beta-cells. *Diabetes* 49: 735–740

Pathak V, Pathak NM, O'Neill CL, Guduric-Fuchs J & Medina RJ (2019) Therapies for Type 1 Diabetes: Current Scenario and Future Perspectives. *Clin Med Insights Endocrinol Diabetes* 12

Patra M, Klochendler A, Condiotti R, Kaffe B, Elgavish S, Drawshy Z, Avrahami D, Narita M, Hofree M, Drier Y, *et al* (2024) Senescence of human pancreatic beta cells enhances functional maturation through chromatin reorganization and promotes interferon responsiveness. *Nucleic Acids Res* 52: 6298

Pitrez PR, Monteiro LM, Borgogno O, Nissan X, Mertens J & Ferreira L (2024) Cellular reprogramming as a tool to model human aging in a dish. *Nature Communications 2024 15:1* 15: 1–11

Pratt EPS, Harvey KE, Salyer AE & Hockerman GH (2019) Regulation of cAMP accumulation and activity by distinct phosphodiesterase subtypes in INS-1 cells and human pancreatic β-cells. *PLoS One* 14: e0215188

Quarta M & Demaria M (2024) On the past, present and future of senotherapeutics. *npj Aging 2024 10:1* 10: 1–2

Ramzy A, Thompson DM, Ward-Hartstonge KA, Ivison S, Cook L, Garcia R V., Loyal J, Kim PTW, Warnock GL, Levings MK, *et al* (2021) Implanted pluripotent stem-cell-derived pancreatic endoderm cells secrete glucose-responsive C-peptide in patients with type 1 diabetes. *Cell Stem Cell* 28: 2047-2061.e5

REICHMAN TW, RICORDI C, NAJI A, MARKMANN JF, PERKINS BA, WIJKSTROM M, PARASKEVAS S, BRUINSMA B, MARIGOWDA G, SHIH

JL, *et al* (2023) 836-P: Glucose-Dependent Insulin Production and Insulin-Independence in Type 1 Diabetes from Stem Cell–Derived, Fully Differentiated Islet Cells—Updated Data from the VX-880 Clinical Trial. *Diabetes* 72

Ren P, Zhang J & Vijg J (2024) Somatic mutations in aging and disease. *Geroscience* 46: 5171

Rezania A, Bruin JE, Arora P, Rubin A, Batushansky I, Asadi A, O'Dwyer S, Quiskamp N, Mojibian M, Albrecht T, *et al* (2014) Reversal of diabetes with insulin-producing cells derived in vitro from human pluripotent stem cells. *Nature Biotechnology 2014 32:11* 32: 1121–1133

Rhinn M, Ritschka B & Keyes WM (2019) Cellular senescence in development, regeneration and disease. *Development (Cambridge)* 146

Ricordi C, Lacy PE & Scharp DW (1989) Automated Islet Isolation From Human Pancreas. *Diabetes* 38: 140–142

Ring NAR, Valdivieso K, Grillari J, Redl H & Ogrodnik M (2022) The role of senescence in cellular plasticity: Lessons from regeneration and development and implications for age-related diseases. *Dev Cell* 57: 1083–1101

Rubin de Celis MF & Bonner-Weir S (2023) Reversing and modulating cellular senescence in beta cells, a new field of opportunities to treat diabetes. *Front Endocrinol (Lausanne)* 14: 1217729

Ruggiero AD, Vemuri R, Blawas M, Long M, DeStephanis D, Williams AG, Chen H, Justice JN, Macauley SL, Day SM, *et al* (2023) Long-term dasatinib plus quercetin effects on aging outcomes and inflammation in nonhuman primates: implications for senolytic clinical trial design. *Geroscience* 45: 2785–2803

Sacks DB (2024) Smart insulin switches itself off in response to low blood sugar. *Nature 2024 634:8035* 634: 785–787

Sagiv A, Biran A, Yon M, Simon J, Lowe SW & Krizhanovsky V (2012) Granule exocytosis mediates immune surveillance of senescent cells. *Oncogene* 32: 1971

Saito Y, Yamamoto S & Chikenji TS (2024) Role of cellular senescence in inflammation and regeneration. *Inflammation and Regeneration 2024 44:1* 44: 1–12

Sanada F, Taniyama Y, Muratsu J, Otsu R, Shimizu H, Rakugi H & Morishita R (2018) IGF Binding Protein-5 Induces Cell Senescence. *Front Endocrinol (Lausanne)* 9: 53

Sapra A & Bhandari P (2023) Diabetes. *StatPearls*

Schmitt CA, Wang B & Demaria M (2022) Senescence and cancer — role and therapeutic opportunities. *Nature Reviews Clinical Oncology 2022 19:10* 19: 619–636

Schwitzgebel VM, Scheel DW, Conners JR, Kalamaras J, Lee JE, Anderson DJ, Sussel L, Johnson JD & German MS (2000) Expression of neurogenin3 reveals an islet cell precursor population in the pancreas. *Development* 127: 3533–3542

Serrano IM, Hirose M, Valentine CC, Roesner S, Schmidt E, Pratt G, Williams L, Salk J, Ibrahim S & Sudmant PH (2024) Mitochondrial somatic mutation and selection throughout ageing. *Nature Ecology & Evolution 2024 8:5* 8: 1021–1034

Shapiro AMJ, Lakey JRT, Ryan EA, Korbutt GS, Toth E, Warnock GL, Kneteman NM & Rajotte R V. (2000) Islet Transplantation in Seven Patients with Type 1 Diabetes Mellitus Using a Glucocorticoid-Free Immunosuppressive Regimen. *New England Journal of Medicine* 343: 230–238

Shapiro AMJ, Pokrywczynska M & Ricordi C (2016) Clinical pancreatic islet transplantation. *Nature Reviews Endocrinology 2016 13:5* 13: 268–277

Shin JS, Kim JM, Kim JS, Min BH, Kim YH, Kim HJ, Jang JY, Yoon IH, Kang HJ, Kim J, *et al* (2015) Long-term control of diabetes in immunosuppressed nonhuman primates (NHP) by the transplantation of adult porcine islets. *American Journal of Transplantation* 15: 2837–2850

Siegel EG, Wollheim CB, Kikuchi M, Renold AE & Sharp GW (1980) Dependency of cyclic AMP-induced insulin release on intra- and extracellular calcium in rat islets of Langerhans. *Journal of Clinical Investigation* 65: 233

Sierra-Ramirez A, López-Aceituno JL, Costa-Machado LF, Plaza A, Barradas M & Fernandez-Marcos PJ (2020) Transient metabolic improvement in obese mice treated with navitoclax or dasatinib/quercetin. *Aging* 12: 11337–11348

Singh A, Afshan N, Singh A, Singh SK, Yadav S, Kumar M, Sarma DK & Verma V (2023) Recent trends and advances in type 1 diabetes therapeutics: A comprehensive review. *Eur J Cell Biol* 102: 151329

Skwarska A & Konopleva M (2023) BCL-xL Targeting to Induce Apoptosis and to Eliminate Chemotherapy-Induced Senescent Tumor Cells: From Navitoclax to Platelet-Sparing BCL-xL PROTACs. *Cancer Res* 83: 3501–3503

Sondka Z, Dhir NB, Carvalho-Silva D, Jupe S, Madhumita, McLaren K, Starkey M, Ward S, Wilding J, Ahmed M, *et al* (2024) COSMIC: a curated database of somatic variants and clinical data for cancer. *Nucleic Acids Res* 52: D1210–D1217

Sordi V, Melzi R, Mercalli A, Formicola R, Doglioni C, Tiboni F, Ferrari G, Nano R, Chwalek K, Lammert E, *et al* (2010) Mesenchymal Cells Appearing in Pancreatic

Tissue Culture Are Bone Marrow-Derived Stem Cells With the Capacity to Improve Transplanted Islet Function. *Stem Cells* 28: 140–151

Sordi V, Monaco L & Piemonti L (2023) Cell Therapy for Type 1 Diabetes: From Islet Transplantation to Stem Cells. *Horm Res Paediatr* 96: 658–669

Soria-Valles C & López-Otín C (2016) iPSCs: On the Road to Reprogramming Aging. *Trends Mol Med* 22: 713–724

Spisak N, de Manuel M, Milligan W, Sella G & Przeworski M (2024) The clock-like accumulation of germline and somatic mutations can arise from the interplay of DNA damage and repair. *PLoS Biol* 22: e3002678

Stein GH, Drullinger LF, Soulard A & Dulić V (1999) Differential Roles for Cyclin-Dependent Kinase Inhibitors p21 and p16 in the Mechanisms of Senescence and Differentiation in Human Fibroblasts. *Mol Cell Biol* 19: 2109

Storer M, Mas A, Robert-Moreno A, Pecoraro M, Ortells MC, Di Giacomo V, Yosef R, Pilpel N, Krizhanovsky V, Sharpe J, *et al* (2013) XSenescence is a developmental mechanism that contributes to embryonic growth and patterning. *Cell* 155: 1119

Strässler ET, Aalto-Setälä K, Kiamehr M, Landmesser U & Kränkel N (2018) Age Is Relative—Impact of Donor Age on Induced Pluripotent Stem Cell-Derived Cell Functionality. *Front Cardiovasc Med* 5: 4

Surmachevska N & Rubio J (2024) Senescence in Osteoarthritis: Overview of Mechanisms and Therapeutics. *Eur J Rheumatol* 11: S3

Suryadevara V, Hudgins AD, Rajesh A, Pappalardo A, Karpova A, Dey AK, Hertzel A, Agudelo A, Rocha A, Soygur B, *et al* (2024) SenNet recommendations for detecting senescent cells in different tissues. *Nature Reviews Molecular Cell Biology 2024 25:12* 25: 1001–1023

Suzuki H, Shibata R, Kito T, Yamamoto T, Ishii M, Nishio N, Ito S, Isobe K ichi & Murohara T (2012) Comparative angiogenic activities of induced pluripotent stem cells derived from young and old mice. *PLoS One* 7

Takahashi K & Yamanaka S (2006) Induction of Pluripotent Stem Cells from Mouse Embryonic and Adult Fibroblast Cultures by Defined Factors. *Cell* 126: 663–676

Takaya K & Kishi K (2024) Combined dasatinib and quercetin treatment contributes to skin rejuvenation through selective elimination of senescent cells in vitro and in vivo. *Biogerontology* 25: 691–704

Talchai C, Xuan S, Lin H V., Sussel L & Accili D (2012) Pancreatic β cell dedifferentiation as a mechanism of diabetic β cell failure. *Cell* 150: 1223–1234

Thompson PJ, Shah A, Ntranos V, Van Gool F, Atkinson M & Bhushan A (2019) Targeted Elimination of Senescent Beta Cells Prevents Type 1 Diabetes. *Cell Metab* 29: 1045-1060.e10

Thorngren J, Brboric A, Vasylovska S, Hjelmqvist D, Westermark GT, Saarimäki-Vire J, Kvist J, Balboa D, Otonkoski T, Carlsson PO, *et al* (2024) Efficient Vascular and Neural Engraftment of Stem Cell–Derived Islets. *Diabetes* 73: 1127–1139

van Tienhoven R, Kracht MJL, van der Slik AR, Thomaidou S, Wolters AHG, Giepmans BNG, Riojas JPR, Nelson MS, Carlotti F, de Koning EJP, *et al* (2023) Presence of immunogenic alternatively spliced insulin gene product in human pancreatic delta cells. *Diabetologia* 66: 884–896

Tremmel DM & Odorico JS (2018) Rebuilding a better home for transplanted islets. *Organogenesis* 14: 163–168

Tuttle KR, Brosius FC, Adler SG, Kretzler M, Mehta RL, Tumlin JA, Tanaka Y, Haneda M, Liu J, Silk ME, *et al* (2018) JAK1/JAK2 inhibition by baricitinib in diabetic kidney disease: results from a Phase 2 randomized controlled clinical trial. *Nephrol Dial Transplant* 33: 1950–1959

Ueda S, Tominaga T, Ochi A, Sakurai A, Nishimura K, Shibata E, Wakino S, Tamaki M & Nagai K (2021) TGF-β1 is involved in senescence-related pathways in glomerular endothelial cells via p16 translocation and p21 induction. *Scientific Reports 2021 11:1* 11: 1–12

Uusitalo L, Nevalainen J, Niinistö S, Alfthan G, Sundvall J, Korhonen T, Kenward MG, Oja H, Veijola R, Simell O, *et al* (2008) Serum α- and γ-tocopherol concentrations and risk of advanced beta cell autoimmunity in children with HLA-conferred susceptibility to type 1 diabetes mellitus. *Diabetologia* 51: 773–780

Vantyghem MC, Chetboun M, Gmyr V, Jannin A, Espiard S, Le Mapihan K, Raverdy V, Delalleau N, MacHuron F, Hubert T, *et al* (2019) Ten-Year Outcome of Islet Alone or Islet After Kidney Transplantation in Type 1 Diabetes: A Prospective Parallel-Arm Cohort Study. *Diabetes Care* 42: 2042–2049

Vecchio I, Tornali C, Bragazzi NL & Martini M (2018) The Discovery of Insulin: An Important Milestone in the History of Medicine. *Front Endocrinol (Lausanne)* 9: 613

Velazco-Cruz L, Song J, Maxwell KG, Goedegebuure MM, Augsornworawat P, Hogrebe NJ & Millman JR (2019) Acquisition of Dynamic Function in Human Stem Cell-Derived β Cells. *Stem Cell Reports* 12: 351–365

Vilas JM, Carneiro C, Da Silva-Álvarez S, Ferreirós A, González P, Gómez M, Ortega S, Serrano M, García-Caballero T, González-Barcia M, *et al* (2018) Adult Sox2+

stem cell exhaustion in mice results in cellular senescence and premature aging. *Aging Cell* 17: e12834

Waibel M, Wentworth JM, So M, Couper JJ, Cameron FJ, MacIsaac RJ, Atlas G, Gorelik A, Litwak S, Sanz-Villanueva L, *et al* (2023) Baricitinib and β-Cell Function in Patients with New-Onset Type 1 Diabetes. *New England Journal of Medicine* 389: 2140–2150

Wang H, Brun T, Kataoka K, Sharma AJ & Wollheim CB (2006) MafA controls Genes implicated in Insulin Biosynthesis and Secretion. *Diabetologia* 50: 348

Wang L, Zhang X, Sheng J, Chen L, Zhi L, Zheng Q, Qi Y, Wang L, Zhang J, Zhao J, *et al* (2023) RBM4 regulates cellular senescence via miR1244/SERPINE1 axis. *Cell Death & Disease 2023 14:1* 14: 1–11

Wang M, Tian T, Zhou H, Jiang SY, Jiao YY, Zhu Z, Xia J, Ma JH & Du RH (2024a) Metformin normalizes mitochondrial function to delay astrocyte senescence in a mouse model of Parkinson's disease through Mfn2-cGAS signaling. *J Neuroinflammation* 21: 1–17

Wang S, Du Y, Zhang B, Meng G, Liu Z, Liew SY, Liang R, Zhang Z, Cai X, Wu S, *et al* (2024b) Transplantation of chemically induced pluripotent stem-cell-derived islets under abdominal anterior rectus sheath in a type 1 diabetes patient. *Cell* 187: 6152-6164.e18

Wang Y, Kuca K, You L, Nepovimova E, Heger Z, Valko M, Adam V, Wu Q & Jomova K (2024c) The role of cellular senescence in neurodegenerative diseases. *Archives of Toxicology 2024 98:8* 98: 2393–2408

Wang Y, Peng F, Yang Z, Cheng L, Cao J, Fu X, He H, Cai R, Zeng W, Dong Y, *et al* (2025) A rapid chemical reprogramming system to generate human pluripotent stem cells. *Nat Chem Biol*

Warncke K, Weiss A, Achenbach P, Von Dem Berge T, Berner R, Casteels K, Groele L, Hatzikotoulas K, Hommel A, Kordonouri O, *et al* (2022) Elevations in blood glucose before and after the appearance of islet autoantibodies in children. *J Clin Invest* 132: e162123

Wen Y, Wani P, Zhou L, Baer T, Phadnis SM, Reijo Pera RA & Chen B (2013) Reprogramming of fibroblasts from older women with pelvic floor disorders alters cellular behavior associated with donor age. *Stem Cells Transl Med* 2: 118–128

Westacott MJ, Farnsworth NL, St Clair JR, Poffenberger G, Heintz A, Ludin NW, Hart NJ, Powers AC & Benninger RKP (2017) Age-dependent decline in the coordinated [Ca2+] and insulin secretory dynamics in human pancreatic islets. *Diabetes* 66: 2436–2445

Wierstra I (2013) The transcription factor FOXM1 (Forkhead box M1): proliferation-specific expression, transcription factor function, target genes, mouse models, and normal biological roles. *Adv Cancer Res* 118: 97–398

Wilson ME, Scheel D & German MS (2003) Gene expression cascades in pancreatic development. *Mech Dev* 120: 65–80

Xiao J, Group for the CND and MDS, Weng J, Group for the CND and MDS, Ji L, Group for the CND and MDS, Jia W, Group for the CND and MDS, Lu J, Group for the CND and MDS, *et al* (2014) Worse Pancreatic β-cell Function and Better Insulin Sensitivity in Older Chinese Without Diabetes. *The Journals of Gerontology: Series A* 69: 463–470

Xu M, Tchkonia T, Ding H, Ogrodnik M, Lubbers ER, Pirtskhalava T, White TA, Johnson KO, Stout MB, Mezera V, *et al* (2015) JAK inhibition alleviates the cellular senescence-associated secretory phenotype and frailty in old age. *Proc Natl Acad Sci U S A* 112: E6301–E6310

Xu M, Tchkonia T & Kirkland JL (2016) Perspective: Targeting the JAK/STAT pathway to fight age-related dysfunction. *Pharmacol Res* 111: 152

Yang B, Li T, Wang Z, Zhu Y, Niu K, Hu S, Lin Z, Zheng X, Jin X & Shen C (2024) Ruxolitinib-based senomorphic therapy mitigates cardiomyocyte senescence in septic cardiomyopathy by inhibiting the JAK2/STAT3 signaling pathway. *Int J Biol Sci* 20: 4314

Yang J, Liu HC, Zhang JQ, Zou JY, Zhang X, Chen WM, Gu Y & Hong H (2023) The effect of metformin on senescence of T lymphocytes. *Immunity and Ageing* 20: 1–15

Yang L, Shi J, Wang X & Zhang R (2022) Curcumin Alleviates D-Galactose-Induced Cardiomyocyte Senescence by Promoting Autophagy via the SIRT1/AMPK/mTOR Pathway. *Evid Based Complement Alternat Med* 2022

Yousefzadeh MJ, Flores RR, Zhu Y, Schmiechen ZC, Brooks RW, Trussoni CE, Cui Y, Angelini L, Lee KA, McGowan SJ, *et al* (2021) An aged immune system drives senescence and ageing of solid organs. *Nature* 594: 100

Zakrzewski W, Dobrzyński M, Szymonowicz M & Rybak Z (2019) Stem cells: past, present, and future. *Stem Cell Res Ther* 10: 68

Zhang W, Qu J, Liu GH & Belmonte JCI (2020) The ageing epigenome and its rejuvenation. *Nature Reviews Molecular Cell Biology 2020 21:3* 21: 137–150

Ziegler AG, Rewers M, Simell O, Simell T, Lempainen J, Steck A, Winkler C, Ilonen J, Veijola R, Knip M, *et al* (2013) Seroconversion to multiple islet autoantibodies and risk of progression to diabetes in children. *JAMA* 309: 2473–2479

Zuckerman V, Wolyniec K, Sionov R V., Haupt S & Haupt Y (2009) Tumour suppression by p53: the importance of apoptosis and cellular senescence. *J Pathol* 219: 3–15

